Ontario

Ontario Geological Survey
Open File Report 6155

Geological Setting of Volcanogenic Massive Sulphide Mineralization in the Kamiskotia Area: Discover Abitibi Initiative

2005

105-05383/

Ontario

ONTARIO GEOLOGICAL SURVEY

Open File Report 6155

Geological Setting of Volcanogenic Massive Sulphide Mineralization in the Kamiskotia Area: Discover Abitibi Initiative

by

B. Hathway, G. Hudak and M.A. Hamilton

2005

Parts of this publication may be quoted if credit is given. It is recommended that reference to this publication be made in the following form:

Hathway, B., Hudak, G. and Hamilton, M.A. 2005. Geological setting of volcanogenic massive sulphide mineralization in the Kamiskotia area: Discover Abitibi Initiative; Ontario Geological Survey, Open File Report 6155, 81p.

Discover Abitibi

Découvrons l'Abitibi

Discover Abitibi Initiative
The Discover Abitibi Initiative is a regional, cluster economic development project based on geoscientific investigations of the western Abitibi greenstone belt. The initiative, centred on the Kirkland Lake and Timmins mining camps, will complete 19 projects developed and directed by the local stakeholders. FedNor, Northern Ontario Heritage Fund Corporation, municipalities and private sector investors have provided the funding for the initiative.

Initiative Découvrons l'Abitibi
L'initiative Découvrons l'Abitibi est un project de développment économique régional dans une grappe d'industries, projet fondé sur des études géoscientifiques de la ceinture de roches vertes de l'Abitibi occidental. Cette initiative, centrée sur les zones minières de Kirkland Lake et de Timmins, ménera à bien 19 projets élaborés et dirigés par des intervenants locaux. FedNor, la Société de gestion du Fonds du patrimoine du Nord de l'Ontario, municipalités et des investisseurs du secteur privé ont fourni les fonds de cette initiative.

FedNor
Canada
Timmins
KIRKLAND LAKE
Ontario
Northern Ontario Heritage Fund
Fonds du patrimoine du Nord de l'Ontario

© Queen's Printer for Ontario, 2005

© Queen's Printer for Ontario, 2005.

Open File Reports of the Ontario Geological Survey are available for viewing at the Mines Library in Sudbury, at the Mines and Minerals Information Centre in Toronto, and at the regional Mines and Minerals office whose district includes the area covered by the report (see below).

Copies can be purchased at Publication Sales and the office whose district includes the area covered by the report. Although a particular report may not be in stock at locations other than the Publication Sales office in Sudbury, they can generally be obtained within 3 working days. All telephone, fax, mail and e-mail orders should be directed to the Publication Sales office in Sudbury. Use of VISA or MasterCard ensures the fastest possible service. Cheques or money orders should be made payable to the *Minister of Finance.*

Mines and Minerals Information Centre (MMIC) Tel: (416) 314-3800
Macdonald Block, Room M2-17
900 Bay St.
Toronto, Ontario M7A 1C3

Mines Library Tel: (705) 670-5615
933 Ramsey Lake Road, Level A3
Sudbury, Ontario P3E 6B5

Publication Sales Tel: (705) 670-5691(local)
933 Ramsey Lake Rd., Level A3 1-888-415-9845(toll-free)
Sudbury, Ontario P3E 6B5 Fax: (705) 670-5770
E-mail: pubsales@ndm.gov.on.ca

Regional Mines and Minerals Offices:

Kenora - Suite 104, 810 Robertson St., Kenora P9N 4J2

Kirkland Lake - 10 Government Rd. E., Kirkland Lake P2N 1A8

Red Lake - Box 324, Ontario Government Building, Red Lake P0V 2M0

Sault Ste. Marie - 70 Foster Dr., Ste. 200, Sault Ste. Marie P6A 6V8

Southern Ontario - P.O. Bag Service 43, 126 Old Troy Rd., Tweed K0K 3J0

Sudbury - Level B3, 933 Ramsey Lake Rd., Sudbury P3E 6B5

Thunder Bay - Suite B002, 435 James St. S., Thunder Bay P7E 6S7

Timmins - Ontario Government Complex, P.O. Bag 3060, Hwy. 101 East, South Porcupine P0N 1H0

Toronto - MMIC, Macdonald Block, Room M2-17, 900 Bay St., Toronto M7A 1C3

This report has not received a technical edit. Discrepancies may occur for which the Ontario Ministry of Northern Development and Mines does not assume any liability. Source references are included in the report and users are urged to verify critical information. Recommendations and statements of opinions expressed are those of the author or authors and are not to be construed as statements of government policy.

If you wish to reproduce any of the text, tables or illustrations in this report, please write for permission to the Team Leader, Publication Services, Ministry of Northern Development and Mines, 933 Ramsey Lake Road, Level B4, Sudbury, Ontario P3E 6B5.

Cette publication est disponible en anglais seulement.

Parts of this report may be quoted if credit is given. It is recommended that reference be made in the following form:

Hathway, B., Hudak, G. and Hamilton, M.A. 2005. Geological setting of volcanogenic massive sulphide mineralization in the Kamiskotia area: Discover Abitibi Initiative; Ontario Geological Survey, Open File Report 6155, 81p.

Contents

Abstract xiii

Introduction 1

Previous Regional Geological Work 1

Regional Geology 1

Kidd–Munro Assemblage 4
  Felsic to Intermediate Metavolcanic Rocks 4
  Mafic Metavolcanic Rocks 6
  Felsic Intrusive Rocks in the Kidd–Munro Assemblage 6
  Mafic to Ultramafic Intrusive Rocks in the Kidd–Munro Assemblage 7

Kamiskotia Volcanic Complex 7
  Felsic Metavolcanic Rocks 9
    South of the Steep Lake Fault 9
    Steep Lake Fault to Halfmoon Lake 9
    Ski-Hill Rhyolite 10
    Godfrey Creek Rhyolite 10
    Northeast of Kam Kotia Mine 11
  Mafic Metavolcanic Rocks 11
  Clastic Sedimentary Rocks 12
  Depositional Depths for the Kamiskotia Volcanic Complex 12

Kamiskotia Gabbroic Complex (KGC) 12
  Steep Lake Granophyre 13

Porcupine Assemblage Sedimentary Rocks 14

Geochemistry 14
  Mafic Metavolcanic Rocks 15
    Kidd–Munro Assemblage: Loveland and Macdiarmid Townships 15
    Carscallen and Bristol Townships 15
    Kamiskotia Volcanic Complex: Godfrey, Jamieson and Robb Townships 17
  Felsic to Intermediate Metavolcanic Rocks 18
    Kidd–Munro Assemblage: Loveland, Macdiarmid, Thorburn and Northernmost Robb Townships 18
    Kamiskotia Volcanic Complex 20

Geochronology 23
  Discussion 24

Structural Geology 24
  Kidd–Munro Assemblage 24
  Kamiskotia Volcanic and Gabbroic Complexes 25
    D_1 25
    D_2 26
    D_{3-4} 26
  Faulting 26

Metamorphism and Alteration 27

Volcanogenic Massive Sulphide Deposits 27
  Kam Kotia Mine 27
    Stratigraphy 30
    Alteration 33
    Structure 35
    Discussion – Kam Kotia Mine 36
  Canadian Jamieson Mine Area 37
    Stratigraphy 37
    Alteration 42
    Structure 44
    Discussion – Canadian Jamieson Mine 44
  Jameland Mine 45
  Steep Lake Prospect 45
  Halfmoon Lake Prospect 46
  Minor showings in the Kamiskotia Volcanic Complex 46
  Kidd–Munro Assemblage 46

Volcanogenic Massive Sulphide Exploration Suggestions 47
  Kidd–Munro Assemblage 47
  Kamiskotia Volcanic Complex 47

Acknowledgements 48

References 48

Appendix 1. Geochemical data for 156 rock samples from Carscallen, Bristol, Turnbull, Godfrey, Robb, Jamieson, Loveland, Macdiarmid and Thorburn townships 53

Metric Conversion Table 81

FIGURES

1. Generalized geological map of the southern Abitibi greenstone belt in Ontario 2
2. Geological sketch map of the Kamiskotia area 3
3. MgO vs. SiO_2 variation diagrams for Kidd–Munro assemblage and KVC metavolcanic rocks 15
4. Classification of Kamiskotia area metavolcanic rocks using Zr/TiO_2 vs. Nb/Y plot and Jensen plot 16
5. Rare earth element patterns for Kamiskotia area mafic metavolcanic rocks 17
6. Plots of TiO_2 against Zr and P_2O_5 for Kamiskotia area mafic metavolcanic rocks 18
7. Rare earth element patterns for Kamiskotia area felsic metavolcanic rocks 19
8. Plots of $[La/Yb]_{CN}$ vs. $[Yb]_{CN}$ and Zr/Y vs. Y for Kidd–Munro assemblage and KVC felsic and intermediate rocks 21
9. Rare earth element patterns for KVC rhyolites stratigraphically beneath the Genex VMS deposit 22
10. Stereoplots showing poles to S_1 and S_2 foliation planes in Jamieson and Godfrey townships 25
11. Alteration box plot of Large et al. (2001) showing Kamiskotia area mafic metavolcanic samples 28
12. Detailed surface geological map of the Kam Kotia Mine area 29
13. Stereonets showing poles to foliation planes in the immediate vicinities of the Kam Kotia and Canadian Jamieson deposits 36
14. Detailed surface geological map of the Canadian Jamieson Mine area 38
15. Apparent stratigraphic correlations between the Kam Kotia and Canadian Jamieson VMS deposits based on composite stratigraphic sections at the two deposits 40

PHOTOS

1. Field and drill core photographs of Kidd–Munro assemblage and Kamiskotia Volcanic Complex lithologies 5
2. Field and drill core photographs of Kamiskotia Volcanic Complex lithologies and related intrusive rocks 8
3. Field photographs of various lithologies in the vicinity of the Kam Kotia VMS deposits 31
4. Alteration in the vicinity of the Kam Kotia VMS orebody 34
5. Field photographs of various lithologies in the vicinity of the Canadian Jamieson VMS deposits 39
6. Alteration in the vicinity of the Canadian Jamieson VMS orebody 43

MAPS

Map P.3544—Revised Precambrian Geology of Parts of Godfrey, Turnbull, Carscallen and Bristol Townships .... back pocket

Map P.3556 Precambrian Geology of Parts of Godfrey, Robb, Jamieson, Loveland, Macdiarmid and Thorburn Townships .... back pocket

Abstract

The main aim of this Discover Abitibi subproject has been to understand the stratigraphy, volcanic facies, alteration and structural style of the late Archean volcanic succession that hosts copper-zinc volcanogenic massive sulphide (VMS) mineralization in the Kamiskotia area (Abitibi greenstone belt, Timmins region). The Archean rocks in the southern part of the study area are assigned to the Kamiskotia Gabbroic Complex (KGC) and Kamiskotia Volcanic Complex (KVC). All the known VMS deposits in the study area occur within a restricted, east-facing stratigraphic interval in the upper part of the KVC. New U-Pb ages for this interval, ranging from 2701.1 ± 1.4 to 2698.6 ± 1.3 Ma, and an age of 2703.1 ± 1.2 Ma from the lower part of the KVC, indicate that the KVC may better be regarded as part of the Blake River assemblage (2701 to 2697 Ma), rather than the older Tisdale assemblage (2710 to 2703 Ma). Future exploration in the KVC is probably best focused on the along-strike extension of the VMS-hosting interval, and in particular on areas close to the intersections of synvolcanic faults. Mafic and felsic volcaniclastic strata, which can be replaced by VMS mineralization, and felsic coherent facies flows and/or domes, appear to be important potential targets. Chlorite and/or sericite alteration is associated with VMS orebodies at Kam-Kotia, Canadian Jamieson and Genex mines. Although these alteration haloes represent a further exploration guide, they appear to be relatively areally restricted, and may prove difficult to locate given the sparse outcrop in much of the study area. Evidence of west-facing sections in northeast Godfrey and southeast Jamieson townships suggests the possibility of repetition of the VMS-hosting interval across a map-scale syncline in that area.

New U-Pb ages of 2714.6 ± 1.2 and 2712.3 ± 2.8 Ma indicate that the northeast-facing succession in the northern part of the study area (Loveland, Macdiarmid and Thorburn townships) forms part of the Kidd–Munro assemblage (2719 to 2710 Ma). A west-northwest-trending faulted contact is inferred between this older succession and the KVC rocks to the south. The Kidd–Munro assemblage rocks were coeval with the Kidd Volcanic Complex, which hosts the giant Kidd Creek VMS deposit 5 km to the east of the study area. The lower part of the succession, in south-central Loveland Township, consists of high-silica FIIIb rhyolites. These rocks are geochemically similar to ore-associated FIIIb rocks from Kidd Creek, and seem likely to represent the most prospective part of this succession.

Geological Setting of Volcanogenic Massive Sulphide Mineralization in the Kamiskotia Area: Discover Abitibi Initiative

B. Hathway[1], G. Hudak[2] and M.A. Hamilton[3]

Ontario Geological Survey
Open File Report 6155
2005

[1] Mineral Exploration Research Centre, Laurentian University, Sudbury, Ontario
[2] Department of Geology, University of Wisconsin Oshkosh, Oshkosh, Wisconsin
[3] Department of Geology, University of Toronto, Toronto, Ontario

Introduction

The main goal of this Discover Abitibi subproject has been to understand the stratigraphy, volcanic facies, alteration and structural style of the Archean volcanic succession that hosts copper-zinc volcanogenic massive sulphide (VMS) mineralization in the Kamiskotia area (Abitibi greenstone belt, Timmins region: Figure 1). With this aim, regional bedrock mapping (by B. Hathway) covered two contiguous mapping corridors. In the initial, 2003 field season, a southern area, located mainly in Godfrey and Turnbull townships, but also including parts of northernmost Bristol and Carscallen townships, was mapped at 1:10 000 scale (Map P.3544—Revised, back pocket; Hathway and Thurston 2003). During the 2004 field season, a larger, northern area, including parts of Godfrey, Robb, Jamieson, Loveland, Macdiarmid and Thorburn townships, was mapped at 1:20 000 scale (Map P.3556, back pocket; Hathway et al. 2004). Deposit-scale work within the regional mapping area by G. Hudak focused on the Kam Kotia and Canadian Jamieson VMS deposits. An additional deposit-scale study of the Genex deposit is detailed in a separate report by Hocker et al. (2005). To facilitate description of the geology, some of the major faults and lithological units have been given informal names (Figure 2). The prefix "meta" has generally been omitted from descriptions of Archean rock types. UTM co-ordinates are NAD 83. Nomenclature for diamond-drill holes follows that used by the relevant company in respective assessment files.

Previous Regional Geological Work

Finley (1926) produced the first comprehensive geological map of Godfrey, Turnbull, Jamieson and Robb townships (1:47 520 scale), as part of the Kamiskotia Lake gold area. Subsequently, Berry (1946) mapped Robb, Jamieson, Loveland and Macdiarmid townships at 1:31 680 scale (1" to 1/2 mile). Hogg (1955) mapped Godfrey Township at 1:12 000 scale in 1949, and Middleton (1975, 1976) incorporated that work into his later 1:31 680 scale map and report covering Godfrey and Turnbull townships. Middleton also produced 1:31 680 scale maps of Robb and Jamieson townships (1973) and Loveland and Macdiarmid townships (1974), both with accompanying reports. More recently Barrie has authored two reports (1992, 2000), with comprehensive reference lists, and a 1:50 000 scale map (1990) covering the southern part of the current study area (including the past-producing VMS deposits). Recent maps by Vaillancourt et al. (2001) and Hall and Smith (2002a) cover Bristol and Carscallen townships, respectively, at 1:20 000 scale.

Regional Geology

The Archean rocks in the southern part of the study area are assigned to the Kamiskotia Gabbroic Complex (KGC), which includes both mafic and felsic intrusive rocks, and the Kamiskotia Volcanic Complex (KVC), both formally defined by Barrie (1992). The KVC includes all the known VMS deposits in the study area. It overlies and is intruded by the KGC, but the two complexes are thought to be broadly coeval (Barrie 1992). Ayer et al. (2002) included these rocks in the Tisdale assemblage (2710-2703 Ma). However new U-Pb ages on KVC rocks, reported here, indicate that they are slightly younger than the youngest previously known Tisdale assemblage rocks. On this basis, the KVC has been included in the Blake River assemblage (2701-2697 Ma: Ayer et al. 2002) by Ayer et al. (2005). Owing to lack of outcrop, the nature and location of the northern and eastern boundaries of the KVC have been poorly constrained. Barrie (1992) suggested a bounding line parallel to stratigraphy and extending from a point 2 km north of the Kam Kotia Mine to a point 2 km east of the Genex Mine, representing a demarcation between metavolcanic rocks with few geophysical conductors to the west, and metavolcanic-metasedimentary rocks with numerous conductors to the east. A U-Pb age of 2719.5 ± 1.7 Ma from southern Thorburn township (*see* Figure 2), reported by Ayer et al. (2002), suggests that rocks to the north of the KVC form part of the older Kidd–Munro assemblage. This is confirmed by new ages reported here from Loveland and Thorburn townships. The boundary between the two successions appears to trend broadly east-west in the area along the Kamiskotia River in northern Robb Township (*see* Figure 2), where there is a distinct break in the airborne geomagnetic signature. Rocks appear to face to the northeast on each side of this boundary, implying a faulted contact with substantial displacement. It is difficult to trace the boundary farther east, where there is little or no outcrop. Although the geology of northern Jamieson Township between the Kamiskotia and Mattagami rivers is constrained by a large number of overburden holes drilled to bedrock (Cominco Limited 1973, 1974; Map P.3556, back pocket), Kidd–Munro assemblage and KVC rocks cannot be differentiated with the available data, and the boundary shown there on Figure 2 is provisional.

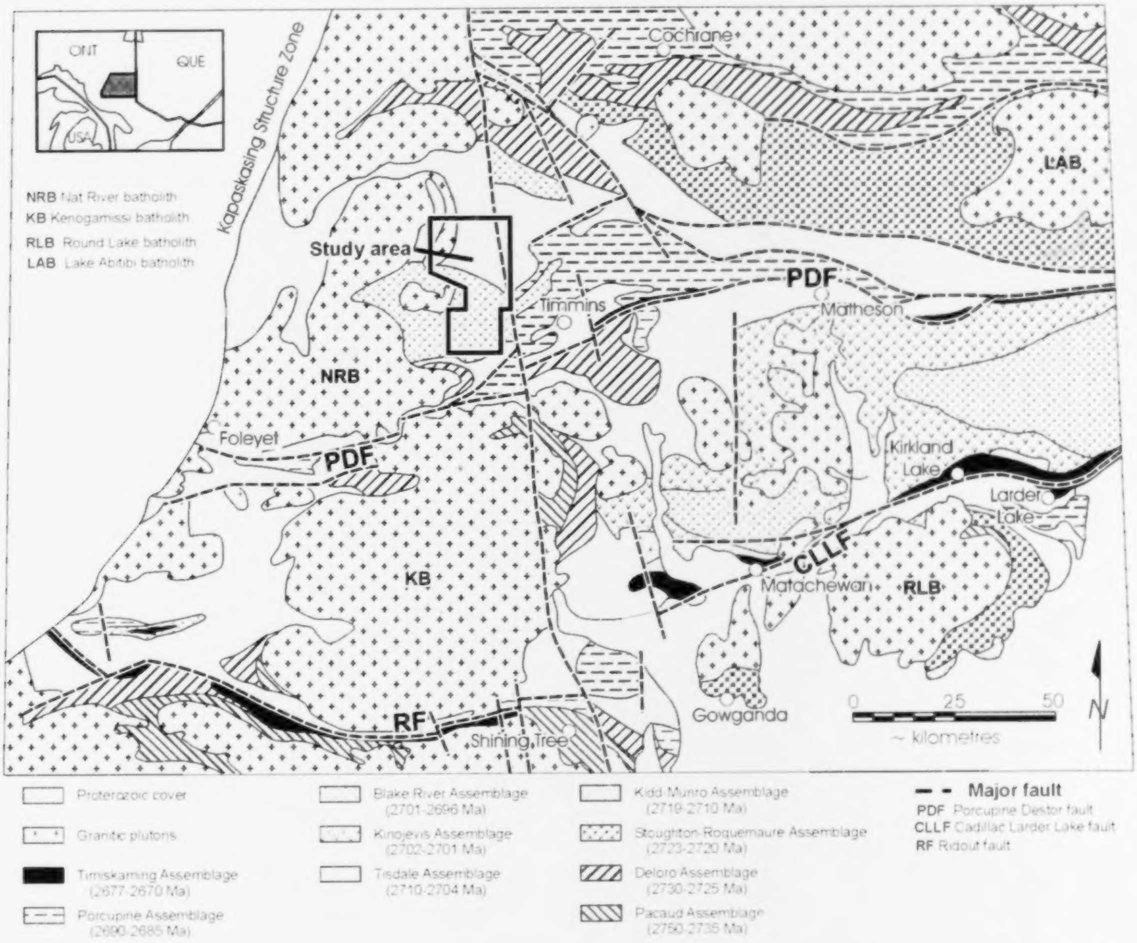
ONT
QUE
USA
Kapaskasing Structure Zone
NRB Nat River batholith
KB Kenogamissi batholith
RLB Round Lake batholith
LAB Lake Abitibi batholith
Cochrane
LAB
Study area
PDF
Timmins
Matheson
NRB
Foleyet
PDF
Kirkland Lake
Larder Lake
CLLF
KB
Matachewan
RLB
RF
Shining Tree
Gowganda
0 25 50
~ kilometres
N
Proterozoic cover
Granitic plutons
Timiskaming Assemblage (2677-2670 Ma)
Porcupine Assemblage (2690-2685 Ma)
Blake River Assemblage (2701-2696 Ma)
Kinojevis Assemblage (2702-2701 Ma)
Tisdale Assemblage (2710-2704 Ma)
Kidd-Munro Assemblage (2719-2710 Ma)
Stoughton-Roquemaure Assemblage (2723-2720 Ma)
Deloro Assemblage (2730-2725 Ma)
Pacaud Assemblage (2750-2735 Ma)
Major fault
PDF Porcupine Destor fault
CLLF Cadillac Larder Lake fault
RF Ridout fault

Figure 1. Generalized geological map of the southern Abitibi greenstone belt in Ontario, with distribution of assemblages and location of the study area. Modified from Ayer et al. (2002).

southern Thorburn township (*see* Figure 2), reported by Ayer et al. (2002), suggests that rocks to the north of the KVC form part of the older Kidd–Munro assemblage. This is confirmed by new ages reported here from Loveland and Thorburn townships. The boundary between the two successions appears to trend broadly east-west in the area along the Kamiskotia River in northern Robb Township (*see* Figure 2), where there is a distinct break in the airborne geomagnetic signature. Rocks appear to face to the northeast on each side of this boundary, implying a faulted contact with substantial displacement. It is difficult to trace the boundary farther east, where there is little or no outcrop. Although the geology of northern Jamieson Township between the Kamiskotia and Mattagami rivers is constrained by a large number of overburden holes drilled to bedrock (Cominco Limited 1973, 1974: Map P.3556, back pocket), Kidd–Munro assemblage and KVC rocks cannot be differentiated with the available data, and the boundary shown there on Figure 2 is provisional.

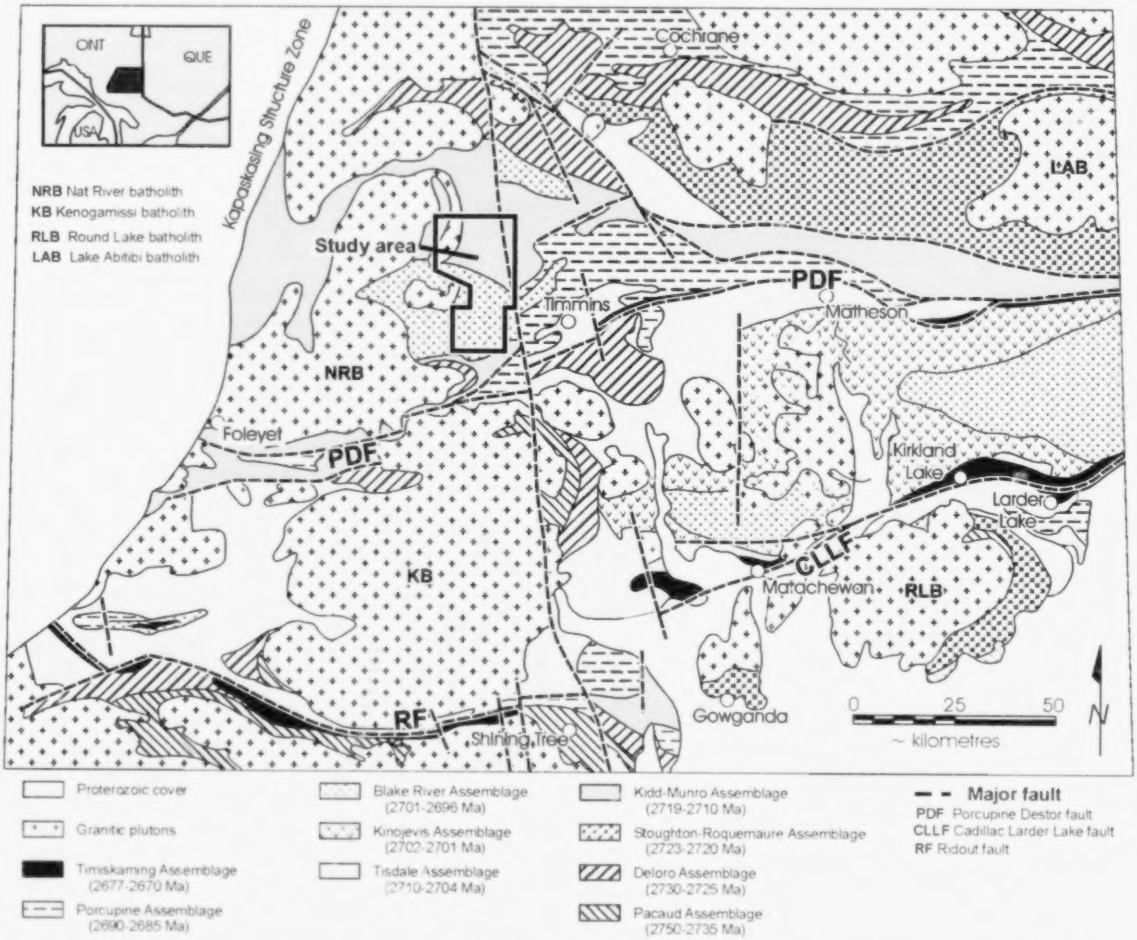
ONT
QUE
USA
Kapuskasing Structure Zone
NRB Nat River batholith
KB Kenogamissi batholith
RLB Round Lake batholith
LAB Lake Abitibi batholith
Study area
Cochrane
LAB
PDF
Matheson
Timmins
NRB
Foleyet
PDF
Kirkland Lake
Larder Lake
CLLF
Matachewan
RLB
KB
RF
Shining Tree
Gowganda
0
25
50
~ kilometres
N
Proterozoic cover
Granitic plutons
Timiskaming Assemblage (2677-2670 Ma)
Porcupine Assemblage (2690-2685 Ma)
Blake River Assemblage (2701-2696 Ma)
Kinojevis Assemblage (2702-2701 Ma)
Tisdale Assemblage (2710-2704 Ma)
Kidd-Munro Assemblage (2719-2710 Ma)
Stoughton-Roquemaure Assemblage (2723-2720 Ma)
Deloro Assemblage (2730-2725 Ma)
Pacaud Assemblage (2750-2735 Ma)
Major fault
PDF Porcupine Destor fault
CLLF Cadillac Larder Lake fault
RF Ridout fault

Figure 1. Generalized geological map of the southern Abitibi greenstone belt in Ontario, with distribution of assemblages and location of the study area. Modified from Ayer et al. (2002).

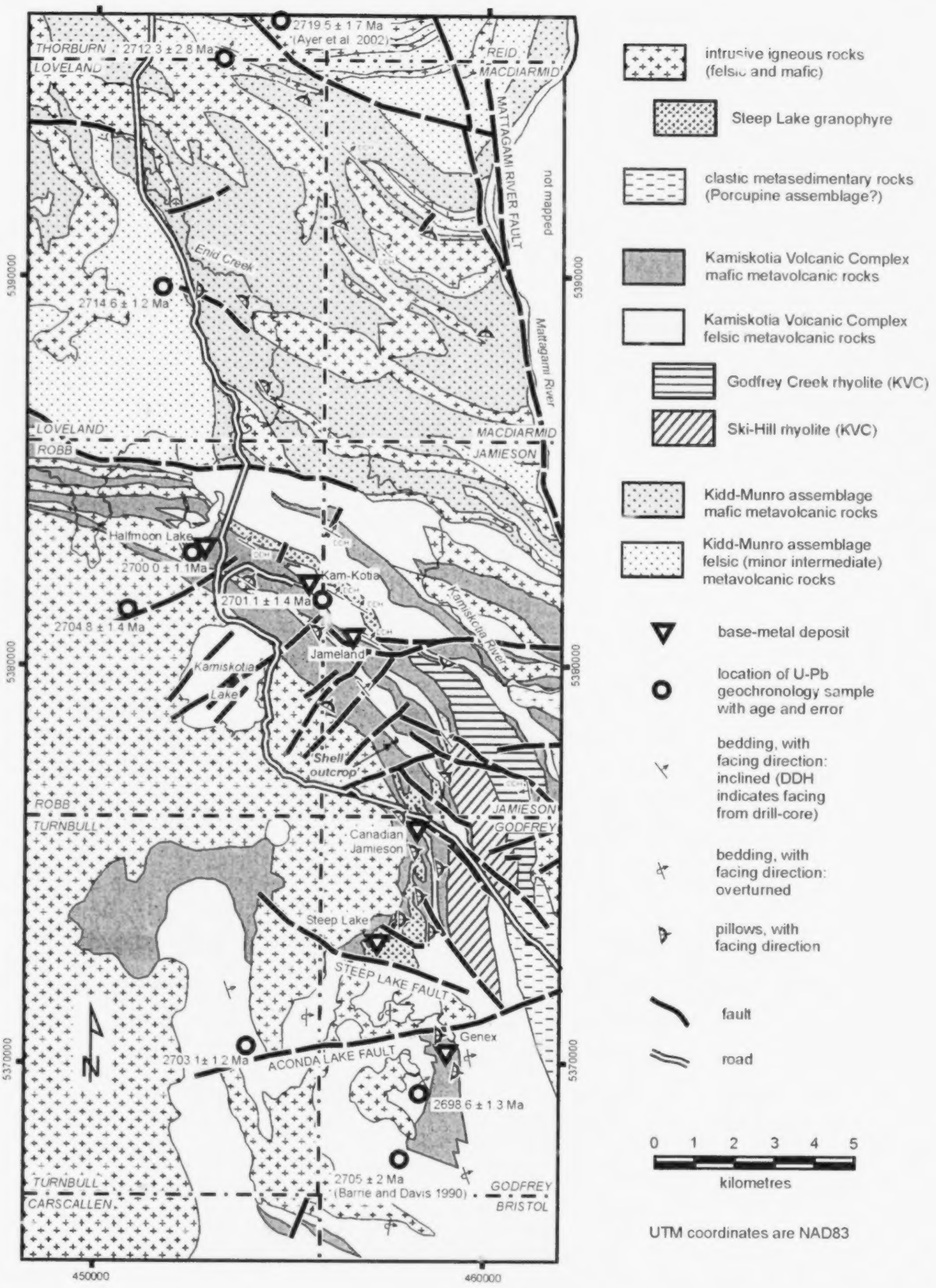
2719.5 ± 1.7 Ma
(Ayer et al. 2002)
THORBURN
2712.3 ± 2.8 Ma
LOVELAND
REID
MACDIARMID
MATTAGAMI RIVER FAULT
not mapped
Enid Creek
2714.6 ± 1.2 Ma
Mattagami River
LOVELAND
MACDIARMID
ROBB
JAMIESON
Halfmoon Lake
2700.0 ± 1.1 Ma
Kam-Kotia
2701.1 ± 1.4 Ma
2704.8 ± 1.4 Ma
Jameland
Kamiskotia River
Kamiskotia Lake
Shell outcrop
ROBB
TURNBULL
JAMIESON
GODFREY
Canadian Jamieson
Steep Lake
STEEP LAKE FAULT
Genex
2703.1 ± 1.2 Ma
ACONDA LAKE FAULT
2698.6 ± 1.3 Ma
N
2705 ± 2 Ma
(Barrie and Davis 1990)
TURNBULL
CARSCALLEN
GODFREY
BRISTOL
5390000
5380000
5370000
450000
460000
intrusive igneous rocks (felsic and mafic)
Steep Lake granophyre
clastic metasedimentary rocks (Porcupine assemblage?)
Kamiskotia Volcanic Complex mafic metavolcanic rocks
Kamiskotia Volcanic Complex felsic metavolcanic rocks
Godfrey Creek rhyolite (KVC)
Ski-Hill rhyolite (KVC)
Kidd-Munro assemblage mafic metavolcanic rocks
Kidd-Munro assemblage felsic (minor intermediate) metavolcanic rocks
base-metal deposit
location of U-Pb geochronology sample with age and error
bedding, with facing direction: inclined (DDH indicates facing from drill-core)
bedding, with facing direction: overturned
pillows, with facing direction
fault
road
0 1 2 3 4 5
kilometres
UTM coordinates are NAD83

Figure 2. Geological sketch map of the Kamiskotia area, with locations of known VMS deposits and samples used for U-Pb geochronology. The boundary between the Kidd–Munro assemblage and the KVC has been extrapolated eastward into Jamieson Township, but its location there is uncertain.

Although the contact is not exposed, bedding orientation suggests there may be an angular unconformity between the KVC and conglomerates exposed in central Godfrey Township, on the eastern margin of the study area (*see* Figure 2). It is suggested that the conglomerates may form part of the Porcupine assemblage (2696 to 2692 Ma: Ayer et al. 2002; *see* "Porcupine Assemblage Sedimentary Rocks" below).

Typically north-northwest-trending diabase dikes of the Paleoproterozoic (circa 2450 Ma, e.g. Barrie 2000) Matachewan swarm are common throughout the area, and are easily recognized as narrow, moderately magnetic linear features on airborne geophysical surveys. Based on their orientation, a small number of northwest-trending diabase dikes in northeast Carscallen (Hall and Smith 2002a, 2002b) and Jamieson and Loveland townships are assigned to the Mesoproterozoic Sudbury swarm (dated at 1238.5 ± 4 Ma: Krogh et al. 1987).

Kidd–Munro Assemblage

FELSIC TO INTERMEDIATE METAVOLCANIC ROCKS

The lowermost part of the Kidd–Munro assemblage in the study area consists of felsic volcanic rocks exposed at scattered locations in northernmost Robb Township and south-central Loveland Township. The extent of these rocks is further delineated by numerous overburden holes drilled to bedrock by Gulf Minerals Canada Ltd. (1979) and more recent diamond drilling (e.g. Mullen 1998). This area has a relatively flat magnetic signature and coincides with a marked gravity low (Ontario Geological Survey 2003a, 2003b). All outcrops appear to consist of massive, commonly flow-banded, medium grey (locally reddish grey) quartz- and feldspar-phyric coherent rhyolite. Phenocrysts in the small exposures along the Kamiskotia River tend to be small (< 1 mm), but the larger outcrops farther north are more coarsely phyric. Aphyric rhyolite and relatively minor felsic volcaniclastic intervals within the rhyolite succession have been intersected by drilling (Mullen 1998). A hole drilled through the eastern contact with overlying mafic pillow lavas (Meunier DDH LDM99-2) encountered 2 m of thin-bedded graphitic argillite and siltstone at the top of the felsic succession. There is no bedding orientation data within the felsic succession west of this north-northwest-trending contact. However, flow-banding in outcrops in the western part of the area shows a consistent northeasterly strike (Map P.3556, back pocket), suggesting a possible discordance with the pillow lavas farther to the northeast.

Felsic rocks stratigraphically higher in the Kidd–Munro assemblage appear to be largely, if not wholly, volcaniclastic. There is no exposure of the felsic lenses lying immediately beneath and within the thick series of broadly concordant mafic-ultramafic intrusions just west of the Mattagami River. Middleton (1974) described rocks sectioned by diamond drilling as felsic pyroclastic units with associated graphitic tuff. The author was able to examine Falconbridge DDH MCD41-03, which penetrated the upper part of the lower lens. Here, the felsic section consists of thick-bedded, redeposited, monomict felsic lapilli tuff (larger lapilli are vesicular and quartz-phyric), with intercalated intervals of thin-bedded tuff, tuffaceous sandstone and graphitic argillite up to 12 m thick. Sharp unit bases, grading, flame structures and load casts (Photo 1A) indicate facing to the northeast. Falconbridge DDH MCD51-03 penetrated a stratigraphically higher felsic lens consisting of amalgamated units of redeposited felsic lapilli tuff up to 2 m thick with stratified sand-grade upper divisions.

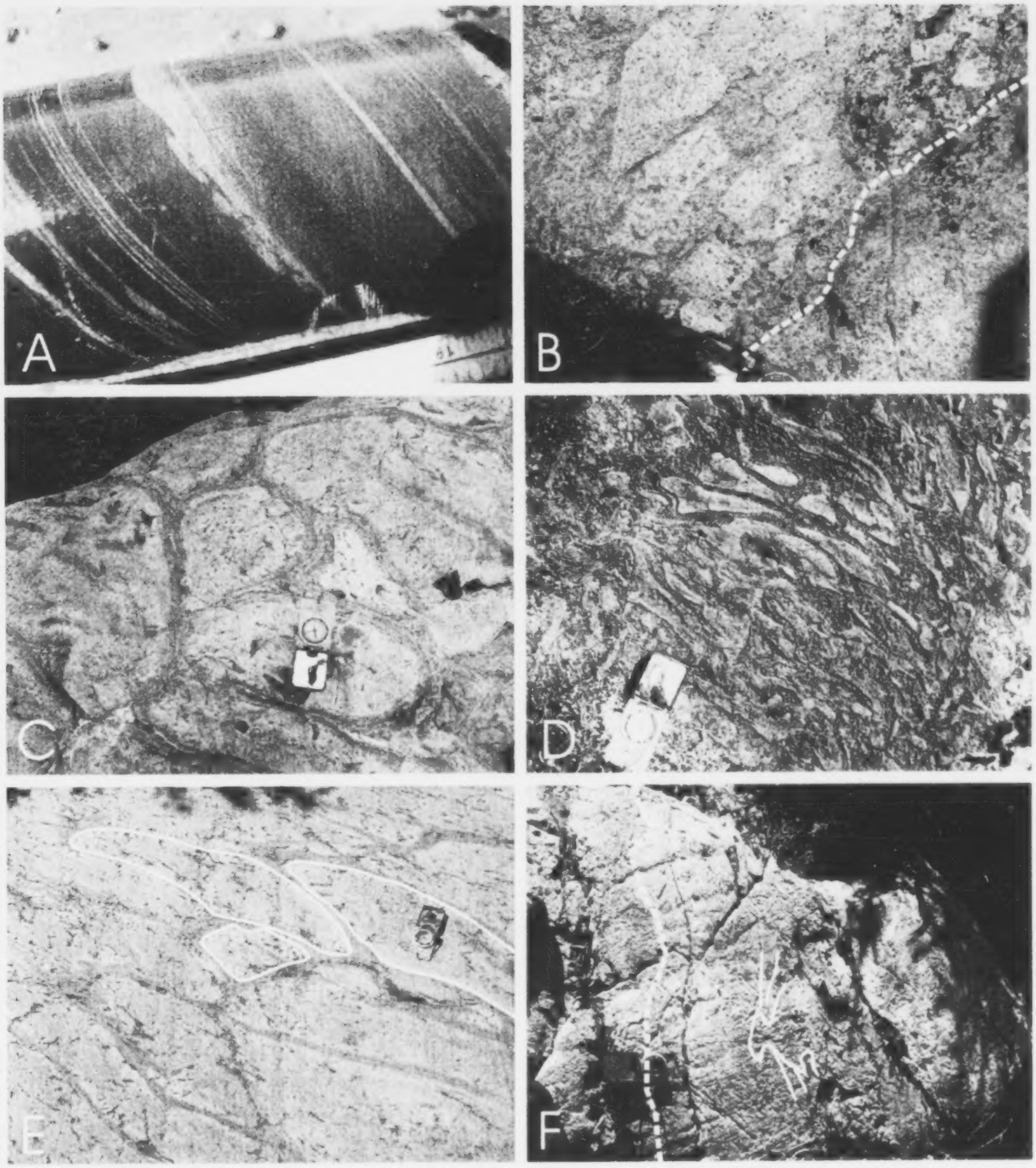

Photo 1. A) Kidd–Munro assemblage, Macdiarmid Township: load-casts at base of volcaniclastic sandstone unit indicate northeast facing (towards right); core 3.5 cm across (Falconbridge DDH MCD41-03, 112.8 m; collar UTME457611, UTMN5390746). B) Kidd–Munro assemblage, Thorburn Township: felsic-intermediate breccia with erosional contact (marked) on flat-stratified, sand- to granule-grade upper division of underlying breccia unit, facing to northeast (04BHA0333: UTM453569, UTME5395774). C) Kidd–Munro assemblage, northeast Loveland Township: mafic pillow lava, facing northeast (towards top-right) (04BHA0340: UTME455396, UTMN5394515). D) Kidd–Munro assemblage, Macdiarmid Township: mafic hyaloclastite breccia (04BHA0315, UTME460202, UTMN5388437). E) KVC, Godfrey Creek, Jamieson Township: mafic pillow lava, facing southwest (towards top-right) (04BHA0086, UTME459050, UTMN5380222). F) KVC, northeast Carscallen Township: top of thin-bedded, 3-4 m thick felsic tuff interval with locally intense soft-sediment deformation (marked) overlain by massive felsic lapilli tuff (sharp base marked), facing northeast (towards left) (03BHA0328: UTME455773, UTMN5366456)

Felsic-intermediate volcaniclastic rocks exposed in northwestern Macdiarmid Township, in the northeast corner of Loveland Township, and on the southern boundary of Thorburn Township, are intercalated with and overlie a thick pillow lava succession to the south. Exposed rocks are largely massive, poorly sorted breccias and tuff breccias. Clasts (up to 1 m across) are angular (rarely subrounded), commonly sparsely vesicular, and either coarsely feldspar-phyric or finely quartz and feldspar-phyric. Secondary feldspar is common in these rocks, with equant, often clustered crystals crossing clast boundaries. Breccias may be polymict, with roughly equal proportions of both clast types, or virtually monomict. Bedding is rarely seen, but the western tip of an outcrop on the Thorburn–Loveland township boundary exposes sharp-based breccia units up to 3.5 m thick with sand- to granule-grade, commonly stratified, upper divisions up to 20 cm thick (facing to the north: Photo 1B). In an outcrop 1.7 km to the east-southeast, massive felsic breccia is overlain by several metres of thin-bedded tuffaceous sandstone (sharp-based, graded units indicate north facing). In drill core, the coarser volcaniclastic facies are seen to be associated with substantial intervals of graphitic argillite (e.g. Falconbridge DDH MCD61-01 and MCD61-02 in westernmost Macdiarmid Township). Spheroidal pyrite nodules are common in the argillites and many sections include thin, intercalated tuffaceous sandstone units. Contorted bedding within the core, and larger-scale reversals of facing provide evidence of soft-sediment deformation.

MAFIC METAVOLCANIC ROCKS

Between the rhyolites in south-central Loveland Township and the felsic volcaniclastic rocks at the northern edge of the study area, the Kidd–Munro assemblage consists largely of massive to pillowed (Photo 1C), variably silicified, mafic volcanic rocks. These rocks are generally sparsely plagioclase-phyric (to 1 mm) with a groundmass of fine-grained chlorite, amphibole and quartz. Quartz- and chlorite-filled amygdules, clots of actinolite up to 1 cm across, and disseminated pyrrhotite grains are common. Patches and veins of epidote are locally abundant. Pillows are commonly large (up to 2 m) and mid-grey weathered, with brownish selvages. Thick intervals of hyaloclastite breccia are found at several locations, notably in the large outcrop in Macdiarmid Township 0.9 km west of the Mattagami River (Photo 1D). Pillow facing directions are to the east-northeast in southeast Loveland Township, swinging to face northeast up-section (*see* Photo 1C).

FELSIC INTRUSIVE ROCKS IN THE KIDD–MUNRO ASSEMBLAGE

Pink to white, typically medium-grained (locally coarse) granitoid rocks (generally consisting of plagioclase, potassium feldspar and quartz) crop out sparsely in western and northern Loveland Township, and have been proven to be present, by overburden drilling, in southeast Thorburn Township (Gulf Minerals Canada Ltd. 1979). These rocks were described as granodiorite and quartz monzonite by Middleton (1974). Although contacts were not seen, xenoliths of mafic volcanic wall-rock are present in some outcrops. These intrusive rocks are likely to be related to granitoid intrusions described by Barrie (1992) farther south (Cote Township and Groundhog River tonalites, with U-Pb zircon ages of 2694 ± 4 Ma and 2696 ± 1.5 Ma, respectively), which are younger than, and not related to, the KGC or KVC. Areas of quartz-feldspar porphyry in eastern Loveland and western Macdiarmid townships seem to represent a southeastward, along-strike continuation of the granitoid rocks in northeast Loveland Township.

MAFIC TO ULTRAMAFIC INTRUSIVE ROCKS IN THE KIDD–MUNRO ASSEMBLAGE

The Kidd–Munro assemblage volcanic rocks are intruded by numerous, broadly concordant, sill-like mafic intrusions. Most of the larger bodies are medium to coarse grained and gabbroic, consisting of amphibole and/or chlorite after pyroxene; plagioclase; iron-titanium oxides (commonly replaced by leucoxene); and locally quartz (e.g. in Loveland Township just west of Enid Creek). Some outcrops include areas of altered pyroxenite (e.g. in the northwest corner of Macdiarmid Township). Quartz-epidote veins are common. Minor, finer grained mafic intrusions (not shown on the map) are also common, for example in the rhyolite in Loveland Township. Limited outcrops of the large intrusion in central-western Macdiarmid Township, which coincides with an intense magnetic anomaly, are of gabbro. However, drilling data shows it to be a composite, layered, ultramafic to mafic intrusion. Falconbridge DDH MCD41-02, for example, penetrated serpentinized dunite (consisting of altered, fine- to medium-grained olivine, with minor plagioclase and magnetite, ± pyroxene) showing gradational contacts with gabbro-gabbronorite (plagioclase and chlorite-altered pyroxene, ± altered olivine). Fibrous chrysotile/lizardite (asbestos) veins may constitute up to 6% of the rock in this intrusion (Middleton 1974). Although there is no geochronological data for these rocks in the study area, numerous mafic to ultramafic intrusions cutting Kidd–Munro assemblage rocks elsewhere in the region are known to be of Tisdale assemblage age (2710 to 2703 Ma; J. Ayer, OGS, personal communication, 2005).

Kamiskotia Volcanic Complex

Facing directions from pillow packing and sharp-based, graded volcaniclastic units in KVC rocks to the south of the Steep Lake fault (southwestern Godfrey, eastern Turnbull, northern Bristol and northeast Carscallen townships) appear to be uniformly to the east or northeast (Photos 1F, 2A, 2B: earlier assertions of westward facing (cf. Hathway and Thurston 2003) have been revised). These rocks generally dip steeply to the west (dips generally ≥ 75°). The east-facing succession continues north into northern Godfrey and southern Jamieson townships, and swings to strike northwestward in northern Robb Township. In these areas the volcanic succession is underlain by intrusive rocks of the KGC to the west and south along the margin of the study area. Observed facing directions in these areas are uniformly to the east or northeast, except in the area of Jamieson Township close to where Godfrey Creek enters the Kamiskotia River (Map P.3556, back pocket). Here, at an outcrop on Godfrey Creek, pillow packing indicates facing to the southwest (Photo 1E). Middleton (1973) recorded similar facing directions for pillows at an outcrop 700 m to the northeast, although reliable facing was not seen there by this author. Westward facing was also noted for graded felsic tuff units in Falconbridge DDH J14-01 (Falconbridge Jamieson Report 52, 1988, unpublished), drilled 4 km to the southeast, and apparently along strike from the Godfrey Creek outcrops (drill core not available to this author, but facing directions from other Falconbridge DDH logs have proved reliable). The reversal in facing direction suggests the presence of a synclinal axis to the west of the Godfrey Creek pillow lavas. During 2004 fieldwork (Hathway et al. 2004), it was thought that, as suggested by Middleton (1973, p.36), a fold axis might lie within the thick felsic volcanic unit that forms Mount Jamieson (Kamiskotia Ski Hill), with repetition of a basal crystal-rich unit on each limb of the fold. However, this now seems less likely (see discussion below) and a syncline axis has not been shown on the map.

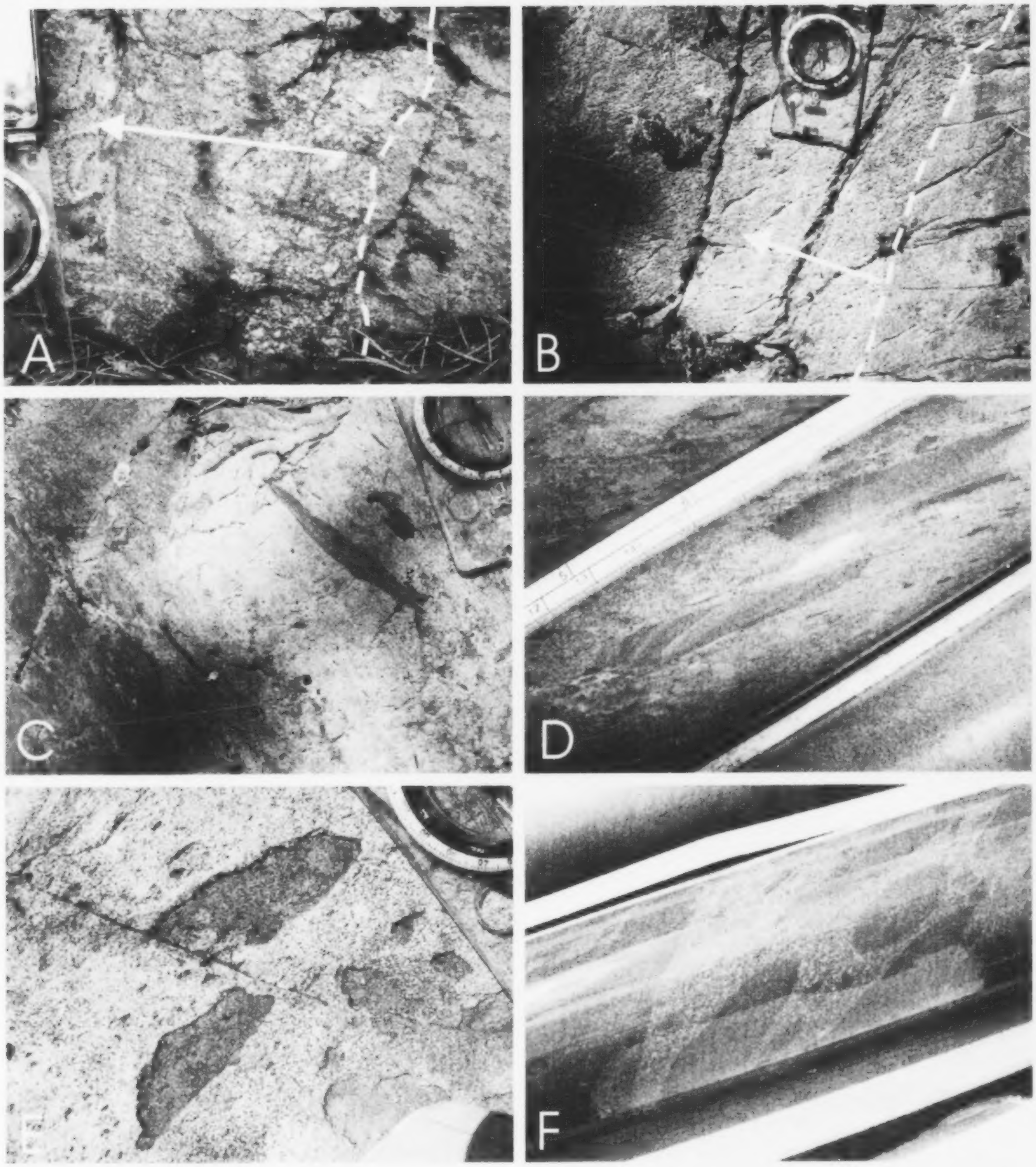

Photo 2. A) KVC, Turnbull Township: normal-graded (arrow) felsic lapilli tuff unit, facing east (03BHA0416; UTME453755, UTMN5371966). B) KVC, Bristol Township: sharp-based, normal-graded (arrow) felsic lapilli tuff-tuff unit, facing east (03BHA0374; UTME457698, UTMN5365882). C) KVC, Godfrey Township: dark green inclusions in vesicular, coherent mid-grey Ski-Hill rhyolite (04BHA0222; UTME460796, UTMN5375105). D) KVC, Jamieson Township: laminated siltstone-mudstone intraclasts in a granule-grade matrix consisting largely of felsic lithic clasts (04BHA0459; Falconbridge DDH J51-02, 82.4 m; collar UTME456185, UTMN5383740). E) Steep Lake granophyre, Godfrey Township (700 m southeast of Steep Lake): finely spherulitic felsic intrusive rock with darker, chlorite-rich inclusions (04BHA0439; UTME458473, UTMN5372758). F) Steep Lake granophyre, Robb Township: inclusion-rich facies as in E; core 3.5 cm across (04BHA0460; Falconbridge DDH R56-29, 448 m; collar UTME455779, UTMN5382669).

FELSIC METAVOLCANIC ROCKS

South of the Steep Lake Fault

KVC rocks in this area are largely felsic. For the lowermost part of the succession, the stratigraphy is most clear in eastern Turnbull Township. Here, a lower western unit consists of coarsely quartz- and feldspar-phyric coherent rhyolite, and associated tuff-breccia and lapilli tuff in which matrix and clasts are characteristically hard to distinguish. This is overlain by a unit consisting of finely quartz- and feldspar-phyric to aphyric, finely flow-banded rhyolite and associated felsic lapilli tuff. The latter is particularly easy to recognize, with very distinct, pale, often texturally diverse, unvesiculated lithic lapilli and more ductile, dark, originally glassy fragments in a dark, sericite-rich matrix. The middle part of the felsic succession is most consistently exposed around and to the west of Keeley Lake, to the north of the Aconda Lake fault (ALF). Here a 3 km thick succession consists of intervals of massive quartz- and feldspar-phyric coherent rhyolite from 100 to 700 m thick, alternating with similar thicknesses of compositionally similar, highly sericitized, commonly bedded lapilli tuff. South of the ALF, the basaltic pillow lavas in the Genex Mine area are underlain by at least 600 m of generally fine felsic lapilli tuff (clasts typically <1 cm), with minor tuff breccia but relatively little coherent rhyolite. A well-exposed felsic volcaniclastic interval (mainly lapilli tuff) is present within the Genex pillow lava pile to the east of the ore bodies (*see* Hocker et al. 2005). There are a number of small outcrops of felsic lapilli tuff to the east of (stratigraphically above) the Genex pillow lavas; sharp-based, graded units in the exposures due east of the Genex Mine indicate eastward facing.

Outcrops to the east and west of Godfrey Lake consist of quartz- and feldpar-phyric rhyolite. Flow banding is rare here and the phenocrysts are locally large (to 2 mm) and abundant. Lapilli tuff exposed in scattered outcrops to the southwest of the rhyolite resembles that associated with the aphyric rhyolites in eastern Turnbull Township. Massive lapilli tuffs with abundant quartz and feldspar crystals are well exposed 1.5 km to the east of Godfrey Lake. A 40 cm thick interval within this succession consists of sharp-based, graded, tuffaceous sandstone units with mudstone tops, indicating tops to the east. The outcrops in northern Bristol Township, 1 km south of Godfrey Lake (south of the intrusive body), include some coherent rhyolite, but appear to consist largely of crystal-rich (quartz and feldspar) lapilli tuff. This is generally massive or very thickly bedded, but on the western edge of the outcrop cluster, 20 cm thick, sharp-based, normal-graded lapilli tuff units with fine tuff tops indicate eastward facing (*see* Photo 2B). A survey undertaken for Hollinger Mines Ltd. (Alexander et al. 1971: not known to this author at the time of fieldwork) shows further felsic volcanic outcrops (mapped as rhyolite) to the southwest of this area.

Steep Lake Fault to Halfmoon Lake

Just north of the Steep Lake fault, there are two lenses of rhyolite and felsic lapilli tuff to the west of Steep Lake. Up-section, to the southeast of Steep Lake, the road to the Genex Mine crosses a large area of strongly foliated quartz- and feldspar-phyric coherent rhyolite and lapilli tuff, with minor intercalated basalt pillow lava. These felsic rocks appear to be continuous with an interval of felsic lapilli tuff that extends north within a mainly mafic volcanic succession to the felsic volcanic intervals in the area of the Canadian Jamieson Mine (*see* "Volcanogenic Massive Sulphide Deposits"). Intervals of rhyolite, rhyolite breccia and lapilli tuff to the northeast of the mine, across the Kamiskotia Highway, seem to be a further northward continuation of this stratigraphic interval, offset to the east across the Kamiskotia Highway fault. The felsic rocks continue along strike to the northwest, through the thick-bedded rhyolite breccia and lapilli tuff exposed in the large, stripped "Shell outcrop" (*see* Figure 2: E457720, N5378300;

described in detail by Comba et al. (1986)) to a cluster of outcrops exposing northeast-facing felsic lapilli tuffs and tuffs to the south of the Little Kamiskotia River, 2.5 km east of the Kamiskotia Highway. Although there is no exposure of felsic rocks in the intervening area, drill-core intersections suggest that this felsic interval is continuous, across a series of further eastward fault offsets, with the rhyolites and felsic volcaniclastic rocks at Kam Kotia Mine (*see* "Volcanogenic Massive Sulphide Deposits"). Although there is no exposure of KVC rocks west of Kam Kotia Mine, diamond drilling indicates that from the mine west to Halfmoon Lake the succession at this level is almost completely mafic. Closely spaced drilling shows that the area around and beneath the southern part of Halfmoon Lake is underlain by a series of stacked lenses of coherent rhyolite (commonly strongly foliated) with subordinate lapilli tuff. Drill logs in an unpublished report by Ore Systems Consulting (2000) show south-facing indicators in felsic volcaniclastic rocks south of the lake. Some of this core was seen by the author, who found evidence for facing inconclusive, and given the firm evidence for northeast-facing at Kam Kotia Mine (see below), it seems likely that the succession here is similarly oriented. West of the Halfmoon Lake area, felsic rocks form a series of relatively thin lenses, commonly enclosed by gabbro.

Ski-Hill Rhyolite

The felsic volcanic interval extending south from Canadian Jamieson Mine is overlain by mafic volcanic rocks, including east-facing pillow lavas. Stratigraphically above these to the east is a thick, lithologically distinct felsic volcanic unit which extends north, offset to the east across the Kamiskotia Highway fault, to a large outcrop 2.5 km north-northwest of Mount Jamieson. This unit, here informally named the Ski-Hill rhyolite, is typically well-exposed, forming Mount Jamieson and the high ground to north and south. Its northern and southern limits appear to be fault-bounded. During fieldwork it was thought that quartz and feldspar crystal-rich intervals along the western and eastern margin of the Ski-Hill unit might represent the same horizon repeated across a syncline. However, thin-section study indicates that the basal, western interval (up to 90 m thick) is a coarse-grained quartz-feldspar intrusive rock (*see* "Steep Lake Granophyre" below), whereas the eastern interval (up to 180 m thick) is a porphyritic rhyolite. The latter has a groundmass that may be spherulitic, but locally shows well-preserved perlitic cracks, and grades westward into the typically aphyric rhyolite that forms the main part of the Ski-Hill rhyolite (approximately 900 m thick). This rhyolite contains generally sparse, but locally abundant, darker, fine-grained chlorite-rich inclusions (usually <1 cm, but locally with long axes up to 20 cm: Photo 2C). The inclusions have tabular to irregular shapes and may show a wide range of orientations within a given outcrop. Towards its eastern edge, the rhyolite contains sparse quartz-filled amygdules, and locally shows a steeply dipping to vertical, generally north-trending fabric defined by less competent, sericitic zones about 30 cm thick. This "layering" is best seen at the top of the ridge 600 m north of the Kamiskotia Highway fault (E460796, N5375105), where the darker green, sericitic zones show a regular 1.5 m scale spacing within massive, more competent, mid-grey, sparsely amygdaloidal rhyolite. Dark green inclusions occur throughout the section, and here many (but not all) tend to lie subparallel to the darker zones. The "layering" is tentatively interpreted as a flow-related shear fabric akin to flow banding, but the absence of typical, fine-scale flow banding, and the dark inclusions distinguish the Ski-Hill unit from other Kamiskotia rhyolites, and during fieldwork it was thought the unit might be volcaniclastic (Hathway et al. 2004).

Godfrey Creek Rhyolite

This thick unit is exposed in scattered outcrops immediately east of the Ski-Hill rhyolite to the north of the Kamiskotia Highway fault, and more extensively farther north, with outcrop extending to the north of a well-exposed section in Godfrey Creek. It consists of massive, commonly flow-banded, typically finely phyric to aphyric, coherent rhyolite, with subordinate rhyolite breccia and minor lapilli tuff. The dark inclusions seen in the Ski-Hill rhyolite are absent. An outcrop just north of the Kamiskotia Highway fault (E460940, N5374487) exposes a sharp, unfaulted contact between the massive, porphyritic eastern interval of the Ski-Hill rhyolite and rhyolite breccia of the Godfrey Creek unit, here passing eastward to flow-banded rhyolite. The southwest facing pillows in Godfrey Creek lie to the northeast (immediately downstream) of this rhyolitic unit. Rhyolitic breccias close to the unexposed contact are intensely sheared. The mafic volcanics, accompanied by sedimentary rocks farther south, appear to form a discontinuous interval on the eastern flank of the rhyolite. Rhyolite and felsic lapilli tuff similar to the Godfrey Creek unit are exposed beyond this to the northeast, in the area towards the Kamiskotia River.

Northeast of Kam Kotia Mine

Sparse diamond drilling and rare outcrops in the area to the north of the Little Kamiskotia River, stratigraphically above the Kam Kotia VMS deposit, indicate the presence of a thick succession of aphyric coherent rhyolite flows and associated rhyolite breccia. This includes subordinate mafic volcanic rocks and, about 1.5 km north of Kam Kotia, a northeast-facing sedimentary interval. Rhyolite in drill core to the east of, and stratigraphically above, the sedimentary interval (Falconbridge DDH J52-01, J52-02, J52-03) locally shows well developed flow-banding. Although these rocks lie broadly along strike from the Ski-Hill and Godfrey Creek rhyolites, it is difficult to correlate between the two areas with the available data.

MAFIC METAVOLCANIC ROCKS

In the southernmost part of the study area, mafic volcanic rocks form a west-northwest-trending lens in northeast Carscallen and northwest Bristol townships. These rocks consist of aphyric to sparsely plagioclase phyric (phenocrysts to 1 mm) massive and pillowed flows, with minor amoeboid pillow breccia. Pillows are typically large (to 3 m) and pinkish grey, with blue-green selvages (Hall and Smith 2002b). Pillow facing directions are inconclusive but suggest tops broadly to the east (at a high angle to the strike of the lens) at two outcrops.

East-facing, typically aphyric, pillowed and massive basaltic lavas in the Genex Mine area, and syndepositional mafic sills in the underlying felsic volcaniclastic succession are described in detail by Hocker et al. (2005). Although it is difficult to make firm correlations across the Aconda Lake and Steep Lake faults to the north, basaltic lavas in the Steep Lake area, and extending north to Canadian Jamieson Mine, seem likely to be broadly stratigraphically equivalent to the Genex basalts (*see* Figure 2). To the southeast of Canadian Jamieson Mine and across the Kamiskotia Highway fault to the northeast, east-facing pillows at the top of this succession immediately underlie the Ski-Hill rhyolite. These basalts appear to extend north, offset by a series of faults, to form the thick, northeast-facing succession of pillowed and massive basalt that underlies the Kam Kotia and Jameland deposits. Subordinate, intercalated felsic volcanic and volcaniclastic rocks occur within the basaltic succession from Genex north to Kam Kotia. Pillows in this area are variably flattened in the plane of the S_2 or S_1/S_2 foliation (see below), which is typically at a high angle to the trend of bedding south of the Canadian Jamieson Mine.

A thick succession of generally aphyric, variably vesicular pillow lavas with associated hyaloclastite and pillow breccia, stratigraphically above the Kam Kotia deposit (1.2 km northeast of the mine, immediately above the northeast-facing sedimentary interval) has been intersected by a number of drill holes (e.g. Falconbridge J51-01, J51-07, J51-07). The southwest-facing basaltic lavas exposed in Godfrey Creek (*see* Photo 1E) consist of a number of approximately 5 m thick flow units, with massive bases and pillowed upper parts. Pillows are flattened in the plane of the S_1/S_2 foliation, here trending subparallel to bedding.

The original mineralogy of the KVC mafic metavolcanic rocks has been almost completely replaced by greenschist-facies alteration assemblages (chlorite, amphibole, carbonate, albite, epidote, quartz and opaque minerals: Hart 1984). Feldspar phenocrysts are generally turbid and albitized.

CLASTIC SEDIMENTARY ROCKS

The sedimentary succession intersected by a series of drill holes northeast of the Kam Kotia Mine (Falconbridge DDH R56-02, J51-02, J51-03, J51-05, J41-13) is up to 150 to 200 m thick and extends for at least 2.3 km along strike. It is underlain and overlain by massive coherent rhyolite and felsic lapilli tuff. The interval consists largely of thin- to medium-bedded, mid-grey tuffaceous sandstone and thick (up to at least 1.3 m), poorly sorted granule- to pebble-grade beds consisting mainly of texturally varied, angular to subrounded felsic volcanic lithic clasts. Sandstone beds commonly have upper divisions of black graphitic mudstone. The thicker, coarser grained beds contain abundant intraclasts of black mudstone and/or grey sandstone (commonly laminated: Photo 2D) and variable amounts of pyrrhotite fragments. Sharp-based, normal-graded units and flame structures indicate facing to the northeast. The sedimentary interval sectioned by several drill holes (e.g. Falconbridge DDH J14-01, J14-02) in southern Jamieson Township to the east of the Godfrey Creek rhyolite is described as graphitic argillite with intercalated felsic tuff and lapilli tuff. It lies broadly along strike from the sedimentary rocks northeast of Kam Kotia and, if the westward facing reported from Falconbridge DDH J14-01 is discounted, could represent a southeastward extension of that interval. These strata occur within, and form part of, the KVC.

DEPOSITIONAL DEPTHS FOR THE KAMISKOTIA VOLCANIC COMPLEX

Reposited volcaniclastic intervals throughout the KVC all appear to have been deposited by sediment gravity flows, and there appears to be no evidence for deposition above storm wave base. Comba et al. (1986) cited evidence for local subaerial deposition in the upper part of the KVC, including fiamme (interpreted as evidence for welding) in a crystal-rich felsic lapilli tuff 3.3 km south of Genex Mine (E459595, N5367140), and in a 40 m thick felsic lapilli tuff interval exposed in the "Shell outcrop", 1.6 km northwest of Canadian Jamieson Mine. Welding is typically a feature of subaerial pyroclastic flows, but is known to occur in shallow-water submarine facies (e.g. Reedman et al. 1987). However, fiamme in themselves are not firm evidence for welding: this must rest on the *association* between fiamme and evidence for high-temperature emplacement (e.g. pseudomorphed perlitic cracks, rheomorphic folding: Branney and Sparks 1990). Where this association is absent, as in the KVC volcaniclastic units, it is likely that flattening and alteration of glassy juvenile fragments to produce fiamme may have taken place during early burial compaction (Branney and Sparks 1990). Additionally, Comba et al. (1986) interpreted a 20 cm thick flat-laminated felsic tuff interval in the "Shell outcrop" as a base-surge deposit. However, the unit lacks key features characteristic of such deposits (unidirectional bedforms, low-angle truncations, accretionary lapilli: e.g. Cas and Wright 1987), and sediment-gravity flow deposition seems more likely.

Kamiskotia Gabbroic Complex (KGC)

Barrie (1992) divided the KGC into four zones, of which only the uppermost two are found in the present study area. Gabbro-norite and hornblende gabbro of the "Upper Zone" are exposed to the northeast and southwest of Kamiskotia Lake and in a small area to the northeast of Steep Lake. Northeast facing directions were determined by Barrie (1992) in Upper Zone cumulates to the south and west of

Kamiskotia Lake. Remaining KGC rocks are generally of felsic to intermediate composition and were included in the "granophyre zone", lying above and along strike with the Upper Zone, by Barrie (1992). To the south of the Steep Lake fault, granophyre zone rocks form numerous sills and broadly concordant sill-like intrusive bodies which are typically fine- to medium-grained and equigranular (microdiorite of Middleton (1976)), but may be plagioclase-phyric (porphyrite or intrusive andesite of Middleton (1976)). Quartz- and feldspar-phyric phases are rare, but do occur (e.g. 100 m west of Keeley Lake). There are also areas of microgabbro in eastern Turnbull Township and to the north and west (Hocker et al. 2005) of the Genex Mine. North of the Steep Lake fault and southeast of Kamiskotia Lake, granophyric rocks described as quartz porphyry and quartz diorite (Hogg 1955; Middleton 1976) occupy a large area along and within the eastern margin of the Upper Zone gabbro. In Robb Township and western Jamieson Township gabbroic sills are common in the KVC up to and above the level of the Kam Kotia and Jameland VMS deposits.

STEEP LAKE GRANOPHYRE

The felsic intrusive rocks exposed to the south and east of Steep Lake, which lie within the east-facing KVC succession, were described as spherulitic granophyre by Hogg (1955), and spherulitic microdiorite by Middleton (1976). Contacts with the KVC volcanic rocks are not exposed. These rocks are feldspar-phyric to aphyric, with a groundmass dominated by crudely spheroidal structures, up to 2 mm across, consisting either of intergrown quartz and feldspar (also seen in the granophyric rocks to the west: Hogg 1955) or of fine radiating feldspar crystals. The groundmass also includes abundant chlorite, calcite, and mosaic quartz. Darker, chlorite-rich inclusions are common (Photo 2E), and locally make up the greater part of the rock (Hogg 1955, p.25). These are generally fine-grained and strongly altered to chlorite, but some outcrops include coarser grained gabbroic inclusions. Coarse-grained, quartz-feldspar intrusive phases (granitic quartz porphyry of Hogg (1955)) form discrete intervals within the spherulitic granophyre to the south of Steep Lake, and also occur locally as rounded inclusions. Texturally similar, equigranular quartz-feldspar intrusive rocks also occur farther up-section, along the basal contact of the Ski-Hill rhyolite. Intermittent outcrops indicate that the Steep Lake granophyre extends north to the Canadian Jamieson Mine, where a finely spherulitic felsic intrusive interval, lithologically similar to the granophyre in the main part of the KGC to the west, intrudes the footwall basalts 400 m southwest of the VMS deposits. The distinctive dark inclusions die out 1.5 km south of the mine.

Spherulitic (locally granophyric) felsic intrusive rocks rich in dark inclusions crop out and occur in drill core across the Kamiskotia Highway fault 1 km north of Canadian Jamieson Mine. These rocks appear to represent a further northward continuation of the Steep Lake granophyre. Another series of outcrops 500 m to the east appears to represent the same interval, offset across another fault. These rocks commonly show intense chlorite-carbonate alteration and include coarse-grained quartz-feldspar inclusions up to 3 m across (e.g. outcrop at E458864, N5376867). Similar rocks are exposed 1 km farther north (outcrop at E459098, N5378396) and in a nearby drill hole (Falconbridge DDH J22-02: rocks described as "mafic volcanics with granitic intrusions").

Farther to the northeast, similar felsic intrusive rocks are found in numerous drill holes beginning 600 m east of the Jameland Mine (Falconbridge DDH J41-12) and extending northeast along strike, through and beyond the Kam Kotia hanging wall, for 4.2 km (to Falconbridge DDH R55-04: E454138, N5383648). The inclusion-rich facies is exposed in a number of small outcrops immediately north of the Kam Kotia open pit. Drill core from Falconbridge DDH R55-04 and R56-29 (collar 300 m north of the Kam Kotia open pit: E455782, N5382670: Photo 2F) was examined in detail by the author, and the unit is easily identifiable in log descriptions for other holes (the inclusion-rich facies is generally described as a spherulitic felsic volcanic rock or lapilli tuff). The rock is typically mid-grey, consisting of small (<1 mm), poorly defined spheroidal structures set in a matrix of quartz, calcite and chlorite, but darker, grey-green, chlorite-rich phases are also common. The dark grey-brown inclusions (*see* Photo 2F) occur in discrete intervals and have shapes ranging from rounded and equant, to tabular (long axes generally <10 cm). Their margins may be irregular and can be quite diffuse (they are not chilled). They consist of finely divided chlorite, quartz and opaque minerals and have no apparent internal structure. Rare gabbroic inclusions and minor intervals of coarse-grained, quartz-feldspar intrusive rock are also present. Barrie and Pattison (1999, e.g. Figure 6) interpreted the inclusion-rich rocks as mixed-magma intermediate lapilli ash tuffs; however, the unit is lithologically identical to finer-grained phases of the granophyre east of Steep Lake (compare Photos 2E and F) and north of Canadian Jamieson Mine, and probably represents part of the same intrusive body.

Porcupine Assemblage Sedimentary Rocks

Poorly sorted, clast- to matrix-supported conglomerates are exposed in a cluster of outcrops in northern Godfrey Township just west of Twentythree Mile Creek (northeast of the Kamiskotia Highway). Clasts of felsic volcanic rock, felsic tuff, volcaniclastic sandstone and/or dark grey silty mudstone predominate, but basaltic-intermediate volcanic clasts and rare massive sulphide fragments also occur. Clasts are generally subrounded to angular and may be up to 30 cm across. Minor, finer grained (granule to sand grade) intervals up to 30 cm thick define bedding, which dips relatively gently (25°) to the southeast, implying an angular discordance with the steeply dipping, north-striking KVC rocks to the north and west. Together with the polymict lithic content, this suggests that these rocks may form part of a younger sedimentary succession resting unconformably on, and probably derived from, the KVC. It seems likely that they may form part of the wholly sedimentary Porcupine assemblage (2696 to 2692 Ma), which unconformably overlies the Kidd–Munro and Tisdale assemblages over a wide area farther to the east (*see* Figure 1; Ayer et al. 2002).

Geochemistry

A total of 156 samples were analysed for major oxides and selected trace elements in order to characterize the volcanic rock units of the mapped area. Crushed samples were processed using an agate mill. Major and minor element values were determined by wavelength-dispersive X-ray fluorescence spectrometry (WD-XRFS) of fused glass disks. Loss-on-ignition (LOI) was determined gravimetrically. Trace element analyses were performed with inductively coupled plasma emission mass spectrometry (ICP-MS) using closed beaker digest solution preparation. Additionally, Nb, Y, Zr and Cr concentrations were determined through WD-XRFS of pressed powder pellets, and Be, Cr, Co, Cu, Li, Ni, Sc, Sr, V,W and Zn were determined by inductively coupled plasma atomic emission spectrometry (ICP-AES). For samples collected in 2003 (03 prefix), all work was completed at Geoscience Laboratories, Sudbury. For samples collected in 2004 (04 prefix), crushing and XRF analysis were carried out by Activation Laboratories Ltd. (www.actlabs.com), and ICP analysis at Geoscience Laboratories. The results of all analyses are provided in Appendix 1. Data are cited and plotted anhydrous. Accuracy and precision data are given by Macdonald et al. (2005).

Plots of MgO vs SiO_2 for volcanic rocks from the Kidd–Munro assemblage and KVC are shown in Figure 3. Both successions are bimodal: the KVC most markedly so, with a compositional gap between 56 and 72 wt% SiO_2. In the Blake River Group in the Rouyn-Noranda district, all rocks display a compositional gap between 64 and 71% SiO_2 (Gélinas et al. 1977).

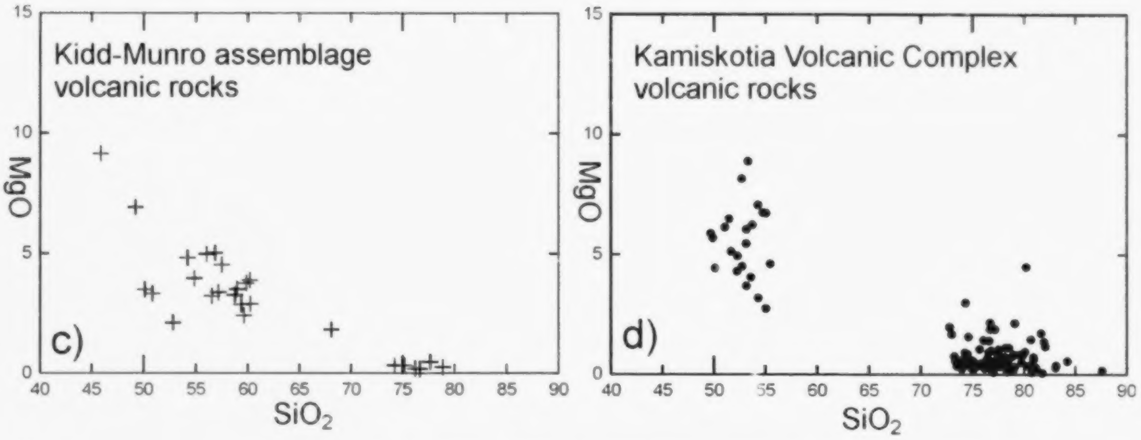

Figure 3. MgO vs SiO_2 variation diagrams for a) Kidd–Munro assemblage and b) KVC metavolcanic rocks.

MAFIC METAVOLCANIC ROCKS

Kidd–Munro Assemblage: Loveland and Macdiarmid Townships

Mafic volcanic rocks from this area form a group across the subalkaline andesite-basalt/basalt boundary on the revised Winchester and Floyd (1977; Pearce 1996) plot of Zr/TiO_2 vs. Nb/Y (Figure 4a). Most samples plot in the calc-alkaline basalt and andesite fields on the Jensen cation plot (Figure 4b; Jensen 1976). Chondrite-normalized rare earth element (REE) patterns for most samples are similar, and are distinct from other groups, with a flat pattern in the middle and heavy REE, a moderately steep negative slope in the light REE, and a slight negative Eu anomaly (Figure 5a). One sample has an anomalous flat REE pattern (pillow lava 04BHA0330).

Carscallen and Bristol Townships

The mafic lavas from Carscallen and Bristol townships have a distinctive geochemistry, falling in the alkali basalt field on the Zr/TiO_2 vs. Nb/Y plot (*see* Figure 4a), with Y/Nb for the main group around 1.3. They form a fairly tight cluster on the calc-alkaline basalt/tholeiitic andesite boundary on the Jensen diagram (*see* Figure 4b). Their REE patterns are also unlike those seen in other groups, showing relatively steep, smoothly S-curved negative slopes in the middle and light REE, and no Eu anomaly (Figure 5b). These rocks are geochemically distinct from the KVC basalts to the northeast (see below), suggesting that they may not form part of the KVC succession. Given their stratigraphic position at or near the base of the KVC, it is possible that they may represent part of the Kidd–Munro assemblage, which is present farther to the southwest in Carscallen Township (Hall and Smith 2002b, Ayer et al. 2002). However, they are also geochemically dissimilar to the Kidd–Munro assemblage basalts in Loveland and Macdiarmid townships.

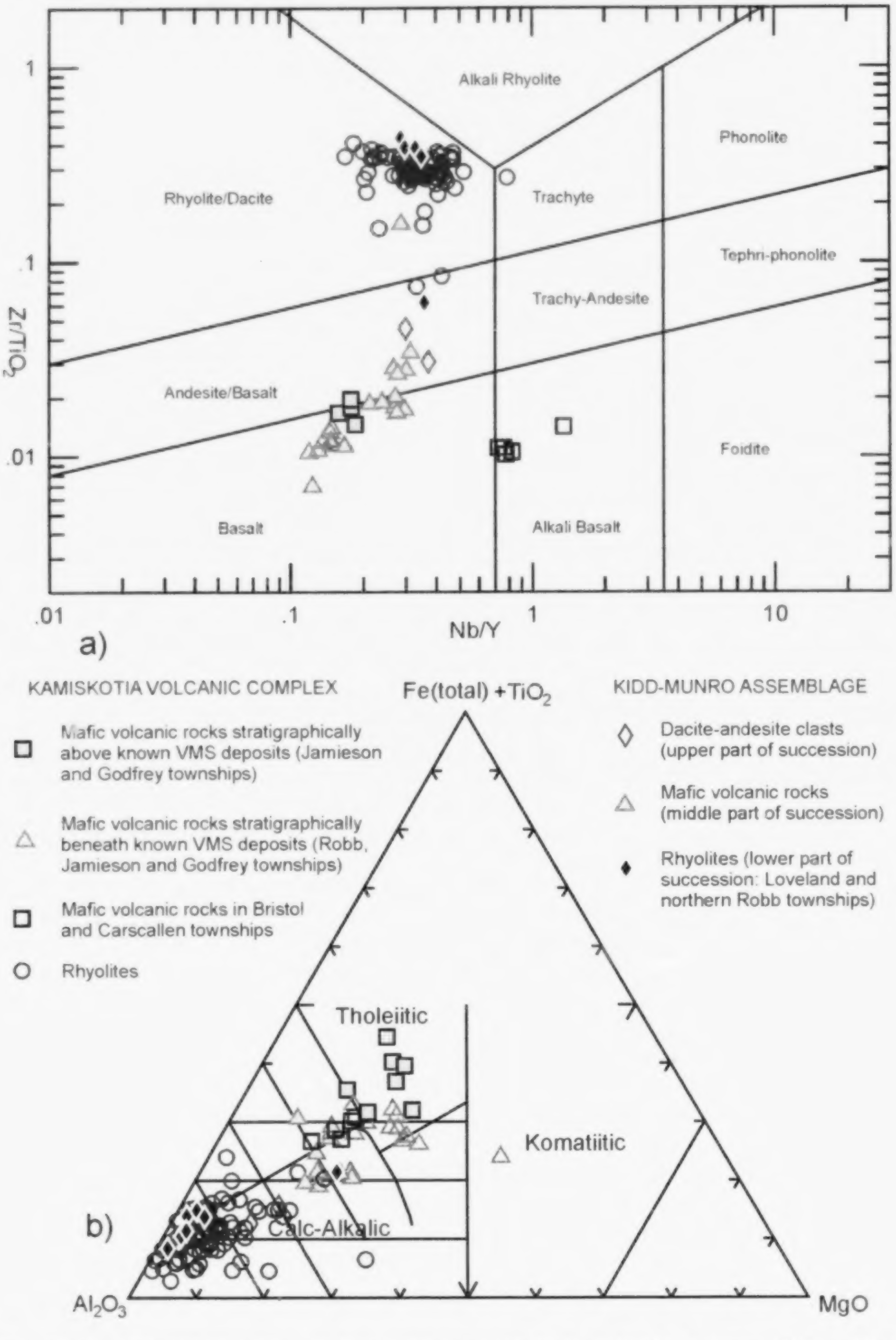

Figure 4. Classification of Kamiskotia area metavolcanic rocks using a) Zr/TiO_2 vs. Nb/Y plot (Pearce 1996, *modified from* Winchester and Floyd 1977) and b) Jensen cation plot (Jensen 1976).

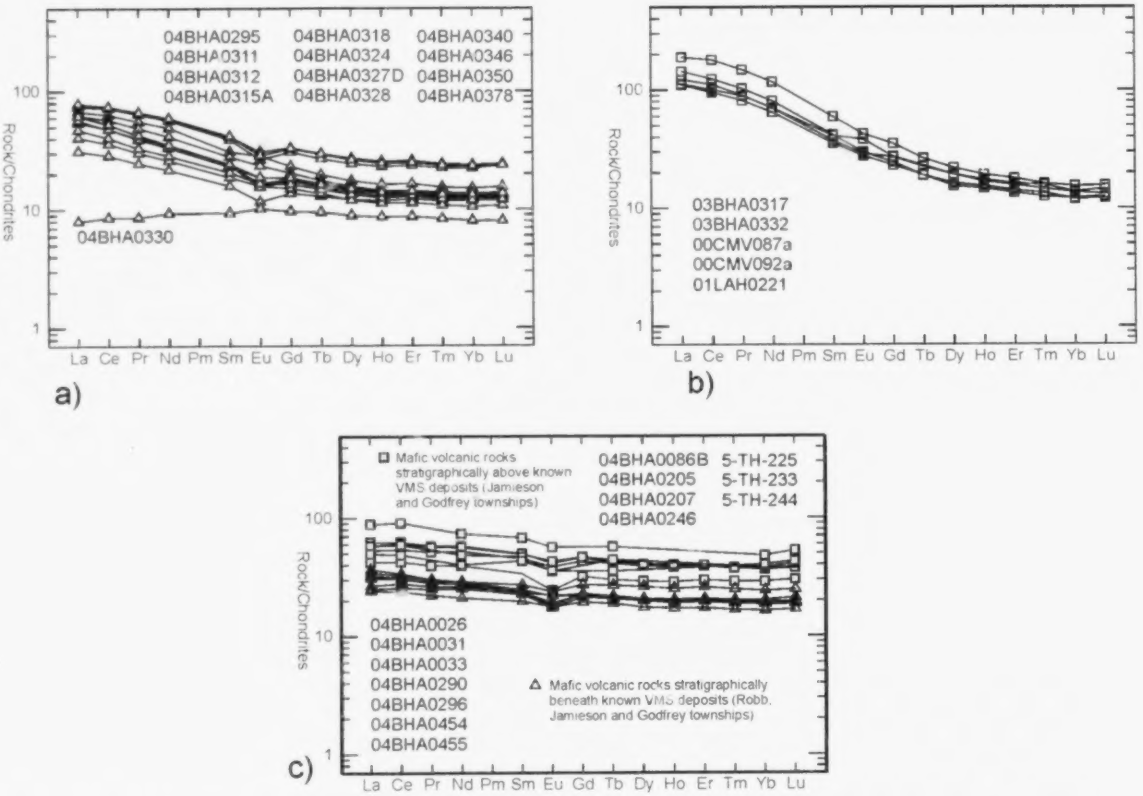

Figure 5. Chondrite-normalised rare earth element (REE) patterns for Kamiskotia area mafic metavolcanic rocks. a) Kidd–Munro assemblage lavas from Loveland and Macdiarmid townships; b) mafic lavas from Carscallen and Bristol townships (00CMV and 01LAH analyses from Vaillancourt and Hall (2003)); c) Kamiskotia Volcanic Complex lavas from Godfrey, Robb and Jamieson townships (5-TH analyses from Hart (1984)). Normalising values from Sun and McDonough (1989). Symbols as in Figure 4.

Kamiskotia Volcanic Complex: Godfrey, Jamieson and Robb Townships

Kamiskotia Volcanic Complex pillow lavas from this area cluster on the subalkaline andesite-basalt/basalt boundary on the Zr/TiO_2 vs. Nb/Y diagram (*see* Figure 4a). Hart (1984, p.51) divided the KVC mafic volcanic rocks into primitive and overlying, more evolved types, with the former having lower Ti, Zr/Y, Zr/TiO2, Zr/Hf and total REE, and higher Mg than the latter. New geochemical data from north of the Steep Lake fault support this division, which is clear on plots of TiO_2 against Zr and P_2O_5 (Figure 6). The division between the two types appears to coincide with the VMS-hosting interval at the Canadian Jamieson and Kam Kotia mines. On the Jensen plot (*see* Figure 4b), both types fall in the tholeiitic basalt field, but lavas lying stratigraphically above the VMS deposits are more Fe-rich than those below. Both types have relatively flat chondrite-normalized REE patterns, generally with slight to moderate negative Eu anomalies, but there is a consistent increase in total REE concentrations stratigraphically upward from the primitive into the more evolved lavas (Figure 5c). The latter are geochemically similar to iron, titanium and incompatible element-enriched tholeiitic basalts ("Fe-Ti basalts": Figure 6) reported by Barrie and Pattison (1999) in their detailed study of the Kam Kotia deposit. There, they describe a

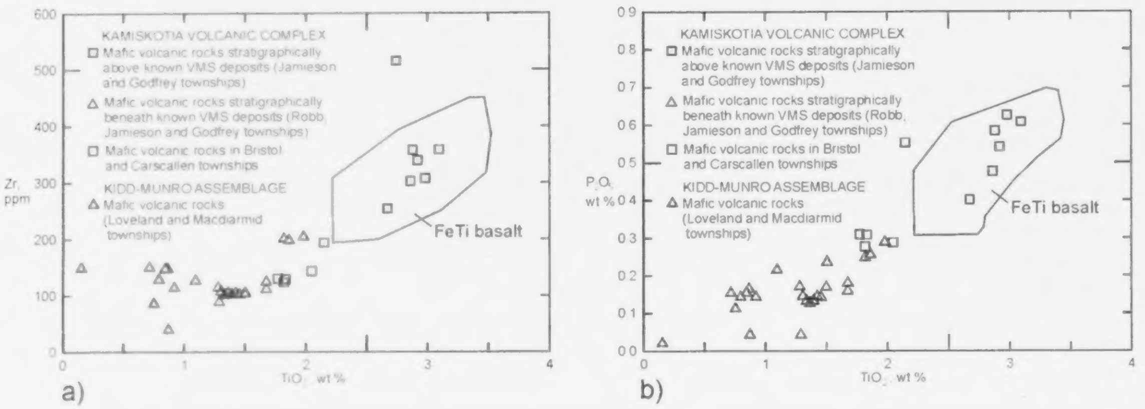

Figure 6. Plots of TiO_2 against a) Zr and b) P_2O_5 for Kamiskotia area mafic metavolcanic rocks. Data are plotted anhydrous. Field for Kam Kotia area Fe-Ti basalts from Barrie and Pattison (1999).

footwall consisting largely of primitive tholeiites, with minor Fe-Ti basalt intrusions, whereas the hanging wall includes thick, evolved Fe-Ti basalt sill-flow units (interpreted here as sills: *see* "Kam Kotia Mine" below).

In the large sample set collected by Hocker from the Genex Mine area, many mafic lavas have REE patterns with distinct negative slopes in the light REE (Hocker et al. 2005). However, unlike samples collected farther north (generally at some distance from known VMS deposits), these tend to be hydrothermally altered, plotting well outside the "least altered box" on the alteration box plot of Large et al. (2001). Samples from Genex that fall within the "least altered box" are geochemically similar (including REE patterns) to the primitive tholeiites farther north.

FELSIC TO INTERMEDIATE METAVOLCANIC ROCKS

Lesher et al. (1986) and Hart et al. (2004) divided Superior Province Archean felsic metavolcanic rocks into five types (FI, FII, FIIIa, FIIIb, and FIV) based on their trace-element geochemistry. These groups are best distinguished using plots of chondrite-normalized La/Yb vs. Yb, and variations in the nature of the Eu anomaly, but if REE data are lacking, discrimination can be made using plots of Zr/Y vs. Y, and (Zr/10)-(Ti/100)-Y projections (Lesher et al. 1986). This classification has proven useful in identifying high- and low-prospectivity areas for VMS exploration. FII to FIV rhyolites are generated under the high-temperature and low-pressure conditions that characterise high heat-flow rift environments, and these settings are conducive to the formation of the large, convective hydrothermal systems necessary for the formation of VMS deposits (Hart et al. 2004). VMS deposits are commonly hosted by FIII to FIV rocks and rarely by FII rocks, and FI rocks are generally barren (Lesher et al. 1986; Hart et al. 2004).

Kidd–Munro Assemblage: Loveland, Macdiarmid, Thorburn and Northernmost Robb Townships

Apart from one altered sample, the rhyolites from the lower, southwestern part of the Kidd–Munro assemblage in northern Robb and central Loveland townships all have high silica contents (SiO_2 = 76-80 wt %) and low TiO_2 (wt % 0.11-0.15). All samples show consistent, relatively flat REE patterns with a strong negative Eu anomaly (Figure 7a), and fall in the FIIIb "tholeiitic" rhyolite field on the Hart et al.

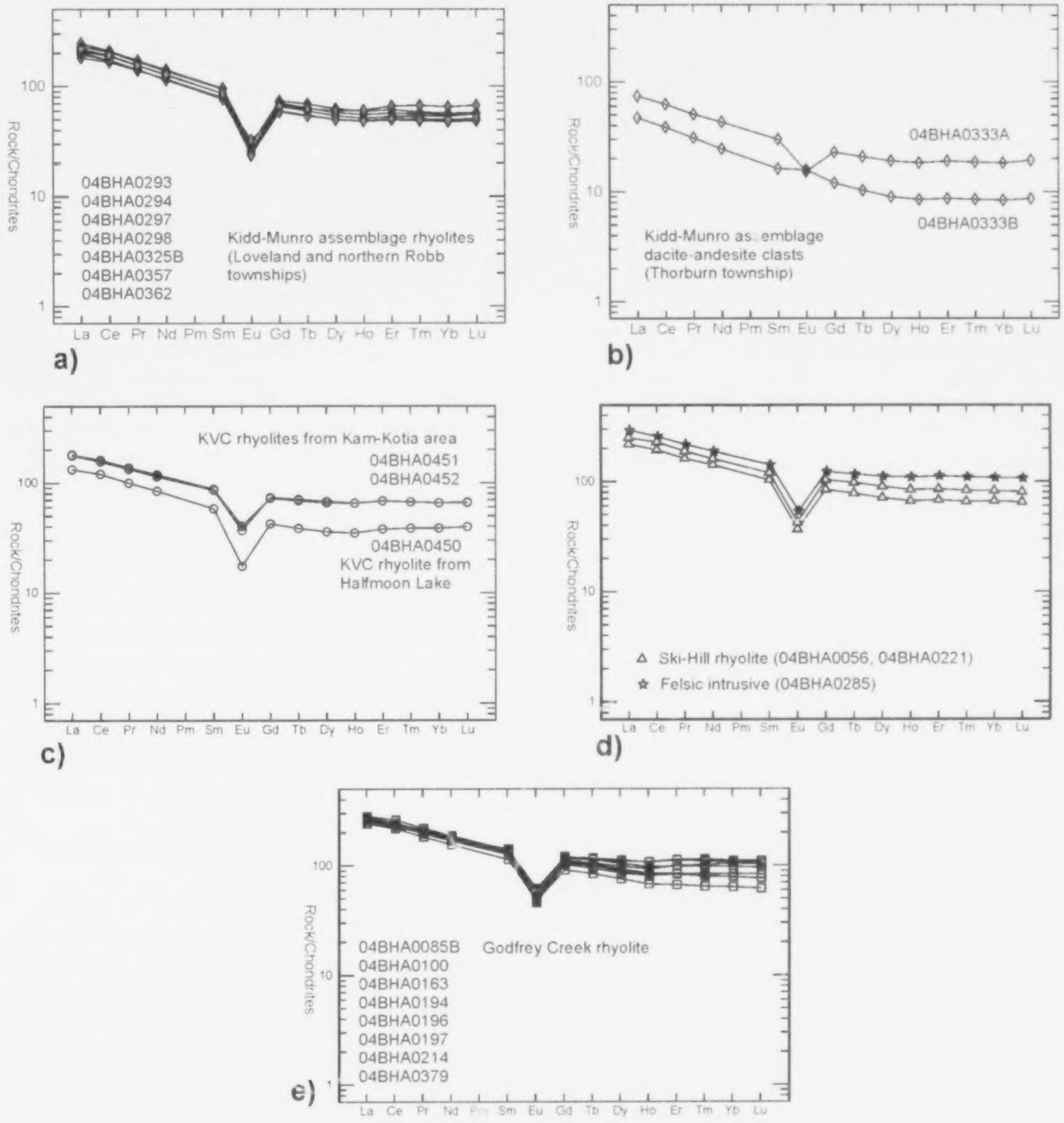

Figure 7. Chondrite-normalised rare earth element (REE) patterns for Kamiskotia area felsic metavolcanic rocks. a) Kidd–Munro assemblage rhyolites from Loveland and northern Robb townships; b) Kidd–Munro assemblage dacite-andesite clasts from Thorburn Township; c) KVC rhyolites from the Kam Kotia area and Halfmoon Lake; d) Ski-Hill rhyolite (upper KVC) with a sample from the Steep Lake granophyre (04BHA0285) for comparison; e) Godfrey Creek rhyolite (upper KVC). Normalising values from Sun and McDonough (1989).

(2004) plot of [La/Yb]$_{CN}$ vs. [Yb]$_{CN}$ (Figure 8a). Two clasts were analysed from the largely volcaniclastic felsic-intermediate succession in the northermost part of the study area (333A, 333B, 327D). They fall in the subalkaline basalt/andesite field on the revised Winchester and Floyd diagram (*see* Figure 4a), and in the calc-alkaline dacite and andesite fields on the Jensen plot (*see* Figure 4b). REE patterns (Figure 7b) are similar to those shown by the underlying pillow lavas, suggesting that they form part of the same suite, and only one sample has a relatively weak Eu anomaly. These rocks plot in the FII "calc-alkaline" field on the [La/Yb]$_{CN}$ vs. [Yb]$_{CN}$ diagram (*see* Figure 8a).

Kamiskotia Volcanic Complex

Rhyolites from the lower part of the KVC in Godfrey, Turnbull, Bristol and Carscallen townships have high silica contents (SiO_2 = 74-82 wt %) and weight % TiO_2 ranging from 0.09 to 0.4. REE patterns for these rocks, lying stratigraphically beneath the Genex VMS deposit, are shown in Figure 9A to O. Most have gentle negative slopes and strong negative Eu anomalies; however, rocks from areas C, G, E, F and N, all in the lower part of the succession, have weaker Eu anomalies. Areas E and F, stratigraphically beneath the geochemically anomalous Carscallen–Bristol township basalt lens, are likely to represent the oldest part of this succession, and may form part of the Kidd–Munro assemblage. Areas C and G were recognized as lithologically similar in the field (aphyric to finely phyric rhyolites with rare, fine-scale flow banding) and are likely to be part of the same unit. On the [La/Yb]$_{CN}$ vs. [Yb]$_{CN}$ diagram (Figure 8c), rocks from the area cluster in the FII field and the low Yb part of the FIIIb field, with most having slightly higher [La/Yb]$_{CN}$ and lower [Yb]$_{CN}$ than the Kidd–Munro assemblage rhyolites. In the stratigraphically higher, eastern part of the area, but still beneath the Genex deposit, samples from area K and several locations in area I are distinctly more heavy REE enriched, plotting well into the FIIIb field on the [La/Yb]$_{CN}$ vs. [Yb]$_{CN}$ diagram.

Data for felsic volcanic rocks from the approximate level of the VMS deposits at Genex, Kam Kotia and Halfmoon Lake are shown in Figures 7c, 8e and 8f. Samples collected by Hocker et al. (2005) from the Genex Mine area plot largely in the FII field on the [La/Yb]$_{CN}$ vs. [Yb]$_{CN}$ diagram (Figure 8e: many of these samples show intense chlorite-sericite alteration). Rhyolites in drill core along strike to the southeast of the Kam Kotia deposit fall in the FIIIb field, and a rhyolite from the felsic lens hosting the Halfmoon Lake deposit falls in the FII field. In a detailed study of the Halfmoon Lake prospect, Ore Systems Consulting (2000) found FIIIa and FIIIb rhyolites, and FII-type "High-Ti dacites" in this lens, although many of their analyses appear to be of volcaniclastic rocks. Representative analyses from their report are plotted on Figure 8f.

Rhyolites from the Ski-Hill and Godfrey Creek units in the upper part of the KVC, above the VMS deposits, have 75-82 weight % SiO_2 and weight% TiO_2 ranging from 0.15 to 0.4. These rocks show flat REE patterns with strong negative Eu anomalies (Figure 7d and e), similar to those from areas K and I farther down section (*see* Figure 9), and plot well into the FIIIb field on the [La/Yb]$_{CN}$ vs. [Yb]$_{CN}$ diagram (*see* Figure 8c). Figure 7d also shows the REE pattern for an inclusion-free phase of the Steep Lake granophyre (04BHA0285, to the south of Canadian Jamieson Mine). The similarity of the REE patterns, together with the presence of unusual chloritic inclusions in both units, suggests the granophyre may represent the intrusive equivalent of the Ski-Hill rhyolite.

To summarize, the data indicates that rhyolites in the lower part of the KVC and at the level of the VMS deposits include FII and low-Yb FIIIb types, with minor high-Yb FIIIb rocks, whereas rhyolites in the upper part of the KVC are uniformly of the high-Yb FIIIb type. This trend is clear in plots of Zr/Y vs. Y as well as [La/Yb]$_{CN}$ vs. [Yb]$_{CN}$ (*see* Figure 8).

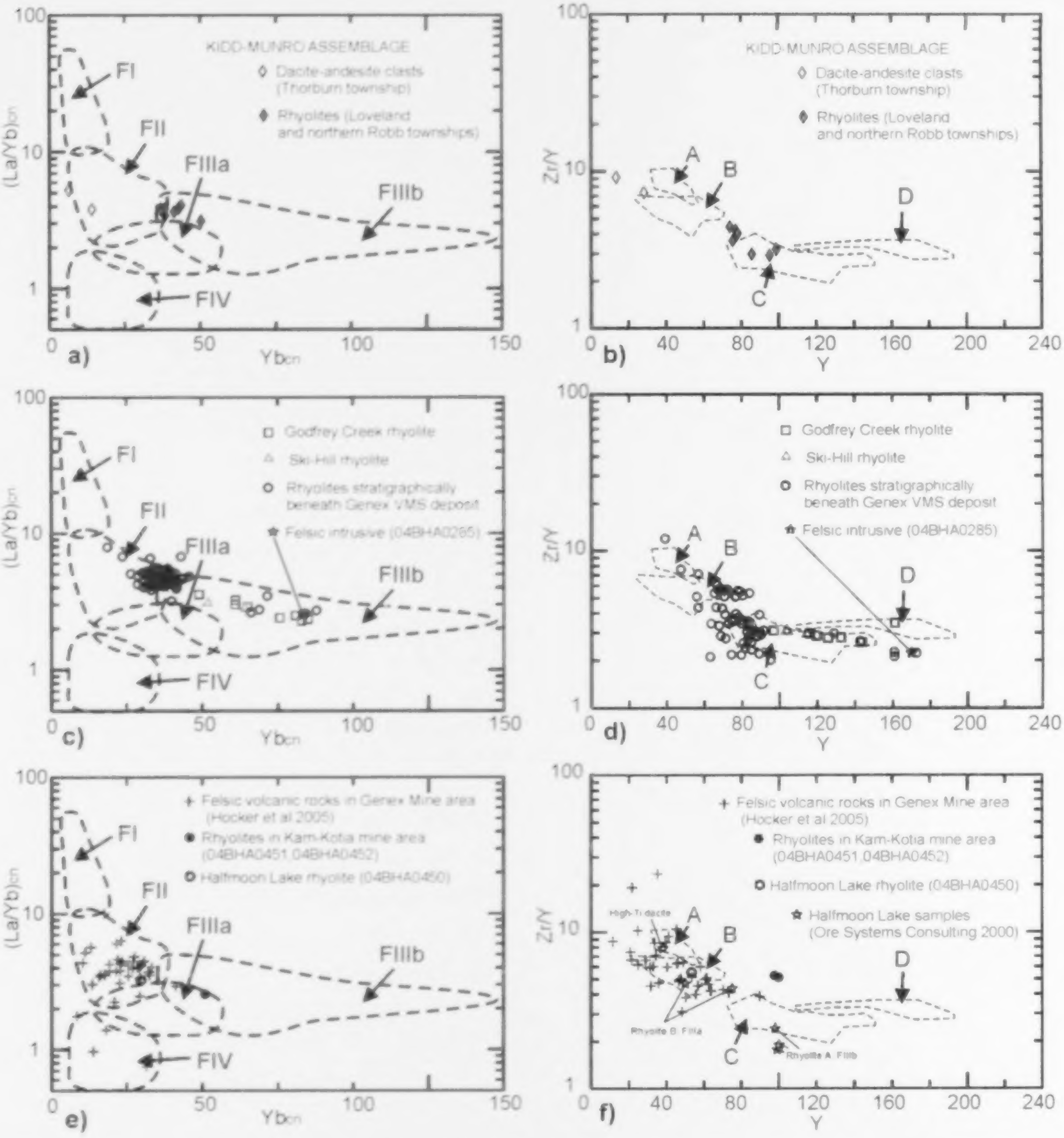

Figure 8. Plots of $[La/Yb]_{CN}$ vs. $[Yb]_{CN}$ and Zr/Y vs. Y for a) and b) Kidd–Munro assemblage felsic and intermediate rocks from Loveland, Robb and Thorburn townships; c) and d) Kamiskotia Volcanic Complex rhyolites stratigraphically below and above the main VMS-hosting interval; e) and f) Kamiskotia Volcanic Complex rhyolites from the VMS-hosting interval. Fields for FI to FIV rhyolites in a), c) and e) from Hart et al. (2004). Fields A to D in b), d) and f) from Lesher et al. (1986): A: 9 ore-associated FII from Sturgeon Lake area; B: 23 ore-associated FIIIa from the Noranda district; C: 21 ore-associated FIIIb from Kamiskotia and Kidd Creek; D: 5 ore-associated FIIIb rhyolites from the Matagami district. Normalising values in a), c) and e) from Nakamura (1974).

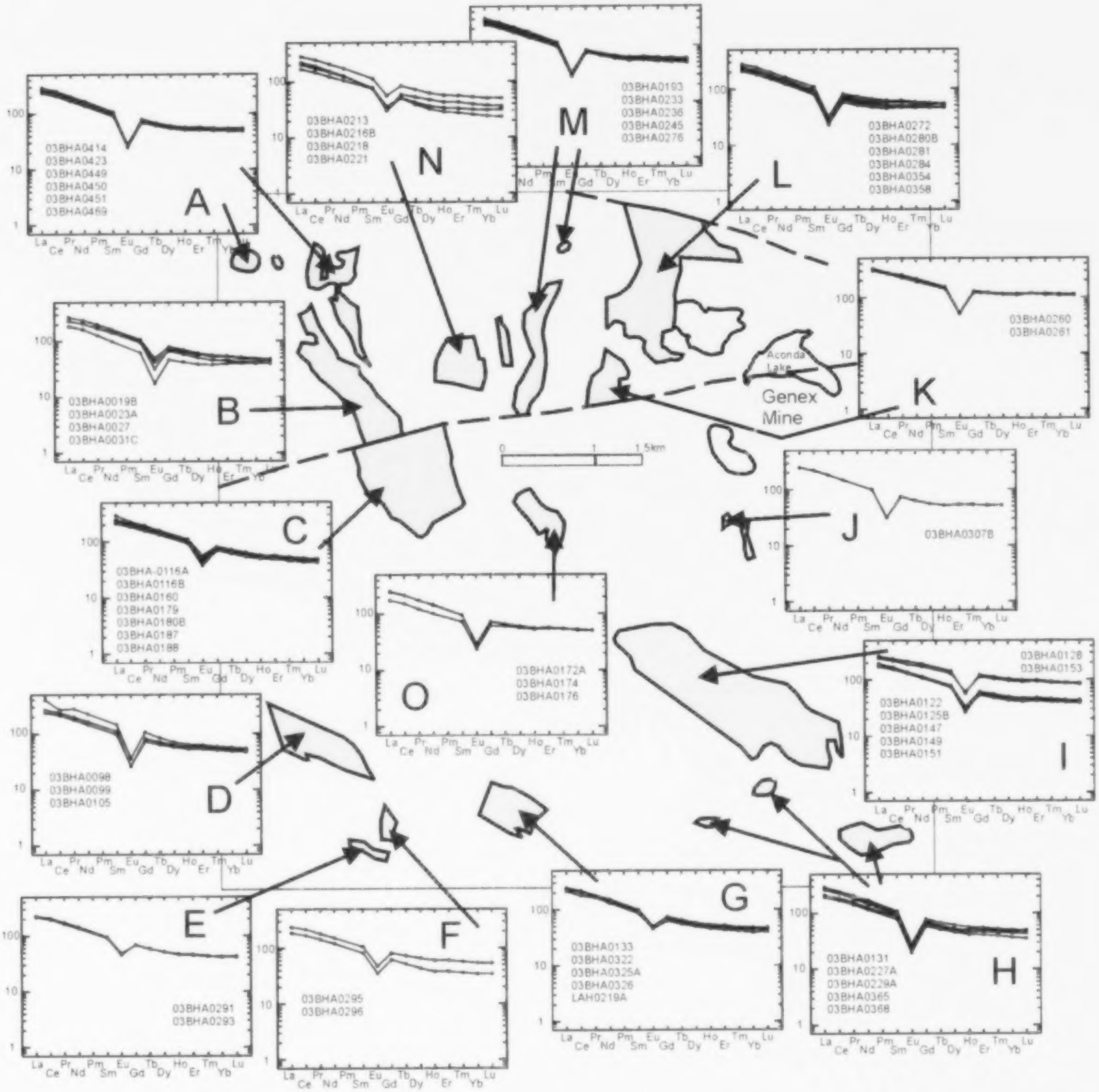

Figure 9. Chondrite-normalised rare earth element (REE) patterns for KVC rhyolites stratigraphically beneath the Genex VMS deposit (LAH analysis in G from Vaillancourt and Hall 2003). REE plots are linked to specific areas of coherent rhyolite (A to O). Normalising values from Sun and McDonough (1989). Y-axis, chondrite-normalized REE.

Geochronology

U-Pb zircon geochronological results for seven samples, together with sample locations (UTM NAD 83) and descriptions, are listed below. Sample locations are also shown in Figure 2 and on maps P.3544—Revised) and P.3556 (both in back pocket).

> Sample 04BHA0297. Kidd–Munro assemblage flow-banded, quartz-phyric rhyolite; outcrop in Loveland Township (UTM E451785, N5389819). Quartz and potassium-feldspar phenocrysts to 2 mm in quartz-sericite (minor calcite and biotite) groundmass. FIIIb geochemistry. Age: 2714.6 ± 1.2 Ma.
>
> Sample 04BHA0333. Kidd–Munro assemblage redeposited, felsic-intermediate volcaniclastic sandstone; western tip of outcrop in southernmost Thorburn Township, about 5 m stratigraphically above gabbro sill (UTM E453583, N5395777). Coarsely plagioclase-phyric lithic clasts (groundmass of felted feldspar laths) and altered plagioclase grains in a matrix of mosaic quartz and pink-green pleochroic epidote. Age: 2712.3 ± 2.8 Ma.
>
> Sample 03BHA0047. KVC felsic lapilli tuff; outcrop in eastern Turnbull Township (UTM E453921, N5370435). Abundant quartz and albitized feldspar crystals to 1 mm, in quartz-sericite-carbonate matrix with relict shard textures. Age: 2703.1 ± 1.2 Ma.
>
> Sample 03BHA0345. KVC felsic lapilli-tuff; outcrop 800 m south-southwest of Genex Mine (UTM E458483, N5369414). Abundant quartz and altered, euhedral feldspar crystals to 1 mm, in quartz-sericite matrix with carbonate rhombs and minor chlorite, locally showing relict shard textures. Age: 2698.6 ± 1.3 Ma.
>
> Sample 03BHA0382. KVC rhyolite from Falconbridge DDH R44-14 (97 to 100.5 m), 200 m south of Halfmoon Lake (projected vertically to surface: UTM E452485, N5383020). Rare rounded quartz phenocrysts to 0.5 mm in strongly foliated, quartz-sericite groundmass. FIIIb geochemistry (Ore Systems Consulting 2000). Age: 2700.0 ± 1.1 Ma.
>
> Sample 03BHA0384. KVC felsic lapilli tuff; outcrop 500 m southeast of Kam Kotia Mine (UTM E455853, N5381788). Quartz and euhedral feldspar crystals to 1 mm, in quartz-actinolite-biotite matrix. Age: 2701.1 ± 1.4 Ma.
>
> Sample 04BHA0462. Granophyric phase of Kamiskotia gabbro (KGC); outcrop in Robb Township, 1.7 km northwest of Kamiskotia Lake (UTM E451049, N5381502). Consists of quartz, altered plagioclase, and areas of granophyric quartz-feldspar intergrowth, with minor opaque minerals, chlorite and epidote. Age: 2704.8 ± 1.4 Ma.

The following two samples were collected for geochronology but did not yield zircons:

> Sample 03BHA0381. Felsic lapilli-tuff from Noranda DDH FPT-89-1, 130.85 to 136.8 m. Northernmost Loveland Township (projected vertically to surface: UTM E454670, N5395502).
>
> Sample 03BHA0383. Spherulitic rhyolite; outcrop in Kam Kotia Mine open pit (UTM E455582, N5382263).

DISCUSSION

There are two previously published age determinations for the volcanic succession in the study area. Ayer et al. (2002) obtained an age of 2719.5 ± 1.7 Ma for a dacite tuff from Noranda DDH TB96-1 in southern Thorburn Township (UTM E454840, N5396597: just north of the present study area), indicating that rocks in that area form part of the Kidd–Munro assemblage (2719 to 2710 Ma). Based on an age of 2705 ± 2 Ma for a KVC rhyolite outcrop in Godfrey Township (Barrie and Davis 1990, location uncertain, but probably east of Godfrey Lake, in area I on Figure 9), Ayer et al. (2002) placed that succession in the Tisdale assemblage (2703-2710 Ma).

New ages of 2714.6 ± 1.2 Ma for the rhyolite in central Loveland Township, and 2712.3 ± 2.8 Ma for a volcaniclastic interval in southernmost Thorburn Township, confirm assignment of those rocks to the Kidd–Munro assemblage. These ages indicate younging to the north, consistent with the northeast-facing indicators seen throughout this succession. The older, Ayer et al. (2002) age of 2719.5 ± 1.7 Ma, not far north of the younger of the two new ages, suggests there may be an intervening structural discontinuity, perhaps similar to that between the Kidd–Munro assemblage rocks and the KVC to the south.

The age of 2703.1 ± 1.2 Ma from Turnbull Township and the ages of 2698.6 ± 1.3 Ma, 2701.1 ± 1.4 Ma and 2700.0 ± 1.1 Ma for stratigraphically higher samples from Genex, Kam Kotia and Halfmoon Lake (all from felsic rocks underlying the main VMS hosting intervals) provide an age range for the greater part of the KVC. The three latter ages are within error of each other, and indicate a similar timing for VMS mineralization in the three areas. The four new ages are at variance with the Barrie and Davis (1990) age, indicating that the KVC is slightly younger than the youngest previously known Tisdale assemblage rocks (2710-2703 Ma), and coeval with the younger Blake River assemblage (2701-2697 Ma: Ayer et al. 2002).

The age of 2704.8 ± 1.4 Ma for a granophyric phase of the Upper Zone (Barrie 1992) of the KGC is younger than a previous age of 2707 ± 2 Ma from the stratigraphically lower, Middle Zone gabbro in Turnbull Township, west of the present study area (Barrie and Davis 1990). The new age is slightly older than (although within error of) the age of 2703.1 ± 1.2 Ma for the lower part of the KVC, which the gabbro appears to intrude. However, it is significantly older than the 2700.0 ± 1.1 Ma KVC rhyolite age from Halfmoon Lake, only 2 km to the northeast. This age relationship is problematic: it is possible that the KGC could intrude an older succession (e.g. Kidd–Munro assemblage) with the KVC deposited on top of such a basement complex (J. Ayer, OGS, personal communication, 2005). However, outcrop east of Kamiskotia Lake indicates an unfaulted, intrusive contact between the Upper Zone gabbro and the "primitive" KVC tholeiitic pillow lavas that underlie the VMS-hosting interval in this area.

Structural Geology

KIDD–MUNRO ASSEMBLAGE

Kidd–Munro assemblage rocks generally show a single, weak, nonpenetrative foliation, which strikes northwest in the rhyolites in south-central Loveland Township and gradually swings to strike west-northwest (broadly parallel to bedding strike) in the northeastern corner of the township. Unlike in much of the KVC, pillows and clasts are not noticeably deformed. As noted by Middleton (1974), the shape of the mafic-ultramafic intrusion in west-central Macdiarmid Township indicates that the succession has been folded to form an open syncline with a broadly north-trending axis.

KAMISKOTIA VOLCANIC AND GABBROIC COMPLEXES

The KVC and KGC have been affected by at least three deformation episodes. These appear to be the same as those recognised by Hall and Smith (2002b) in Carscallen Township, and the same terminology is used here (D_1, D_2 and D_{3-4})

D_1

D_1 is represented by a steeply dipping penetrative foliation (S_1) most easily recognized in relatively fine-grained, phyllosilicate-altered felsic volcaniclastic (KVC) and felsic-intermediate intrusive (KGC) rocks in southern Jamieson and northern Godfrey townships. Here it strikes northwest (mean 320° in south Jamieson and northernmost Godfrey townships; 305° in the Steep Lake area) and generally dips to the northeast (Figure 10a and c). Elsewhere, as noted by Hall and Smith (2002b), S_1 is typically transposed into the plane of the later S_2 foliation to form an west- to west-northwest-striking composite planar fabric. This composite S_1/S_2 foliation (shown as "unknown generation" on the accompanying maps in the back pocket) is the dominant structural fabric south of the Steep Lake fault, where S_1 is difficult to recognise.

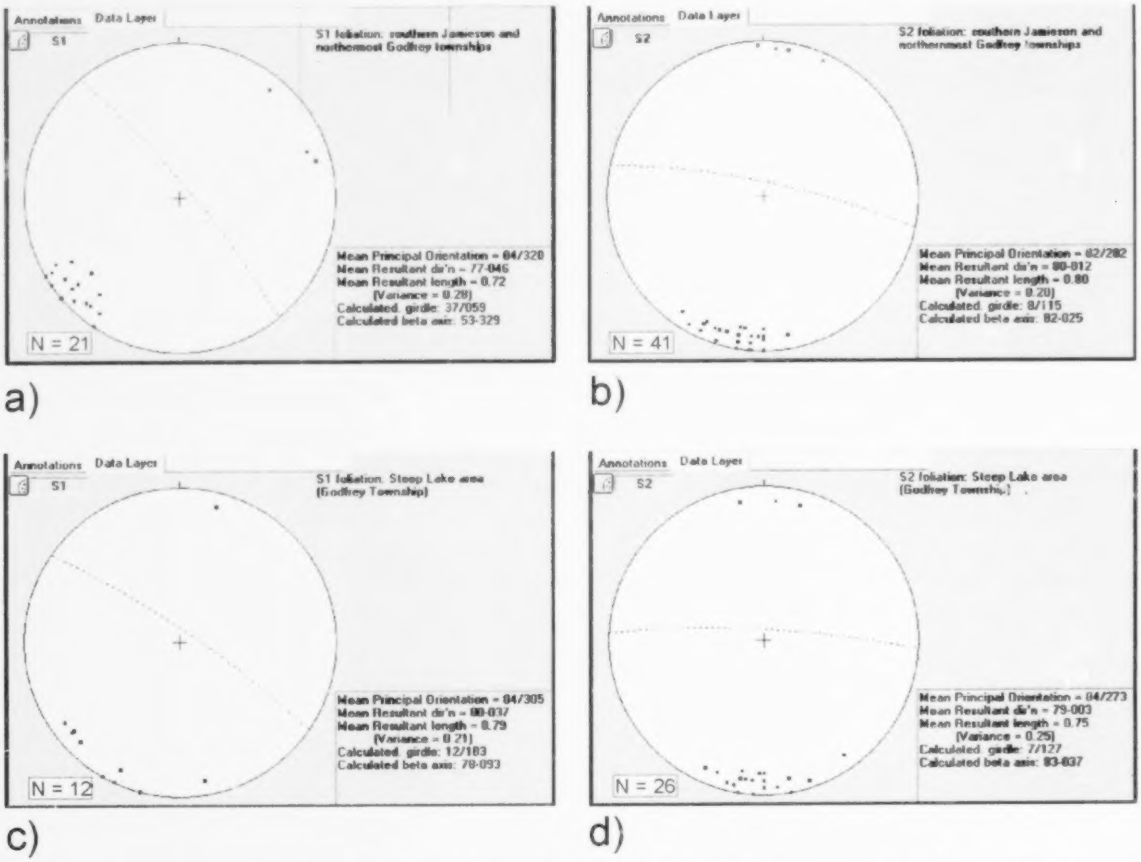

S1 foliation: southern Jamieson and northernmost Godfrey townships

Mean Principal Orientation = 04/320
Mean Resultant dir'n = 77-046
Mean Resultant length = 0.72
(Variance = 0.28)
Calculated. girdle: 37/059
Calculated beta axis: 53-329

a)

S2 foliation: southern Jamieson and northernmost Godfrey townships

Mean Principal Orientation = 02/282
Mean Resultant dir'n = 80-012
Mean Resultant length = 0.80
(Variance = 0.20)
Calculated. girdle: 8/115
Calculated beta axis: 82-025

b)

S1 foliation: Steep Lake area (Godfrey Township)

Mean Principal Orientation = 04/305
Mean Resultant dir'n = 80-037
Mean Resultant length = 0.79
(Variance = 0.21)
Calculated. girdle: 12/183
Calculated beta axis: 78-093

c)

S2 foliation: Steep Lake area (Godfrey Townshi.)

Mean Principal Orientation = 04/273
Mean Resultant dir'n = 79-003
Mean Resultant length = 0.75
(Variance = 0.25)
Calculated. girdle: 7/127
Calculated beta axis: 83-037

d)

Figure 10. Stereoplots showing poles to S_1 and S_2 foliation planes in a) and b) southern Jamieson and northernmost Godfrey townships; c) and d) Steep Lake area (Godfrey Township).

KAMISKOTIA VOLCANIC AND GABBROIC COMPLEXES

The KVC and KGC have been affected by at least three deformation episodes. These appear to be the same as those recognised by Hall and Smith (2002b) in Carscallen Township, and the same terminology is used here (D_1 D_2 and D_{3-4})

D_1

D_1 is represented by a steeply dipping penetrative foliation (S_1) most easily recognized in relatively fine-grained, phyllosilicate-altered felsic volcaniclastic (KVC) and felsic-intermediate intrusive (KGC) rocks in southern Jamieson and northern Godfrey townships. Here it strikes northwest (mean 320° in south Jamieson and northernmost Godfrey townships; 305° in the Steep Lake area) and generally dips to the northeast (Figure 10a and c). Elsewhere, as noted by Hall and Smith (2002b), S_1 is typically transposed into the plane of the later S_2 foliation to form an west- to west-northwest-striking composite planar fabric. This composite S_1/S_2 foliation (shown as "unknown generation" on the accompanying maps in the back pocket) is the dominant structural fabric south of the Steep Lake fault, where S_1 is difficult to recognise.

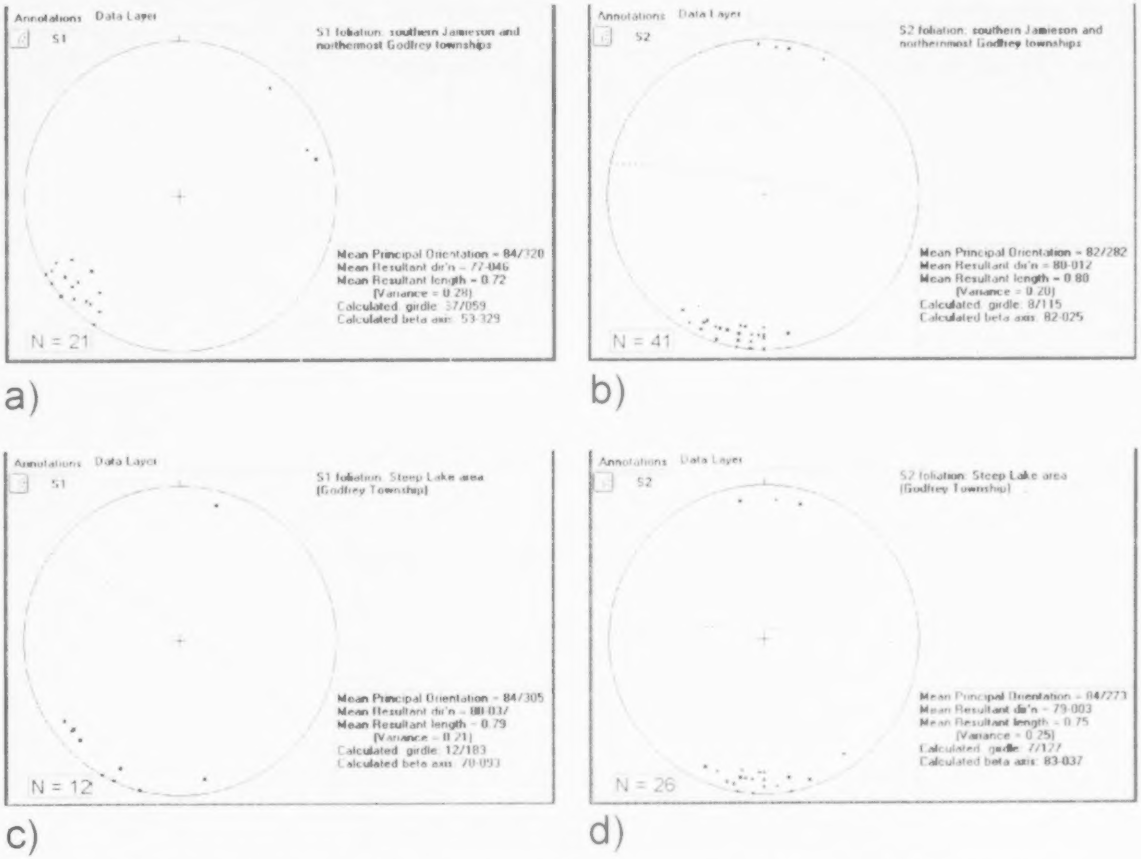

Figure 10. Stereoplots showing poles to S_1 and S_2 foliation planes in a) and b) southern Jamieson and northernmost Godfrey townships; c) and d) Steep Lake area (Godfrey Township).

Hall and Smith (2002b) interpreted a map-scale, north-trending antiform-synform pair in southeast Carscallen Township as D_1-associated (F_1), and the north-northwest-trending anticline in Godfrey and Turnbull townships is also likely to be an F_1 fold. The relationship of the S_1 foliation to bedding on the east-facing limb of the fold is consistent with the observed anticlinal closure to the south. Unfortunately S_1 was not recognized on the western limb of the anticline. Hall and Smith (2002b) noted rare mesoscopic folds associated with D_1 but these were not seen in the present study area.

D_2

In areas where it can be distinguished from D_1, D_2 is typically represented by a steeply dipping, west- to west-northwest-striking spaced foliation (S_2) which is generally the most obvious structural fabric. In northern Godfrey and southern Jamieson townships there is a relatively consistent 32 to 38° angle between S_2 and the more northwest-striking, penetrative S_1 foliation (*see* Figure 10). Mesoscopic F_2 folds similar to those identified by Hall and Smith (2000b) are common to the northeast of Kamiskotia Lake (e.g. in the outcrops around the Kam Kotia Mine), but rare elsewhere. They are typically tight, asymmetric (usually Z-shaped), have east-northeast-trending axes and fold the earlier S_1 foliation.

$D_{3/4}$

The locally developed D_3 deformation of Hall and Smith (2000b), represented by crenulations on earlier foliation surfaces, was not recognized in this study. However, locally abundant kink folds with vertical axial planes and variable orientations (sometimes forming conjugate sets) can be attributed to their D_4 deformation.

FAULTING

There is a well-defined break in the KVC stratigraphy across the east-northeast-trending Aconda Lake fault (*see* Figure 2) in Godfrey and Turnbull townships. Although there appears to be a small amount of late dextral offset with respect to the Matachewan diabase dikes, the nature of the displacement within the KVC is uncertain owing to lack of marker horizons. This fault seems to have localized the emplacement of KGC "granophyre zone" intrusive rocks in the Aconda Lake area, suggesting an early syn-intrusion/synvolcanic history. The series of northwest-trending faults inferred farther south in Godfrey Township may be related to the similarly oriented, but better constrained, fault system in northern Godfrey and southern Jamieson townships, which includes the Steep Lake and Kamiskotia Highway faults (*see* Figure 2). Offset of marker intervals (e.g. Steep Lake granophyre, Ski-Hill rhyolite) across these faults is consistently dextral in map view. Although there is little firm evidence for synvolcanic movement, the Ski-Hill rhyolite terminates abruptly to the north across one of these faults. The fault inferred to divide the Kidd–Munro assemblage from the KVC to the south appears to trend broadly west-northwest in the Loveland–Robb township boundary area, and is likely to extend eastward into Jamieson Township, although its location there is uncertain.

A system of northeast-trending faults is well developed in Robb Township, southwest Jamieson Township, and northern Godfrey Township. These are marked by offset of felsic volcanic intervals in outcrop to the southeast of Mount Jamieson. Farther west (Kamiskotia Lake area), offset of magnetic phases of the KGC and gabbroic sills in the KVC is clear from aeromagnetic data (*see* Map P.3556). These faults appear to have no consistent sense of movement. Although the relationship of these faults to the northwest-trending faults is uncertain, there is evidence for synvolcanic displacement on northeast-trending faults in the Kam Kotia Mine area (see below).

Middleton (1973, 1974) mapped a series of late north-northwest-trending faults with inferred sinistral displacement along the trend of many of the Matachewan diabase dikes. Although sinistral offsets across diabase dikes are clear in some places (e.g. 400 m south of Halfmoon Lake), displacements generally appear to be small, and these faults have not been shown on the maps. The Mattagami River fault trends parallel to, and may have originated as part of, the Matachewan dike-related fault system (Middleton 1973). However, large-scale, sinistral strike-slip movement on this fault, with an estimated offset of at least 11 km (Middleton 1973), postdates emplacement of Matachewan swarm (Middleton 1973, 1974). A number of northwest- and northeast-trending faults offset the Matachewan dike swarm in northern Loveland and Macdiarmid townships.

Metamorphism and Alteration

All the Archean volcanic rocks in the area have undergone greenschist-facies metamorphism. Hydrothermal alteration zones proximal to the past-producing VMS deposits are discussed in detail below (Canadian Jamieson and Kam Kotia) and by Hocker et al. (2005: Genex). Lithogeochemical samples for the regional study, collected at some distance from known VMS deposits, are plotted on the "alteration box plot" of (Large et al. 2001) in Figure 11. This plot, consisting of the Ishikawa alteration index (AI = 100 (K_2O + MgO)/(K_2O + MgO + Na_2O + CaO) plotted against the chlorite-carbonate-pyrite index (CCP = 100 (MgO + FeO)/(MgO + FeO + Na_2O + K_2O), should help to distinguish VMS-related hydrothermal alteration from regional greenschist-facies metamorphism (Large et al. 2001). Most mafic volcanic rocks cluster within the "least altered" field, in contrast to samples collected from the Genex Mine area (*see* Hocker et al. 2005), a large number of which plot near the top right corner of the box plot (chlorite-pyrite alteration). Similarly, most felsic volcanic samples plot in the relevant "least altered" box, whereas felsic samples from Genex tend to plot close to the chlorite-sericite join along the upper right-hand side of the box plot. Some felsic samples, notably from the Godfrey Creek and Ski-Hill rhyolites in the upper part of the KVC, have AI values in excess of 80, indicating sericitic alteration. However, they do not show the elevated CCP indices (greater than 50) seen in samples with similar AI values from Genex (Hocker et al. 2005).

Volcanogenic Massive Sulphide Deposits

KAM KOTIA MINE

Surface geological mapping at 1:5000 to 1:1000 scales, supplemented with petrographic observations, was completed to evaluate the volcanic stratigraphy, alteration mineralogy, and structural deformation present in the immediate vicinity of the former Kam Kotia Mine orebodies (Figure 12). These deposits produced 5 840 000 tonnes (6 436 000 tons) of massive sulphide ore with an average grade of 1.11% Cu and 1.21% Zn (Barrie and Pattison 1999; Barrie 2000). Descriptions of the VMS mineralization at Kam Kotia can be found in Binney and Barrie (1991), Barrie and Pattison (1999), and Barrie (2000).

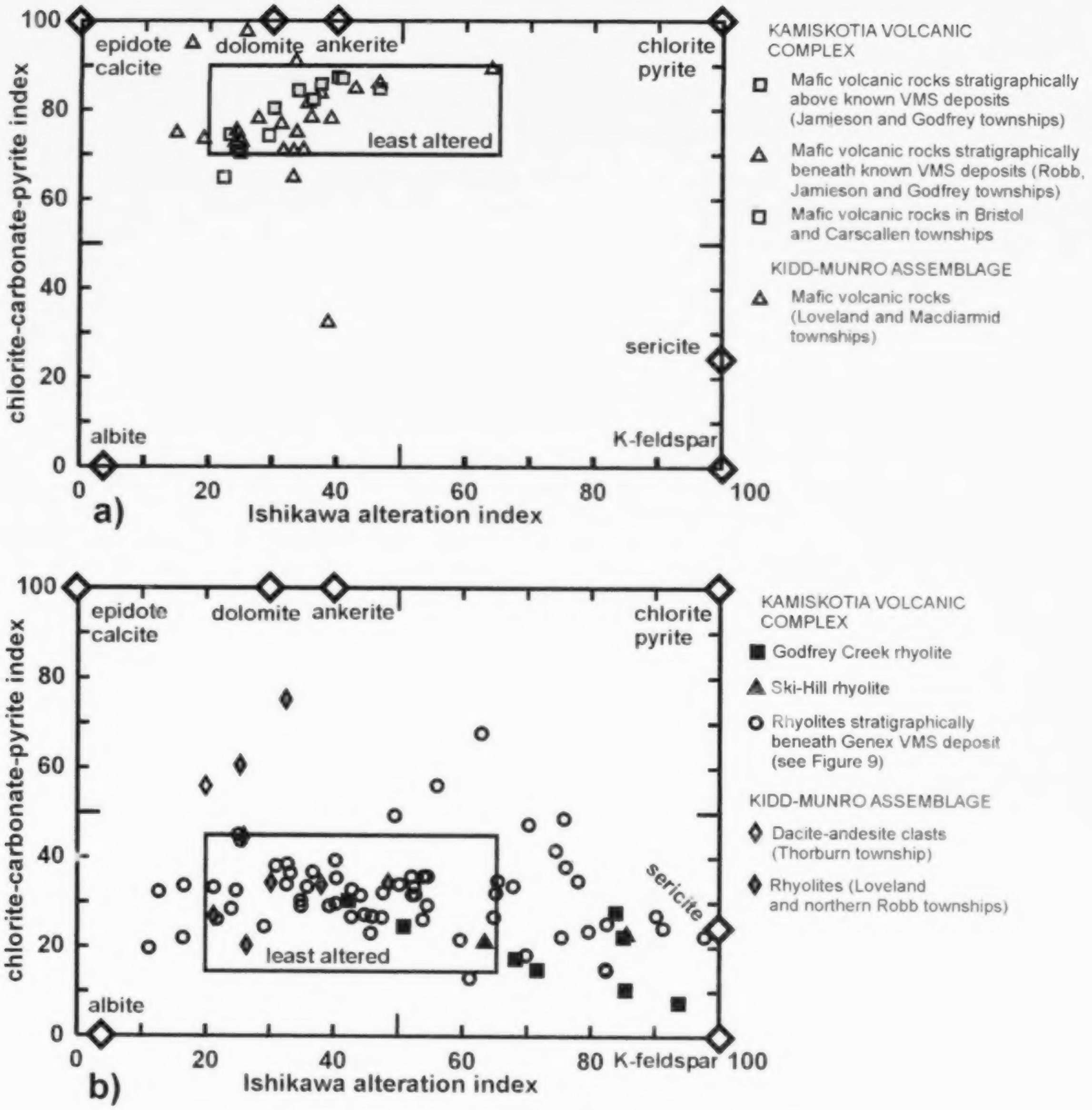

Figure 11. Alteration box plot of Large et al. (2001) showing a) Kamiskotia area mafic metavolcanic samples; b) felsic metavolcanic samples. "Least altered" fields of Large et al. (2001) are shown for illustration.

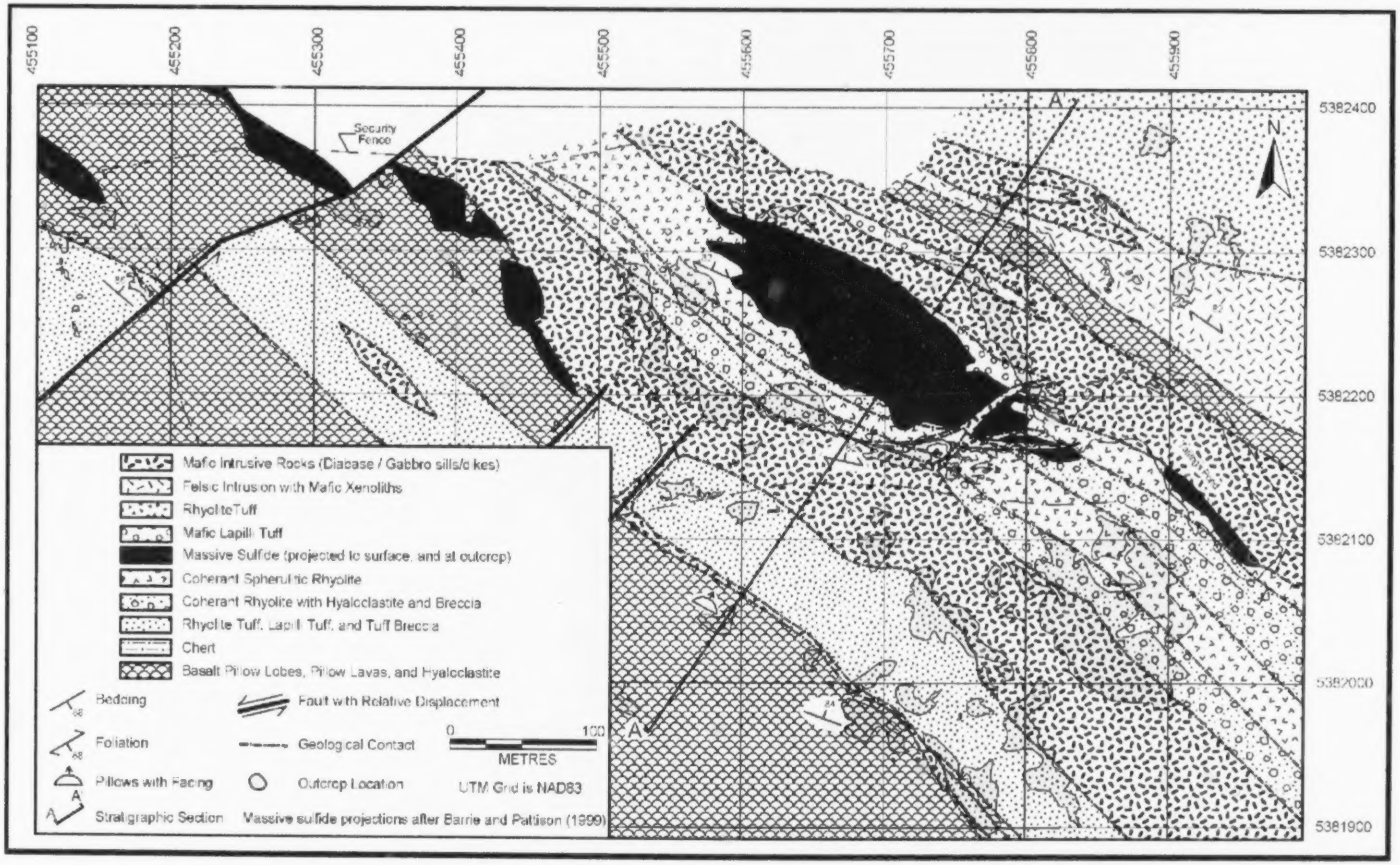

455100
455200
455300
455400
455500
455600
455700
455800
455900
5382400
5382300
5382200
5382100
5382000
5381900
N
A
A'
Security Fence
Mafic Intrusive Rocks (Diabase / Gabbro sills/dikes)
Felsic Intrusion with Mafic Xenoliths
RhyoliteTuff
Mafic Lapilli Tuff
Massive Sulfide (projected to surface, and at outcrop)
Coherent Spherulitic Rhyolite
Coherent Rhyolite with Hyaloclastite and Breccia
Rhyolite Tuff, Lapilli Tuff, and Tuff Breccia
Chert
Basalt Pillow Lobes, Pillow Lavas, and Hyaloclastite
Bedding
Foliation
Pillows with Facing
Stratigraphic Section
Fault with Relative Displacement
Geological Contact
Outcrop Location
0
100
METRES
UTM Grid is NAD83
Massive sulfide projections after Barrie and Pattison (1999)

Figure 12. Detailed surface geological map of the Kam Kotia Mine area. Cross-section A-A' is presented in Figure 15.

Stratigraphy

Geological mapping during previous studies (Somerville 1967; Binney and Barrie 1991; Barrie and Pattison 1999; Barrie 2000), as well as this study, indicate that the strata in the vicinity of the Kam Kotia Mine comprise a steeply northeast-dipping, northeast-younging succession of subaqueously deposited mafic and felsic lavas and volcaniclastic strata, chemical metasedimentary rocks (chert exhalites and massive sulphide deposits), and mafic intrusive rocks (*see* Figure 12). Detailed volcanological facies mapping performed during this study slightly modifies the geological section developed by Barrie and Pattison (1999).

The base of the stratigraphic sequence comprises at least 155 m of west- to northwest-striking (278°-300°) basalt pillow lavas, pillow lobes, and associated hyaloclastite deposits (Photo 3A). Bun- to mattress-shaped pillows (*see* Dimroth et al. 1978) vary from 0.1 to 0.4 m thick and 0.8 to 1.0 m wide. Pillow lobes range from 0.5 to 2.0 m thick and 2.0 to 4.0 m wide. Both the pillows and the pillow lobes are variably amygdaloidal, containing 10 to 15% oval quartz-filled amygdules ranging from 0.3 to 1.5 cm in diameter. Locally, pipe amygdules up to 0.4 cm wide by 5 cm long are present and are radially oriented within pillow selvedges. Hyaloclastite deposits up to 1 cm thick occur between individual pillows and lobes. The basal contact of this unit was not encountered during mapping.

A 60 to 80 m thick succession of interbedded, commonly fining-upward sequences comprising thinly bedded to very thickly bedded, commonly vaguely normal-graded rhyolite tuff breccias, lapilli tuffs and tuffs overlies the pillow basalts and can be traced for at least 500 m along strike. These volcaniclastic strata occur approximately 100 m into the footwall of the Kam Kotia orebodies. At the base of this unit, a chert horizon up to 2 m thick with local gossan-like sulphide staining occurs. Overlying volcaniclastic units vary from very thinly bedded to massive, and comprise up to 25% angular to subangular coherent rhyolite lapilli and blocks in a fine-grained recrystallized felsic ash matrix (Photo 3B). Petrographic observations indicate the presence of 5 to 28% angular, broken, and locally sliver-like <1 mm diameter quartz and/or feldspar crystals. Petrographic observations also indicate that exceptionally well-preserved perlitic fractures occur within the coherent rhyolite lapilli and blocks.

A second, up to 95 m thick, horizon of basalt pillow lavas and associated hyaloclastite crops out approximately 100 m west-southwest of the Kam Kotia open pit, and can be traced up to 400 m west of the open pit. Outcrops typically are stained a deep brownish red due to the presence of oxidized sulphide minerals. Sparsely to moderately (5-10%) amygdaloidal bun- and mattress-shaped pillows strike west-northwest to northwest (285°-305°), and range from 0.3 to 0.4 m thick and 0.5 to 1.0 m wide, whereas pillow lobes are up to 1 m thick and up to 3 m wide. Interpillow hyaloclastite deposits generally range from <1 to 2 cm in thickness. Well-preserved hyaloclastite breccias and pillow breccias crop out approximately 50 m west of the Kam Kotia open pit. These deposits are characterized by a fine- to coarse-grained, chlorite-rich recrystallized ash matrix which contains 50 to 60% angular, cuspate, blocky and locally lens-shaped, 0.3 to 3.0 cm, sparsely quartz amygdaloidal basalt clasts and 10 to 20% sub-rounded to angular amygdaloidal basalt lapilli and blocks containing 10 to 20%, 1 to 3 mm quartz amygdules. Both types of mafic clasts locally exhibit fine-grained, up to 0.1 cm thick chilled margins. Barrie and Pattison (1999) note that this unit hosted the western, subsurface lenses of the Kam Kotia orebody.

Coherent spherulitic rhyolite and associated autoclastic and hyaloclastite breccias comprise the immediate footwall and host strata to the main Kam Kotia massive sulphide lens. Stratigraphically

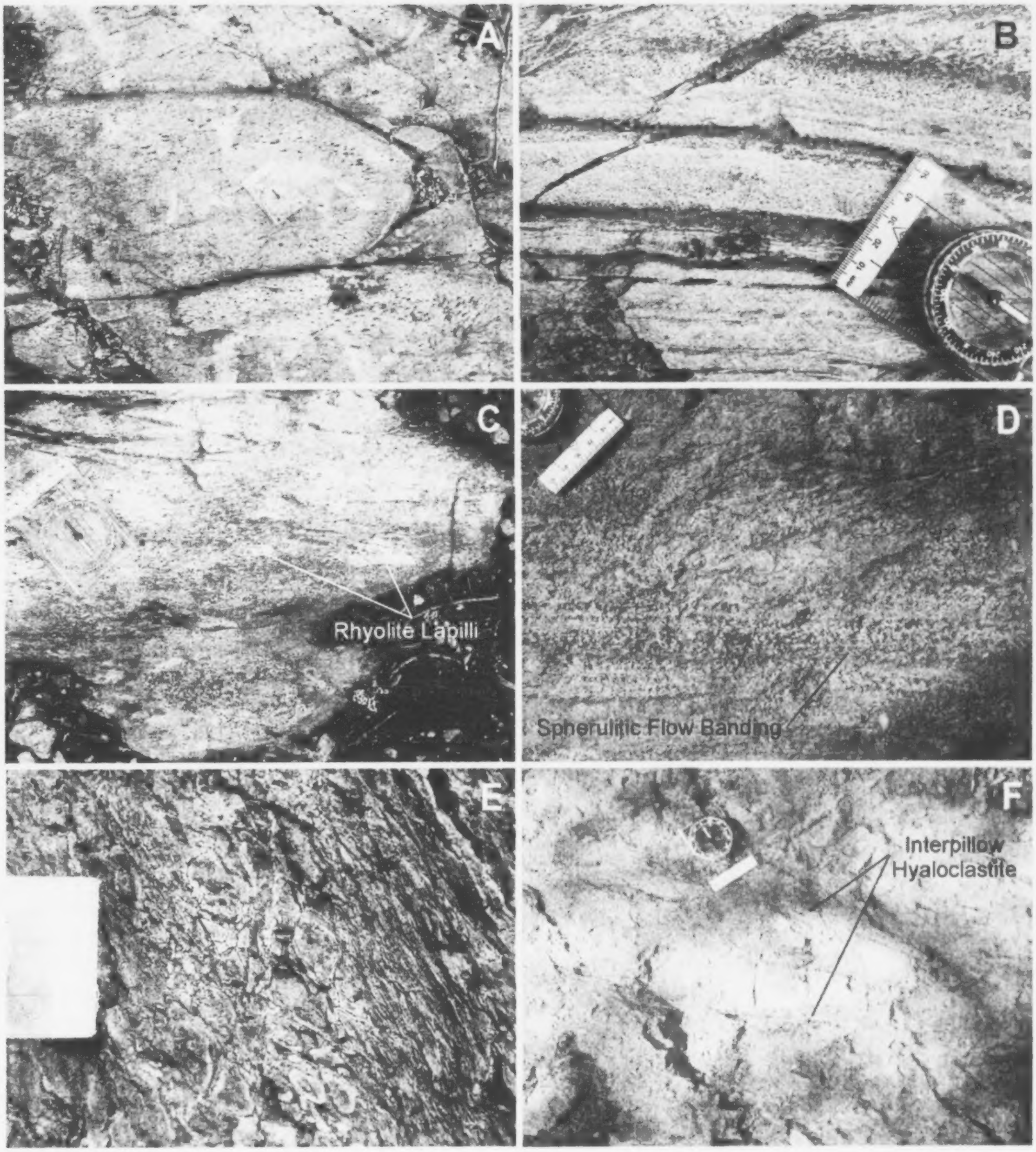

Photo 3. Field photographs of various lithologies in the vicinity of the Kam Kotia VMS deposits: A) Pillow basalts located 200 m south of the Kam Kotia Mine open pit; B) laminated to very thinly bedded, normal-graded tuffs located 400 m west of the Kam Kotia Mine open pit; C) angular coherent rhyolite lapilli within lapilli tuffs located approximately 300 m south-southeast of the Kam Kotia Mine open pit; D) flow banded spherulitic rhyolite located approximately 15 m south of the southeastern edge of the Kam Kotia Mine open pit; E) hydrothermally altered rhyolite hyaloclastite located on the western edge of the Kam Kotia Mine open pit; F) pillow basalts located approximately 75 m north of the Kam Kotia Mine open pit. The compass in all photos is 55 mm wide.

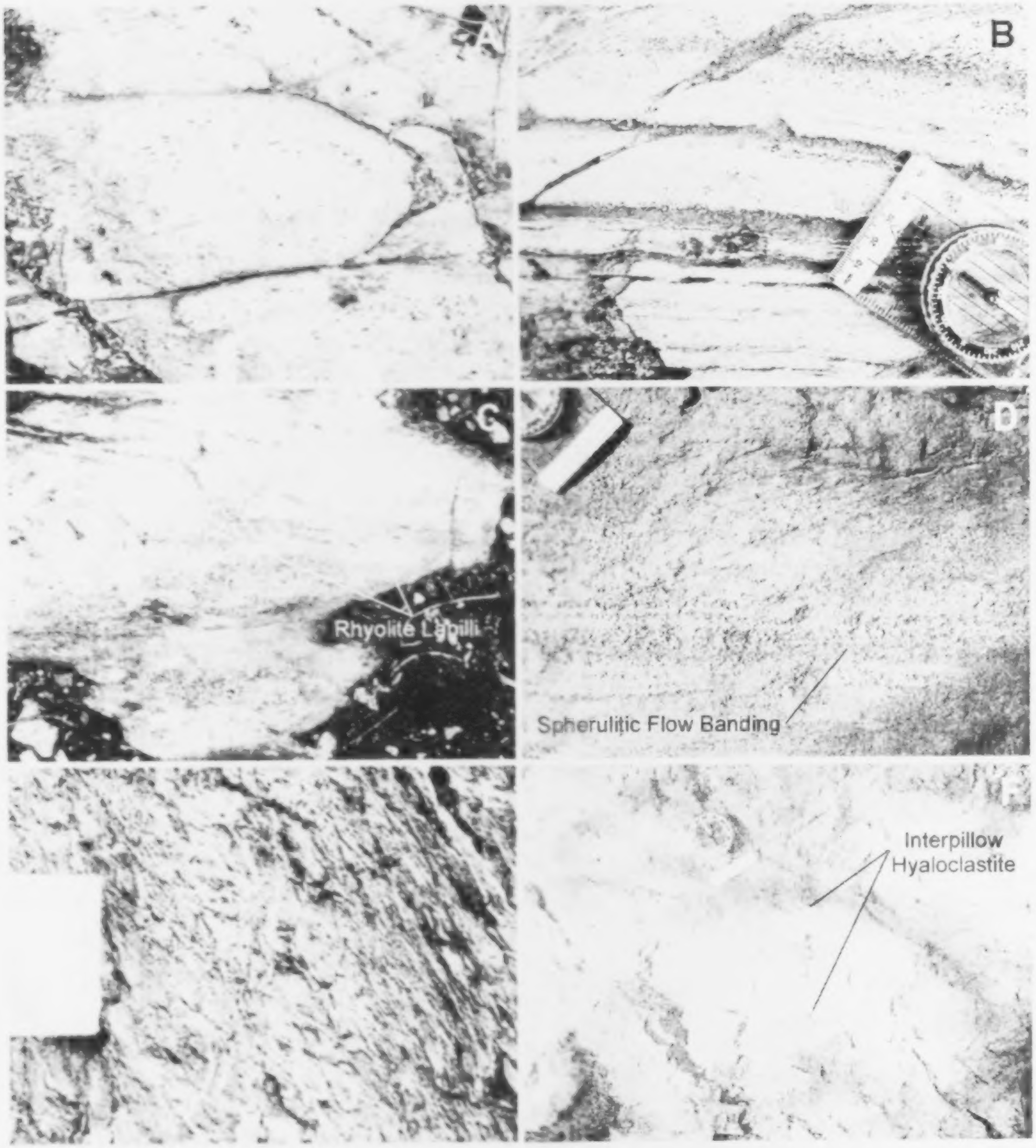

Photo 3. Field photographs of various lithologies in the vicinity of the Kam Kotia VMS deposits: A) Pillow basalts located 200 m south of the Kam Kotia Mine open pit; B) laminated to very thinly bedded, normal-graded tuffs located 400 m west of the Kam Kotia Mine open pit; C) angular coherent rhyolite lapilli within lapilli tuffs located approximately 300 m south-southeast of the Kam Kotia Mine open pit; D) flow banded spherulitic rhyolite located approximately 15 m south of the southeastern edge of the Kam Kotia Mine open pit; E) hydrothermally altered rhyolite hyaloclastite located on the western edge of the Kam Kotia Mine open pit; F) pillow basalts located approximately 75 m north of the Kam Kotia Mine open pit. The compass in all photos is 55 mm wide.

upward, four mappable facies were identified. The lowermost of these facies comprises a 4 to 25 m thick sequence of coherent spherulitic rhyolite with localized autoclastic and hyaloclastite breccias and tuff breccias that are locally replaced by pyrite-rich, semi-massive to massive sulphide mineralization up to 1 m thick on the southwestern wall of the Kam Kotia open pit. Nondeformed parts of this unit are characterized by up to 60% subangular, blocky to cuspate shard-shaped, commonly jigsaw puzzle-fit chloritized, locally quartz-phyric (1-2%, <1-2 mm phenocrysts) coherent rhyolite lapilli which have silicified clast margins ranging from 1 to 3 mm in thickness. Commonly, the unit is moderately to strongly sericitized (see below), sulphide mineralized, and moderately to strongly sheared, features which typically combine to obscure the original volcanic fabrics. Overlying this volcaniclastic facies is an 8 to 16 m thick, medium to dark grey, locally flow banded coherent spherulitic rhyolite facies (Photo 3D). This unit can be traced from approximately 50 m west of the Kam Kotia open pit to 400m east-southeastward. The coherent rhyolite is sparsely quartz-phyric (up to 3%, ≤ 1 mm euhedral to subhedral phenocrysts), sparsely to moderately amygdaloidal (2-10%, 0.3-2.0 cm rounded quartz ± carbonate amygdules) and contains up to 90%, 0.1 to 1.0 cm rounded to oval spherulites. Upwards, a second, 8 to 25 m thick horizon of coherent spherulitc rhyolite with localized autoclastic and hyaloclastite breccias and tuff breccias is present. This facies can be traced along strike east-southeastward from outcrops within the western part of the Kam Kotia open pit to the southeastern pit wall, where it has been significantly to totally replaced by up to several meters of semi-massive to massive pyrite, minor sphalerite, and minor chalcopyrite. Outcrops in the western part of the open pit display exceptional blocky, chlorite- and quartz-altered angular hyaloclastite (Photo 3E) that is locally crosscut by several generations of quartz-sulphide veins ranging from 0.5 to 10 cm thick. The uppermost facies of this sequence comprises an 8 to 33 m thickness of pale grey, locally flow-banded, sparsely quartz-phyric (1-2%, ≤ 1 mm subhedral to euhedral quartz phenocrysts), spherulitic (10-30%) rhyolite. Locally, exceptionally well-preserved perlitic fractures are preserved in this unit (*see* Barrie and Pattison 1999, Figure 5a). A lack of outcrop exposure does not permit surface observation of the upper contact of this unit.

Two lenses of mafic lapilli tuff, ranging from 11 m to 16 m in thickness, crop out along and above the northern wall of the Kam Kotia open pit. These massive deposits are characterized by a dark green, chlorite-rich matrix which contains up to 10%, <1 to 2 mm pale orange to pale green iron-carbonate and/or chlorite-altered, subhedral tabular feldspars and 15 to 20% oval, lens-shaped, and locally amoeboid scoria lapilli ranging from <1 to 6 cm in length. Scoria fragments are characterized by 20 to 30%, <1 mm oval to lens-shaped chlorite amygdules. A diabase sill obscures the contact relationships between this unit and both the underlying and overlying volcanic and volcaniclastic strata.

A third pillow basalt unit, ranging from at least 16 to 25 m thick, crops out approximately 65 m into the hangingwall of the largest Kam Kotia orebody. Northwest-striking (290°-298°), steeply north-dipping (82°-90°), bun- to mattress-shaped pillows vary from 0.2 to 0.5 m thick and 0.5 to 1.2 m wide, and are moderately flattened parallel to the northwest-trending foliation. The pillows locally contain 10 to 12%, 0.2 to 3.0 cm, oval to elliptical, locally radial pipe-like quartz ± carbonate amygdules. Blocky hyaloclastite deposits up to 3 cm thick surround individual pillows.

The uppermost stratigraphic unit mapped in the vicinity of the Kam Kotia Mine comprises feldspar- and quartz-phyric rhyolite tuffs and lapilli tuff. In outcrop, the unit is characterized by light- to medium-grey matrix which contains 5 to 10%, <1 mm blocky feldspar phenocrysts and up to 1%, <1 to 2 mm quartz pheonocrysts. Two distinctive types of lapilli are present in this unit: a) 2 to 5%, medium grey, commonly weathered-out, 0.5 to 5.0 cm diameter round to subround pumice; and b) 3 to 5%, medium grey, blocky to subround, locally amoeboid feldspar-phyric rhyolite lapilli. Petrographic observations indicate the presence of a very fine-grained, recrystallized quartz-feldspar matrix.

Three distinctive intrusive units occur in the vicinity of the Kam Kotia Mine: 1) Fine-grained diabase dikes and fine- to medium-grained diabasic to gabbroic sills and dikes occur in the immediate footwall and hanging wall to the largest of the Kam Kotia orebodies. Previous workers (Barrie and Pattison 1999) have mapped these rocks as massive basalt flows. However, the presence of sharp, fine-grained (apparently chilled) contacts, the lack of hyaloclastite and breccias along the contacts, and apparent cross-cutting relationships suggest that these mafic bodies are intrusive. The footwall sill is up to 90 m thick and is characterized by a distinctly amygdaloidal zone (up to 20%, 1 mm to 1 cm quartz amygdules) that is up to 4 m thick, occurs 1 to 3 m south of its sharp, fine-grained northern contact, and can be traced along strike for at least 450 m. Petrographic observations indicate that this unit is characterized by a fine- to medium-grained subophitic texture. The hanging wall sill varies from 50 to 65 m thick and is similar in field and petrographic characteristics to the footwall sill. 2) Fine-grained mafic dikes (described by Barrie and Pattison (1999) as pyroxenite dikes), ranging from less than one to several meters in width, occur locally on outcrops rimming the Kam Kotia open pit and appear to have crosscut the massive sulphide mineralization. 3) A third intrusion, the Steep Lake intrusion, strikes west-northwest, and can be observed in outcrop approximately 60 m north of the north wall of the Kam Kotia open pit, and approximately 150 m northeast of the northeast wall of the Kam Kotia open pit. This unit, which has previously been described as "mixed magma tuff" (Barrie and Pattison 1999) and "intermediate lapilli-tuff" or "Steep Lake tuff" (Hathway et al. 2004), is characterized by a pale grey to tan, locally spherulitic groundmass which contains 10 to 15%, 0.5 to 5.0 cm lens-, oval-, and amoeboid-shaped green to tannish-green chlorite- ± carbonate-rich lapilli-sized xenoliths.

Based on vertical projections of the former massive sulphide deposits (Barrie and Pattison 1990), the main Kam Kotia ore zone appears to have been hosted within rhyolite lava flows and associated rhyolite breccias and hyaloclastites. The common relationship between semi-massive and massive sulphide mineralization and rhyolite hyaloclastite suggests that the Kam Kotia deposits may have largely formed as a synvolcanic replacement-type (Doyle and Allen 2003) massive sulphide deposit. Up-dip ore projections, as well as descriptions of the ore geology by Somerville (1967) suggest that ore lenses to the west of the main Kam Kotia ore zone were hosted in mafic volcanic and volcaniclastic strata.

Alteration

Hydrothermal alteration in the vicinity of the Kam Kotia deposits (Photo 4) varies in intensity from moderate to strong, and affects all lithologies present. Chlorite, sericite, and locally, quartz, are the major alteration minerals present, with epidote, zoisite/clinozoisite, iron carbonate, and very fine-grained biotite or stilpnomelane occurring in minor amounts. Alteration mineral assemblage mapping indicates that chlorite alteration with local silicification is most prominent in the mafic and felsic footwall volcanic strata within approximately 150 m of the northeast-trending faults located southwest of the Kam Kotia open pit, and in the mafic volcanic and volcaniclastic rocks that make up the north wall of the open pit. Intense sericite alteration affects both coherent and volcaniclastic facies felsic rocks east of the zone of chlorite alteration in the immediate footwall to the main Kam Kotia deposit, suggesting the presence of a chlorite-sericite alteration pipe with a chlorite-rich core and sericite-rich margin. Less intense sericite alteration occurs in the felsic strata up-section from the deposit.

Mafic volcanic and volcaniclastic rocks, as well as mafic intrusive rocks, are moderately to strongly chlorite altered, and may be moderately to strongly silicified. Locally, chlorite-rich (up to 70%) domains of these strata are crosscut by veins up to several centimeters wide comprising quartz ± sulphide minerals (pyrite ± chalcopyrite) immediately southwest of the Kam Kotia open pit. This region has been interpreted by Barrie and Pattison (1999) to represent a zone of stringer mineralization associated with the overlying Kam Kotia VMS mineralization. Thin (up to several millimeters wide), pale green veins of

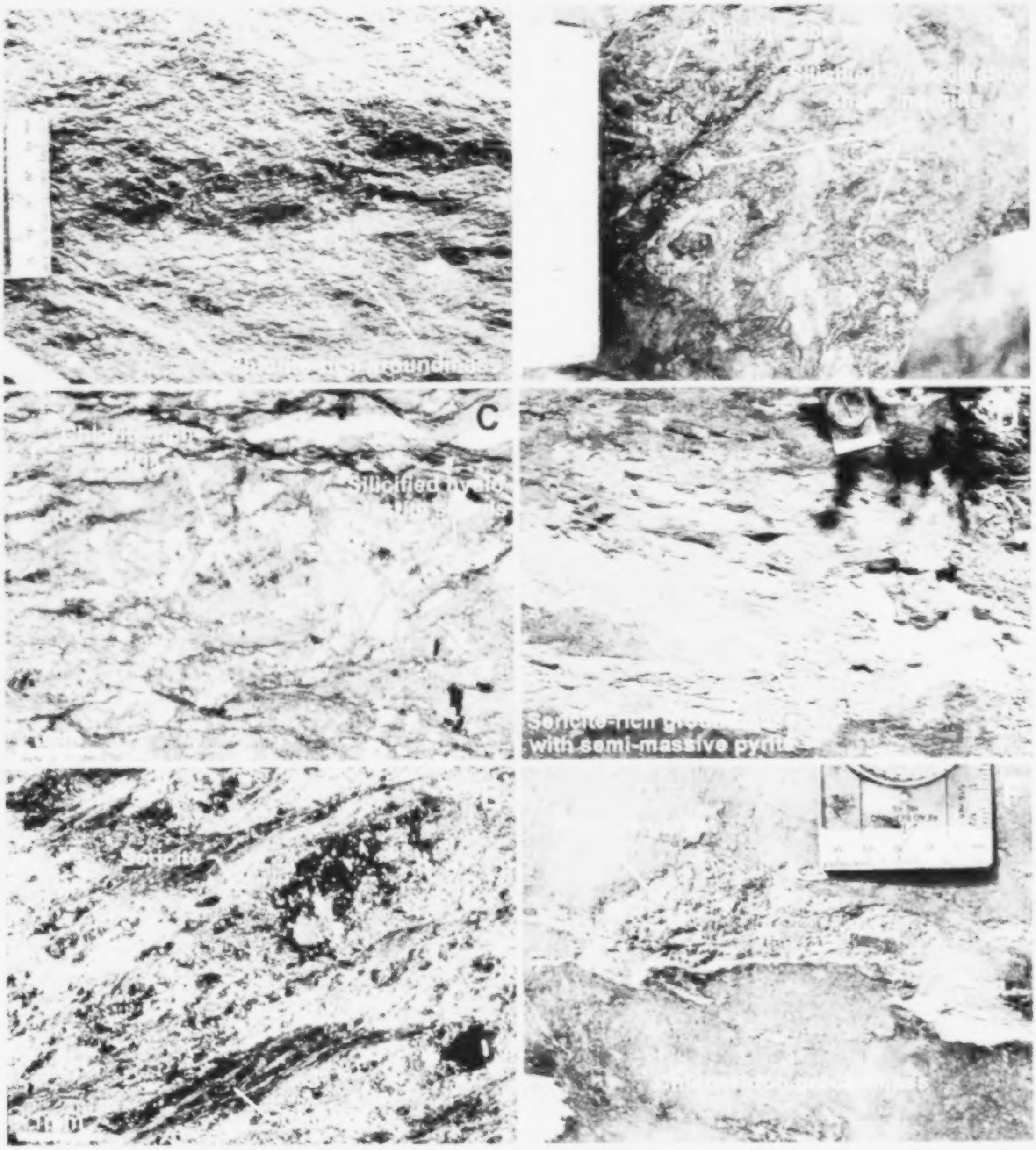
C
Silicified hyalo
Sericite-rich groundmass
with semi-massive pyrite
Sericite

Photo 4. Alteration in the vicinity of the Kam Kotia VMS orebody: A) chlorite-altered coherent spherulitic rhyolite, west wall of the Kam Kotia open pit; B) chloritized matrix and silicified clasts within rhyolite hyaloclastite deposits, west wall of Kam Kotia open pit; C) photomicrograph (crossed-polarized light) of chloritized and silicified rhyolite hyaloclastite, west wall of Kam Kotia open pit; D) sericite-altered rhyolite hyaloclastite from southeast wall of Kam Kotia open pit; E) photomicrograph (cross-polarized light) of chlorite- and sericite-altered hyaloclastite, southeast wall of Kam Kotia open pit; F) massive garnet within chloritized mafic footwall sill, south wall of Kam Kotia open pit.

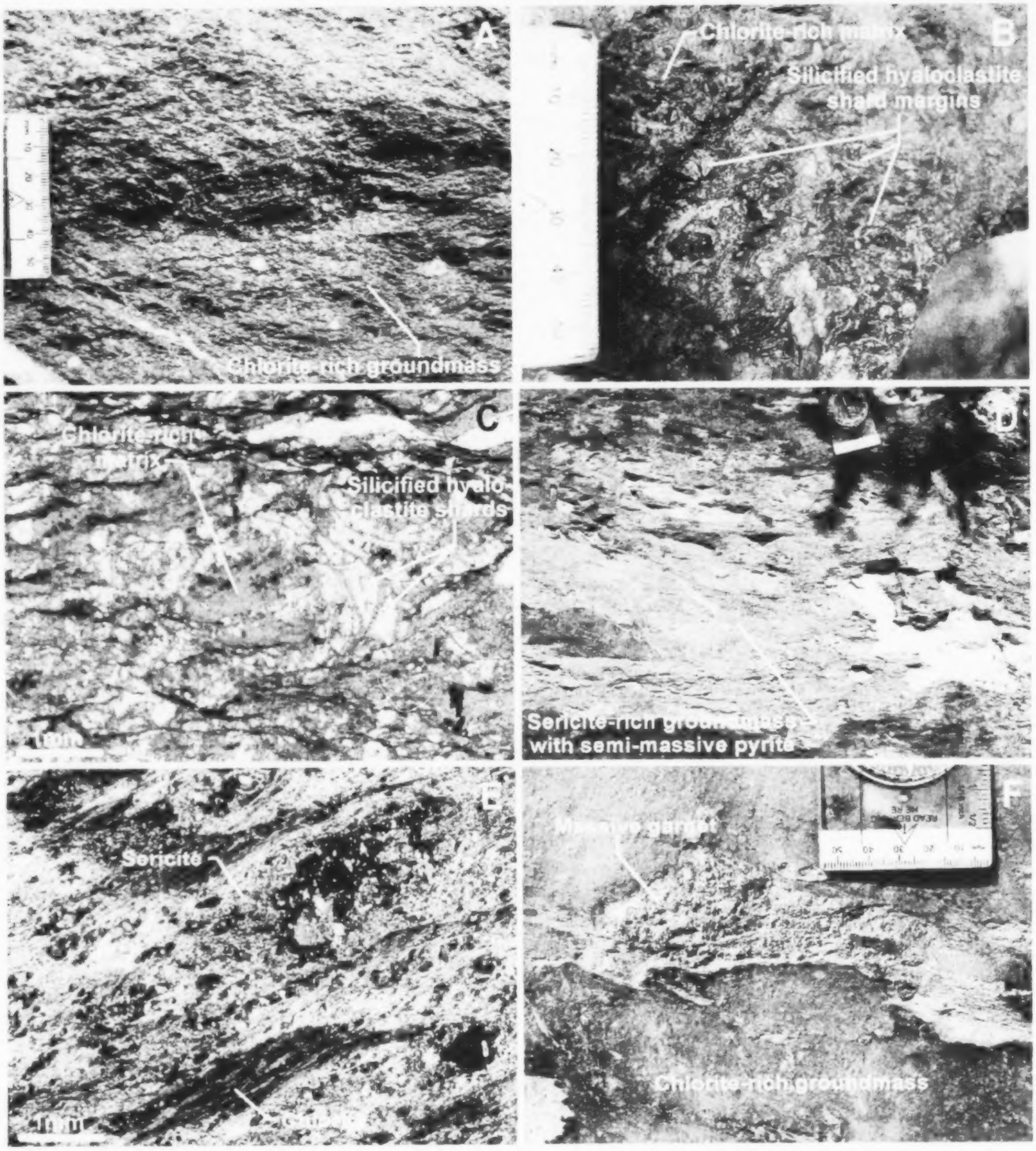
A
Chlorite-rich groundmass
B
Chlorite-rich matrix
Silicified hyaloclastite shard margins
C
Chlorite-rich matrix
Silicified hyaloclastite shards
1mm
D
Sericite-rich groundmass with semi-massive pyrite
E
Sericite
1mm
F
Massive garnet
Chlorite-rich groundmass

Photo 4. Alteration in the vicinity of the Kam Kotia VMS orebody: A) chlorite-altered coherent spherulitic rhyolite, west wall of the Kam Kotia open pit; B) chloritized matrix and silicified clasts within rhyolite hyaloclastite deposits, west wall of Kam Kotia open pit; C) photomicrograph (crossed-polarized light) of chloritized and silicified rhyolite hyaloclastite, west wall of Kam Kotia open pit; D) sericite-altered rhyolite hyaloclastite from southeast wall of Kam Kotia open pit; E) photomicrograph (cross-polarized light) of chlorite- and sericite-altered hyaloclastite, southeast wall of Kam Kotia open pit; F) massive garnet within chloritized mafic footwall sill, south wall of Kam Kotia open pit.

epidote ± quartz are also present. Petrographic observations indicate that the chlorite is consistently "Berlin-blue" to violet birefringent, which is characteristic of iron-rich chlorites based on electron microprobe analyses (Hudak 1996; Hocker et al. 2003). Epidote (up to 28%) is commonly present, and locally, anomalous blue birefringent, very fine-grained zoisite/clinozoisite (up to 30%) also occurs. Actinolite (up to 60%) locally occurs as pseudomorphs of original ferromagnesian phases within the mafic intrusive rocks.

Felsic volcanic and volcaniclastic strata vary from intensely chlorite altered, to moderately to intensely sericite altered. In general, both the chlorite and sericite are aligned parallel to the predominant S_2 foliation present in the strata. Intense chlorite alteration is present in felsic volcanic and volcaniclastic strata along the southwestern and western margins of the Kam Kotia open pit. Chlorite is evenly disseminated within coherent facies rhyolite. Rhyolite hyaloclastite deposits contain intensely chloritized cuspate lapilli rimmed by silicified zones <0.1 to 0.3 cm wide. Petrographic observations indicate that chlorite (up to 58%) is Berlin-blue birefringent and iron-rich. Strong (up to 75%) sericite alteration commonly occurs within, and immediately adjacent to, massive sulphide mineralization that crops out along the southeastern part of the Kam Kotia open pit. Sericite commonly occurs as an alteration product of the quartzo-feldspathic matrix or groundmass of the felsic strata, and varies in abundance from trace amounts to 40%. Locally, minor amounts of very fine-grained biotite or stilpnomelane (up to 11%) occur in thin (<1-2 mm wide) veins which typically crosscut the fabric formed by chlorite and/or sericite. Epidote and iron-carbonate locally occur in minor abundances.

Iron-rich chlorites commonly occur in hydrothermal upflow zones associated with VMS deposits (Hendry 1981; Larson 1984; Reed 1984; Kranidiotis and MacLean 1987; Morton and Franklin 1987; Koopman et al. 1999; Hannington et al. 2002). Sericite also commonly occurs proximal to hydrothermal upflow zones, but can also form extensive semiconformable alteration zones in felsic volcanic strata (Morton and Franklin 1987; Gibson et al. 1999). The presence of zoisite/clinozoisite in the mafic volcanic and intrusive rocks proximal to the Kam Kotia mineralization may be indicative of alteration proximal to hydrothermal upflow zones. Hannington et al. (2002) have found that epidote compositions associated with the VMS deposits in the Blake River Group of the Noranda mining camp in Quebec vary systematically, with zoisite/clinozoisite-bearing rocks occuring in hydrothermal upflow areas that experienced anomalous fluid flow at high water to rock ratios and higher temperatures.

Structure

The most prominent structures in the vicinity of the Kam Kotia mine are west- to northwest-striking, generally steeply north-dipping foliations. Foliation intensity is variable within the strata, with phyllosilicate-altered volcaniclastic strata commonly exhibiting more developed, more tightly spaced cleavage than less altered or coherent volcanic strata. It is commonly difficult to distinguish S_1 and S_2 foliations, perhaps due to transposition of the S_1 foliation into the later S_2 foliation (Hall and Smith 2002b). Where these two foliations can be distinguished (Figure 13a), S_1 is steeply north dipping and northwest trending (mean principle orientation 314°/81°N), whereas S_2 is west-northwest striking and generally steeply north dipping (mean principle orientation 285°/79°N). S_2 is the most prominent fabric in the strata in the vicinity of the Kam Kotia Mine.

Asymmetric, tight Z-shaped F_2 folds with east-northeast-trending fold axes locally occur in boudinaged fragments of felsic tuff deposits approximately 180 m northeast of the north wall of the Kam Kotia open pit, and in very thinly bedded to thinly bedded felsic tuffs approximately 400 m west of the

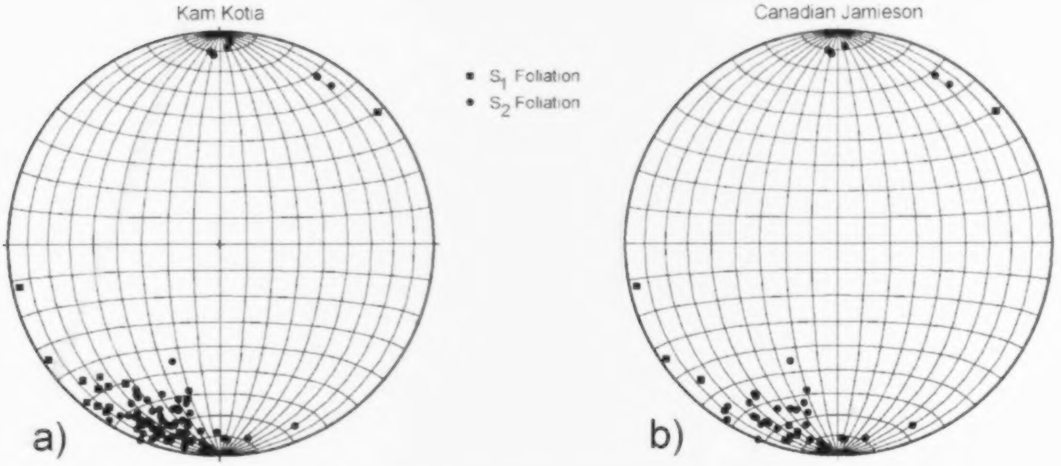

Figure 13. Stereonets showing poles to foliation planes in the immediate vicinities of a) the Kam Kotia and b) Canadian Jamieson deposits.

Kam Kotia pit. Rare, tight W-shaped folds with east-southeast-trending fold axes occur in laminated to very thinly bedded tuff deposits located approximately 80 m north of the Kam Kotia open pit, and may be related to synvolcanic soft sediment deformation.

Three northeast-striking faults have been tentatively identified in the region south and west of the Kam-Kotia open pit based on offsets in stratigraphy, VMS horizons, and the presence of diabase dikes (*see* Figure 12). The orientation of the most westerly of these faults is poorly constrained due to a lack of outcrop, and is based largely on offsets in the vertical projections in VMS horizons. The most recent movement on this fault likely occurred during the D_2 deformation event (Barrie and Pattison 1999). The two faults located immediately south-southwest of the Kam Kotia open pit are believed to be synvolcanic structures that may have been reactivated during D_2. Evidence for synvolcanic faults includes the presence of dikes or apophyses of synvolcanic intrusions, abrupt changes in unit thicknesses, and offsets of a unit with subsequent units not offset (Gibson et al. 1999). Note on Figure 12 that the second horizon of basalt pillow lavas and associated hyaloclastite deposits does not crop out east of the westernmost of these faults, suggesting that a synvolcanic basin may have been developed west of this structure. The easternmost of these faults has been identified by the presence of a disconformable diabase intrusion which may have been a feeder to the footwall sill.

Discussion – Kam Kotia Mine

Detailed mapping has identified the various volcanic facies and intrusive strata that occur in outcrops in the immediate vicinity of the Kam Kotia massive sulphide orebodies. In summary, the sequence comprises a bimodal sequence of supracrustal Neoarchean coherent and volcaniclastic mafic and felsic rocks and chemical sedimentary rocks, along with mafic intrusive rocks. Pillowed basalts, mafic and felsic hyaloclastite deposits, chert horizons, massive sulphide mineralization, and hydrothermal alteration assemblages consistent with those found in modern seafloor hydrothermal systems indicate that the volcanic section in this region was originally deposited in a subaqueous environment. Field alteration mineral assemblage mapping, supplemented by petrographic studies, suggests the presence of a northeast-oriented discordant iron-rich chlorite alteration pipe that is at least 200 m wide and extends upward to the southwestern part of the Kam Kotia open pit. Sericite alteration is most prevalent in footwall volcanic strata along the southeastern part of the Kam Kotia open pit, and in felsic volcaniclastic strata which occur up-section from the VMS mineralization.

Although the presence of amygdule-rich coherent facies strata has been used by previous authors (Barrie and Pattison 1999) to suggest formation in a shallow submarine environment, the depth of water at which the VMS and associated volcanic and volcaniclastic strata were deposited remains poorly constrained. The lack of wave-generated bedforms in the volcaniclastic strata indicates deposition in at least 150 to 200 m of water (Draper 1967; Butman et al. 1979). The presence of copper-zinc VMS mineralization indicates that synvolcanic hydrothermal solutions genetically associated with the mineralization were under sufficient hydrostatic pressure to prevent extensive boiling of the hydrothermal fluids. This occurs only in water depths of at least several hundred metres in modern seafloor VMS hydrothermal systems (Herzig and Hannington 1995).

CANADIAN JAMIESON MINE AREA

Surface geological mapping, at a scale of 1:5000 to 1:1000, was completed to evaluate the volcanic stratigraphy, alteration mineralogy, and structural deformation present in the immediate vicinity of the Canadian Jamieson orebodies (Figure 14). These deposits produced 740 000 tonnes (816 000 tons) of massive sulphide ore averaging 2.4% Cu and 4.2% Zn between 1966 and 1971 (Binney and Barrie 1991; Barrie 2000). Descriptions of the VMS mineralization at Canadian Jamieson can be found in Binney and Barrie (1991) and Barrie (2000).

Stratigraphy

Geological mapping indicates that the Canadian Jamieson area is composed of an east-northeast-younging, northwest-striking sequence of subaqueously deposited mafic and felsic coherent and volcaniclastic facies strata, chemical metasedimentary rocks (exhalites), and intermediate to mafic intrusive rocks. The surface geology, based on mapping for this study, is presented in Figure 14.

A sequence of north-northwest-striking (350°), steeply east-dipping and east-topping pillow basalts and associated hyaloclastite deposits at least 140 m thick comprise the base of the stratigraphic sequence in the vicinity of the Canadian Jamieson deposits. Bun- and mattress-shaped pillows are relatively well-preserved, and vary from 0.5 to 2.0 m thick by 1.0 to 3.0 m wide. Pillow selvedges typically contain 5 to 8%, 0.1 to 0.3 cm, oval to round quartz ± carbonate-filled amygdules. Fine-grained interpillow hyaloclastite zones vary from 2 to 8 cm in width, and are strongly chloritic. The easternmost contact of this unit is intruded by olivine diabase and diabase dikes.

Laminated to thinly bedded, locally cross-bedded felsic tuffs (Photo 5A) comprise an up to 6.5 m thick sequence that occurs immediately east of the olivine diabase and diabase dikes, and appears to occur immediately up-section from the pillow basalts described above. The orientation of bedding in the tuffs generally varies from 328°/80°E to 343°/80°E, and is locally tightly folded about northwest-trending D_2 fold axes (described below). Petrographic studies indicate that these rocks are characterized by a variably altered, very fine-grained matrix of recrystallized quartz and feldspar. Up to 1%, <1 mm angular quartz phenocrysts are locally present. A massive basalt lava flow or sill up to 22 m thick immediately stratigraphically overlies, and occurs in sharp contact with, the felsic tuffs.

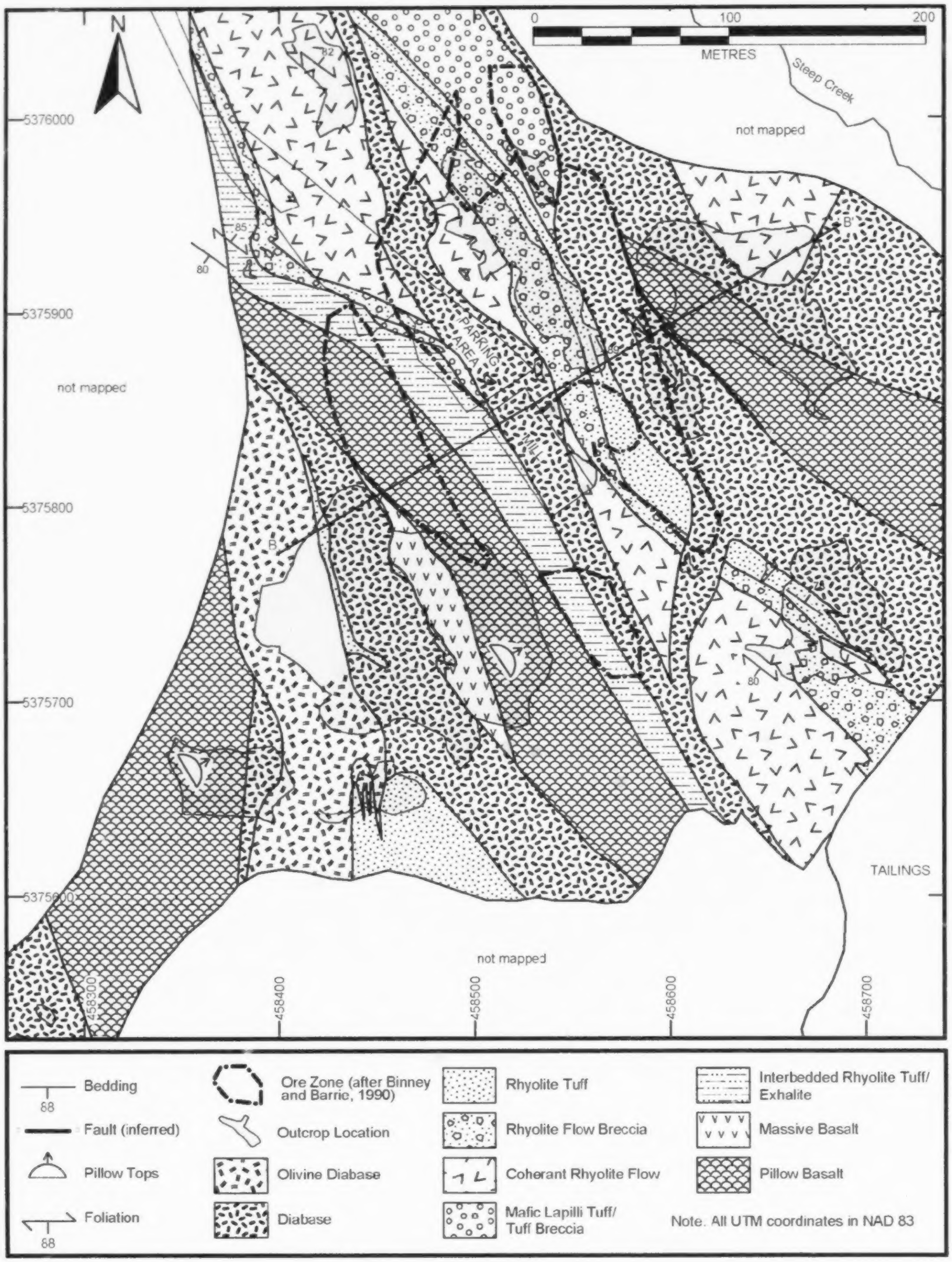
N
0
100
200
METRES
Steep Creek
not mapped
5376000
5375900
5375800
5375700
5375600
not mapped
PARKING AREA
MILL
B
B'
82
85
80
80
TAILINGS
not mapped
458300
458400
458500
458600
458700
Bedding
88
Fault (inferred)
Pillow Tops
Foliation
88
Ore Zone (after Binney and Barrie, 1990)
Outcrop Location
Olivine Diabase
Diabase
Rhyolite Tuff
Rhyolite Flow Breccia
Coherant Rhyolite Flow
Mafic Lapilli Tuff/ Tuff Breccia
Interbedded Rhyolite Tuff/ Exhalite
Massive Basalt
Pillow Basalt
Note. All UTM coordinates in NAD 83

Figure 14. Detailed surface geological map of the Canadian Jamieson Mine area. Cross-section B-B′ is presented in Figure 15.

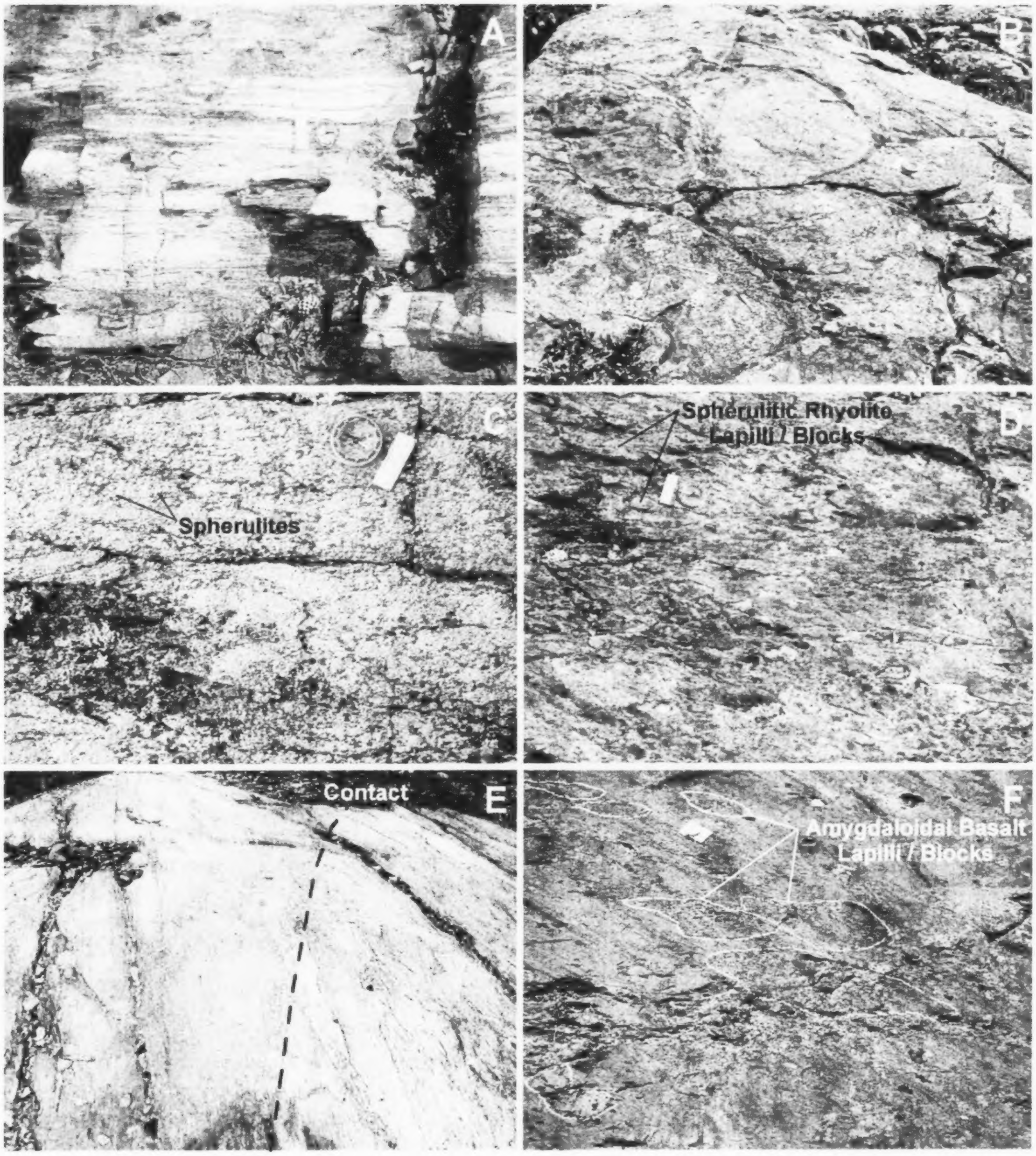
A
B
C
Spherulites
Spherulitic Rhyolite Lapilli / Blocks
D
Contact
E
F
Amygdaloidal Basalt Lapilli / Blocks

Photo 5. Field photographs of various lithologies in the vicinity of the Canadian Jamieson VMS deposits. A) laminated to very thinly bedded tuffs located 100 m southwest of the former mill; B) pillow basalts and associated interpillow hyaloclastite deposits located 50 m south of the former mill; C) spherulitic coherent rhyolite located 100 m north of the former mill; D) rhyolite flow breccia located 70 m north of the former mill; E) contact between rhyolite flow breccia (left side of photo) and stratigraphically overlying rhyolite tuff; and F) mafic tuff breccia containing lapilli- and block-sized amygdaloidal basalt fragments (outlined on outcrop with white chalk). The compass in all photos is 55 mm wide.

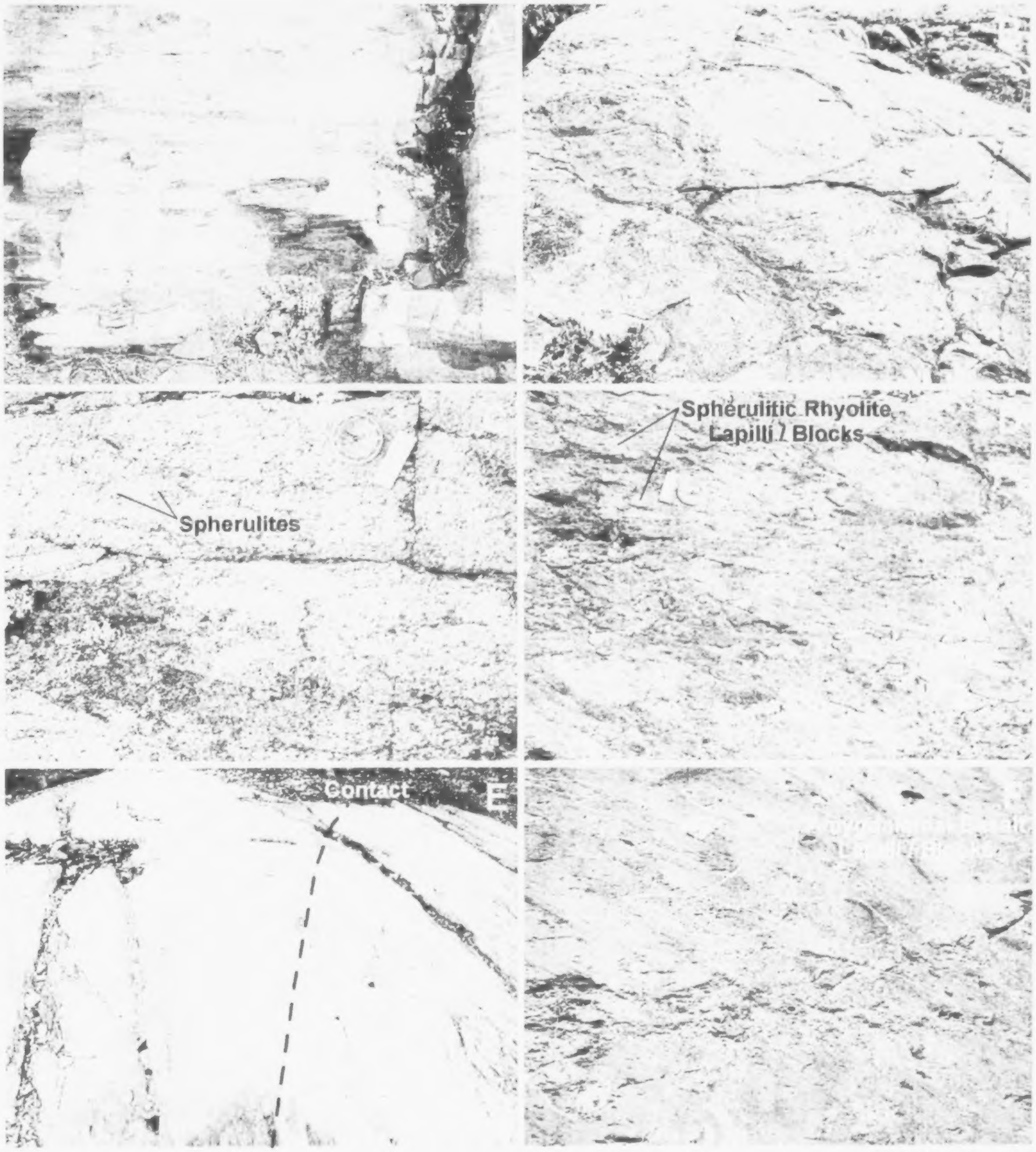

Photo 5. Field photographs of various lithologies in the vicinity of the Canadian Jamieson VMS deposits. A) laminated to very thinly bedded tuffs located 100 m southwest of the former mill; B) pillow basalts and associated interpillow hyaloclastite deposits located 50 m south of the former mill; C) spherulitic coherent rhyolite located 100 m north of the former mill; D) rhyolite flow breccia located 70 m north of the former mill; E) contact between rhyolite flow breccia (left side of photo) and stratigraphically overlying rhyolite tuff; and F) mafic tuff breccia containing lapilli- and block-sized amygdaloidal basalt fragments (outlined on outcrop with white chalk). The compass in all photos is 55 mm wide.

A second horizon of north- to northwest-striking, east-facing pillowed basalt and associated hyaloclastite up to 60 m thick occurs immediately up-section from the massive basalt (Photo 5B). These rocks are similar in appearance and lithological characteristics to the pillow lava/hyaloclastite unit described above.

Overlying the pillowed flows is a 10 to 25 m thick sequence of interbedded felsic tuff and sulphide-bearing exhalite horizons. This unit crops out approximately 140 m northwest of the former mill and comprises interbedded northwest-striking, steeply west-dipping, locally sulphide-stained chert horizons (up to 10 cm thick), and laminated to very thinly bedded tuff horizons.

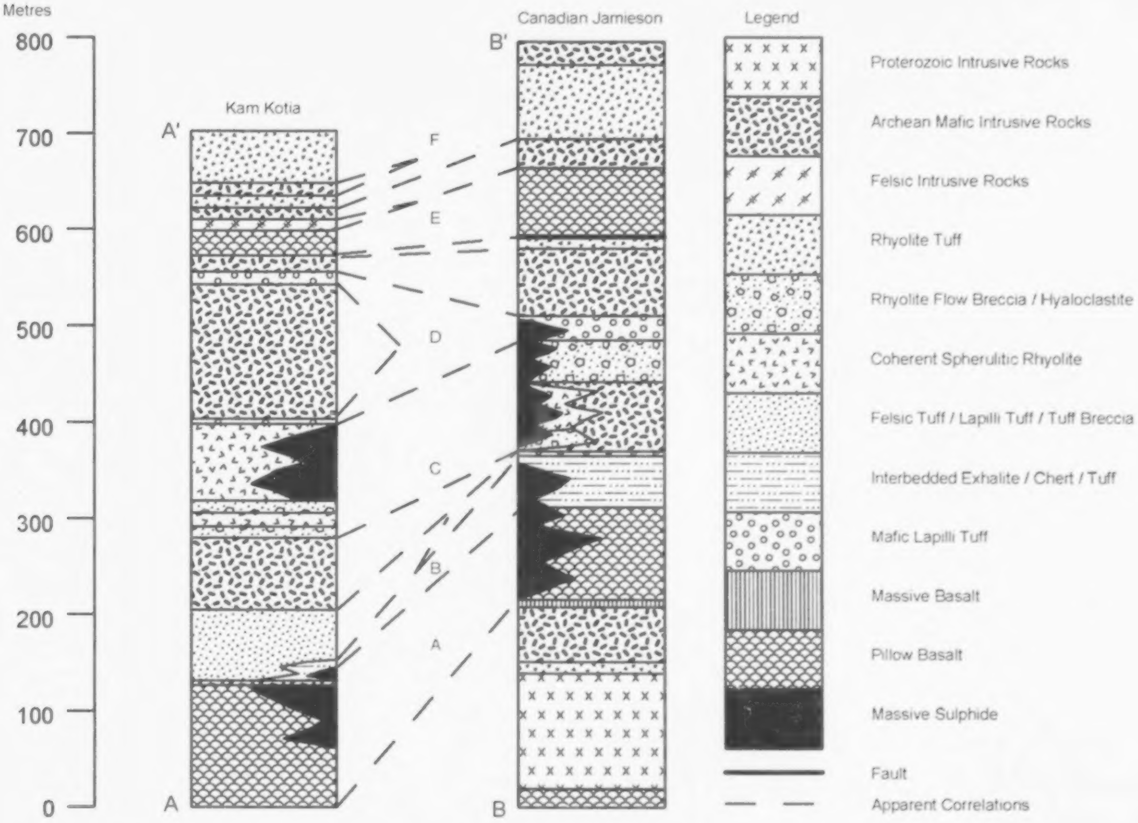
Metres
800
700
600
500
400
300
200
100
0
Kam Kotia
A'
A
Canadian Jamieson
B'
B
F
E
D
C
B
A
Legend
Proterozoic Intrusive Rocks
Archean Mafic Intrusive Rocks
Felsic Intrusive Rocks
Rhyolite Tuff
Rhyolite Flow Breccia / Hyaloclastite
Coherent Spherulitic Rhyolite
Felsic Tuff / Lapilli Tuff / Tuff Breccia
Interbedded Exhalite / Chert / Tuff
Mafic Lapilli Tuff
Massive Basalt
Pillow Basalt
Massive Sulphide
Fault
Apparent Correlations

Figure 15. Apparent stratigraphic correlations between the Kam Kotia and Canadian Jamieson VMS deposits based on composite stratigraphic sections at the two deposits (*see* Figures 12 and 14 for locations of sections A-A′ and B-B′, respectively). Note that the detailed lithostratigraphic sequences and stratigraphic positioning of VMS mineralization at the two deposits are similar. From the base of the stratigraphic sections, these correlations include A) pillowed basalt with VMS mineralization; B) exhalites, cherts, and tuffs and associated VMS mineralization; C) rhyolite lavas flows and associated volcaniclastic facies with VMS mineralization; D) mafic lapilli tuffs and tuff breccias with VMS mineralization; E) pillow basalts; and F) felsic tuffs. Stratigraphic positions of the VMS mineralization at the Kam Kotia deposit based on Barrie and Pattison (1999). Stratigraphic positions of the VMS mineralization at the Canadian Jamieson Mine based on Binney and Barrie (1991).

The interbedded exhalite and tuff deposits are overlain by a sequence of mafic, monomict to polymict lapilli tuffs. The deposits are characterized by a fine- to coarse-ash, chlorite-rich matrix which contains up to 1% angular chert lapilli and up to 5% subrounded to rounded amygdaloidal basalt lapilli containing 5 to 10% oval to rounded quartz amygdules. The unit appears to be massive and nongraded.

Coherent spherulitic rhyolite and associated autoclastic and hyaloclastite breccias (Photos 5C and D) occur up-section from the exhalite and tuff deposits, and based on vertical projections of the VMS mineralization, comprise the immediate footwall and host strata to VMS mineralization at the Canadian Jamieson Mine. The base of this sequence crops out approximately 125 m northwest of the former mill, and comprises an autoclastic rhyolite breccia which is up to 13 m thick and contains up to 10% angular to subrounded, locally spherulitic coherent rhyolite lapilli in a fine-grained felsic matrix. Coherent rhyolite occurs immediately up-section, and is up to 65 m thick. This facies comprises massive to faintly flow-banded rhyolite containing <1 to 2%, 1-2 mm quartz phenocrysts and up to 40%, 1 to 3 mm, pale grey round to oval spherulites. Petrographic observations indicate that the groundmass is composed of fine- to medium-grained recrystallized polygonal quartz and feldspar mosaics. The coherent rhyolite grades eastward and stratigraphically upward into a second horizon of rhyolite autoclastic and hyaloclastic breccia which is up to 25 m thick. This sequence of facies is similar to those noted by Gibson (1990) for Archean felsic lobe-hyaloclastite flows in the Noranda mining camp of Quebec, and by Yamagishi (1991) for submarine felsic lava flows of Neogene age in Japan.

An obscure but sharp contact trending beween 335° and 350° occurs between rhyolite autoclastic and hyaloclastite breccias and a stratigraphically overlying 10 to 20 m thick sequence of very thinly bedded to medium-bedded felsic tuffs (Photo 5E). These tuffs are generally normal graded, with individual graded beds comprising coarse, locally <0.1 cm diameter quartz crystal chip-rich bases which grade upward into finer, crystal-poor tops. The sequence likely represents deposits from low-concentration subaqueous mass flows.

A sulfide-rich, clast-bearing, strongly chlorite and/or carbonate-altered, matrix-supported mafic lapilli tuff/tuff breccia immediately overlies the felsic tuffs. This massive mafic unit is up to 40 m thick, and comprises 10 to 15% subangular to subrounded lapilli- to block-sized amygdaloidal basalt clasts (Photo 5F), with subordinate angular coherent rhyolite lapilli in a fine-grained chorite-rich matrix. Lens-shaped clasts (up to 15 cm in diameter) consisting of dark grey quartz and semi-massive pyrite comprise 10 to 12% of the unit. Barrie (2000) notes that this unit forms the on-strike extension to the Canadian Jamieson "north ore zone", which occurred approximately 70 m north of the former mill site 10 m below surface.

A third horizon of pillowed basalt and associated hyaloclastite occurs up-section from the mafic tuffs and tuff breccias, and is up to 70 m thick. The unit comprises bun- to mattress-shaped pillows that are similar in morphology to mafic pillows found lower in the section, but contain only up to 5% rounded to oval quartz vesicles up to 1 cm in diameter.

The uppermost stratigraphic unit mapped in the vicinity of the Canadian Jamieson Mine comprises a sparsely quartz-phyric rhyolite tuff. The unit is massive, and is up to 80 m thick. No sulphide mineralization was observed within these deposits.

Two distinctive intrusive units crosscut the volcanic and sedimentary stratigraphy in the vicinity of the Canadian Jamieson deposits. Fine- to medium-grained, north-northwest-trending Archean diabase dikes occur in the central and eastern parts of the study area. These dikes commonly contain polygonal tortoise-shell jointing, as well as columnar jointing which is now horizontally inclined due to the steep dip of the strata. Such structures suggest these dikes are synvolcanic and were quenched by cool seawater (McPhie et al. 1993). Coarser-grained olivine diabase dikes (Matachewan dikes) occur in the south-central part of the field area. Crosscutting relationships clearly indicate that the diabase dikes pre-date the olivine diabase dikes.

Based on vertical projections of the ore horizons (Binney and Barrie 1991, *see* Figure 40.2), massive sulphide mineralization at the Canadian Jamieson deposit appears to be associated with interbedded rhyolitic tuffs and chert-rich chemical metasedimentary rocks, rhyolitic lava flows and associated flow breccias, and mafic lapilli tuffs and tuff breccias. Based on surface exposures observed during field mapping, sulphide mineralization in the Canadian Jamieson area appears to have at least locally replaced the matrix of the volcaniclastic strata, suggesting that this deposit may also, in part, be of the synvolcanic replacement-type (Doyle and Allen 2003).

Alteration

Hydrothermal alteration in the vicinity of the Canadian Jamieson deposit is dependent upon both stratigraphic position and lithological composition. Rocks in the vicinity of the mineralization are generally chloritized and sericitized, although local silicification and epidotization are also present (Photo 6). Binney and Barrie (1991) note that the Canadian Jamieson Mine lacks a significant alteration zone stratigraphically below the VMS mineralization. Field and petrographic observations made during this study, however, indicate evidence for the local presence of high temperature, likely acidic hydrothermal fluids believed to be associated with the VMS mineralization.

Mafic coherent and volcaniclastic rocks are generally chlorite altered. In the field, chloritic alteration varies from patchy and disseminated to pervasive. Petrographic observations indicate that the chlorite is fine grained, and is characterized by anomalous "Berlin-blue" birefringence characteristic of an iron-rich composition. Chlorite (11-42%) is commonly associated with fine-grained, disseminated carbonate, with iron carbonate (based on brown-stained grain margins) appearing only in the footwall volcanic strata (up to 2%) and calcite (3-25%) occurring in both the hanging wall and footwall rocks. Patchy to dendritic veins (up to 1 cm across) of epidote are locally present in the mafic volcanic strata. Petrographic observations indicate that epidote (up to 22%) is found in mafic volcanic rocks in both the hanging wall and footwall, whereas anomalous, blue-birefringent, very fine-grained zoisite/clinozoisite (up to 36%) occurs only in the footwall mafic strata. Patchy silicification (5-8%) locally occurs in pillowed mafic flows and associated hyaloclastite deposits 50 to 100 m south-southwest of the former mill. Similar iron-chlorite alteration, patchy silicification, and patchy to vein epidote alteration occur in the Archean diabase dike that occurs in proximity to the Canadian Jamieson mineralization.

Felsic coherent and volcaniclastic rocks are generally sericite-altered in the vicinity of the Canadian Jamieson deposits, although chloritic alteration is locally present. Both varieties of phyllosilicate minerals are oriented parallel to the major foliations present in the strata. Alteration intensity in the coherent facies strata varies from moderate to intense. These rocks contain 15 to 43% fine-grained sericite and up to 10% fine-grained, "Berlin-blue" birefringent iron-rich chlorite. Sericitic alteration is most intense in coherent facies rocks that crop out approximately 50 to 100 m north of the former mill. Chloritic alteration is most intense in coherent facies strata which crop out approximately 100 m south-southeast of the former mill. Sphalerite occurs locally in trace quantities within the altered coherent facies strata. Felsic volcaniclastic facies strata are generally sericite-altered (up to 40% sericite), but locally contain up to 20% fine-grained iron-rich chlorite. One sample from footwall felsic tuffs located approximately 100 m southwest of the former mill also contained up to 1% andalusite. Andalusite alteration occurs proximal to VMS mineralization in the Archean Sturgeon Lake VMS camp (Morton et al. 1991; Morton and Franklin 1987; Hudak 1996), the Archean Onaman VMS prospect (Osterberg et al. 1987), and the Archean Bousquet

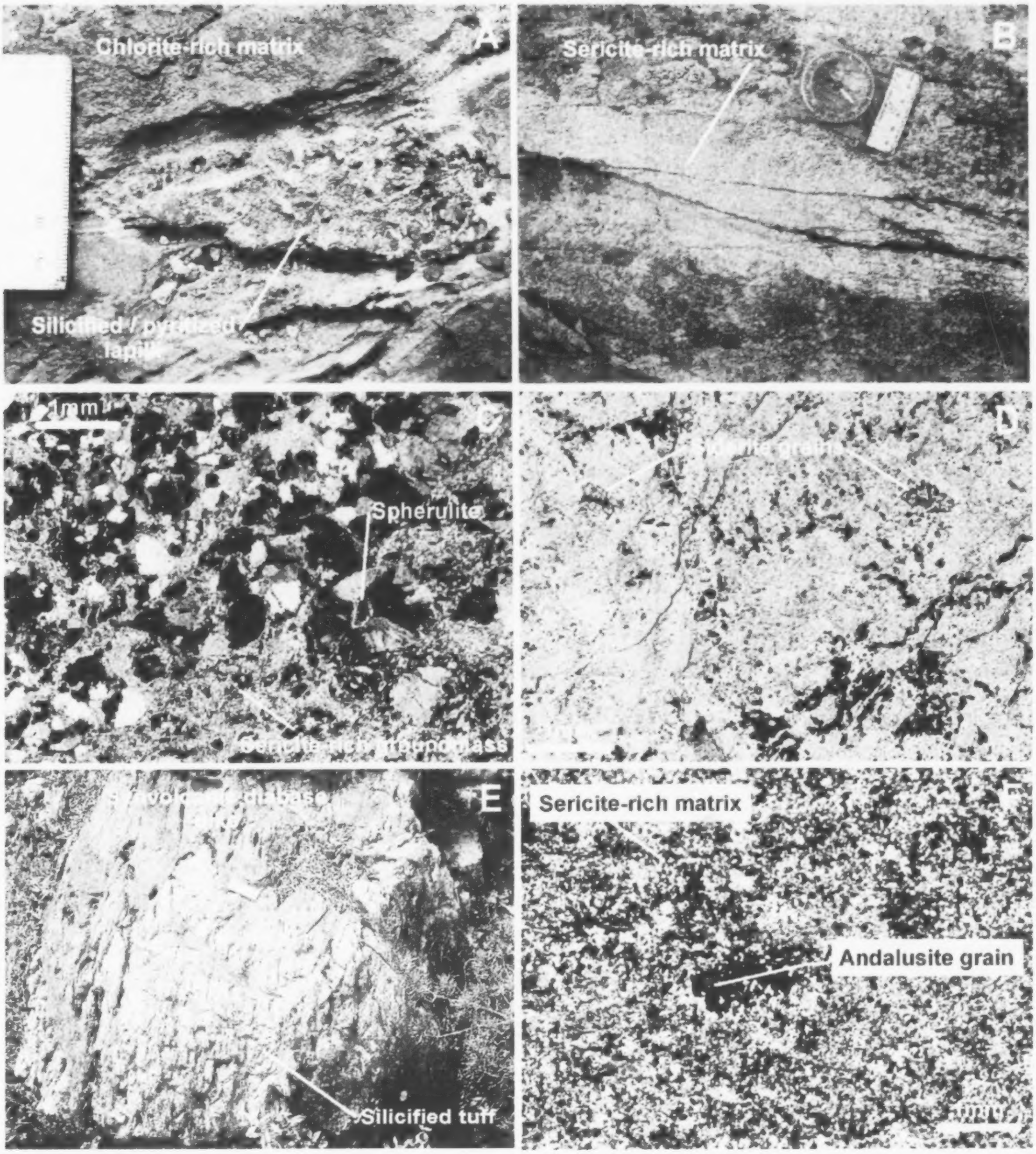
Chlorite-rich matrix
A
Silicified / pyritized lapilli
Sericite-rich matrix
B
1mm
C
Spherulite
Sericite-rich groundmass
D
Siderite grains
Synvolcanic diabase
E
Silicified tuff
Sericite-rich matrix
F
Andalusite grain
1mm

Photo 6. Alteration in the vicinity of the Canadian Jamieson VMS orebody: A) chloritized pillow breccia containing pyrite- and quartz-replaced lapilli located immediately along strike with the north ore zone; B) sericitized spherulitic coherent rhyolite located 75 m north of former Canadian Jamieson mill; C) photomicrograph (cross-polarized light) of sericite-altered spherulitic coherent rhyolite; D) photomicrograph (plane-polarized light) illustrating siderite grains in rhyolite tuffs in footwall to the Canadian Jamieson VMS orebodies; E) silicified rhyolite tuffs in footwall to the Canadian Jamieson VMS orebodies; F) photomicrograph of andalusite grain in strongly sericite-altered rhyolite tuffs occurring in the footwall to the Canadian Jamieson VMS deposits.

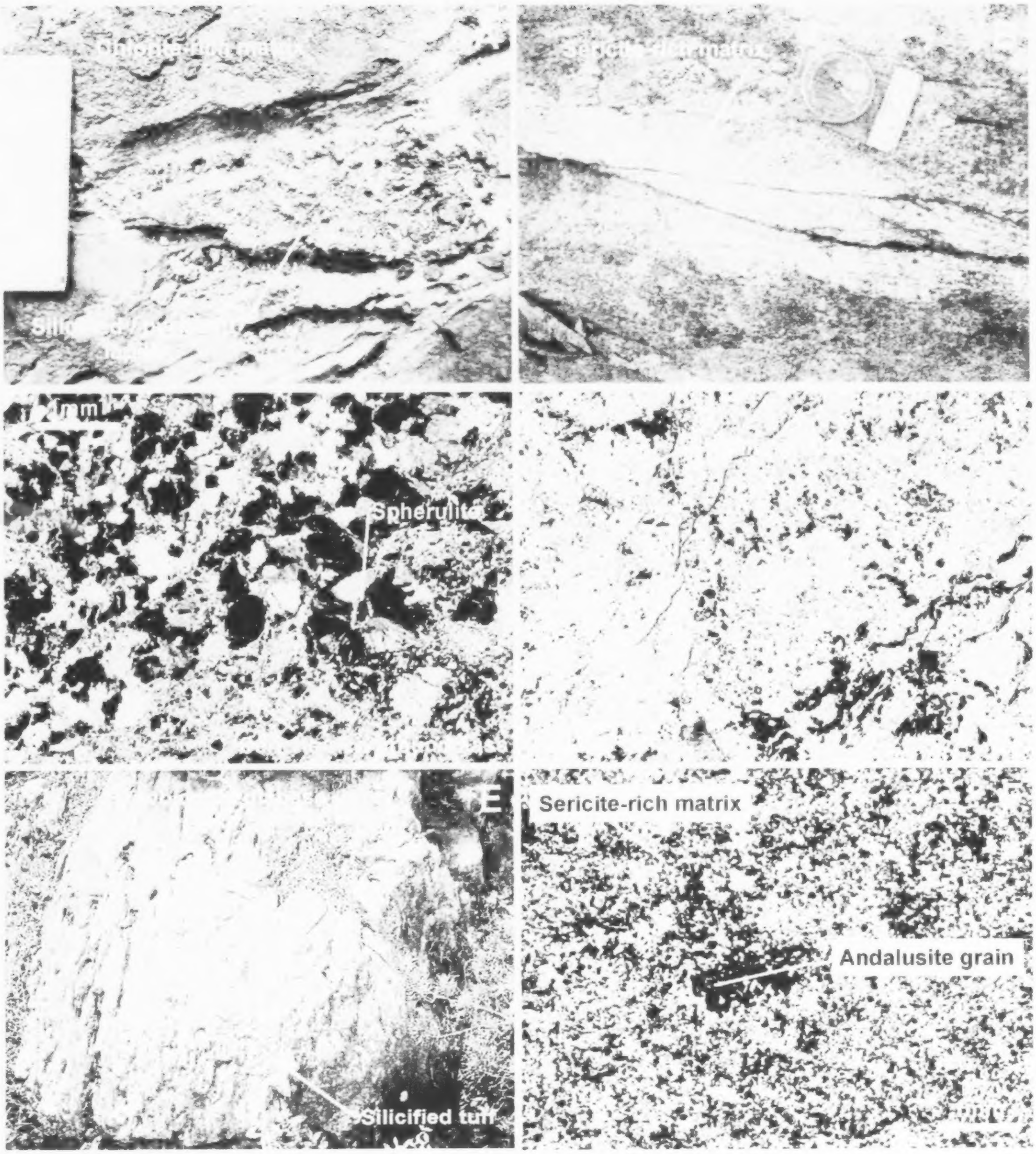

Photo 6. Alteration in the vicinity of the Canadian Jamieson VMS orebody: A) chloritized pillow breccia containing pyrite- and quartz-replaced lapilli located immediately along strike with the north ore zone; B) sericitized spherulitic coherent rhyolite located 75 m north of former Canadian Jamieson mill; C) photomicrograph (cross-polarized light) of sericite-altered spherulitic coherent rhyolite; D) photomicrograph (plane-polarized light) illustrating siderite grains in rhyolite tuffs in footwall to the Canadian Jamieson VMS orebodies; E) silicified rhyolite tuffs in footwall to the Canadian Jamieson VMS orebodies; F) photomicrograph of andalusite grain in strongly sericite-altered rhyolite tuffs occurring in the footwall to the Canadian Jamieson VMS deposits.

gold-rich polymetallic sulfide deposit (Tourigny et al. 1993) and is believed to represent alteration by high temperature, metalliferous, acidic fluids which have caused extreme alkali depletion. At the Canadian Jamieson deposit, the region in which andalusite alteration occurs may represent proximity to synvolcanic faults and hydrothermal upflow zones that were genetically associated with VMS mineralization.

Structure

The most prominent structures in the vicinity of the Canadian Jamieson Mine are west- to northwest-striking, generally steeply north-dipping foliations (*see* Figure 13). Foliation intensity varies significantly within the strata, being significantly better developed where phyllosilicate (typically sericitic) alteration is more intense. In the northeast part of the study area, structural deformation was largely confined to pre-existing, phyllosilicate-rich hydrothermal alteration zones associated with massive sulphide mineralization in the volcanic and volcaniclastic strata.

As in the vicinity of the Kam Kotia deposit, it is generally difficult to distinguish S_1 and S_2 foliations. Where distinguishable, S_1 is steeply north dipping and northwest trending (mean principle orientation 327°/85°N), whereas S_2 is west-northwest striking and generally steeply north dipping (mean principle orientation 283°/79°N). S_2 is the most prominent fabric in the strata in the vicinity of the Kam Kotia Mine.

Two distinct types of folds are present in the vicinity of the Canadian Jamieson deposits. Asymmetric, tight Z-shaped and W-shaped folds located approximately 100 m southeast of the southeastern corner of the former mill have fold axes which trend 320° and plunge 21°SE. These folds deform the northwest-trending S_1 foliation, and are at least D_2 in age. Broad F_3 folds with northeast-trending axes are locally present in strongly S_2-foliated coherent rhyolite approximately 100 m north of the former mill site.

Structural deformation in the northeastern part of the property consists of north-northwest-trending D_2 shear zones, up to 1 m wide, in sericite-altered felsic lava flows and associated volcaniclastic rocks, approximately 130 m north of the former mill. Approximately 75 m northeast of the former mill, northwest-trending boudin-like bodies of felsic tuff occur within diabase dikes adjacent to a 0.2 to 0.6 m wide chlorite-rich shear zone.

Post-volcanic fault zones were not identified by the regionally limited mapping performed in the Canadian Jamieson area. A possible north-northeast-trending synvolcanic fault zone may be present where the disconformable diabase dike occurs approximately 100 m southeast of the former Canadian Jamieson mill, and a disconformable synvolcanic fault zone may occur in proximity to andalusite-altered felsic strata in the footwall.

Discussion – Canadian Jamieson Mine

Detailed mapping has recognized the volcanic facies that occur in the vicinity of the Canadian Jamieson deposits. In summary, the region comprises a bimodal stratigraphic sequence composed of Archean mafic to intermediate lava flows and volcaniclastic rocks, felsic lava flows and volcaniclastic rocks, chemical sedimentary rocks, and diabase dikes, as well as Proterozoic olivine diabase dikes. Pillowed mafic to intermediate lava flows, exhalite deposits, and massive sulphide mineralization suggest deposition of the volcanic strata in a subaqueous environment. Due to a lack of subsurface data at the present time, it is difficult to determine with any certainty the spatial relationships of mineralization and stratigraphy in the Canadian Jamieson area. Based on field data collected during this study, it appears that massive sulphide mineralization occurs within interbedded rhyolite tuffs and chert-rich chemical metasedimentary rocks, rhyolite lava flows and associated flow breccias, and mafic lapilli tuffs and tuff breccias. The most eastern of the ore lenses, the "north ore zone" (Barrie 2000), is closely spatially related to strongly sheared felsic volcanic and volcaniclastic strata and Archean diabase dikes.

Tortoise-shell jointing and epidote-rich alteration veins within the Archean diabase dikes suggest thermal and chemical interaction with seawater. These jointed and altered intrusive rocks may represent synvolcanic feeder dikes to basalt lava flows that occur up-section of the Canadian Jamieson area. The distribution of these dikes may indicate the presence of synvolcanic structures that could be associated with hydrothermal upflow zones and possible base-metal sulphide mineralization.

Sericite- and chlorite-rich alteration mineral assemblages locally present in the Archean metavolcanic, metasedimentary, and meta-intrusive rocks are consistent with mineral assemblages developed by subaqueous hydrothermal systems proximal to VMS mineralization (Franklin 1986; Morton and Franklin 1987; Gibson et al. 1999). Minor andalusite that occurs locally in the footwall rhyolite tuffs may represent areas which have undergone extensive synvolcanic alteration by high temperature acidic hydrothermal fluids moving upward toward the paleoseafloor near synvolcanic fault zones. Such aluminium-silicate-bearing alteration assemblages occur in close proximity to Archean VMS mineralization in the Sturgeon Lake camp of northwestern Ontario (Morton et al. 1991; Hudak 1996), the Onaman VMS prospect of northwestern Ontario (Osterberg et al. 1987), and the Archean Bousquet gold-rich VMS deposit in Quebec (Tourigny et al. 1993). The occurrence of strongly alkali-depleted aluminium silicate alteration zones may be the result of attack by acidic hydrothermal fluids generated by phase separation of a boiling hydrothermal fluid (Franklin 1986), by alteration at relatively high water:rock ratios of an evolved seawater hydrothermal fluid, or by hydrothermal fluids which contain high concentrations of magmatic gases (Giggenbach 1992).

JAMELAND MINE

This past-producing deposit lies along strike with Kam-Kotia deposit, 1.2 km to the southeast (Barrie 2000). Pyke and Middleton (1971) and Middleton (1973) describe the ore-bodies as a series of lenses hosted by chloritized and brecciated mafic volcanic rocks and felsic tuffs, with the whole group plunging 30° to 35° to the southeast. As at Kam Kotia, the lower lenses consisted of massive, zinc-rich sulphide, and the upper lenses of copper-rich, stringer-type ore.

STEEP LAKE PROSPECT

This prospect has been described by Watkins (1974) and Mullen (1977). The main showing lies 500 m west of Steep Lake (*see* Figure 2) along a north-trending contact between chlorite- and sericite-altered felsic volcaniclastic rocks and younger, east-facing basaltic pillow lavas. Based on drilling data, mineralization, which includes chalcopyrite, sphalerite, pyrite and minor pyrrhotite, is described as forming lenses up to 6.1 m wide along the steeply east-dipping (overturned) contact (Watkins 1974). Chalcopyrite occurs as "blotches and narrow stringers" in the felsic and mafic rocks, and sphalerite as "blotches" in the basalts.

HALFMOON LAKE PROSPECT

There is no outcrop in this area, and the following brief description is drawn largely from a detailed report on this deposit by Ore Systems Consulting (2000) for Prospectors Alliance. The deposits occur largely within a steeply southwest-dipping, but probably northeast-facing felsic volcanic lens up to 100 m thick, about 200 m south of Halfmoon Lake (*see* Figure 2). The felsic rocks are underlain and overlain by low-Ti "primitive", commonly pillowed mafic lavas, although in the stratigraphic footwall these are largely cut out by a thick Fe-Ti gabbro sill. The main showing consists of massive and semi-massive pyrite and sphalerite, plus or minus chalcopyrite and/or galena, in an interval generally less than 8 m thick hosted by chlorite- and sericite-altered felsic volcaniclastic rocks at or close to the top of the felsic lens. Subordinate intervals of semi-massive sulphide, dominated by pyrrhotite and sphalerite, occur down-section within the felsic succession. The felsic rocks form the lowermost of a series of stacked felsic volcanic lenses (Map P.3556, back pocket). Drilling through the upper lenses (e.g. Falconbridge R44-13, 15, 17) has shown locally intense chloritization and sericitization, with minor mineralization (mainly disseminated pyrite) but no significant intersections.

MINOR SHOWINGS IN THE KAMISKOTIA VOLCANIC COMPLEX

Dispersed, 1 cm scale sulphide-rich clasts occurring locally in bedded, crystal-rich felsic lapilli tuffs in Turnbull Township, 300 m northwest of the 03BHA0047 U-Pb age outcrop, are important in that they demonstrate the possibility of VMS mineralization in the lower part of the KVC. Higher in the KVC succession, blebs of massive pyrite and pyrrhotite to 10 cm are abundant in a 5.5 m thick interval in basaltic breccia immediately beneath overlying felsic tuffs in the "Shell outcrop" (*see* Figure 2) midway between, and at a similar stratigraphic level to, the Canadian Jamieson and Jameland mines.

KIDD–MUNRO ASSEMBLAGE

Volcanogenic massive sulphide exploration in the Kidd–Munro assemblage rocks has largely focused on the rhyolites in south-central Loveland Township and on the felsic-intermediate volcaniclastic rocks at the northern margin of the study area. Although hydrothermal alteration is generally weak within the lower rhyolite succession, drilling encountered up to 1% disseminated sphalerite over 1.5 m in one coarse-grained volcaniclastic interval (Mullen 1998). Meunier DDH LDM99-2 encountered disseminated pyrite and trace chalcopyrite and sphalerite in argillites and siltstones at the top of this felsic succession, and in underlying sericitized felsic tuffs and tuff breccias, with alteration and zinc-copper mineralization decreasing down section. Minor massive sulphide showings are associated with felsic-mafic contacts in the upper part of the Kidd–Munro assemblage. For example, 60 cm of submassive pyrrhotite and pyrite occur at the contact of basalt with overlying felsic volcaniclastic rocks in Noranda DDH FPT89-1 in northernmost Loveland Township. Pyrite, pyrrhotite and trace chalcopyrite occur as stringers and disseminations in rocks above and below this level.

Volcanogenic Massive Sulphide Exploration Suggestions

KIDD–MUNRO ASSEMBLAGE

New U-Pb ages of 2714.6 ± 1.2 and 2712.3 ± 2.8 Ma indicate that the Kidd–Munro assemblage rocks in Loveland, Macdiarmid and Thorburn townships were coeval with the Kidd Volcanic Complex (2717.0 ± 2.6 to 2711.5 ± 1.5 Ma: Bleeker et al. 1999), which hosts the giant Kidd Creek VMS deposit 5 km to the east of the study area. The high-silica FIIIb rhyolites in south-central Loveland Township are geochemically similar to ore-associated FIIIb rocks from Kidd Creek (e.g. Lesher et al. 1986), and seem likely to represent the most prospective part of the succession. Although the stratigraphy and bedding orientation of these rocks are poorly known owing to the scattered nature of the outcrop, drilling has indicated the presence of volcaniclastic intervals representing lulls in volcanism during which VMS deposits may have developed (Mullen 1998). One such interval is known to be present immediately beneath the unexposed and largely unexplored contact with overlying mafic lavas which trends north-northwest through Loveland Township. Drilling has also indicated mineralization associated with the FII felsic-intermediate volcaniclastic rocks at the top of the Kidd–Munro succession, particularly along felsic-mafic contacts at the base of and within this interval.

KAMISKOTIA VOLCANIC COMPLEX

U-Pb ages from the Genex, Kam Kotia and Halfmoon Lake deposits indicate a similar timing for VMS mineralization in the three areas. The volcanic successions in the Kam Kotia and Canadian Jamieson areas are stratigraphically similar, with a similar stratigraphic positioning for the VMS deposits in the two areas (*see* Figure 15). This suggests that the Kam Kotia, Canadian Jamieson, and probably the Jameland (Barrie 2000) orebodies are likely to have formed along the same time-stratigraphic horizon. If this hypothesis is correct, this time-stratigraphic interval offers an important exploration target for future VMS deposits, as many VMS orebodies may occur along a single stratigraphic level (Franklin et al. 1981; Gibson et al. 1991). Mafic and felsic volcaniclastic strata which can be replaced by VMS mineralization, and felsic coherent facies flows and/or domes, appear to be important potential targets. The apparent change in mafic volcanic geochemistry from "primitive" to "evolved" Fe-Ti rich lavas across the VMS-hosting interval may aid in locating this stratigraphic level. Indicators of west-facing in KVC rocks along the eastern edge of the study area suggest the possibility of repetition of the stratigraphic interval hosting the known VMS deposits. On this basis, the area with little or no outcrop and sparse drill-core data towards the Mattagami River in Godfrey and southern Jamieson townships may merit further investigation.

Evidence for early movement on the Aconda Lake fault immediately north of the Genex deposit, and for increased alteration intensity along northeast-trending faults in the Kam Kotia Mine area, suggests that synvolcanic faulting may have played an important role in localizing VMS mineralization. Areas where such faults intersect the VMS-hosting interval may provide a tighter focus for more detailed exploration. The detailed studies at Canadian Jamieson and Kam Kotia suggest that the presence of high concentrations of synvolcanic diabase intrusions may also be an important exploration guide. These intrusive rocks may have been emplaced within synvolcanic structural zones which could have also acted as conduits for mineralizing, base-metal-rich hydrothermal fluids. Anomalous chlorite and/or sericite alteration such as that associated with VMS orebodies at Kam Kotia, Canadian Jamieson and Genex (Hocker et al. 2005) represents a further possible exploration guide. However, these alteration haloes appear to be relatively areally restricted, and may prove difficult to locate given the sparse outcrop in much of the study area.

Acknowledgements

This work has been funded by the Discover Abitibi Initiative, managed by the Timmins Economic Development Corporation. We have benefited from discussions with local prospectors and mining companies, especially Falconbridge Exploration and Lionel Bonhomme.

References

Alexander, D.R., Laine, B.M. and Smith, J. 1971. Report on geological survey: Bristol, Carscallen, Godfrey and Turnbull townships, Hollinger Mines Ltd.; Timmins Resident Geologist's office, unpublished assessment file with maps: AFRI no. 42A12SE0402.

Ayer, J.A., Amelin, Y., Corfu, F., Kamo, S.L., Ketchum, J.W.F., Kwok, K. and Trowell, N. 2002. Evolution of the southern Abitibi greenstone belt based on U-Pb geochronology: autochthonous volcanic construction followed by plutonism, regional deformation and sedimentation; Precambrian Research, v.115, p.63-95.

Ayer, J.A., Thurston, P.C., Bateman, R., Dubé, B., Gibson, H.L., Hamilton, M.A., Hathway, B., Hocker, S.M., Houlé, M., Hudak, G., Lafrance, B., Lesher, C.M., Ispolatov, V., MacDonald, P.J., Péloquin, A.S., Piercey, S.J., Reed, L.E. and Thompson, P.H. 2005. Overview of results from the Greenstone Architecture Project: Discover Abitibi Initiative; Ontario Geological Survey, Open File Report 6154.

Barrie, C.T. 1990. The geology of the Kamiskotia area; Ontario Geological Survey, Preliminary Map P.3396, scale 1:50 000.

Barrie, C.T. 1992. Geology of the Kamiskotia area; Ontario Geological Survey, Open File Report 5829, p.180.

Barrie, C. T. 2000. Geology of the Kamiskotia area; Ontario Geological Survey, Study 59, 79p.

Barrie, C.T. and Davis, D.W. 1990. Timing of magmatism and deformation in the Kamiskotia–Kidd Creek area, western Abitibi Subprovince, Canada; Precambrian Research, v.46, p.217-240.

Barrie, C.T. and Pattison, J. 1999. Fe-Ti basalts, high silica rhyolites, and the role of magmatic heat in the genesis of the Kam-Kotia volcanic-associated massive sulfide deposit, Western Abitibi Subprovince, Canada; *in* Hannington, M. D. and Barrie, C.T. (eds.), Economic Geology Monograph 10, The Giant Kidd Creek Volcanogenic Massive Sulfide Deposit, Western Abitibi Subprovince, Canada, p.577-592.

Berry, L.G. 1946. Geology of the Robb–Jamieson area; Ontario Department of Mines, v.53 (1944), pt.4, p.1-16. Accompanied by Map 53c, scale 1:31 680.

Binney, P. and Barrie, C.T. 1991. Kamiskotia area; *in* Geology and Ore Deposits of the Timmins District, Ontario (Field Trip 6), Geological Survey of Canada, Open File 2161, p.52-65.

Bleeker, W., Parrish, R.R. and Sager-Kinsman, S. 1999. High-precision U-Pb geochronology of the late Archean Kidd Creek deposit and surrounding Kidd volcanic complex; *in* Hannington, M.D. and Barrie, C.T. (eds.), Economic Geology Monograph 10, The Giant Kidd Creek Volcanogenic Massive Sulfide Deposit, Western Abitibi Subprovince, Canada, p.43-69.

Branney, M.J. and Sparks, R.S.J. 1990. Fiamme formed by diagenesis and burial-compaction in soils and subaqueous sediments; Journal of the Geological Society, London, v.147, p.919-922.

Butman, B., Noble, M. and Folger, D.W. 1979. Long-term observations of bottom current and bottom sediment movement on the Mid-Atlantic continental shelf; Journal of Geophysical Research, v.84, p. 1187-1205.

Cas, R.A.F. and Wright, J.V. 1987. Volcanic successions: modern and ancient: a geological approach to processes, products and successions; Allen & Unwin Ltd., 528p.

Comba, C.D.A., Binney, W.P., Stewart, R.D., Cunnison, K.M. and Mullen, D.V. 1986. Timmins, Ontario: exceptional exposures of Archean subaerial and shallow subaqueous volcanic rocks, and associated ore deposits; GAC-MAC 1986 Field Trip Guidebook No.5, 25p.

COMINCO Limited. 1973. Jamieson overburden drilling, Report 40; Timmins Resident Geologist's office, unpublished assessment file: AFRI no. 42A12NE0669.

COMINCO Limited. 1974. Jamieson overburden drilling, Report 41; Timmins Resident Geologist's office,unpublished assessment file: AFRI no. 42A12NE0668.

Dimroth, E., Cousineau, P., Leduc, M. and Sanschagrin, Y. 1978. Structure and organization of Archean subaqueous basalt flows, Rouyn-Noranda area, Quebec, Canada; Canadian Journal of Earth Science, v.15, p.902-918.

Doyle, M.G., and Allen, R.L. 2003. Subsea-floor replacement in volcanic-hosted massive sulfide deposits; Ore Geology Reviews, v.23, no.3-4, p.183-222.

Draper, L. 1967. Wave activity at the sea bed around northwestern Europe; Marine Geology, v.5, p.133.

Finley, F.L. 1926. Kamiskotia gold area; Ontario Department of Mines, v.34 (1925), pt.6, p.43-64. Accompanied by Map 34f, scale 1:47 520.

Franklin, J.M. 1986. Volcanic-associated massive sulfide deposits – an update; *in* Andrew, C.J., Crowe, R.W.A., Finlay, S., Pennell, W.M., and Pyne, J.F. (eds), Geology and Genesis of Mineral Deposits in Ireland: Irish Association for Economic Geology, p.49-69.

Franklin, J.M., Sangster, D.M. and Lydon, J.W. 1981. Volcanic-associated massive sulfide deposits; Economic Geology 75th Anniversary Volume, p.485-627.

Gélinas, L., Brooks, C., Perrault, G., Carignan, J., Trudel, P. and Grasso, F. 1977. Chemo-stratigraphic divisions within the Abitibi Volcanic Belt, Rouyn-Noranda district, Quebec; *in* Baragar, W.R.A., Coleman, L.C. and Hall, J.M. (eds), Volcanic Regimes in Canada: Geological Association of Canada, Special Paper 16, p.265-295.

Gibson, H.L. 1990. The mine sequence of the Central Noranda Volcanic Complex: Geology, alteration, massive sulphide deposits and volcanological reconstruction; unpublished PhD thesis, Carleton University, Ottawa, Ontario, 800p.

Gibson, H.L., Morton, R.L. and Hudak, G.J. 1999. Chapter 2: Submarine volcanic processes, deposits, and environments favorable for the location of volcanic-associated massive sulfide deposits; Reviews in Economic Geology, v.8., p.13-51.

Giggenbach, W.F. 1992. Magma degassing and mineral deposition in hydrothermal systems along convergent plate boundaries; Economic Geology, v.87, p.1927-1944.

Gulf Minerals Canada Limited. 1979. Reid Overburden Drilling Project; Timmins Resident Geologist's office, unpublished assessment file: AFRI no. 42A14SW0105.

Hall, L.A.F. and Smith, M.D. 2002a. Precambrian geology, Denton and Carscallen townships; Ontario Geological Survey, Preliminary Map P.3517, scale 1:20 000.

Hall, L.A.F. and Smith, M.D. 2002b. Precambrian geology of Denton and Carscallen townships, Timmins West area; Ontario Geological Survey, Open File Report 6093, 75p.

Hannington, M.D., Kjarsgaard, I.M., Santaguida, F., and Cathles, L.M. 2002. Mineral-chemical studies of regional scale hydrothermal alteration in the Central Blake Group, Western Abitibi Subprovince: Part 1. Summary of results from the Noranda Volcanic Complex; Geological Survey of Canada, Open File 94E07, p.47-76.

Hart, T.R. 1984. The geochemistry and petrogenesis of a metavolcanic and intrusive sequence in the Kamiskotia area, Timmins, Ontario; unpublished MSc thesis, University of Toronto, Toronto, Ontario, 174p.

Hart, T.R, Gibson, H.L. and Lesher, C.M. 2004. Trace element geochemistry and petrogenesis of felsic volcanic rocks associated with volcanogenic massive Cu-Zn-Pb sulfide deposits; Economic Geology, v.99, p.1003-1013.

Hathway, B. and Thurston, P.C. 2003. Discover Abitibi. Base Metal Subproject 1. Volcanogenic massive sulphide mineralization in the Kamiskotia Area; *in* Summary of Field Work and Other Activities 2003, Ontario Geological Survey, Open File Report 6120, p.39-1 to 39-4.

Hathway, B., Hudak, G. and Hamilton, M. 2004. Discover Abitibi. Base Metal Subproject 1. Geological setting of volcanogenic massive sulphide mineralization in the Kamiskotia Area; *in* Summary of Field Work and Other Activities 2004, Ontario Geological Survey, Open File Report 6145, p. 38-1 to 38-8.

Hendry, D.A.F. 1981. Chlorites, phengites and siderites from the Prince Lyell ore deposit, Tasmania, and the origin of the deposit; Economic Geology, v.76, p. 285-303.

Herzig, P.M. and Hannington, M.D. 1995. Polymetallic massive sulfides at the modern seafloor - a review; Ore Geology Reviews, v.10, p.95-115.

Hocker, S.M., Hudak, G.J. and Heine, J. 2003. Electron microprobe analysis of alteration mineralogy at the Archean Fivemile Lake volcanic-associated massive sulfide prospect in the Vermilion District of northeastern Minnesota; Natural Resources Research Institute Report of Investigation NRRI/RI-2003/17, 49p.

Hocker, S.M., Thurston, P.C. and Gibson, H.L. 2005. Volcanic stratigraphy and controls on mineralization in the Genex Mine area, Kamiskotia area: Discover Abitibi Initiative; Ontario Geological Survey, Open File Report 6156, 143p.

Hogg, N. 1955. Geology of Godfrey Township, District of Cochrane; Ontario Department of Mines, v.63 (1954), pt.7. Accompanied by Map 1954-4, scale 1:12 000.

Hudak, G. J. 1996. The physical volcanology and hydrothermal alteration associated with late caldera volcanic and volcaniclastic rocks and volcanogenic massive sulfide deposits in the Sturgeon Lake region of northwestern Ontario, Canada; unpublished PhD thesis, University of Minnesota, Minneapolis, Minnesota, 463p.

Jensen, L.S. 1976. A new cation plot for classifying subalkalic volcanic rocks; Ontario Division of Mines, Miscellaneous Paper 66, 22p.

Kranidiotis, P. and MacLean, W.H. 1987. Systematics of chlorite alteration at the Phelps Dodge massive sulfide deposit, Matagami, Quebec; Economic Geology, v.82, p.1898-1911.

Krogh, T.E., Corfu, F., Davis, D.W., Dunning, G.R., Heaman, L.M., Kamo, S.L., Machado, N., Greenhough, J.D. and Nakamura, E. 1987. Precise U-Pb isotopic ages of diabase dikes and mafic to ultramafic rocks using trace amounts of baddeleyite and zircon; *in* Mafic Dike Swarms, Geological Association of Canada, Special Paper 34, p.147-152.

Koopman, E.R., Hannington, M.D., Santaguida, F. and Cameron, B.I. 1999. Petrology and geochemistry of proximal hydrothermal alteration in the Mine Rhyolite at Kidd Creek; Economic Geology Monography 10, p.267-296.

Large, R.R., Gemmell, J.B., Paulick, H. and Huston, D.L. 2001. The Alteration Box Plot: a simple approach to understanding the relationship between alteration mineralogy and lithogeochemistry associated with volcanic-hosted massive sulfide deposits; Economic Geology, v. 96 , p.957-971.

Larson, P.B. 1984. Geochemistry of the alteration pipe at the Bruce Cu-Zn volcanogenic massive sulfide deposit, Arizona; Economic Geology, v.79, p.1880-1896.

Lesher, C.M., Goodwin, A.M., Campbell, I.H. and Gorton, M.P. 1986. Trace-element geochemistry of ore-associated and barren, felsic metavolcanic rocks in the Superior Province, Canada; Canadian Journal of Earth Science, v.23, p.222-237.

Macdonald, P.J., Piercey, S.J. and Hamilton, M.A. 2005. An integrated study of intrusive rocks spatially associated with gold and base metal mineralization in Abitibi Greenstone Belt, Timmins area and Clifford Township: Discover Abitibi Initiative; Ontario Geological Survey, Open File Report 6160, 210p.

McPhie, J., Doyle, M. and Allen, R. 1993. Volcanic textures: A guide to the interpretation of textures in volcanic rocks; CODES Key Center, University of Tasmania, Hobart, Tasmania, Australia, 198p.

Middleton, R.S. 1973. Magnetic survey of Robb and Jamieson townships, District of Cochrane; Ontario Division of Mines, Geophysical Report 1, p.56. Accompanied by Map 2255, scale 1:31 680.

Middleton, R.S. 1974. Magnetic survey of Loveland and Macdiarmid townships, District of Cochrane; Ontario Division of Mines, Geophysical Report 2, p.26. Accompanied by Map 2288, scale 1:31 680.

Middleton, R.S. 1975. Magnetic, petrochemical and geological survey of Turnbull and Godfrey Townships, District of Cochrane; Ontario Division of Mines, Open File Report 5118, 267p.

Middleton, R.S. 1976. Turnbull and Godfrey townships; Ontario Division of Mines, Map 2330, scale 1:31 680.

Morton, R.L. and Franklin, J.M. 1987. Two-fold classification of Archean volcanic-associated massive sulphide deposits; Economic Geology, v.82, p.1057-1063.

Morton, R.L., Walker, J.S., Hudak, G.J. and Franklin, J.M. 1991. The early development of an Archean submarine caldera complex with emphasis on the Mattabi ash-flow tuff and its relationship to the Mattabi massive sulfide deposit; Economic Geology; v.86, p.1002-1011.

Mullen, D. 1977. Geology report, Godfrey 51 property, Texasgulf Canada Ltd; Timmins Resident Geologist's office, unpublished assessment file: AFRI no. 42A12SE0412.

Mullen, D. 1998. ATNA Resources Limited, Diamond drilling and relogging report, Meunier Option, Loveland and Robb townships; Timmins Resident Geologist's office, unpublished assessment file: AFRI no. 42A1NE2006.

Nakamura, N. 1974. Determination of REE, Ba, Fe, Mg, Na and K in carbonaceous and ordinary chondrites; Geochimica et Cosmochimica Acta, v.38, p.757-775.

Ontario Geological Survey 2003a. Ontario airborne geophysical surveys magnetic and electromagnetic surveys, Timmins area; Ontario Geological Survey, Geophysical Data Set 1004.

Ontario Geological Survey 2003b. Ontario airborne geophysical surveys, magnetic and electromagnetic data, Kamiskotia area MEGATEM® II; Ontario Geological Survey, Geophysical Data Set 1042.

Ore Systems Consulting, Vancouver. 2000. Report for Prospectors Alliance on the Halfmoon VMS prospect, Robb Township (unpublished report).

Osterberg, S.A., Morton, R.L. and Franklin, J.M. 1987. Hydrothermal alteration and physical volcanology of Archean rocks in the vicinity of the Headway–Couilee massive sulfide occurrence, Onaman area, northwestern Ontario; Economic Geology, v.82, p.311-332.

Pearce, J.A. 1996. A user's guide to basalt discrimination diagrams; Geological Association of Canada, Short Course Notes, v.12, p.79-113.

Pyke, D.R. and Middleton, R.S. 1971. Distribution and characteristics of the sulphide ores of the Timmins Area; The Canadian Mining and Metallurgical (CIM) Bulletin, v.64, p.55-66.

Reed, M. H. 1984. Geology, wall-rock alteration, and massive sulfide mineralization in a portion of the West Shasta district, California; Economic Geology, v.79, p.1299-1318.

Reedman, A.J., Howells, M.F., Orton, G. and Campbell, S.D.J. 1987. The Pitts Head Tuff Formation: a subaerial to submarine welded ash-flow tuff of Ordovician age, North Wales; Geological Magazine, v.124, p.427-439.

Somerville, R. 1967. Kam Kotia Mine; *in* Abel, M.K. (ed.), Canadian Institute of Mining and Metallurgy, Centenial Field Excursion, Northwestern Quebec – Northern Ontario, October 1967, p.132-134.

Sun, S.S. and McDonough, W.F. 1989. Chemical and isotopic systematics of oceanic basalts: Implications for mantle composition and processes; *in* Magmatism in Ocean Basins, Geological Society of London, Special Publication 42, p. 313-345.

Tourigny, G., Doucet, D. and Bourget, A. 1993. Geology of the Bousquet No. 2 Mine: an example of a deformed, gold-bearing, polymetallic sulfide deposit; Economic Geology, v.88, p.1578-1597.

Vaillancourt, C. and Hall, L.A.F. 2003. Lithogeochemical data for the Timmins West area: Carscallen, Denton, Bristol, Ogden and Deloro townships; Ontario Geological Survey, Miscellaneous Release—Data 123.

Vaillancourt, C., Pickett, C.L. and Dinel, E. 2001. Precambrian geology, Timmins West–Bristol and Ogden townships; Ontario Geological Survey, Preliminary Map P.3436, scale 1:20 000.

Watkins, J.J. 1974. Report on the geology of the Godfrey 51 claim group, Godfrey Township. Texasgulf Inc. files (unpublished report).

Winchester, J.A. and Floyd, P.A. 1977. Geochemical discrimination of different magma series and their differentiation products using immobile elements; Chemical Geology, v.20, p.325-343.

Yamagishi, H. 1991. Morphological and sedimentological characteristics of the Neogene submarine coherent lavas and hyaloclastites in Southwest Hokkaido, Japan; Sedimentary Geology, v.74, p.5-23.

Appendix 1

Geochemical data for 156 rock samples from Carscallen, Bristol, Turnbull, Godfrey, Robb, Jamieson, Loveland, Macdiarmid and Thorburn townships

ActLabs = Activation Laboratories Ltd.
N.D. = not detected
LOI = loss on ignition
d.l. = detection limit
ICP-AES = inductively coupled plasma atomic emission spectroscopy
ICP-MS = inductively coupled plasma mass spectrometry
OGL = Ontario Geoscience Laboratories
XRF = X-ray fluorescence
asterisk (*) indicates over-range ICP-MS values

Sample number		03-BHA-0019B	03-BHA-0023A	03-BHA-0027	03-BHA-0031C	03-BHA-0098	03-BHA-0099
Township		Turnbull Township	Turnbull Township	Turnbull Township	Turnbull Township	Turnbull Township	Turnbull Township
UTM East NAD83		453595	453795	453662	454055	453460	453678
UTM North NAD83		5371331	5371180	5370879	5370932	5366763	5366914
Rock type		rhyolite	rhyolite	rhyolite	rhyolite	rhyolite	rhyolite
Note		porphyritic, flow-banded	quartz and feldspar phyric	quartz and feldspar phyric	quartz and feldspar phyric	flow-banded	flow-banded
laboratory: method		OGL: XRF	OGL: XRF	OGL: XRF	OGL: XRF	OGL: XRF	OGL: XRF
	2003 d.l.						
SiO2 (wt%)	0.01	73.18	78.78	72.18	74.83	76.82	77.96
TiO2 (wt%)	0.01	0.22	0.1	0.23	0.26	0.09	0.1
Al2O3 (wt%)	0.01	11.78	10.24	12.96	12.53	10.62	11.49
Fe2O3 (wt%)	0.01	3.22	1.48	3	2.58	1.88	1.57
MgO (wt%)	0.01	0.52	0.79	0.58	1.41	0.57	0.31
CaO (wt%)	0.01	2.29	1.14	1.25	0.5	1.2	0.48
Na2O (wt%)	0.01	3.56	1.73	3.67	1.52	2.81	2.59
K2O (wt%)	0.01	2.88	4.5	3.9	4.99	4.11	4.23
MnO (wt%)	0.01	0.06	0.04	0.04	0.01	0.05	0.04
P2O5 (wt%)	0.01	0.03	N.D.	0.04	0.03	N.D.	N.D.
Cr2O3 (wt%)							
LOI (wt%)	0.05	2.92	2.32	2.02	2.07	2.44	1.51
TOTAL		100.66	101.13	99.87	100.74	100.61	100.29
laboratory: method		OGL: XRF	OGL: XRF	OGL: XRF	OGL: XRF	OGL: XRF	OGL: XRF
Cr (ppm)	4	21	17	9	N.D.	35	10
Ni (ppm)							
Nb (ppm)	2	25	24	28	16	26	27
Y (ppm)	1	69	75	72	51	78	90
Zr (ppm)	3	324	182	358	246	161	175
V (ppm)							
laboratory: method		OGL: ICP-AES	OGL: ICP-AES	OGL: ICP-AES	OGL: ICP-AES	OGL: ICP-AES	OGL: ICP-AES
Al (ppm)	100	53708	47956	62270	59467	49262	55091
Ba (ppm)	1	498	657	910	725	810	771
Be (ppm)	0.1	1.25	1.31	1.66	1.17	1.06	1.44
Ca (ppm)	50	10614	6876	8470	3349	7342	3120
Cd (ppm)	2	N.D.	N.D.	N.D.	N.D.	N.D.	N.D.
Co (ppm)	1	3	1	3	4	2	2
Cr (ppm)	6	23.4	17.6	15.58	15.25	38	20.93
Cu (ppm)	3	15	9	N.D.	N.D	N.D.	5
Fe (ppm)	100	20070	10266	20670	18507	13086	11272
K (ppm)	60	17299	27266	25352	30413	24579	25766
Li (ppm)	1	9	10	21	15	6	11
Mg (ppm)	70	2655	4147	3301	7694	2877	1746
Mn (ppm)	1	286	257	269	80	351	285
Mo (ppm)	8	N.D.	N.D.	N.D	N.D.	N.D.	N.D.
Na (ppm)	150	22662	11625	24758	10583	18503	16740
Ni (ppm)	3	5	N.D.	5	7	4	N.D.
P (ppm)	10	64	N.D.	66	98	N.D.	N.D.
S (ppm)	43	127	90	112	79	163	388
Sc (ppm)	3	3.9	2	3.8	4	2	2.2
Sr (ppm)	0.7	36.1	31	52.6	16.7	43.2	18.9
Ti (ppm)	10	935	472	1046	1182	418	458
V (ppm)	0.6	4.6	N.D.	3.1	8.6	N.D.	N.D.
W (ppm)	2	7	8	5	7	6	9
Y (ppm)	0.2	50.8	61.9	60.2	41.9	61.7	71.7
Zn (ppm)	2	115	52	69	36	39	111
laboratory: method		OGL: ICP-MS	OGL: ICP-MS	OGL: ICP-MS	OGL: ICP-MS	OGL: ICP-MS	OGL: ICP-MS
Ce (ppm)	0.07	127.79	127.08	146.73	100.27	130.83	163.28
Cs (ppm)	0.007	0.543	0.636	0.411	0.76	0.414	0.87
Dy (ppm)	0.008	12.932	14.686	15.494	9.813	14.595	17.875
Er (ppm)	0.008	7.479	8.704	8.964	6.597	8.75	10.25
Eu (ppm)	0.005	2.502	1.874	2.89	1.02	1.539	2.111
Gd (ppm)	0.009	13.935	14.888	16.344	9.519	14.9	21.89*
Hf (ppm)	0.1	9	7.3	12.1	8.7	6.8	7.7
Ho (ppm)	0.003	2.592	3.008	3.157	2.135	3.023	3.572
La (ppm)	0.02	54.98	55.67	64.28	44.29	56.45	95.5
Lu (ppm)	0.003	1.027	1.139	1.193	1.019	1.185	1.358
Nb (ppm)	0.2	28.1	28.1	33.3	19.9	29.3	32.2
Nd (ppm)	0.03	67.63	68.89	77.14	47.03	67.41	105.02*
Pr (ppm)	0.006	16.399	16.88	19.109	12.274	16.894	26.45*
Rb (ppm)	0.05	65.57	91.17	73.96	110.45	86.48	110.33
Sm (ppm)	0.01	14.67	15.02	16.57	9.62	14.82	22.29
Sr (ppm)	0.5	39.6	33.4	58.2	17.7	46.9	20.3
Ta (ppm)	0.17	1.83	2	2.17	1.65	2.05	2.32
Tb (ppm)	0.003	2.195	2.418	2.624	1.586	2.394	3.159
Th (ppm)	0.06	6.3	7.7	7.75	9.57	8.55	9.45
Tm (ppm)	0.003	1.092	1.242	1.302	1.025	1.286	1.48
U (ppm)	0.007	1.582	1.831	1.872	2.064	1.828	2.146
Y (ppm)	0.02	68.93	81.38	79.89	55.34	79.08	94.72
Yb (ppm)	0.01	7	7.88	8.26	6.74	8.16	9.47
Zr (ppm)	4	300.2	199	420	286.7	174	193.9

Sample number		03-BHA-0102	03-BHA-0105	03-BHA-0116A	03-BHA-0116B	03-BHA-0122	03-BHA-0125A
Township		Turnbull Township	Turnbull Township	Turnbull Township	Turnbull Township	Godfrey Township	Godfrey Township
UTM East NAD83		453679	453999	454265	454258	458910	458677
UTM North NAD83		5367130	5366857	5369714	5369648	5367060	5367381
Rock type		rhyolite	rhyolite	rhyolite	rhyolite	rhyolite	rhyolite
Note		quartz and feldspar phyric	flow-banded	sparsely porphyritic	sparsely porphyritic	quartz and feldspar phyric	quartz and feldspar phyric
laboratory: method		OGL: XRF	OGL: XRF	OGL: XRF	OGL: XRF	OGL: XRF	OGL: XRF
	2003 d.l.						
SiO2 (wt%)	0.01	77.81	77.35	74.07	72.58	75.56	74.08
TiO2 (wt%)	0.01	0.1	0.1	0.22	0.24	0.24	0.35
Al2O3 (wt%)	0.01	11.28	11.86	12.03	12.88	10.35	13.36
Fe2O3 (wt%)	0.01	1.53	1.11	3.97	4	2.24	2.43
MgO (wt%)	0.01	0.27	0.44	1.03	0.89	0.7	0.85
CaO (wt%)	0.01	0.79	0.5	0.78	1.19	1.43	0.88
Na2O (wt%)	0.01	2.75	1.2	5.15	5.05	2.57	5.07
K2O (wt%)	0.01	4.04	7.46	0.95	1.24	3.75	2.56
MnO (wt%)	0.01	0.04	0.02	0.04	0.05	0.06	0.03
P2O5 (wt%)	0.01	N.D.	0.01	0.03	0.03	0.03	0.07
Cr2O3 (wt%)							
LOI (wt%)	0.05	1.69	1.38	1.67	1.94	2.2	1.52
TOTAL		100.31	101.44	99.94	100.06	99.13	101.2
laboratory: method		OGL: XRF	OGL: XRF	OGL: XRF	OGL: XRF	OGL: XRF	OGL: XRF
Cr (ppm)	4	13	15	11	9	13	13
Ni (ppm)							
Nb (ppm)	2	27	28	27	26	17	6
Y (ppm)	1	82	78	70	66	66	17
Zr (ppm)	3	161	181	353	372	357	155
V (ppm)							
laboratory: method		OGL: ICP-AES	OGL: ICP-AES	OGL: ICP-AES	OGL: ICP-AES	OGL: ICP-AES	OGL: ICP-AES
Al (ppm)	100	53288	56481	57724	63218	50426	64043
Ba (ppm)	1	776	1085	376	496	602	509
Be (ppm)	0.1	1.07	1.15	1.04	1.62	1.05	0.68
Ca (ppm)	50	5217	3395	5021	7893	7404	5432
Cd (ppm)	2	N.D.	N.D.	N.D.	N.D.	N.D.	N.D.
Co (ppm)	1	1	1	9	4	2	5
Cr (ppm)	6	16.33	21.22	16.1	12.75	18.08	22.44
Cu (ppm)	3	N.D.	N.D.	N.D.	3	N.D.	N.D.
Fe (ppm)	100	10832	8708	26835	27621	14473	16490
K (ppm)	60	24582	46501	5909	7980	23417	16430
Li (ppm)	1	11	6	7	9	11	17
Mg (ppm)	70	1559	2255	5939	5257	3676	4872
Mn (ppm)	1	226	169	236	312	328	219
Mo (ppm)	8	N.D.	N.D.	N.D.	N.D.	N.D.	N.D.
Na (ppm)	150	18284	7594	33909	34252	17926	33495
Ni (ppm)	3	N.D.	3	6	5	4	5
P (ppm)	10	N.D.	N.D.	94	96	75	244
S (ppm)	43	296	222	90	>400	95	100
Sc (ppm)	3	1.9	2	3.5	3.7	4.2	4.3
Sr (ppm)	0.7	25.5	22.3	36.2	60	19	43.5
Ti (ppm)	10	425	472	976	1040	1081	1566
V (ppm)	0.6	N.D.	N.D.	1.8	2.5	0.8	14
W (ppm)	2	4	7	4	7	6	4
Y (ppm)	0.2	64.4	64.7	59	54.4	52.3	13.3
Zn (ppm)	2	83	41	46	72	50	44
laboratory: method		OGL: ICP-MS	OGL: ICP-MS	OGL: ICP-MS	OGL: ICP-MS	OGL: ICP-MS	OGL: ICP-MS
Ce (ppm)	0.07	138.22	145.32	140.57	130.5	94.32	74.14
Cs (ppm)	0.007	0.486	0.686	0.387	0.362	0.988	1.821
Dy (ppm)	0.008	16.054	15.823	14.537	13.695	12.28	3.171
Er (ppm)	0.008	9.554	9.509	8.29	8.031	7.667	1.907
Eu (ppm)	0.005	1.59	1.521	3.057	2.752	1.907	1.026
Gd (ppm)	0.009	16.405	16.63	15.001	14.539	12.311	3.907
Hf (ppm)	0.1	7.2	7.9	11.4	11.8	11.1	4.9
Ho (ppm)	0.003	3.26	3.241	2.927	2.79	2.541	0.648
La (ppm)	0.02	59.24	62.59	70.77	58.42	41.84	37.2
Lu (ppm)	0.003	1.257	1.296	1.063	1.126	1.097	0.296
Nb (ppm)	0.2	31.4	33	31.8	30.2	19.7	7.3
Nd (ppm)	0.03	72.87	76.27	73.79	70.4	51.26	31.33
Pr (ppm)	0.006	18.094	18.842	18.677	17.195	12.34	8.639
Rb (ppm)	0.05	100.1	141.89	22.26	24.18	70.75	63.96
Sm (ppm)	0.01	16.37	16.85	15.32	15.06	11.61	4.97
Sr (ppm)	0.5	27.4	23.7	40.3	65.7	20.7	47.1
Ta (ppm)	0.17	2.24	2.36	2	2.01	1.4	0.64
Tb (ppm)	0.003	2.654	2.66	2.434	2.286	2.007	0.556
Th (ppm)	0.06	9.08	9.67	6.72	7.03	6.19	6.46
Tm (ppm)	0.003	1.372	1.409	1.142	1.167	1.11	0.283
U (ppm)	0.007	2.101	2.083	1.566	1.66	1.327	1.346
Y (ppm)	0.02	85.83	84.58	75.88	71.67	66.7	17.3
Yb (ppm)	0.01	8.78	8.89	7.23	7.49	7.29	1.97
Zr (ppm)	4	176.7	200.8	391.3	410.9	381.7	178.5

Sample number		03-BHA-0125B	03-BHA-0128	03-BHA-0131	03-BHA-0133	03-BHA-0144A	03-BHA-0147
Township		Godfrey Township	Godfrey Township	Godfrey Township	Carscallen	Godfrey Township	Godfrey Township
UTM East NAD83		458631	458102	458048	455759	459536	457798
UTM North NAD83		5367369	5367123	5366635	5366364	5367175	5367533
Rock type		rhyolite	rhyolite	rhyolite	rhyolite	rhyolite (block)	rhyolite
Note		quartz and feldspar phyric	quartz and feldspar phyric	flow-banded	flow-banded	block in felsic lapilli tuff	sparsely quartz phyric
laboratory: method	2003 d.l.	OGL: XRF	OGL: XRF	OGL: XRF	OGL: XRF	OGL: XRF	OGL: XRF
SiO2 (wt%)	0.01	76.53	74.44	83.78	73.39	76.04	76.39
TiO2 (wt%)	0.01	0.24	0.17	0.08	0.24	0.14	0.22
Al2O3 (wt%)	0.01	11.59	10.5	8.51	12.83	11.78	11.06
Fe2O3 (wt%)	0.01	2.03	3.14	0.64	2.78	2.08	2.42
MgO (wt%)	0.01	0.65	1.36	0.55	0.46	0.53	0.65
CaO (wt%)	0.01	0.04	1.53	0.61	1.59	0.65	1.29
Na2O (wt%)	0.01	0.19	0.82	1.35	6.13	0.91	2.8
K2O (wt%)	0.01	9.09	5.49	3.99	0.66	6.81	3.82
MnO (wt%)	0.01	0.01	0.03	0.02	0.03	0.04	0.03
P2O5 (wt%)	0.01	0.03	N.D.	N.D.	0.03	N.D.	0.02
Cr2O3 (wt%)							
LOI (wt%)	0.05	0.89	3.25	1.31	1.88	1.5	
TOTAL		101.29	100.72	100.86	100.03	100.49	100.55
laboratory: method		OGL: XRF	OGL: XRF	OGL: XRF	OGL: XRF	OGL: XRF	OGL: XRF
Cr (ppm)	4	11	22	15	21	28	13
Ni (ppm)							
Nb (ppm)	2	18	20	18	26	24	19
Y (ppm)	1	70	121	62	65	146	68
Zr (ppm)	3	376	340	124	370	310	342
V (ppm)							
laboratory: method		OGL: ICP-AES	OGL: ICP-AES	OGL: ICP-AES	OGL: ICP-AES	OGL: ICP-AES	OGL: ICP-AES
Al (ppm)	100	51732	50001	39924	60154	56764	52835
Ba (ppm)	1	517	699	808	89	823	527
Be (ppm)	0.1	0.5	1.07	1.17	1.29	2.36	0.92
Ca (ppm)	50	364	10212	3504	9770	4396	8203
Cd (ppm)	2	N.D.	N.D.	N.D.	N.D.	N.D.	N.D.
Co (ppm)	1	2	2	2	4	2	3
Cr (ppm)	6	17.56	20.23	20.45	19.3	18.86	13.39
Cu (ppm)	3	N.D.	N.D.	4	N.D.	N.D.	N.D.
Fe (ppm)	100	15367	23555	4599	18239	15300	16855
K (ppm)	60	>50000	32601	23930	4389	42332	24006
Li (ppm)	1	6	10	11	8	8	12
Mg (ppm)	70	2415	7680	2887	2713	3003	3562
Mn (ppm)	1	78	221	130	152	250	197
Mo (ppm)	8	N.D.	N.D.	N.D.	N.D.	N.D.	N.D.
Na (ppm)	150	1607	5998	9410	40192	6852	19095
Ni (ppm)	3	N.D.	5	N.D.	4	3	3
P (ppm)	10	80	N.D.	N.D.	79	N.D.	35
S (ppm)	43	96	178	95	89	125	83
Sc (ppm)	3	2.9	2.1	1.4	3.4	2	4.1
Sr (ppm)	0.7	7.4	29.6	15	69.8	49.3	22.8
Ti (ppm)	10	1143	779	337	1019	641	998
V (ppm)	0.6	N.D.	N.D.	N.D.	1.8	N.D.	N.D.
W (ppm)	2	5	10	7	7	9	3
Y (ppm)	0.2	45.2	104.2	49.2	51.8	>120.0	54.2
Zn (ppm)	2	120	65	22	18	148	59
laboratory: method		OGL: ICP-MS	OGL: ICP-MS	OGL: ICP-MS	OGL: ICP-MS	OGL: ICP-MS	OGL: ICP-MS
Ce (ppm)	0.07	93.46	132.61	104.93	126.31	183.07	99.98
Cs (ppm)	0.007	0.736	0.682	0.499	0.36	2.365	0.574
Dy (ppm)	0.008	10.916	24.34*	11.626	13.029	29.97*	12.62
Er (ppm)	0.008	6.973	15.395	6.809	7.765	17.838	7.818
Eu (ppm)	0.005	1.643	3.513	1.143	2.785	2.749	1.789
Gd (ppm)	0.009	11.067	23.16*	12.046	13.969	31.03*	12.57
Hf (ppm)	0.1	11.8	12.6	5.3	11.5	12.4	10.7
Ho (ppm)	0.003	2.324	5.18	2.367	2.63	6.214	2.638
La (ppm)	0.02	40.5	57.06	46.25	54.94	81.68	45.6
Lu (ppm)	0.003	0.991	2.123	0.895	1.097	2.254	1.065
Nb (ppm)	0.2	21	25.6	21.2	30.4	29.3	22.3
Nd (ppm)	0.03	50.1	80.33	54.11	67.44	110.83*	53.04
Pr (ppm)	0.006	12.21	17.933	13.55	16.248	24.991	12.856
Rb (ppm)	0.05	96.81	81.26	72.02	20.79	161.91*	76.3
Sm (ppm)	0.01	11.2	19.72	11.98	14.33	27.82	11.95
Sr (ppm)	0.5	7.3	31.6	15.7	79	53.1	24.3
Ta (ppm)	0.17	1.62	1.61	1.61	1.96	2.11	1.51
Tb (ppm)	0.003	1.786	3.877	1.926	2.195	4.998	2.064
Th (ppm)	0.06	6.46	8.18	6.54	6.92	11.73	6.6
Tm (ppm)	0.003	1.027	2.259	0.999	1.131	2.551	1.159
U (ppm)	0.007	1.53	2.054	1.377	1.675	2.564	1.516
Y (ppm)	0.02	56.09	128.41*	62.54	69.95	160.31*	70.13
Yb (ppm)	0.01	6.72	14.55	6.32	7.47	15.73	7.4
Zr (ppm)	4	404	387.2	134.1	401.1	345.4	363.8

Sample number		03-BHA-0149	03-BHA-0151	03-BHA-0153	03-BHA-0160	03-BHA-0172A	03-BHA-0174
Township		Godfrey Township	Godfrey Township	Godfrey Township	Turnbull Township	Godfrey Township	Godfrey Township
UTM East NAD83		457551	457544	457303	455101	456225	456237
UTM North NAD83		5367614	5368014	5367970	5369907	5369091	5369276
Rock type		rhyolite	rhyolite	rhyolite	rhyolite	rhyolite	rhyolite
Note		quartz and feldspar phyric	sparsely porphyritic	quartz and feldspar phyric	aphyric to finely phyric	aphyric	aphyric
laboratory: method	2003 d.l.	OGL: XRF	OGL: XRF	OGL: XRF	OGL: XRF	OGL: XRF	OGL: XRF
SiO2 (wt%)	0.01	74	76.08	75.56	74.96	76.76	77.1
TiO2 (wt%)	0.01	0.19	0.25	0.18	0.14	0.16	0.15
Al2O3 (wt%)	0.01	10.96	10.94	11.28	12.61	11.59	11.2
Fe2O3 (wt%)	0.01	2.62	2.38	2.45	2.02	1.99	1.73
MgO (wt%)	0.01	0.96	0.8	0.83	0.9	0.37	0.74
CaO (wt%)	0.01	1.15	1.56	1.62	0.55	1.32	1.61
Na2O (wt%)	0.01	1.9	1.22	2.22	4.44	3.1	2.7
K2O (wt%)	0.01	4.81	5.06	3.67	2.48	3.22	2.67
MnO (wt%)	0.01	0.04	0.03	0.04	0.01	0.02	0.02
P2O5 (wt%)	0.01	0.02	0.03	0.01	0.01	0.01	0.01
Cr2O3 (wt%)							
LOI (wt%)	0.05	2.54	2.45	2.6	1.64	1.97	2.42
TOTAL		99.19	100.8	100.48	99.77	100.52	100.33
laboratory: method		OGL: XRF	OGL: XRF	OGL: XRF	OGL: XRF	OGL: XRF	OGL: XRF
Cr (ppm)	4	14	6	9	19	8	6
Ni (ppm)							
Nb (ppm)	2	20	18	21	30	22	21
Y (ppm)	1	71	63	137	74	84	72
Zr (ppm)	3	313	375	319	272	253	245
V (ppm)							
laboratory: method		OGL: ICP-AES	OGL: ICP-AES	OGL: ICP-AES	OGL: ICP-AES	OGL: ICP-AES	OGL: ICP-AES
Al (ppm)	100	52269	51905	51506	60325	53345	52933
Ba (ppm)	1	871	417	565	659	556	441
Be (ppm)	0.1	0.92	1.15	1.04	1.33	1	1.01
Ca (ppm)	50	7526	10045	9791	3444	7927	10884
Cd (ppm)	2	N.D.	N.D.	N.D.	N.D.	N.D.	N.D.
Co (ppm)	1	2	2	2	3	2	2
Cr (ppm)	6	9.49	10.71	13.13	10.49	11.1	10.97
Cu (ppm)	3	3	8	N.D.	N.D.	N.D.	N.D.
Fe (ppm)	100	18138	16891	16159	13378	13136	12096
K (ppm)	60	29632	30108	22344	15566	19422	16334
Li (ppm)	1	9	6	6	7	5	7
Mg (ppm)	70	5291	4374	4340	4986	2012	4146
Mn (ppm)	1	255	200	257	72	135	109
Mo (ppm)	8	N.D.	N.D.	N.D.	N.D.	N.D.	N.D.
Na (ppm)	150	12803	8589	14612	30248	22459	18315
Ni (ppm)	3	4	3	3	3	N.D.	N.D
P (ppm)	10	31	65	N.D.	N.D.	N.D.	N.D.
S (ppm)	43	147	123	89	88	117	94
Sc (ppm)	3	3.8	4.5	2.4	2.1	3.1	3.1
Sr (ppm)	0.7	15.6	10.2	12.5	38.1	24.3	12.7
Ti (ppm)	10	886	1140	781	602	661	673
V (ppm)	0.6	N.D.	N.D.	1	N.D.	N.D.	N.D.
W (ppm)	2	2	3	6	4	5	N.D.
Y (ppm)	0.2	57.9	49.3	106.8	57.3	64	59.4
Zn (ppm)	2	87	52	33	26	32	20
laboratory: method		OGL: ICP-MS	OGL: ICP-MS	OGL: ICP-MS	OGL: ICP-MS	OGL: ICP-MS	OGL: ICP-MS
Ce (ppm)	0.07	95.67	101.84	143.97	117	131.86	93.94
Cs (ppm)	0.007	0.548	0.43	0.433	0.643	0.495	0.673
Dy (ppm)	0.008	12.086	12.039	26.23*	14.389	15.271	14.416
Er (ppm)	0.008	7.353	7.458	16.322	8.741	9.43	9.132
Eu (ppm)	0.005	1.534	1.919	3.303	2.178	1.71	1.375
Gd (ppm)	0.009	12.008	12.175	24.99*	14.373	15.007	12.703
Hf (ppm)	0.1	8.9	11.4	12.4	9.8	9.2	9.4
Ho (ppm)	0.003	2.509	2.524	5.579	2.984	3.162	3.009
La (ppm)	0.02	42.76	45.32	62.34	51.5	58.84	41.78
Lu (ppm)	0.003	1.041	1.053	2.215	1.21	1.292	1.292
Nb (ppm)	0.2	20.2	21	24	35.9	24.3	25.3
Nd (ppm)	0.03	50.91	53.5	89.45	63.84	68.7	47.5
Pr (ppm)	0.006	12.427	12.951	20.085	15.464	16.727	11.669
Rb (ppm)	0.05	71.33	96.28	60.25	56.7	70.43	75.05
Sm (ppm)	0.01	11.47	12.06	21.88	14.47	14.76	11.21
Sr (ppm)	0.5	14.2	10.4	13.1	41.7	26.7	13.5
Ta (ppm)	0.17	1.39	1.46	1.58	2.38	1.75	1.76
Tb (ppm)	0.003	1.962	1.957	4.2	2.352	2.477	2.277
Th (ppm)	0.06	6.16	6.38	9.05	8.1	8.16	8.48
Tm (ppm)	0.003	1.085	1.09	2.367	1.292	1.39	1.371
U (ppm)	0.007	1.439	1.469	1.938	2.119	1.908	1.9
Y (ppm)	0.02	65.69	66.12	142.18*	77.72	86.04	79.27
Yb (ppm)	0.01	7.07	7.09	15.15	8.28	8.9	8.78
Zr (ppm)	4	290.7	406.7	383.6	296.8	270.3	275.9

Sample number		03-BHA-0176	03-BHA-0179	03-BHA-0180B	03-BHA-0187	03-BHA-0188	03-BHA-0193
Township		Godfrey Township	Turnbull Township	Turnbull Township	Turnbull Township	Turnbull Township	Godfrey Township
UTM East NAD83		456040	454673	454606	455017	454994	456022
UTM North NAD83		5369367	5369935	5369817	5369438	5369541	5370941
Rock type		rhyolite	rhyolite	rhyolite	rhyolite	rhyolite	rhyolite
Note		aphyric	aphyric to finely phyric	aphyric	aphyric	aphyric	aphyric
laboratory: method		OGL: XRF	OGL: XRF	OGL: XRF	OGL: XRF	OGL: XRF	OGL: XRF
	2003 d.l.						
SiO2 (wt%)	0.01	76.25	75.12	75.17	76.04	75.41	74.62
TiO2 (wt%)	0.01	0.15	0.14	0.15	0.14	0.13	0.16
Al2O3 (wt%)	0.01	11.08	12.64	12.69	12.55	12.29	13.18
Fe2O3 (wt%)	0.01	2	2.22	2.55	2.99	2.04	1.96
MgO (wt%)	0.01	0.49	0.25	0.37	0.66	0.45	0.38
CaO (wt%)	0.01	1.25	0.88	0.59	0.26	0.37	0.83
Na2O (wt%)	0.01	3.66	5.31	5.71	5.14	4.57	3.27
K2O (wt%)	0.01	3.18	2.3	1.62	1.96	3.72	3.11
MnO (wt%)	0.01	0.03	0.01	0.02	0.03	N.D.	0.02
P2O5 (wt%)	0.01	0.01	0.01	0.01	0.01	0.01	0.01
Cr2O3 (wt%)							
LOI (wt%)	0.05	2.3	1.27	1.11	0.9	0.95	2.26
TOTAL		100.41	100.17	100	100.68	99.97	99.79
laboratory: method		OGL: XRF	OGL: XRF	OGL: XRF	OGL: XRF	OGL: XRF	OGL: XRF
Cr (ppm)	4	19	20	18	13	60	11
Ni (ppm)							
Nb (ppm)	2	21	31	32	30	29	27
Y (ppm)	1	78	78	73	78	80	89
Zr (ppm)	3	250	277	285	280	272	264
V (ppm)							
laboratory: method		OGL: ICP-AES	OGL: ICP-AES	OGL: ICP-AES	OGL: ICP-AES	OGL: ICP-AES	OGL: ICP-AES
Al (ppm)	100	51922	58455	59960	58913	57082	61438
Ba (ppm)	1	647	633	510	810	1147	685
Be (ppm)	0.1	1.06	1.48	1.7	1.04	1.38	1.85
Ca (ppm)	50	8298	5626	3770	1690	2539	5458
Cd (ppm)	2	N.D.	N.D.	N.D.	N.D.	N.D.	N.D.
Co (ppm)	1	2	2	3	3	2	2
Cr (ppm)	6	23.17	23.05	22.71	16.39	67.35	16.02
Cu (ppm)	3	N.D.	N.D.	N.D.	N.D.	N.D.	N.D.
Fe (ppm)	100	14378	14908	17133	20416	14716	13472
K (ppm)	60	20151	14556	10109	12568	23639	19761
Li (ppm)	1	8	5	6	6	7	12
Mg (ppm)	70	2837	1579	2210	3797	2638	2122
Mn (ppm)	1	213	76	106	163	64	123
Mo (ppm)	8	N.D.	N.D.	N.D.	N.D.	N.D.	N.D.
Na (ppm)	150	24414	33509	36704	34396	30561	21642
Ni (ppm)	3	4	3	3	4	4	N.D.
P (ppm)	10	N.D.	N.D.	N.D.	N.D.	N.D.	N.D.
S (ppm)	43	87	86	83	102	76	72
Sc (ppm)	3	3.1	2.1	2.1	2.2	1.8	3.2
Sr (ppm)	0.7	43.7	48.1	42.3	44.2	43.6	24
Ti (ppm)	10	664	600	634	617	632	692
V (ppm)	0.6	N.D.	N.D.	N.D	N.D.	N.D.	N.D.
W (ppm)	2	3	5	5	5	N.D.	2
Y (ppm)	0.2	62.6	61.1	56.9	61	62.4	65.9
Zn (ppm)	2	57	23	33	31	19	36
laboratory: method		OGL: ICP-MS	OGL: ICP-MS	OGL: ICP-MS	OGL: ICP-MS	OGL: ICP-MS	OGL: ICP-MS
Ce (ppm)	0.07	133.57	123.94	114.89	130.51	126.87	159.15
Cs (ppm)	0.007	0.477	0.298	0.422	0.689	0.705	0.599
Dy (ppm)	0.008	14.729	15.539	14.222	16.301	15.355	16.788
Er (ppm)	0.008	9.179	9.069	8.572	9.072	9.213	10.478
Eu (ppm)	0.005	1.703	2.445	2.342	3.266	2.787	1.864
Gd (ppm)	0.009	14.915	15.276	14.564	16.774	15.608	16.981
Hf (ppm)	0.1	9.2	10.1	10.2	10.1	9.8	10.4
Ho (ppm)	0.003	3.1	3.129	2.92	3.216	3.196	3.513
La (ppm)	0.02	60.02	53.35	50.25	59.5	55.36	72.73
Lu (ppm)	0.003	1.268	1.228	1.201	1.205	1.22	1.494
Nb (ppm)	0.2	25.1	34.4	35.8	34.5	34	30.8
Nd (ppm)	0.03	67.59	67.9	63.34	74.96	71.08	83.23
Pr (ppm)	0.006	16.702	16.169	14.985	17.802	16.753	20.435
Rb (ppm)	0.05	74.73	35.24	40.87	37.45	57.72	91.49
Sm (ppm)	0.01	14.61	15.61	14.29	16.99	15.66	17.47
Sr (ppm)	0.5	49.1	54.6	47.8	50.9	49.7	26
Ta (ppm)	0.17	1.75	2.38	2.31	2.3	2.33	2.27
Tb (ppm)	0.003	2.429	2.518	2.287	2.691	2.491	2.723
Th (ppm)	0.06	8.27	8.06	7.8	7.8	8.09	10.25
Tm (ppm)	0.003	1.38	1.306	1.27	1.294	1.331	1.538
U (ppm)	0.007	2.007	1.899	1.932	1.832	1.815	2.245
Y (ppm)	0.02	82.52	82.54	76.2	83.78	84	91.16
Yb (ppm)	0.01	8.68	8.34	8.14	8.12	8.44	10.05
Zr (ppm)	4	276.5	298	306.2	296.7	288.5	287.2

Sample number		03-BHA-0196A	03-BHA-0213	03-BHA-0216B	03-BHA-0218	03-BHA-0221	03-BHA-0227A
Township		Turnbull Township	Turnbull Township	Turnbull Township	Turnbull Township	Turnbull Township	Bristol Township
UTM East NAD83		455882	455186	455084	455181	455384	459951
UTM North NAD83		5371123	5370850	5370850	5371108	5371141	5365830
Rock type		rhyolite	rhyolite	rhyolite	rhyolite	rhyolite	rhyolite
Note		spherulitic	quartz and feldspar phyric	flow-banded	coarsely feldspar phyric	mineralized	massive rhyolite, finely quartz phyric
laboratory: method		OGL: XRF	OGL: XRF	OGL: XRF	OGL: XRF	OGL: XRF	OGL: XRF
	2003 d.l.						
SiO2 (wt%)	0.01	74.81	71.51	72.33	71.54	79.76	80.11
TiO2 (wt%)	0.01	0.2	0.23	0.28	0.23	0.11	0.1
Al2O3 (wt%)	0.01	11.58	12.61	11.83	12.85	9.3	10.43
Fe2O3 (wt%)	0.01	2.54	3.93	5.89	3.18	2.75	0.98
MgO (wt%)	0.01	0.08	1.51	2.91	0.23	1.68	0.35
CaO (wt%)	0.01	1.58	0.82	0.41	1.9	0.85	0.13
Na2O (wt%)	0.01	5.77	3.18	2.38	5.01	1.79	1.3
K2O (wt%)	0.01	0.8	2.4	1.81	2.04	1.68	6.34
MnO (wt%)	0.01	0.04	0.03	0.05	0.05	0.04	0.01
P2O5 (wt%)	0.01	0.01	0.04	0.03	0.03	N.D.	0.01
Cr2O3 (wt%)							
LOI (wt%)	0.05	1.9	2.6	2.59	2.67	2.53	0.72
TOTAL		99.31	98.85	100.5	99.73	100.5	100.47
laboratory: method		OGL: XRF	OGL: XRF	OGL: XRF	OGL: XRF	OGL: XRF	OGL: XRF
Cr (ppm)	4	21	10	5	18	6	35
Ni (ppm)							
Nb (ppm)	2	24	16	25	27	22	23
Y (ppm)	1	126	42	56	72	58	67
Zr (ppm)	3	383	318	406	387	200	182
V (ppm)							
laboratory: method		OGL: ICP-AES	OGL: ICP-AES	OGL: ICP-AES	OGL: ICP-AES	OGL: ICP-AES	OGL: ICP-AES
Al (ppm)	100	53907	59354	43622	62218	44749	49484
Ba (ppm)	1	168	214	146	572	187	1042
Be (ppm)	0.1	0.98	1.08	0.84	1.35	0.94	1.06
Ca (ppm)	50	9724	5194	2613	13015	5686	940
Cd (ppm)	2	N.D.	N.D.	N.D.	N.D.	N.D.	N.D.
Co (ppm)	1	2	7	13	3	3	2
Cr (ppm)	6	21.6	14.12	10.77	13.47	12.11	35.64
Cu (ppm)	3	N.D.	N.D.	N.D.	N.D.	N.D.	6
Fe (ppm)	100	15904	25968	39142	22771	19257	7351
K (ppm)	60	4710	14100	10306	13776	10147	38421
Li (ppm)	1	2	9	12	15	8	8
Mg (ppm)	70	705	8213	10402	1510	9668	1899
Mn (ppm)	1	212	204	286	366	278	71
Mo (ppm)	8	N.D.	N.D.	N.D.	N.D.	N.D.	N.D.
Na (ppm)	150	37896	22169	16332	32603	12495	8741
Ni (ppm)	3	N.D.	6	14	3	4	N.D.
P (ppm)	10	N.D.	131	108	100	N.D.	N.D.
S (ppm)	43	86	>400	84	104	61	260
Sc (ppm)	3	2.4	4.4	1.7	3.9	1.6	2.1
Sr (ppm)	0.7	65.7	28.9	12.7	91.1	19.1	27
Ti (ppm)	10	832	987	1178	1061	455	485
V (ppm)	0.6	N.D.	4.2	6.9	2.9	N.D.	N.D.
W (ppm)	2	N.D.	N.D.	N.D.	N.D.	N.D.	N.D.
Y (ppm)	0.2	96	34.1	29.1	57.5	48.5	54.3
Zn (ppm)	2	48	47	71	32	43	65
laboratory: method		OGL: ICP-MS	OGL: ICP-MS	OGL: ICP-MS	OGL: ICP-MS	OGL: ICP-MS	OGL: ICP-MS
Ce (ppm)	0.07	114.98	118.22	106.01	151.93	90.53	140.33
Cs (ppm)	0.007	0.202	0.558	0.462	0.653	0.343	1.105
Dy (ppm)	0.008	22.68*	9.176	8.154	15.615	11.979	13.391
Er (ppm)	0.008	14.954	5.436	4.563	9.14	7.033	8.131
Eu (ppm)	0.005	2.913	1.769	2.099	3.27	1.796	1.512
Gd (ppm)	0.009	19.564	10.605	10.372	17.121	11.99	14.75
Hf (ppm)	0.1	13.8	9.4	12.6	13	7.3	7.3
Ho (ppm)	0.003	4.9	1.894	1.623	3.174	2.409	2.727
La (ppm)	0.02	50.34	52.53	48.48	66.97	39.93	62.42
Lu (ppm)	0.003	2.247	0.796	0.595	1.263	0.905	1.121
Nb (ppm)	0.2	27.8	18.8	30.3	35.5	26.7	26.4
Nd (ppm)	0.03	67.06	59.45	58.04	80.88	49.22	72.54
Pr (ppm)	0.006	15.317	14.682	14.236	19.613	11.739	17.709
Rb (ppm)	0.05	14.11	67.01	48.34	58.66	49.07	93.24
Sm (ppm)	0.01	16.68	11.65	11.93	17.47	11.5	15.07
Sr (ppm)	0.5	73.7	31.5	13.8	109.3	20.4	29
Ta (ppm)	0.17	1.96	1.29	1.86	2.21	1.75	1.91
Tb (ppm)	0.003	3.363	1.58	1.454	2.68	1.979	2.247
Th (ppm)	0.06	8.45	4.45	6.09	8.13	5.98	8.46
Tm (ppm)	0.003	2.249	0.802	0.655	1.335	0.994	1.193
U (ppm)	0.007	1.89	1.075	1.382	1.62	1.41	1.949
Y (ppm)	0.02	127.82*	46.92	38.54	83.48	63.07	70.78
Yb (ppm)	0.01	14.72	5.2	4.1	8.46	6.31	7.6
Zr (ppm)	4	414.5	361.4	466.4	454.1	219.8	198.5

Sample number		03-BHA-0229A	03-BHA-0233	03-BHA-0236	03-BHA-0241B	03-BHA-0245	03-BHA-0248
Township		Bristol Township	Godfrey Township	Godfrey Township	Godfrey Township	Godfrey Township	Godfrey Township
UTM East NAD83		459673	455916	456030	456389	456253	458218
UTM North NAD83		5365833	5370613	5370925	5371453	5371754	5371414
Rock type		rhyolite	rhyolite	rhyolite	rhyolite (block)	rhyolite	rhyolite
Note		finely quartz phyric	sparsely porphyritic	sparsely porphyritic	quartz and feldspar phyric	sparsely porphyritic	flow-banded, porphyritic
laboratory: method		OGL: XRF	OGL: XRF	OGL: XRF	OGL: XRF	OGL: XRF	OGL: XRF
	2003 d.l.						
SiO2 (wt%)	0.01	80.18	75.96	75.59	81.98	76.52	80.63
TiO2 (wt%)	0.01	0.11	0.14	0.15	0.11	0.16	0.12
Al2O3 (wt%)	0.01	9.86	11.5	12.21	9.5	11.55	9.78
Fe2O3 (wt%)	0.01	1.31	1.96	2.12	0.97	1.86	2.26
MgO (wt%)	0.01	0.61	0.53	0.37	0.36	0.41	1.14
CaO (wt%)	0.01	0.41	2.12	1.21	0.58	1.04	0.46
Na2O (wt%)	0.01	1.49	2.31	3.42	3.21	5.12	1.92
K2O (wt%)	0.01	5.21	2.79	2.63	1.97	1.3	2.09
MnO (wt%)	0.01	0.04	0.02	0.02	0.02	0.02	0.05
P2O5 (wt%)	0.01	N.D.	0.01	0.01	N.D.	0.01	0.01
Cr2O3 (wt%)							
LOI (wt%)	0.05	1.17	2.88	2.49	1.41	2.1	2.01
TOTAL		100.4	100.22	100.22	100.12	100.09	100.47
laboratory: method		OGL: XRF	OGL: XRF	OGL: XRF	OGL: XRF	OGL: XRF	OGL: XRF
Cr (ppm)	4	21	16	10	16	13	10
Ni (ppm)							
Nb (ppm)	2	17	22	25	21	22	14
Y (ppm)	1	63	80	87	71	80	58
Zr (ppm)	3	178	227	246	169	258	177
V (ppm)							
laboratory: method		OGL: ICP-AES	OGL: ICP-AES	OGL: ICP-AES	OGL: ICP-AES	OGL: ICP-AES	OGL: ICP-AES
Al (ppm)	100	47815	55133	57616	45152	53649	47781
Ba (ppm)	1	721	301	568	349	371	359
Be (ppm)	0.1	0.78	1.28	1.58	0.82	1.02	0.84
Ca (ppm)	50	3020	14000	7797	3977	6301	3125
Cd (ppm)	2	N.D.	N.D.	N.D.	N.D.	N.D.	N.D.
Co (ppm)	1	2	1	1	N.D.	1	2
Cr (ppm)	6	32.15	12.89	12.38	19.61	19.98	15.74
Cu (ppm)	3	N.D.	N.D.	N.D.	63	N.D.	N.D.
Fe (ppm)	100	9777	13464	14195	6938	11759	16081
K (ppm)	60	32213	17988	17322	12114	7973	12794
Li (ppm)	1	8	8	11	6	2	3
Mg (ppm)	70	3455	2866	2012	2103	2297	6398
Mn (ppm)	1	267	123	139	130	108	320
Mo (ppm)	[illegible]	N.D.	N.D.	N.D.	N.D.	N.D.	N.D.
Na (ppm)	150	10596	15829	22932	21419	33146	14028
Ni (ppm)	3	4	3	N.D.	N.D.	N.D.	5
P (ppm)	10	N.D.	N.D.	N.D.	N.D.	N.D.	N.D.
S (ppm)	43	64	49	75	62	72	63
Sc (ppm)	3	2.2	2.8	2.8	1.8	3	2.2
Sr (ppm)	0.7	29.5	18.1	27.6	11.1	36.3	12.7
Ti (ppm)	10	503	647	647	452	684	510
V (ppm)	0.6	N.D.	N.D.	N.D.	N.D.	N.D.	N.D.
W (ppm)	2	3	N.D.	N.D.	N.D.	N.D.	N.D.
Y (ppm)	0.2	52	63.6	66	55.9	61.4	48
Zn (ppm)	2	56	31	75	37	15	48
laboratory: method		OGL: ICP-MS	OGL: ICP-MS	OGL: ICP-MS	OGL: ICP-MS	OGL: ICP-MS	OGL: ICP-MS
Ce (ppm)	0.07	136.84	138.7	149.27	123.24	127.92	126.19
Cs (ppm)	0.007	0.682	0.678	0.55	0.401	0.287	0.341
Dy (ppm)	0.008	12.355	15.463	16.365	12.941	15.504	10.976
Er (ppm)	0.008	7.749	9.759	10.025	7.731	9.548	7.007
Eu (ppm)	0.005	1.349	1.64	1.734	1.562	1.723	1.303
Gd (ppm)	0.009	13.596	15.318	16.539	14.082	15.351	12.331
Hf (ppm)	0.1	7	9.1	9.4	6.8	9.6	6.9
Ho (ppm)	0.003	2.64	3.226	3.361	2.65	3.212	2.282
La (ppm)	0.02	62.68	61.45	66.96	57.57	56.13	57.72
Lu (ppm)	0.003	1.115	1.388	1.415	1.019	1.315	1.043
Nb (ppm)	0.2	20.6	26.6	28.7	24.3	26.5	17.4
Nd (ppm)	0.03	68.74	71.05	76.16	66.46	65.67	65.86
Pr (ppm)	0.006	17.217	17.783	18.642	16.147	16.144	16.115
Rb (ppm)	0.05	70.93	83.64	79.81	52.53	31.55	55.09
Sm (ppm)	0.01	14.29	15.14	16.24	14	14.57	13.27
Sr (ppm)	0.5	32.5	19.9	30.7	12	42.5	14.3
Ta (ppm)	0.17	1.56	1.93	2.07	1.68	1.89	1.28
Tb (ppm)	0.003	2.083	2.487	2.666	2.093	2.484	1.803
Th (ppm)	0.06	7.93	8.93	9.68	7.6	8.69	6.91
Tm (ppm)	0.003	1.152	1.428	1.494	1.102	1.398	1.06
U (ppm)	0.007	1.728	1.688	2.211	1.403	2.071	1.49
Y (ppm)	0.02	68.19	87.75	89.7	74.23	84.59	65.37
Yb (ppm)	0.01	7.49	9.27	9.64	6.91	9.08	6.98
Zr (ppm)	4	198.6	253.6	265.9	184.7	283.3	203.4

Sample number		03-BHA-0260	03-BHA-0261	03-BHA-0262	03-BHA-0272	03-BHA-0276	03-BHA-0280B
Township		Godfrey Township	Godfrey Township	Godfrey Township	Godfrey Township	Godfrey Township	Godfrey Township
UTM East NAD83		456950	456935	456633	456817	456345	457352
UTM North NAD83		5370860	5370788	5370537	5371574	5372291	5372197
Rock type		rhyolite	rhyolite	rhyolite	rhyolite	rhyolite	rhyolite
Note		quartz phyric	quartz phyric	mineralized	quartz phyric	sparsely porphyritic	finely quartz and feldspar phyric
laboratory: method		OGL: XRF	OGL: XRF	OGL: XRF	OGL: XRF	OGL: XRF	OGL: XRF
	2003 d.l.						
SiO2 (wt%)	0.01	76.22	73.59	78.63	78.03	76.95	79.52
TiO2 (wt%)	0.01	0.17	0.17	0.13	0.16	0.17	0.15
Al2O3 (wt%)	0.01	11.18	10.91	10.8	11.43	12.18	11.48
Fe2O3 (wt%)	0.01	3.55	3.53	1.65	1.89	2.11	0.87
MgO (wt%)	0.01	1.86	2.07	4.4	0.81	0.39	1.44
CaO (wt%)	0.01	0.1	0.12	N.D.	0.46	0.36	0.32
Na2O (wt%)	0.01	2.27	1.84	0.35	2.69	4.09	2
K2O (wt%)	0.01	3.73	4.04	2.19	2.67	2	2.89
MnO (wt%)	0.01	0.03	0.03	0.02	0.05	0.03	N.D.
P2O5 (wt%)	0.01	N.D.	N.D.	0.01	0.01	0.01	N.D.
Cr2O3 (wt%)							
LOI (wt%)	0.05	1.79	3.79	2.8	2.41	1.89	2
TOTAL		100.9	100.09	100.98	100.61	100.18	100.68
laboratory: method		OGL: XRF	OGL: XRF	OGL: XRF	OGL: XRF	OGL: XRF	OGL: XRF
Cr (ppm)	4	26	21	16	10	20	7
Ni (ppm)							
Nb (ppm)	2	29	29	25	21	22	21
Y (ppm)	1	150	145	64	67	74	68
Zr (ppm)	3	321	307	212	261	265	226
V (ppm)							
laboratory: method		OGL: ICP-AES	OGL: ICP-AES	OGL: ICP-AES	OGL: ICP-AES	OGL: ICP-AES	OGL: ICP-AES
Al (ppm)	100	52330	51453	38965	53916	57338	54826
Ba (ppm)	1	723	637	385	675	516	536
Be (ppm)	0.1	1.09	1.22	1.74	1.26	1.11	1.37
Ca (ppm)	50	742	866	N.D.	2893	2534	2221
Cd (ppm)	2	N.D.	N.D.	N.D.	N.D.	N.D.	N.D.
Co (ppm)	1	3	2	4	2	1	2
Cr (ppm)	6	12.88	13.15	10.04	12.32	11.33	13.07
Cu (ppm)	3	N.D.	8	N.D.	N.D.	N.D.	N.D.
Fe (ppm)	100	25432	24581	11239	12916	14962	6303
K (ppm)	60	22875	23924	11921	16114	13003	17648
Li (ppm)	1	14	10	11	2	2	6
Mg (ppm)	70	10018	11232	18385	4387	2283	8083
Mn (ppm)	1	206	192	99	308	188	53
Mo (ppm)	8	N.D.	N.D.	N.D.	N.D.	N.D.	N.D.
Na (ppm)	150	15623	12600	2787	18280	26231	13368
Ni (ppm)	3	6	6	6	4	4	4
P (ppm)	10	N.D.	N.D.	N.D.	N.D.	N.D.	N.D.
S (ppm)	43	67	72	56	64	63	60
Sc (ppm)	3	1.8	1.9	1.7	2.7	3.1	2.4
Sr (ppm)	0.7	12.3	12.7	19.7	16	18.8	22.6
Ti (ppm)	10	767	746	545	699	741	623
V (ppm)	0.6	N.D.	N.D.	N.D.	N.D.	N.D.	N.D.
W (ppm)	2	N.D.	N.D.	N.D.	3	N.D.	N.D.
Y (ppm)	0.2	>120.0	>120.0	36.8	52.8	57.4	53.3
Zn (ppm)	2	89	78	31	33	28	27
laboratory: method		OGL: ICP-MS	OGL: ICP-MS	OGL: ICP-MS	OGL: ICP-MS	OGL: ICP-MS	OGL: ICP-MS
Ce (ppm)	0.07	170.2	162.86	32.08	130	144.01	112.96
Cs (ppm)	0.007	0.731	0.662	0.323	0.593	0.446	0.574
Dy (ppm)	0.008	29.46*	28.42*	8.802	13.542	14.862	13.199
Er (ppm)	0.008	19.524	19.157	6.655	8.357	9.003	8.344
Eu (ppm)	0.005	3.035	2.973	0.3	1.717	1.769	1.36
Gd (ppm)	0.009	26.69*	25.01*	4.311	13.958	15.827	12.787
Hf (ppm)	0.1	13.9	13.2	8.4	9.4	10.1	8.8
Ho (ppm)	0.003	6.49	6.169	2.034	2.78	3.058	2.779
La (ppm)	0.02	78.23	71.35	8.72	56.57	63.89	49.79
Lu (ppm)	0.003	2.866	2.748	0.99	1.178	1.255	1.199
Nb (ppm)	0.2	37.5	35.5	28.7	24.9	27.1	26.1
Nd (ppm)	0.03	100.67*	89.99	10.52	65.21	75.12	57.75
Pr (ppm)	0.006	23.865	21.421	2.757	16.211	18.628	14.312
Rb (ppm)	0.05	73.29	87.71	33.94	62.28	45.84	63.25
Sm (ppm)	0.01	23.56	21.76	2.86	14.19	16.12	12.43
Sr (ppm)	0.5	14	13.9	23.2	18	21.5	26.6
Ta (ppm)	0.17	2.66	2.46	2.05	1.8	1.96	1.97
Tb (ppm)	0.003	4.575	4.363	1.112	2.239	2.46	2.115
Th (ppm)	0.06	12.63	11.88	7.24	8.51	9.2	9.07
Tm (ppm)	0.003	2.965	2.83	1.036	1.226	1.321	1.239
U (ppm)	0.007	2.986	2.75	1.887	1.981	1.793	1.938
Y (ppm)	0.02	172.11*	160.34*	55.17	70.44	79.52	72.4
Yb (ppm)	0.01	19.31	18.49	6.63	8.01	8.6	8.06
Zr (ppm)	4	390.2	368.7	230.2	280.6	290.7	252.2

Sample number		03-BHA-0281	03-BHA-0284	03-BHA-0291	03-BHA-0293	03-BHA-0295	03-BHA-0296
Township		Godfrey Township	Godfrey Township	Carscallen	Carscallen	Carscallen	Carscallen
UTM East NAD83		457366	457607	454301	454161	454260	454416
UTM North NAD83		5372216	5372179	5365641	5365591	5365979	5365873
Rock type		rhyolite	rhyolite	rhyolite	rhyolite	rhyolite	rhyolite
Note		quartz and feldspar phyric	quartz and feldspar phyric	sparsely quartz phyric	sparsely quartz-phyric	aphyric rhyolite; fine flow banding	aphyric rhyolite; fine flow banding
laboratory: method		OGL: XRF	OGL: XRF	OGL: XRF	OGL: XRF	OGL: XRF	OGL: XRF
	2003 d.l.						
SiO2 (wt%)	0.01	77.99	76.22	73.48	72.19	80.36	74.79
TiO2 (wt%)	0.01	0.15	0.14	0.22	0.2	0.12	0.17
Al2O3 (wt%)	0.01	11.74	10.83	12	11.68	9.92	12.47
Fe2O3 (wt%)	0.01	1.07	0.86	2.81	3.78	1.01	3.56
MgO (wt%)	0.01	0.82	2.06	0.34	0.65	0.11	0.46
CaO (wt%)	0.01	0.3	1.04	1.53	2.19	0.33	0.22
Na2O (wt%)	0.01	6.25	2.96	4.4	3.58	2.75	3.37
K2O (wt%)	0.01	0.47	2.29	2.84	3.24	4.73	3.85
MnO (wt%)	0.01	0.01	0.03	0.07	0.08	0.04	0.02
P2O5 (wt%)	0.01	0.02	N.D.	0.03	0.03	0.01	0.02
Cr2O3 (wt%)							
LOI (wt%)	0.05	0.95	2.8	2.66	2.28	1.01	1.31
TOTAL		99.76	99.24	100.4	99.89	100.38	100.26
laboratory: method		OGL: XRF	OGL: XRF	OGL: XRF	OGL: XRF	OGL: XRF	OGL: XRF
Cr (ppm)	4	45	15	21	29	18	17
Ni (ppm)							
Nb (ppm)	2	23	21	23	25	22	29
Y (ppm)	1	83	77	61	65	54	84
Zr (ppm)	3	247	231	340	328	227	312
V (ppm)			227	54			
laboratory: method		OGL: ICP-AES	OGL: ICP-AES	OGL: ICP-AES	OGL: ICP-AES	OGL: ICP-AES	OGL: ICP-AES
Al (ppm)	100	56283	53624	56697	56710	47790	61166
Ba (ppm)	1	154	427	545	521	876	636
Be (ppm)	0.1	1.29	1.32	0.83	1.35	0.32	1.55
Ca (ppm)	50	1879	7290	10685	14814	2119	1652
Cd (ppm)	2	N.D.	N.D.	N.D.	N.D.	N.D.	N.D.
Co (ppm)	1	2	3	2	2	N.D.	2
Cr (ppm)	6	53.65	16.47	17.82	14.82	22.95	16.02
Cu (ppm)	3	N.D.	N.D.	N.D.	3	30	N.D.
Fe (ppm)	100	7177	6193	19586	26266	6983	24976
K (ppm)	60	2984	14994	18384	20981	29396	25695
Li (ppm)	1	3	9	13	11	N.D.	8
Mg (ppm)	70	4706	12062	2044	3638	670	2634
Mn (ppm)	1	60	177	460	493	236	164
Mo (ppm)	8	N.D.	N.D.	N.D.	N.D.	N.D.	N.D.
Na (ppm)	150	41024	19932	29236	23850	19594	23160
Ni (ppm)	3	5	5	4	5	N.D.	4
P (ppm)	10	N.D.	N.D.	105	74	18	49
S (ppm)	43	59	56	81	110	162	191
Sc (ppm)	3	3.1	2.9	2.9	3.1	1.3	2.7
Sr (ppm)	0.7	45.8	60.9	82.8	61.4	26	26.7
Ti (ppm)	10	661	613	1007	863	535	783
V (ppm)	0.6	N.D.	N.D.	2.7	2.3	N.D.	0.8
W (ppm)	2	N.D.	N.D.	4	2	N.D.	N.D.
Y (ppm)	0.2	65.1	63	49.6	51.5	42.2	66
Zn (ppm)	2	10	17	94	189	28	41
laboratory: method		OGL: ICP-MS	OGL: ICP-MS	OGL: ICP-MS	OGL: ICP-MS	OGL: ICP-MS	OGL: ICP-MS
Ce (ppm)	0.07	151.04	122.63	125.84	120.6	102.79	132.53
Cs (ppm)	0.007	0.134	0.455	1.024	1.127	0.418	0.488
Dy (ppm)	0.008	16.785	14.716	12.976	13.131	10.994	16.557
Er (ppm)	0.008	10.116	9.551	7.414	7.662	6.226	9.877
Eu (ppm)	0.005	1.8	1.324	2.795	2.642	2.036	2.753
Gd (ppm)	0.009	16.619	13.887	13.925	14.13	12.6	16.608
Hf (ppm)	0.1	9.4	8.7	11.3	11.1	7.9	11
Ho (ppm)	0.003	3.474	3.12	2.588	2.651	2.133	3.384
La (ppm)	0.02	66.39	53.6	53.26	51.16	43.88	56.34
Lu (ppm)	0.003	1.382	1.355	1.041	1.079	0.87	1.362
Nb (ppm)	0.2	28.1	25	27.4	29.3	25.6	34.1
Nd (ppm)	0.03	75.93	63.13	67.19	63.3	56.11	71
Pr (ppm)	0.006	18.921	15.517	16.381	15.423	13.515	17.216
Rb (ppm)	0.05	8.49	47.36	62.04	76.39	82.35	80.64
Sm (ppm)	0.01	16.72	13.54	14.6	13.92	12.44	16.03
Sr (ppm)	0.5	53.4	68.8	94.2	68.7	28.4	29.2
Ta (ppm)	0.17	2.02	1.84	1.9	1.89	1.7	2.24
Tb (ppm)	0.003	2.714	2.312	2.184	2.185	1.929	2.702
Th (ppm)	0.06	9.29	8.75	6.63	6.61	5.99	7.91
Tm (ppm)	0.003	1.467	1.393	1.087	1.109	0.911	1.442
U (ppm)	0.007	2.2	2.257	1.777	1.509	1.377	2.078
Y (ppm)	0.02	89.13	84.29	67.66	69.02	56.09	88.83
Yb (ppm)	0.01	9.47	9.14	6.98	7.14	5.81	9.14
Zr (ppm)	4	272.3	251.7	393.8	392.6	247.4	352.6

Sample number		03-BHA-0300	03-BHA-0301	03-BHA-0307B	03-BHA-0317	03-BHA-0320	03-BHA-0322
Township		Godfrey Township	Godfrey Township	Godfrey Township	Carscallen	Carscallen	Bristol Township
UTM East NAD83		458282	458446	458085	455858	455602	455986
UTM North NAD83		5368958	5368962	5369178	5365869	5365928	5366111
Rock type		rhyolite	basalt	rhyolite	basalt	basalt	rhyolite
Note		abundant quartz phenocrysts	massive basalt	flow-banded	pillow lava	massive basalt	aphyric rhyolite
laboratory: method		OGL: XRF	OGL: XRF	OGL: XRF	OGL: XRF	OGL: XRF	OGL: XRF
	2003 d.l.						
SiO2 (wt%)	0.01	68.9	46.58	71.68	47.14	51.01	72.37
TiO2 (wt%)	0.01	0.3	1.24	0.14	1.6	1.66	0.26
Al2O3 (wt%)	0.01	9.95	13.87	12.02	14.09	15.76	13.12
Fe2O3 (wt%)	0.01	3.36	13.4	2.52	11.21	13.22	3.45
MgO (wt%)	0.01	1.58	5.6	0.74	3.88	4.36	0.44
CaO (wt%)	0.01	3.1	8.21	0.8	7.87	9.24	1.1
Na2O (wt%)	0.01	0.06	3.36	0.22	5.14	2.29	4.44
K2O (wt%)	0.01	7.33	0.04	9.94	0.04	0.02	2.32
MnO (wt%)	0.01	0.14	0.21	0.08	0.12	0.19	0.03
P2O5 (wt%)	0.01	0.03	0.1	0.01	0.28	0.3	0.04
Cr2O3 (wt%)							
LOI (wt%)	0.05	5.48	8.77	2.02	8.71	3.23	2.64
TOTAL		100.24	101.38	100.18	100.08	101.27	100.22
laboratory: method		OGL: XRF	OGL: XRF	OGL: XRF	OGL: XRF	OGL: XRF	OGL: XRF
Cr (ppm)	4	17	132	22	233	218	20
Ni (ppm)							
Nb (ppm)	2	13	3	18	15	17	26
Y (ppm)	1	57	22	72	22	23	70
Zr (ppm)	3	305	85	256	111	118	382
V (ppm)							
laboratory: method		OGL: ICP-AES	OGL: ICP-AES	OGL: ICP-AES	OGL: ICP-AES	OGL: ICP-AES	OGL: ICP-AES
Al (ppm)	100	46854	64530	59720	65758	71084	63111
Ba (ppm)	1	739	8	>1400	43	15	726
Be (ppm)	0.1	0.49	0.35	0.69	0.54	0.54	1.91
Ca (ppm)	50	20947	55402	4552	42646	60465	7498
Cd (ppm)	2	N.D.	N.D.	N.D.	N.D.	N.D.	N.D.
Co (ppm)	1	3	43	2	37	37	3
Cr (ppm)	6	21.26	81.7	24.47	146.2	148.86	11.63
Cu (ppm)	3	N.D.	74	3	N.D.	N.D.	N.D.
Fe (ppm)	100	24016	84819	16391	68494	82803	23365
K (ppm)	60	46135	185	>50000	356	103	15470
Li (ppm)	1	5	30	3	22	8	21
Mg (ppm)	70	8624	31345	3323	20277	23067	2570
Mn (ppm)	1	982	1278	459	637	1118	219
Mo (ppm)	8	N.D.	N.D.	N.D.	N.D.	N.D.	N.D.
Na (ppm)	150	720	23263	1782	35060	16010	29092
Ni (ppm)	3	7	58	4	100	106	6
P (ppm)	10	77	414	13	1197	1302	119
S (ppm)	43	>400	176	>400	79	60	91
Sc (ppm)	3	4.6	32.7	2.5	17.2	18.7	3.8
Sr (ppm)	0.7	50.3	79.1	16.1	255.1	509.1	51
Ti (ppm)	10	1442	5806	683	7975	8183	1161
V (ppm)	0.6	6.1	274.5	1	175.8	172.7	5.4
W (ppm)	2	2	N.D.	N.D.	N.D.	N.D.	N.D.
Y (ppm)	0.2	45.3	16.8	56.6	18.1	17.5	55.5
Zn (ppm)	2	128	106	240	62	45	28
laboratory: method		OGL: ICP-MS	OGL: ICP-MS	OGL: ICP-MS	OGL: ICP-MS	OGL: ICP-MS	OGL: ICP-MS
Ce (ppm)	0.07	84.09	12.84	134.18	68.39	61.95	132.97
Cs (ppm)	0.007	0.959	0.125	0.645	0.084	0.077	0.657
Dy (ppm)	0.008	10.822	4.228	14.023	4.893	4.89	14.26
Er (ppm)	0.008	6.443	2.755	8.813	2.602	2.705	8.366
Eu (ppm)	0.005	1.851	0.939	1.798	1.675	1.806	2.834
Gd (ppm)	0.009	10.511	3.716	15.042	5.565	5.559	15.065
Hf (ppm)	0.1	9	2.5	9.3	3	3.1	12.1
Ho (ppm)	0.003	2.21	0.9	2.941	0.95	0.972	2.846
La (ppm)	0.02	37.35	4.96	58.88	29.06	24.85	58.4
Lu (ppm)	0.003	0.897	0.397	1.317	0.335	0.356	1.187
Nb (ppm)	0.2	16.4	3.8	21.6	17.7	19.4	30.6
Nd (ppm)	0.03	43.06	9.17	68.8	32.83	31.53	69.94
Pr (ppm)	0.006	10.644	1.905	17.306	8.596	7.875	17.131
Rb (ppm)	0.05	93.87	0.43	85.99	0.87	0.54	50.4
Sm (ppm)	0.01	9.58	2.76	15.08	5.74	5.8	15.32
Sr (ppm)	0.5	56	90.9	17.3	303.4	618.6	57.7
Ta (ppm)	0.17	1.35	0.25	1.7	0.94	1.02	1.99
Tb (ppm)	0.003	1.729	0.64	2.329	0.839	0.831	2.392
Th (ppm)	0.06	5.3	0.59	8.46	1.86	1.88	7.32
Tm (ppm)	0.003	0.935	0.398	1.351	0.37	0.377	1.211
U (ppm)	0.007	1.293	0.148	2.081	0.376	0.431	1.782
Y (ppm)	0.02	58.54	22.3	74.3	24.47	24.7	77.17
Yb (ppm)	0.01	6.04	2.63	8.82	2.32	2.4	7.82
Zr (ppm)	4	319.4	88.6	276.9	117.5	122.3	434.4

Sample number		03-BHA-0325A	03-BHA-0326	03-BHA-0332	03-BHA-0354	03-BHA-0358	03-BHA-0363
Township		Carscallen	Carscallen	Bristol Township	Godfrey Township	Godfrey Township	Bristol Township
UTM East NAD83		455645	455789	456491	457015	457437	459594
UTM North NAD83		5366260	5366128	5365457	5371318	5371370	5366499
Rock type		rhyolite	rhyolite	basalt	rhyolite	rhyolite	rhyolite
Note		massive, finely phyric rhyolite	finely feldspar phyric	pillow lava	sparsely porphyritic	flow-banded	aphyric to sparsely phyric
laboratory: method		OGL: XRF	OGL: XRF	OGL: XRF	OGL: XRF	OGL: XRF	OGL: XRF
	2003 d.l						
SiO2 (wt%)	0.01	73.64	71.45	51.09	79.17	80.26	86.78
TiO2 (wt%)	0.01	0.25	0.25	2.02	0.16	0.13	0.08
Al2O3 (wt%)	0.01	12.96	12.88	16.22	11.39	9.93	6.93
Fe2O3 (wt%)	0.01	3.43	3.85	9.35	0.85	1.06	0.5
MgO (wt%)	0.01	0.2	0.56	3	0.78	1.33	0.16
CaO (wt%)	0.01	0.62	1.64	6.02	0.35	0.57	0.62
Na2O (wt%)	0.01	5.76	4.82	6.2	6.58	3.7	3.02
K2O (wt%)	0.01	1.52	2.34	0.49	0.09	1.06	0.99
MnO (wt%)	0.01	0.02	0.04	0.12	N.D	0.02	0.02
P2O5 (wt%)	0.01	0.04	0.04	0.52	0.01	0.01	0.01
Cr2O3 (wt%)							
LOI (wt%)	0.05	1.37	2.11	4.96	0.93	1.79	0.92
TOTAL		99.79	99.96	99.99	100.33	99.86	100.02
laboratory: method		OGL: XRF	OGL: XRF	OGL: XRF	OGL: XRF	OGL: XRF	OGL: XRF
Cr (ppm)	4	7	13	185	23	27	30
Ni (ppm)							
Nb (ppm)	2	27	28	32	21	19	15
Y (ppm)	1	69	73	26	76	63	50
Zr (ppm)	3	383	387	169	234	205	128
V (ppm)							
laboratory: method		OGL: ICP-AES	OGL: ICP-AES	OGL: ICP-AES	OGL: ICP-AES	OGL: ICP-AES	OGL: ICP-AES
Al (ppm)	100	61573	61764	74218	54443	48081	33458
Ba (ppm)	1	485	604	298	21	263	146
Be (ppm)	0.1	1.59	1.44	0.8	0.57	0.82	0.33
Ca (ppm)	50	4091	12111	36276	2050	3625	4591
Cd (ppm)	2	N.D.	N.D.	N.D.	N.D.	N.D.	N.D.
Co (ppm)	1	3	3	38	2	3	1
Cr (ppm)	6	10.88	14.63	138.63	30.17	21.51	41.16
Cu (ppm)	3	51	N.D.	N.D.	N.D.	N.D.	N.D.
Fe (ppm)	100	23700	26994	60545	5957	7389	3587
K (ppm)	60	9866	15491	3367	567	6814	5907
Li (ppm)	1	9	12	12	5	7	3
Mg (ppm)	70	1244	3382	17058	4623	7520	1006
Mn (ppm)	1	106	239	775	46	96	124
Mo (ppm)	8	N.D.	N.D.	N.D.	N.D.	N.D.	N.D.
Na (ppm)	150	38215	32118	40136	42156	24787	20464
Ni (ppm)	3	5	6	126	4	4	N.D.
P (ppm)	10	115	116	2367	N.D.	N.D.	28
S (ppm)	43	>400	69	56	N.D.	N.D.	45
Sc (ppm)	3	3.6	3.9	17.6	2.5	2.4	1
Sr (ppm)	0.7	53.4	63.8	278.6	46.8	34.2	24.4
Ti (ppm)	10	1164	1131	10526	676	548	318
V (ppm)	0.6	3	3.6	181.5	0.8	N.D.	N.D.
W (ppm)	2	N.D.	N.D.	N.D.	N.D.	N.D.	N.D.
Y (ppm)	0.2	56.3	58.3	18.4	61.4	51.4	40.7
Zn (ppm)	2	15	39	80	15	10	18
laboratory: method		OGL: ICP-MS	OGL: ICP-MS	OGL: ICP-MS	OGL: ICP-MS	OGL: ICP-MS	OGL: ICP-MS
Ce (ppm)	0.07	128.85	134.48	110.35	132.82	114.61	104.91
Cs (ppm)	0.007	0.503	2.021	0.237	0.1	0.241	0.665
Dy (ppm)	0.008	14.638	14.615	5.548	15.067	11.89	10.401
Er (ppm)	0.008	8.528	8.602	2.944	9.546	7.666	6.474
Eu (ppm)	0.005	2.75	2.913	2.472	1.871	1.372	1.045
Gd (ppm)	0.009	14.783	15.244	7.212	15.149	11.94	10.734
Hf (ppm)	0.1	11.4	12.1	4.2	9.1	7.9	5.2
Ho (ppm)	0.003	2.952	2.997	1.086	3.155	2.509	2.17
La (ppm)	0.02	55.03	58.47	44.78	59.4	50.02	46.39
Lu (ppm)	0.003	1.153	1.205	0.394	1.344	1.166	0.995
Nb (ppm)	0.2	33.8	33.5	36.6	26.1	23.5	18.3
Nd (ppm)	0.03	67.27	71.74	54.83	68	57.86	52.86
Pr (ppm)	0.006	16.579	17.12	14.123	16.709	14.478	13.206
Rb (ppm)	0.05	34.2	58.17	11.68	1.74	23.77	26.42
Sm (ppm)	0.01	14.41	15.26	9.12	14.71	12.17	11.34
Sr (ppm)	0.5	60.8	72.4	332.7	54	37.9	27.2
Ta (ppm)	0.17	2.13	2.08	1.86	1.84	1.67	1.25
Tb (ppm)	0.003	2.341	2.443	0.987	2.422	1.899	1.718
Th (ppm)	0.06	7.09	7.1	3.28	8.61	7.75	5.47
Tm (ppm)	0.003	1.219	1.225	0.409	1.381	1.169	0.98
U (ppm)	0.007	1.673	1.758	0.689	1.849	1.967	1.376
Y (ppm)	0.02	76.28	78.53	27.13	82.23	67.36	52.9
Yb (ppm)	0.01	7.85	8.11	2.61	8.94	7.73	6.51
Zr (ppm)	4	395.4	436.6	182.5	253.9	227.5	143.4

Sample number		03-BHA-0365	03-BHA-0368	03-BHA-0379	03-BHA-0380B	03-BHA-0387	03-BHA-0403
Township		Bristol Township	Bristol Township	Godfrey Township	Godfrey Township	Godfrey Township	Godfrey Township
UTM East NAD83		458486	457831	459036	459116	459689	457978
UTM North NAD83		5366357	5366012	5371247	5371051	5371168	5370692
Rock type		rhyolite	rhyolite	basalt/andesite	microgabbro	andesite	basalt
Note		massive, aphyric to finely phyric	massive, aphyric	massive	massive, intrusive	massive	massive
laboratory: method		OGL: XRF	OGL: XRF	OGL: XRF	OGL: XRF	OGL: XRF	OGL: XRF
	2003 d.l.						
SiO2 (wt%)	0.01	78.27	77.15	45.49	46.62	56.88	44.07
TiO2 (wt%)	0.01	0.1	0.11	1.06	1.3	0.87	1.22
Al2O3 (wt%)	0.01	9.59	11.71	13.21	14.77	12.77	13.98
Fe2O3 (wt%)	0.01	2.2	1.96	11.07	15.57	9.44	13.62
MgO (wt%)	0.01	0.92	1.09	7.44	7.65	1.22	8.35
CaO (wt%)	0.01	1.85	0.45	8.72	7.18	7.94	7.56
Na2O (wt%)	0.01	3.36	3.27	2.61	3.21	3.11	2.45
K2O (wt%)	0.01	1.62	2.66	0.77	0.17	0.91	0.07
MnO (wt%)	0.01	0.04	0.03	0.17	0.19	0.2	0.21
P2O5 (wt%)	0.01	N.D.	N.D.	0.1	0.1	0.18	0.1
Cr2O3 (wt%)							
LOI (wt%)	0.05	2.35	1.63	9.93	4.59	7.95	9.59
TOTAL		100.31	100.06	100.57	101.35	101.47	101.22
laboratory: method		OGL: XRF	OGL: XRF	OGL: XRF	OGL: XRF	OGL: XRF	OGL: XRF
Cr (ppm)	4	25	23	128	133	30	128
Ni (ppm)							
Nb (ppm)	2	22	26	2	2	7	2
Y (ppm)	1	69	84	24	23	34	24
Zr (ppm)	3	149	183	77	81	214	79
V (ppm)							
laboratory: method		OGL: ICP-AES	OGL: ICP-AES	OGL: ICP-AES	OGL: ICP-AES	OGL: ICP-AES	OGL: ICP-AES
Al (ppm)	100	45538	53820	62007	66560	58334	64638
Ba (ppm)	1	274	304	124	68	152	14
Be (ppm)	0.1	0.99	1.14	0.31	0.34	0.31	0.3
Ca (ppm)	50	12569	3011	56537	43686	50100	49604
Cd (ppm)	2	N.D.	N.D.	N.D.	N.D.	N.D.	N.D.
Co (ppm)	1	1	2	36	47	13	44
Cr (ppm)	6	17.02	12.88	75.34	73.66	15.44	75.86
Cu (ppm)	3	17	3	81	85	17	N.D.
Fe (ppm)	100	14613	12968	67788	94633	60440	84234
K (ppm)	60	10165	16643	5111	1040	6490	414
Li (ppm)	1	12	22	20	12	31	20
Mg (ppm)	70	5169	5803	40263	40630	6493	45917
Mn (ppm)	1	274	151	1030	1171	1230	1297
Mo (ppm)	8	N.D.	N.D.	N.D.	N.D.	N.D.	N.D.
Na (ppm)	150	23584	21481	18580	21473	21414	16771
Ni (ppm)	3	4	5	69	81	16	80
P (ppm)	10	N.D.	N.D.	369	354	807	391
S (ppm)	43	67	N.D.	358	201	101	60
Sc (ppm)	3	1.8	2	29.3	31.8	12.4	30.4
Sr (ppm)	0.7	32.5	16	56.9	64.8	52.9	52.5
Ti (ppm)	10	400	465	5771	6405	4133	5550
V (ppm)	0.6	N.D.	N.D.	260.4	269.5	73	255.2
W (ppm)	2	N.D.	N.D.	N.D.	N.D.	N.D.	N.D.
Y (ppm)	0.2	55.7	63.4	19.5	18.5	26.4	18.4
Zn (ppm)	2	125	79	92	122	127	130
laboratory: method		OGL: ICP-MS	OGL: ICP-MS	OGL: ICP-MS	OGL: ICP-MS	OGL: ICP-MS	OGL: ICP-MS
Ce (ppm)	0.07	116.07	149.71	13.21	14.38	48.35	14.52
Cs (ppm)	0.007	0.814	0.837	0.226	0.573	0.705	0.093
Dy (ppm)	0.008	13.38	15.538	4.671	4.637	6.49	4.564
Er (ppm)	0.008	8.258	9.07	2.969	2.993	3.971	2.914
Eu (ppm)	0.005	1.371	1.607	1.182	1.081	1.483	1.187
Gd (ppm)	0.009	13.282	16.034	4.14	4.029	6.645	4.092
Hf (ppm)	0.1	6.3	7.6	2.3	2.4	5.9	2.3
Ho (ppm)	0.003	2.767	3.145	1.016	1.002	1.357	0.982
La (ppm)	0.02	50.29	69.94	5.07	5.73	20.69	5.73
Lu (ppm)	0.003	1.259	1.256	0.439	0.456	0.605	0.425
Nb (ppm)	0.2	26.7	31.5	3.8	3.9	9.4	3.6
Nd (ppm)	0.03	59.64	79.87	10.39	10.18	26.77	10.31
Pr (ppm)	0.006	14.794	19.749	2.053	2.118	6.32	2.1
Rb (ppm)	0.05	42	70.6	9.87	3.3	26.34	1.43
Sm (ppm)	0.01	13.16	16.51	3.19	2.97	6.05	3.07
Sr (ppm)	0.5	36.3	18.2	66.9	78.4	61	63.5
Ta (ppm)	0.17	1.81	2.21	0.23	0.25	0.62	0.22
Tb (ppm)	0.003	2.206	2.536	0.723	0.704	1.044	0.702
Th (ppm)	0.06	7.89	9.29	0.56	0.5	2.81	0.49
Tm (ppm)	0.003	1.26	1.32	0.439	0.457	0.594	0.431
U (ppm)	0.007	1.625	2.009	0.136	0.144	0.715	0.136
Y (ppm)	0.02	73.86	88.7	26.07	25.6	36.65	25.73
Yb (ppm)	0.01	8.2	8.49	2.88	3.02	3.91	2.81
Zr (ppm)	4	163.2	198.7	84	87.1	239.8	88.7

Sample number		03-BHA-0407	03-BHA-0414	03-BHA-0423	03-BHA-0449	03-BHA-0450A	03-BHA-0451
Township		Godfrey Township	Turnbull Township	Turnbull Township	Turnbull Township	Turnbull Township	Turnbull Township
UTM East NAD83		458115	453978	453920	452981	452851	452951
UTM North NAD83		5370698	5371421	5371780	5372017	5372031	5372120
Rock type		basalt	rhyolite	rhyolite	rhyolite	rhyolite	rhyolite
Note		massive, aphyric	flow-banded	flow-banded	spherulitic	spherulitic	flow-banded, mineralized
laboratory method		OGL XRF	OGL XRF	OGL XRF	OGL XRF	OGL XRF	OGL XRF
	2003 d.l						
SiO2 (wt%)	0.01	43.02	76.69	77.25	79.77	76.37	76.08
TiO2 (wt%)	0.01	1.14	0.13	0.12	0.14	0.16	0.12
Al2O3 (wt%)	0.01	12.98	11.73	11.41	10.99	11.22	11.04
Fe2O3 (wt%)	0.01	17.92	1.67	1.6	1.55	2.1	2.32
MgO (wt%)	0.01	11.47	1.03	0.6	0.71	1.09	0.32
CaO (wt%)	0.01	3.04	0.55	0.93	0.12	1.08	0.96
Na2O (wt%)	0.01	0.05	0.32	0.84	2.73	3.68	3.54
K2O (wt%)	0.01	0.18	6.96	6.31	2.71	2.14	3.75
MnO (wt%)	0.01	0.18	0.01	0.03	N.D.	0.03	0.05
P2O5 (wt%)	0.01	0.08	N.D.	N.D.	0.01	0.01	N.D.
Cr2O3 (wt%)							
LOI (wt%)	0.05	8.5	2.03	2.27	1.42	2.49	1.8
TOTAL		98.56	101.13	101.37	100.17	100.37	99.98
laboratory method		OGL XRF	OGL XRF	OGL XRF	OGL XRF	OGL XRF	OGL XRF
Cr (ppm)	4	139	5	7	7	27	16
Ni (ppm)							
Nb (ppm)	2	N.D.	25	24	20	20	24
Y (ppm)	1	20	76	78	71	78	78
Zr (ppm)	3	70	214	204	243	247	193
V (ppm)							
laboratory method		OGL ICP-AES	OGL ICP-AES	OGL ICP-AES	OGL ICP-AES	OGL ICP-AES	OGL ICP-AES
Al (ppm)	100	64425	55658	53816	51178	51566	52287
Ba (ppm)	1	39	715	850	454	452	726
Be (ppm)	0.1	0.31	1.19	1.11	1.27	0.93	0.79
Ca (ppm)	50	21046	3884	6095	711	7350	6235
Cd (ppm)	2	N.D.	N.D.	N.D.	N.D.	N.D.	N.D.
Co (ppm)	1	56	2	2	3	3	2
Cr (ppm)	6	79.9	10.74	12.25	13.99	16.47	24.8
Cu (ppm)	3	N.D.	8	5	19	N.D.	4
Fe (ppm)	100	>100000	12453	11513	10653	13880	15504
K (ppm)	60	1177	42755	37985	16144	12976	23424
Li (ppm)	1	22	10	9	9	7	14
Mg (ppm)	70	>60000	5478	3172	3843	5896	1743
Mn (ppm)	1	1144	91	193	49	166	300
Mo (ppm)	8	N.D.	N.D.	N.D.	N.D.	N.D.	N.D.
Na (ppm)	150	296	2403	5721	17825	24062	22294
Ni (ppm)	3	88	4	4	5	5	4
P (ppm)	10	405	N.D.	N.D.	N.D.	N.D.	N.D.
S (ppm)	43	68	198	101	>400	>400	62
Sc (ppm)	3	28.1	2.7	2.5	2.7	3	2.4
Sr (ppm)	0.7	17.2	11.5	24.7	10.7	53.2	31.7
Ti (ppm)	10	5025	594	559	639	658	519
V (ppm)	0.6	246.5	0.9	N.D.	N.D.	N.D.	N.D.
W (ppm)	2	N.D.	N.D.	7	3	9	3
Y (ppm)	0.2	15.4	61	61.5	54.1	60.4	59.8
Zn (ppm)	2	430	61	49	12	13	85
laboratory method		OGL ICP-MS	OGL ICP-MS	OGL ICP-MS	OGL ICP-MS	OGL ICP-MS	OGL ICP-MS
Ce (ppm)	0.07	8.93	154.72	141.72	135.06	126.88	148.45
Cs (ppm)	0.007	0.221	0.934	0.744	0.378	0.247	0.21
Dy (ppm)	0.008	3.487	15.232	14.856	13.674	14.352	14.715
Er (ppm)	0.008	2.319	9.298	8.918	8.333	9.012	8.862
Eu (ppm)	0.005	0.6	1.535	1.624	1.442	1.621	1.631
Gd (ppm)	0.009	2.94	16.263	15.551	14.326	13.939	15.535
Hf (ppm)	0.1	2.1	8.8	8.1	8.8	9.1	7.7
Ho (ppm)	0.003	0.778	3.178	3.068	2.857	3.073	3.035
La (ppm)	0.02	3.46	68.57	64.61	61.24	55.74	66.97
Lu (ppm)	0.003	0.377	1.359	1.256	1.213	1.316	1.232
Nb (ppm)	0.2	3.2	31.6	28.3	23.8	25.1	28.7
Nd (ppm)	0.03	6.75	77.89	72.09	68.65	64.26	73.62
Pr (ppm)	0.006	1.351	19.333	18.018	17.09	15.97	18.5
Rb (ppm)	0.05	4.52	124.34	120.12	63.57	45.8	57.09
Sm (ppm)	0.01	2.05	16.34	15.3	14.24	13.75	15.6
Sr (ppm)	0.5	20.2	12.4	27.6	12.3	64.2	35.7
Ta (ppm)	0.17	0.2	2.19	1.97	1.62	1.73	1.9
Tb (ppm)	0.003	0.515	2.536	2.455	2.256	2.303	2.459
Th (ppm)	0.06	0.43	10.01	9.31	7.89	8.22	8.67
Tm (ppm)	0.003	0.343	1.379	1.313	1.247	1.352	1.299
U (ppm)	0.007	0.125	1.979	1.627	1.592	1.192	1.684
Y (ppm)	0.02	20.43	83.68	82.77	74.6	83.78	80.2
Yb (ppm)	0.01	2.3	9.05	8.58	8.21	8.81	8.39
Zr (ppm)	4	78.2	244	227.7	267.6	275.8	209.9

Sample number		03-BHA-0463	03-BHA-0469	03-BHA-0474
Township		Turnbull Township	Turnbull Township	Godfrey Township
UTM East NAD83		454245	453948	459499
UTM North NAD83		5371603	5372142	5371323
Rock type		rhyolite	rhyolite	microgabbro
Note		possibly intrusive	flow-banded	intrusive
laboratory method		OGL XRF	OGL XRF	OGL XRF
	2003 d.l.			
SiO2 (wt%)	0.01	74.21	73.48	49.62
TiO2 (wt%)	0.01	0.31	0.11	1.38
Al2O3 (wt%)	0.01	11.58	11.04	13.94
Fe2O3 (wt%)	0.01	3.52	2.18	10.75
MgO (wt%)	0.01	1.82	1.37	4.87
CaO (wt%)	0.01	1.53	1.91	8.28
Na2O (wt%)	0.01	1.97	0.28	3.56
K2O (wt%)	0.01	2.09	6.37	0.04
MnO (wt%)	0.01	0.04	0.05	0.21
P2O5 (wt%)	0.01	0.05	N.D.	0.11
Cr2O3 (wt%)				
LOI (wt%)	0.05	2.71	3.91	7.66
TOTAL		99.82	100.7	100.42
laboratory method		OGL XRF	OGL XRF	OGL XRF
Cr (ppm)	4	13	20	136
Ni (ppm)				
Nb (ppm)	2	15	22	3
Y (ppm)	1	51	79	25
Zr (ppm)	3	272	201	90
V (ppm)				
laboratory method		OGL ICP-AES	OGL ICP-AES	OGL ICP-AES
Al (ppm)	100	53744	52552	64450
Ba (ppm)	1	324	1012	17
Be (ppm)	0.1	0.53	1	0.41
Ca (ppm)	50	9584	13174	54995
Cd (ppm)	2	N.D.	N.D.	N.D.
Co (ppm)	1	7	2	33
Cr (ppm)	6	16.8	10.89	73.79
Cu (ppm)	3	74	N.D.	93
Fe (ppm)	100	23254	15482	67767
K (ppm)	60	11844	39114	187
Li (ppm)	1	11	10	31
Mg (ppm)	70	9797	7395	27629
Mn (ppm)	1	231	310	1336
Mo (ppm)	8	N.D.	N.D.	N.D.
Na (ppm)	150	13436	2088	23876
Ni (ppm)	3	9	5	47
P (ppm)	10	139	N.D.	409
S (ppm)	43	>400	52	>400
Sc (ppm)	3	4.1	2.4	34.8
Sr (ppm)	0.7	28.6	28.1	93.6
Ti (ppm)	10	1384	534	6212
V (ppm)	0.6	10.6	N.D.	286
W (ppm)	2	5	5	N.D.
Y (ppm)	0.2	37.9	63.1	19
Zn (ppm)	2	84	84	106
laboratory method		OGL ICP-MS	OGL ICP-MS	OGL ICP-MS
Ce (ppm)	0.07	91.41	152.44	16.22
Cs (ppm)	0.007	0.314	0.864	0.097
Dy (ppm)	0.008	9.302	15.167	4.622
Er (ppm)	0.008	5.863	9.203	2.934
Eu (ppm)	0.005	1.119	1.569	1.196
Gd (ppm)	0.009	9.191	15.579	4.135
Hf (ppm)	0.1	8.6	8.1	2.6
Ho (ppm)	0.003	1.97	3.152	1.001
La (ppm)	0.02	42.14	68.31	6.58
Lu (ppm)	0.003	0.9	1.282	0.453
Nb (ppm)	0.2	18.6	28.1	4
Nd (ppm)	0.03	45.51	75.86	11.28
Pr (ppm)	0.006	11.509	19.208	2.408
Rb (ppm)	0.05	45.4	122.5	0.95
Sm (ppm)	0.01	9.31	15.77	3.25
Sr (ppm)	0.5	32.7	31	110.9
Ta (ppm)	0.17	1.37	1.88	0.25
Tb (ppm)	0.003	1.46	2.467	0.715
Th (ppm)	0.06	6.87	8.85	0.62
Tm (ppm)	0.003	0.884	1.35	0.45
U (ppm)	0.007	1.658	2.393	0.16
Y (ppm)	0.02	52.76	84.52	25.14
Yb (ppm)	0.01	5.83	8.74	2.93
Zr (ppm)	4	296.1	224.2	93.3

Sample number		04-BHA-0019	04-BHA-0026	04-BHA-0031	04-BHA-0033	04-BHA-0045	04-BHA-0048A
Township		Robb Township	Robb Township	Jamieson	Robb Township	Jamieson	Jamieson
UTM East NAD83		454083	455898	456332	455590	457561	457409
UTM North NAD83		5382294	5379064	5379364	5380030	5379560	5379072
Rock type		massive mafic volcanic	pillow lava	pillow lava	pillow lava	massive mafic volcanic	massive mafic
Note							
laboratory: method		ActLabs: XRF	ActLabs: XRF	ActLabs: XRF	ActLabs: XRF	ActLabs: XRF	ActLabs: XRF
	2004 d.l.						
SiO2 (wt%)	0.01	51.17	50.94	51.92	53.25	49.33	51.49
TiO2 (wt%)	0.01	0.99	1.36	1.2	1.38	1.82	1.84
Al2O3 (wt%)	0.01	14.3	16.34	13.33	14.02	12.87	11.02
Fe2O3 (wt%)	0.01	12.06	12.27	11.29	11.3	13.52	17.24
MgO (wt%)	0.01	8.53	4.81	4.32	6.51	5.73	2.57
CaO (wt%)	0.01	4.54	7.37	7.89	6.03	6.32	5.39
Na2O (wt%)	0.01	4.89	4.59	4.16	4.71	2.75	4.02
K2O (wt%)	0.01	0.45	0.6	0.20	0.34	0.3	0.75
MnO (wt%)	0.001	0.148	0.247	0.226	0.177	0.3	0.256
P2O5 (wt%)	0.01	0.11	0.13	0.16	0.14	0.23	0.71
Cr2O3 (wt%)	0.01	0.02	0.01	-0.01	0.01	-0.01	-0.01
LOI (wt%)	0.01	2.86	1.71	5.67	1.98	6.94	5.02
TOTAL		100.07	100.38	100.41	99.85	100.1	100.29
laboratory: method		ActLabs: XRF	ActLabs: XRF	ActLabs: XRF	ActLabs: XRF	ActLabs: XRF	ActLabs: XRF
Cr (ppm)	5	164	100	19	37	10	-8
Ni (ppm)	5	75	71	23	27	11	-4
Nb (ppm)	2	-1	2	4	1	3	11
Y (ppm)	2	22	29	28	29	39	78
Zr (ppm)	5	87	97	98	98	161	450
V (ppm)	5	261	320	285	310	423	70
laboratory: method		OGL: ICP-AES	OGL: ICP-AES	OGL: ICP-AES	OGL: ICP-AES	OGL: ICP-AES	OGL: ICP-AES
Al (ppm)	100	66387	75888	63075	66362	61370	50978
Ba (ppm)	1	96	258	176	129	63	165
Be (ppm)	0.1	0.25	0.24	0.3	0.27	0.58	0.91
Ca (ppm)	50	29531	46827	53207	39550	42174	35377
Cd (ppm)	2	N.D.	N.D.	N.D.	N.D.	N.D.	N.D.
Co (ppm)	1	47	48	39	45	34	23
Cr (ppm)	1	143.48	88.81	17.68	40.44	7.89	13.52
Cu (ppm)	3	N.D.	N.D.	46	132	25	N.D.
Fe (ppm)	100	77903	77330	73367	73222	89362	>100000
K (ppm)	60	1740	3824	1687	2471	2115	5178
Li (ppm)	1	9	6	7	8	23	10
Mg (ppm)	70	47032	25819	23836	36482	32469	14052
Mn (ppm)	1	935	1590	1437	1138	1901	1636
Mo (ppm)	8	N.D.	N.D.	N.D.	N.D.	N.D.	N.D.
Na (ppm)	150	31536	29797	28027	30699	18801	26760
Ni (ppm)	3	88	83	39	45	27	19
P (ppm)	10	385	484	575	535	947	3056
S (ppm)	43	N.D.	N.D.	>400	>400	>400	N.D.
Sc (ppm)	0.3	31.9	37.4	34.2	39	35.4	28.5
Sr (ppm)	0.7	28.4	100.9	135	55.8	45.8	74
Ti (ppm)	10	4910	6980	6208	7176	10202	10161
V (ppm)	1	222.6	279.5	255	280.3	>320.0	40.8
W (ppm)	2	N.D.	N.D.	N.D.	2	N.D.	3
Y (ppm)	0.2	18.8	23.2	24	24.9	35.4	69.2
Zn (ppm)	2	107	124	97	130	424	99
laboratory: method		OGL: ICP-MS	OGL: ICP-MS	OGL: ICP-MS	OGL: ICP-MS	OGL: ICP-MS	OGL: ICP-MS
Ce (ppm)	0.07	20.82	15.62	20.54	18.54	34.11	59.65
Cs (ppm)	0.007	0.07	0.051	0.049	0.056	0.075	0.489
Dy (ppm)	0.008	3.862	5.016	4.998	5.185	7.492	14.718
Er (ppm)	0.008	2.527	3.192	3.234	3.279	4.64	9.578
Eu (ppm)	0.005	0.803	0.998	1.093	1.051	2.282	3.306
Gd (ppm)	0.009	3.505	4.378	4.564	4.604	7.223	13.808
Hf (ppm)	0.1	2.3	2.7	2.8	2.7	4.6	11.1
Ho (ppm)	0.003	0.844	1.064	1.082	1.107	1.608	3.196
La (ppm)	0.02	9.59	5.88	8.64	7.29	14.45	22.57
Lu (ppm)	0.003	0.372	0.476	0.471	0.487	0.658	1.458
Nb (ppm)	0.2	3.3	4.2	4.3	4.1	7.1	15.3
Nd (ppm)	0.03	11.9	11.7	13.34	12.75	21.76	41.77
Pr (ppm)	0.006	2.75	2.35	2.829	2.661	4.664	8.721
Rb (ppm)	0.05	2.27	5.84	2.98	6.19	2.96	20.17
Sm (ppm)	0.01	2.97	3.42	3.56	3.54	5.9	11.19
Sr (ppm)	0.5	32.1	111	149.3	62.6	51	81.6
Ta (ppm)	0.17	0.2	0.24	0.26	0.25	0.46	0.97
Tb (ppm)	0.003	0.598	0.779	0.77	0.802	1.193	2.308
Th (ppm)	0.06	0.59	0.58	0.79	0.64	1.62	2.43
Tm (ppm)	0.003	0.375	0.475	0.477	0.494	0.68	1.432
U (ppm)	0.007	0.11	0.152	0.227	0.189	0.425	0.674
Y (ppm)	0.02	22.22	28.42	28.98	29.99	43.22	84.07
Yb (ppm)	0.01	2.49	3.16	3.13	3.22	4.45	9.42
Zr (ppm)	4	87.7	99.7	106.9	100.7	173.3	473.1

Sample number		04-BHA-0056	04-BHA-0085B	04-BHA-0086B	04-BHA-0087	04-BHA-0100	04-BHA-0102
Township		Godfrey Township	Jamieson	Jamieson	Jamieson	Jamieson	Jamieson
UTM East NAD83		459771	459046	459050	459139	460266	458694
UTM North NAD83		5374593	5380148	5380222	5380352	5379313	5379258
Rock type		rhyolite	rhyolite block	pillow lava	gabbro	rhyolite	massive mafic
Note							
laboratory method		ActLabs XRF	ActLabs XRF	ActLabs XRF	ActLabs XRF	ActLabs XRF	ActLabs XRF
	2004 d.l.						
SiO2 (wt%)	0.01	75.2	79.58	50.18	49.06	76.2	47.69
TiO2 (wt%)	0.01	0.23	0.16	2.7	1.19	0.26	2.85
Al2O3 (wt%)	0.01	10.54	9.35	14.97	14.36	11.91	12.63
Fe2O3 (wt%)	0.01	2.2	1.16	13.98	13.31	2.95	18.67
MgO (wt%)	0.01	0.36	0.08	3.49	7.42	0.25	4.22
CaO (wt%)	0.01	0.32	1.21	5.38	11.14	0.69	7.25
Na2O (wt%)	0.01	1.04	1.17	3.82	2.13	4.09	2.1
K2O (wt%)	0.01	7.71	5.92	0.46	0.46	3.26	0.81
MnO (wt%)	0.001	0.05	0.03	0.358	0.196	0.057	0.254
P2O5 (wt%)	0.01	0.03	0.02	0.45	0.12	0.03	0.56
Cr2O3 (wt%)	0.01	-0.01	-0.01	0.02	0.04	-0.01	0.01
LOI (wt%)	0.01	1.39	1.16	4.14	0.68	0.73	3.39
TOTAL		99.06	99.83	99.94	100.1	100.42	100.43
laboratory method		ActLabs XRF	ActLabs XRF	ActLabs XRF	ActLabs XRF	ActLabs XRF	ActLabs XRF
Cr (ppm)	5	-8	-8	128	125	-8	49
Ni (ppm)	5	-4	-4	53	86	-4	26
Nb (ppm)	2	20	30	7	5	39	7
Y (ppm)	2	92	112	55	25	143	55
Zr (ppm)	5	288	310	273	80	517	315
V (ppm)	5	13	-5	378	289	-5	266
laboratory method		OGL ICP-AES	OGL ICP-AES	OGL ICP-AES	OGL ICP-AES	OGL ICP-AES	OGL ICP-AES
Al (ppm)	100	49636	43456	67967	68696	55109	59199
Ba (ppm)	1	739	>1400	200	109	554	215
Be (ppm)	0.1	0.41	1.47	0.57	0.27	1.68	0.57
Ca (ppm)	50	2227	8421	34018	73093	4812	47580
Cd (ppm)	2	N.D.	N.D.	N.D.	N.D.	N.D.	N.D.
Co (ppm)	1	3	1	46	52	2	36
Cr (ppm)	1	44.17	11.17	115.7	142.66	18.21	59.38
Cu (ppm)	3	3	12	28	124	7	10
Fe (ppm)	100	15660	8038	87456	86231	20144	>100000
K (ppm)	60	>50000	41562	3063	3277	22747	5677
Li (ppm)	1	3	4	12	6	5	11
Mg (ppm)	70	1999	364	18465	41275	1354	23437
Mn (ppm)	1	355	211	2267	1283	369	1646
Mo (ppm)	8	N.D.	N.D.	N.D.	N.D.	N.D.	N.D.
Na (ppm)	150	6891	7878	24801	14895	26498	14188
Ni (ppm)	3	4	N.D.	68	112	4	50
P (ppm)	10	91	33	1832	470	52	2406
S (ppm)	43	98	90	>400	177	47	>400
Sc (ppm)	0.3	2.9	1.9	40.3	34.9	3.2	35
Sr (ppm)	0.7	10.3	43.6	88.4	150.5	44.8	82.5
Ti (ppm)	10	1123	776	15667	6142	1330	>16000
V (ppm)	1	12.8	0.8	285	294.2	4.9	218.8
W (ppm)	2	2	N.D.	N.D.	N.D.	6	5
Y (ppm)	0.2	85.7	102	45.6	19	>120.0	47.4
Zn (ppm)	2	69	73	114	113	35	171
laboratory method		OGL ICP-MS	OGL ICP-MS	OGL ICP-MS	OGL ICP-MS	OGL ICP-MS	OGL ICP-MS
Ce (ppm)	0.07	120.42	143.71	33.11	16.92	149.2	39.53
Cs (ppm)	0.007	0.342	0.421	0.132	0.219	0.224	3.945
Dy (ppm)	0.008	18.267	23.389*	9.895	4.189	27.818*	10.596
Er (ppm)	0.008	11.377	13.989	6.446	2.585	18.693	6.59
Eu (ppm)	0.005	2.164	2.894	2.226	1.098	3.008	2.522
Gd (ppm)	0.009	17.593	22.281*	8.839	3.916	23.611*	9.87
Hf (ppm)	0.1	10.7	11.8	6.7	2.3	17.2	7.8
Ho (ppm)	0.003	3.816	4.771	2.157	0.889	6.12	2.276
La (ppm)	0.02	52.53	60.27	12.61	6.98	65.45	15.95
Lu (ppm)	0.003	1.673	1.927	0.963	0.374	2.804	0.995
Nb (ppm)	0.2	21.4	29.7	9.3	4.2	38.2	10.8
Nd (ppm)	0.03	67.31	81.53	24.37	11.46	85.35	28
Pr (ppm)	0.006	15.659	18.873	4.895	2.47	19.823	5.785
Rb (ppm)	0.05	122.25	79.54	10.01	9.49	66.94	38.89
Sm (ppm)	0.01	16.08	20.35	6.92	3.17	20.47	7.73
Sr (ppm)	0.5	10.3	46.4	99.6	169	47.7	90.3
Ta (ppm)	0.17	1.75	2.02	0.58	0.23	2.55	0.69
Tb (ppm)	0.003	2.954	3.825	1.539	0.648	4.216	1.643
Th (ppm)	0.06	9.08	9.52	1.49	0.68	11.6	1.86
Tm (ppm)	0.003	1.696	2.041	0.946	0.371	2.889	0.967
U (ppm)	0.007	2.012	2.5	0.399	0.171	2.871	0.53
Y (ppm)	0.02	103.51	125.356*	58.52	23.27	160.786*	58.43
Yb (ppm)	0.01	11.41	13.41	6.33	2.46	18.71	6.32
Zr (ppm)	4	323	353.6	285.9	85.9	562.9	338.7

Sample number		04-BHA-0144	04-BHA-0163	04-BHA-0183	04-BHA-0194	04-BHA-0196	04-BHA-0197
Township		Jamieson	Jamieson	Jamieson	Jamieson	Jamieson	Jamieson
UTM East NAD83		458610	460840	459036	460889	460274	460173
UTM North NAD83		5377304	5376700	5377363	5377704	5378136	5378352
Rock type		rhyolite block	rhyolite	massive mafic volcanic	rhyolite	rhyolite	rhyolite
Note							
laboratory: method		ActLabs: XRF	ActLabs: XRF	ActLabs: XRF	ActLabs: XRF	ActLabs: XRF	ActLabs: XRF
	2004 d.l.						
SiO2 (wt%)	0.01	81.86	77.21	49.03	78.65	80.44	75.6
TiO2 (wt%)	0.01	0.13	0.17	2.28	0.18	0.14	0.16
Al2O3 (wt%)	0.01	8.51	11.11	13.43	11.23	8.89	10.46
Fe2O3 (wt%)	0.01	1.1	2.09	15.49	1.48	0.81	2.36
MgO (wt%)	0.01	0.27	0.26	6.18	0.16	0.06	0.11
CaO (wt%)	0.01	0.23	0.65	6.46	0.22	0.61	1.11
Na2O (wt%)	0.01	0.69	3.33	2.87	2.39	0.58	0.36
K2O (wt%)	0.01	5.84	3.87	0.55	5.46	6.89	8.26
MnO (wt%)	0.001	0.014	0.058	0.193	0.017	0.02	0.068
P2O5 (wt%)	0.01	0.02	0.02	0.36	0.03	0.02	0.02
Cr2O3 (wt%)	0.01	-0.01	-0.01	0.02	-0.01	-0.01	-0.01
LOI (wt%)	0.01	0.36	1.68	3.45	0.5	0.4	1.11
TOTAL		99.01	100.44	100.31	100.31	98.85	99.61
laboratory: method		ActLabs: XRF	ActLabs: XRF	ActLabs: XRF	ActLabs: XRF	ActLabs: XRF	ActLabs: XRF
Cr (ppm)	5	-8	-8	93	-8	-8	-8
Ni (ppm)	5	-4	-4	50	-4	-4	-4
Nb (ppm)	2	17	35	4	35	28	32
Y (ppm)	2	72	110	40	115	86	99
Zr (ppm)	5	246	319	206	332	265	300
V (ppm)	5	-5	-5	376	-5	-5	-5
laboratory: method		OGL: ICP-AES	OGL: ICP-AES	OGL: ICP-AES	OGL: ICP-AES	OGL: ICP-AES	OGL: ICP-AES
Al (ppm)	100	39839	50424	63392	52257	43532	47854
Ba (ppm)	1	1018	630	145	912	773	782
Be (ppm)	0.1	0.61	1.68	0.64	1.97	0.92	1.59
Ca (ppm)	50	1580	4302	42425	1478	4522	7693
Cd (ppm)	2	N.D.	N.D.	N.D.	N.D.	N.D.	N.D.
Co (ppm)	1	1	2	59	2	1	2
Cr (ppm)	1	26.69	22.98	84.21	22.04	64.64	13.68
Cu (ppm)	3	7	N.D.	54	N.D.	6	7
Fe (ppm)	100	7653	13971	98958	10284	5846	16064
K (ppm)	60	41863	26644	3838	37297	49766	>50000
Li (ppm)	1	3	4	14	5	1	5
Mg (ppm)	70	1400	1384	34178	798	245	424
Mn (ppm)	1	72	392	1215	114	130	462
Mo (ppm)	8	N.D.	N.D.	N.D.	N.D.	N.D.	N.D.
Na (ppm)	150	4605	22217	19996	15970	3837	2265
Ni (ppm)	3	N.D.	N.D.	68	N.D.	N.D.	N.D.
P (ppm)	10	31	25	1462	64	46	29
S (ppm)	43	55	N.D.	>400	43	81	53
Sc (ppm)	0.3	1.5	1.7	40	2	1.3	2
Sr (ppm)	0.7	30	36.8	89.6	28.9	25.7	21.7
Ti (ppm)	10	654	828	13069	879	715	789
V (ppm)	1	1.3	N.D.	310.5	0.9	0.8	N.D.
W (ppm)	2	6	9	4	3	4	8
Y (ppm)	0.2	65.7	95.1	35.6	104.5	79.4	93.5
Zn (ppm)	2	24	15	150	93	56	144
laboratory: method		OGL: ICP-MS	OGL: ICP-MS	OGL: ICP-MS	OGL: ICP-MS	OGL: ICP-MS	OGL: ICP-MS
Ce (ppm)	0.07	84.13	142.46	29.26	136.69	133.69	149.64
Cs (ppm)	0.007	0.227	0.578	0.106	0.449	0.507	0.756
Dy (ppm)	0.008	15.329	21.581*	7.558	26.344*	19.068	22.478*
Er (ppm)	0.008	9.971	13.751	4.86	16.348	10.986	13.756
Eu (ppm)	0.005	1.797	2.667	2.083	2.884	2.794	2.879
Gd (ppm)	0.009	12.734	21.006*	7.128	24.67*	18.666	21.583*
Hf (ppm)	0.1	9.1	12.3	5.2	13.4	10.8	11.9
Ho (ppm)	0.003	3.333	4.582	1.662	5.474	3.819	4.646
La (ppm)	0.02	34.79	61.45	11.82	59.69	57.39	64.87
Lu (ppm)	0.003	1.369	2.118	0.745	2.43	1.564	1.937
Nb (ppm)	0.2	20.6	33.7	7.4	35.5	29.5	33.6
Nd (ppm)	0.03	47.58	78.78	20.55	82.75	72.5	82.29
Pr (ppm)	0.006	11.189	18.576	4.241	19.269	17.377	19.612
Rb (ppm)	0.05	72.74	66.27	6.1	99.57	111.18	128.43
Sm (ppm)	0.01	11.7	19.3	5.74	21.51	17.34	20.1
Sr (ppm)	0.5	32.5	39.2	97.5	31.5	26	23.4
Ta (ppm)	0.17	1.37	2.31	0.47	2.46	2.04	2.23
Tb (ppm)	0.003	2.342	3.526	1.181	4.241	3.144	3.714
Th (ppm)	0.06	6.2	11.09	1.19	11.74	9.86	10.69
Tm (ppm)	0.003	1.472	2.129	0.726	2.494	1.637	2.025
U (ppm)	0.007	1.609	2.595	0.314	2.908	2.37	2.759
Y (ppm)	0.02	81.4	119.22	43.27	132.234*	96.57	115.8
Yb (ppm)	0.01	9.44	14.29	4.81	16.65	10.78	13.42
Zr (ppm)	4	271.2	347.4	216.2	374.4	302.8	346.8

Sample number		04-BHA-0205	04-BHA-0207	04-BHA-0214	04-BHA-0221	04-BHA-0227B	04-BHA-0227G
Township		Godfrey Township	Godfrey Township	Jamieson	Godfrey Township	Jamieson	Jamieson
UTM East NAD83		458874	458823	469363	460806	458479	458479
UTM North NAD83		5374910	5375014	5378084	5375066	5376671	5376671
Rock type		pillow lava	pillow lava	rhyolite	rhyolite	basalt	gabbro
Note							
laboratory: method		ActLabs: XRF	ActLabs: XRF	ActLabs: XRF	ActLabs: XRF	ActLabs: XRF	ActLabs: XRF
	2004 d.l.						
SiO2 (wt%)	0.01	47.56	45.75	77.36	76.55	47.73	47.47
TiO2 (wt%)	0.01	2.46	2.85	0.18	0.38	1.26	2.34
Al2O3 (wt%)	0.01	12.84	12.76	10.8	11.78	13.74	12.36
Fe2O3 (wt%)	0.01	17.36	17.24	0.65	1.77	11.53	17.57
MgO (wt%)	0.01	4.72	5.42	0.11	0.32	4.9	5.42
CaO (wt%)	0.01	5.02	5.64	0.28	0.65	8.14	7.02
Na2O (wt%)	0.01	2.75	2.92	0.33	2.59	0.68	3.19
K2O (wt%)	0.01	0.44	0.44	9.07	5.31	2.6	0.86
MnO (wt%)	0.001	0.291	0.283	0.015	0.037	0.285	0.257
P2O5 (wt%)	0.01	0.37	0.56	0.04	0.06	0.12	0.42
Cr2O3 (wt%)	0.01	-0.01	0.01	-0.01	-0.01	0.01	0.06
LOI (wt%)	0.01	6.57	6.61	0.24	0.89	9.26	3.13
TOTAL		100.37	100.48	99.07	100.33	100.26	100.09
laboratory: method		ActLabs: XRF	ActLabs: XRF	ActLabs: XRF	ActLabs: XRF	ActLabs: XRF	ActLabs: XRF
Cr (ppm)	5	59	60	-8	-8	94	119
Ni (ppm)	5	45	29	-4	-4	41	35
Nb (ppm)	2	6	6	35	26	-1	6
Y (ppm)	2	40	53	122	102	26	46
Zr (ppm)	5	223	315	333	305	85	230
V (ppm)	5	384	322	-5	32	378	302
laboratory: method		OGL: ICP-AES	OGL: ICP-AES	OGL: ICP-AES	OGL: ICP-AES	OGL: ICP-AES	OGL: ICP-AES
Al (ppm)	100	58752	59611	51143	54898	63940	59434
Ba (ppm)	1	142	149	1116	723	629	254
Be (ppm)	0.1	0.35	0.36	0.96	1.45	0.81	0.45
Ca (ppm)	50	32389	36175	1921	4398	52162	45334
Cd (ppm)	2	N.D.	N.D.	N.D.	N.D.	N.D.	N.D.
Co (ppm)	1	40	39	2	2	40	42
Cr (ppm)	1	55.69	60.12	18.66	17.18	77.79	108.89
Cu (ppm)	3	37	24	8	5	N.D.	43
Fe (ppm)	100	>100000	>100000	4502	11978	74014	>100000
K (ppm)	60	3011	3037	>50000	37424	18539	6311
Li (ppm)	1	17	16	2	10	21	9
Mg (ppm)	70	25600	29901	354	1587	26643	30305
Mn (ppm)	1	1824	1784	113	250	1719	1681
Mo (ppm)	8	N.D.	N.D.	N.D.	N.D.	N.D.	N.D.
Na (ppm)	150	18327	19642	2042	17059	4355	21889
Ni (ppm)	3	60	51	3	N.D.	54	57
P (ppm)	10	1590	2382	104	195	430	1773
S (ppm)	43	130	>400	53	N.D.	N.D.	>400
Sc (ppm)	0.3	37	34.8	1.5	5.5	38.2	39.6
Sr (ppm)	0.7	87.3	99.5	27.8	22.8	28.7	122.8
Ti (ppm)	10	14061	>16000	922	1903	6282	13575
V (ppm)	1	282.4	230.5	3	26.5	306.2	271.2
W (ppm)	2	N.D.	12	8	11	10	5
Y (ppm)	0.2	34.1	47.6	113.2	89.3	22.3	40.8
Zn (ppm)	2	172	183	N.D.	77	103	133
laboratory: method		OGL: ICP-MS	OGL: ICP-MS	OGL: ICP-MS	OGL: ICP-MS	OGL: ICP-MS	OGL: ICP-MS
Ce (ppm)	0.07	26.02	38.17	159.36	141.91	12.85	32.32
Cs (ppm)	0.007	0.311	0.171	0.529	0.61	0.375	3.456
Dy (ppm)	0.008	7.35	10.063	24.8*	23.195*	4.661	8.606
Er (ppm)	0.008	4.885	6.453	16.364	14.321	2.912	5.542
Eu (ppm)	0.005	1.402	2.4	3.362	2.497	1.18	2.084
Gd (ppm)	0.009	6.555	9.476	22.739*	21.551*	4.002	7.876
Hf (ppm)	0.1	5.6	7.8	13.4	11.4	2.4	5.8
Ho (ppm)	0.003	1.613	2.195	5.277	4.836	0.994	1.868
La (ppm)	0.02	10.03	14.76	66.41	59.95	5.29	12.49
Lu (ppm)	0.003	0.762	0.977	2.621	2.074	0.415	0.831
Nb (ppm)	0.2	7.8	10.4	33.5	26.6	3.7	8.2
Nd (ppm)	0.03	18.41	27.01	86.95	76.51	9.1	22.4
Pr (ppm)	0.006	3.766	5.521	20.739	18.148	1.861	4.743
Rb (ppm)	0.05	7.58	4.96	124.65	94.14	55.43	31.86
Sm (ppm)	0.01	5.16	7.63	20.98	18.68	2.97	6.44
Sr (ppm)	0.5	98.8	110.7	29.7	24.8	31.3	135.7
Ta (ppm)	0.17	0.51	0.67	2.46	1.88	0.23	0.51
Tb (ppm)	0.003	1.116	1.566	3.93	3.712	0.719	1.345
Th (ppm)	0.06	1.4	1.71	11.77	9.71	0.57	1.32
Tm (ppm)	0.003	0.734	0.957	2.589	2.143	0.424	0.82
U (ppm)	0.007	0.441	0.465	2.522	2.023	0.138	0.347
Y (ppm)	0.02	42.05	58.07	143.321*	114.43	27	48.74
Yb (ppm)	0.01	4.89	6.23	17.8	14.12	2.77	5.38
Zr (ppm)	4	233.9	330.2	378.3	341.4	87.8	240.5

Sample number		04-BHA-0246	04-BHA-0255	04-BHA-0256	04-BHA-0280	04-BHA-0281	04-BHA-0285
Township		Godfrey Township	Godfrey Township	Loveland	Robb Township	Robb Township	Godfrey Township
UTM East NAD83		459041	459041	453082	450343	451224	458424
UTM North NAD83		5374062	5372296	5391219	5384438	5385874	5374989
Rock type		pillow lava	rhyolite block	massive mafic	gabbro	rhyolite	felsic intrusive
Note							
laboratory method		ActLabs: XRF	ActLabs: XRF	ActLabs: XRF	ActLabs: XRF	ActLabs: XRF	ActLabs: XRF
	2004 d.l.						
SiO2 (wt%)	0.01	51.55	68.72	59.37	43.86	75.03	75.77
TiO2 (wt%)	0.01	2.71	0.46	0.71	1.42	0.16	0.19
Al2O3 (wt%)	0.01	13.03	10.44	16.68	10.99	11.82	11.19
Fe2O3 (wt%)	0.01	12.78	4.99	7.46	14.92	2.61	3.1
MgO (wt%)	0.01	6.36	1.86	2.87	4.89	0.49	1.92
CaO (wt%)	0.01	4.83	4.26	8.76	7.79	1.11	0.6
Na2O (wt%)	0.01	3.01	0.8	3.09	2.35	2.19	3.74
K2O (wt%)	0.01	0.45	3.21	0.47	0.49	4.3	1.72
MnO (wt%)	0.001	0.173	0.09	0.119	0.236	0.059	0.074
P2O5 (wt%)	0.01	0.55	0.11	0.15	0.15	0.02	0.02
Cr2O3 (wt%)	0.01	0.01	-0.01	0.01	0.01	-0.01	-0.01
LOI (wt%)	0.01	4.94	4.94	0.69	12.99	2.4	1.49
TOTAL		100.4	99.87	100.38	100.09	100.18	99.8
laboratory method		ActLabs: XRF	ActLabs: XRF	ActLabs: XRF	ActLabs: XRF	ActLabs: XRF	ActLabs: XRF
Cr (ppm)	5	52	9	40	15	-8	-8
Ni (ppm)	5	22	5	57	26	-4	-4
Nb (ppm)	2	7	2	4	1	23	41
Y (ppm)	2	54	24	21	30	64	150
Zr (ppm)	5	317	192	142	97	287	339
V (ppm)	5	280	90	132	372	-5	-5
laboratory method		OGL: ICP-AES	OGL: ICP-AES	OGL: ICP-AES	OGL: ICP-AES	OGL: ICP-AES	OGL: ICP-AES
Al (ppm)	100	61474	50578	80358	51370	55632	54689
Ba (ppm)	1	87	583	167	606	867	724
Be (ppm)	0.1	0.46	1.04	0.37	0.25	1.9	1.1
Ca (ppm)	50	31434	30154	59870	50925	8045	4225
Cd (ppm)	2	N.D.	N.D.	N.D.	N.D.	N.D.	N.D.
Co (ppm)	1	38	12	23	57	2	3
Cr (ppm)	1	52.83	12.83	58.62	15.63	9.54	9.59
Cu (ppm)	3	20	N.D.	12	20	N.D.	N.D.
Fe (ppm)	100	81771	33085	49381	94891	17793	21078
K (ppm)	60	3228	24280	3358	3401	31268	12902
Li (ppm)	1	17	22	6	9	23	9
Mg (ppm)	70	35479	10636	16057	26850	2613	11051
Mn (ppm)	1	1069	590	799	1337	403	502
Mo (ppm)	8	N.D.	N.D.	N.D.	N.D.	N.D.	N.D.
Na (ppm)	150	20475	5528	22005	15633	15243	26056
Ni (ppm)	3	45	14	69	43	3	5
P (ppm)	10	2352	400	535	576	23	56
S (ppm)	43	>400	56	N.D.	>400	53	46
Sc (ppm)	0.3	32.7	8.9	16.6	34.8	5.4	2.4
Sr (ppm)	0.7	74.4	37.3	173.6	60.2	49	40.1
Ti (ppm)	10	>16000	2319	3558	7285	799	933
V (ppm)	1	210.4	78.8	119	291.2	N.D.	3.5
W (ppm)	2	7	9	4	8	11	10
Y (ppm)	0.2	47.6	19.6	17.7	26.5	57.4	>120.0
Zn (ppm)	2	122	19	51	91	79	29
laboratory method		OGL: ICP-MS	OGL: ICP-MS	OGL: ICP-MS	OGL: ICP-MS	OGL: ICP-MS	OGL: ICP-MS
Ce (ppm)	0.07	36.81	48.58	34.86	17.31	103.05	156.38
Cs (ppm)	0.007	0.401	0.71	0.719	0.106	0.452	0.288
Dy (ppm)	0.008	10.271	4.012	3.655	5.537	12.417	28.103*
Er (ppm)	0.008	6.55	2.656	2.257	3.603	8.355	18.541
Eu (ppm)	0.005	2.475	1.099	1.065	1.121	1.321	3.094
Gd (ppm)	0.009	9.543	4.658	3.884	4.821	11.836	25.238*
Hf (ppm)	0.1	7.9	5.6	3.7	2.8	10.1	13.4
Ho (ppm)	0.003	2.251	0.861	0.788	1.186	2.69	6.151
La (ppm)	0.02	13.85	21.42	16.15	6.97	43.94	69.19
Lu (ppm)	0.003	0.953	0.452	0.357	0.533	1.374	2.708
Nb (ppm)	0.2	10.6	7.9	6.3	4.3	27.2	35.2
Nd (ppm)	0.03	26.4	24.06	17.06	12.15	52.79	87.33
Pr (ppm)	0.006	5.405	6.063	4.227	2.504	13.006	20.474
Rb (ppm)	0.05	5.71	91.13	9.16	7.01	106.62	31.02
Sm (ppm)	0.01	7.56	5.29	3.73	3.61	11.66	21.7
Sr (ppm)	0.5	83.5	38.8	189.4	66	51.6	42.6
Ta (ppm)	0.17	0.68	0.63	0.46	0.28	1.79	2.43
Tb (ppm)	0.003	1.638	0.692	0.62	0.848	1.976	4.328
Th (ppm)	0.06	1.91	4.12	1.92	0.79	6.73	11.87
Tm (ppm)	0.003	0.955	0.407	0.337	0.531	1.29	2.788
U (ppm)	0.007	0.511	0.974	0.522	0.208	1.464	2.705
Y (ppm)	0.02	59.4	23.78	21.19	31.5	72.82	169.547*
Yb (ppm)	0.01	6.21	2.83	2.26	3.4	8.84	18.31
Zr (ppm)	4	337.2	218.2	149.9	103	325.3	383.8

Sample number		04-BHA-0290	04-BHA-0293	04-BHA-0294	04-BHA-0295	04-BHA-0296	04-BHA-0297
Township		Godfrey Township	Loveland	Loveland	Loveland	Godfrey Township	Loveland
UTM East NAD83		458119	451406	449649	454392	457939	451789
UTM North NAD83		5375378	5386130	5386850	5387373	5373600	5389811
Rock type		pillow lava	rhyolite	rhyolite	pillow lava	pillow lava	rhyolite
Note							
laboratory: method		ActLabs: XRF	ActLabs: XRF	ActLabs: XRF	ActLabs: XRF	ActLabs: XRF	ActLabs: XRF
	2004 d.l.						
SiO2 (wt%)	0.01	48.51	75.2	78.9	50.12	47.58	76.66
TiO2 (wt%)	0.01	1.33	0.15	0.11	0.74	1.21	0.12
Al2O3 (wt%)	0.01	13.49	12.04	10.59	16.86	13.72	10.87
Fe2O3 (wt%)	0.01	11.7	3.25	1.89	10.08	11.55	2.68
MgO (wt%)	0.01	5.52	0.32	0.25	3.49	7.37	0.18
CaO (wt%)	0.01	6.81	1.01	1.02	16.75	6.62	2.27
Na2O (wt%)	0.01	4.17	3.21	4.58	0.65	2.54	3.27
K2O (wt%)	0.01	0.62	3.64	1.25	0.08	0.54	2.21
MnO (wt%)	0.001	0.178	0.052	0.044	0.174	0.192	0.078
P2O5 (wt%)	0.01	0.13	0.02	0.02	0.11	0.12	0.02
Cr2O3 (wt%)	0.01	0.01	-0.01	-0.01	0.02	0.02	-0.01
LOI (wt%)	0.01	7.3	1.38	1.09	1.16	8.63	1.66
TOTAL		99.77	100.26	99.73	100.24	100.09	100
laboratory: method		ActLabs: XRF	ActLabs: XRF	ActLabs: XRF	ActLabs: XRF	ActLabs: XRF	ActLabs: XRF
Cr (ppm)	5	52	-8	-8	118	100	-8
Ni (ppm)	5	33	-4	-4	87	43	-4
Nb (ppm)	2	1	24	26	-1	-1	25
Y (ppm)	2	31	71	76	18	25	73
Zr (ppm)	5	93	288	226	79	86	274
V (ppm)	5	342	-5	-5	173	371	-5
laboratory: method		OGL: ICP-AES	OGL: ICP-AES	OGL: ICP-AES	OGL: ICP-AES	OGL: ICP-AES	OGL: ICP-AES
Al (ppm)	100	63171	53910	48890	81676	65531	49203
Ba (ppm)	1	175	827	340	24	195	455
Be (ppm)	0.1	0.35	1.41	0.83	0.19	0.39	1.15
Ca (ppm)	50	44191	6640	7027	>100000	45022	15996
Cd (ppm)	2	N.D.	N.D.	N.D.	N.D.	N.D.	N.D.
Co (ppm)	1	33	3	2	37	46	2
Cr (ppm)	1	45.13	10.28	38.71	129.1	82.95	14.31
Cu (ppm)	3	N.D.	17	9	N.D.	81	16
Fe (ppm)	100	75434	21466	12787	65773	76212	17507
K (ppm)	60	4516	25463	8976	463	4013	15770
Li (ppm)	1	36	4	6	N.D.	16	14
Mg (ppm)	70	30523	1722	1304	19284	42143	810
Mn (ppm)	1	1064	330	293	1181	1270	495
Mo (ppm)	8	N.D.	N.D.	N.D.	N.D.	N.D.	N.D.
Na (ppm)	150	28600	20455	31230	4356	17638	24023
Ni (ppm)	3	46	3	3	100	59	4
P (ppm)	10	507	36	N.D.	352	463	N.D.
S (ppm)	43	N.D.	>400	>400	N.D.	>400	N.D.
Sc (ppm)	0.3	36.2	4.5	3.6	22.7	37.6	3.2
Sr (ppm)	0.7	60.6	33.4	39	72.4	53.3	187.7
Ti (ppm)	10	6881	740	555	3714	6347	591
V (ppm)	1	284.5	N.D.	0.7	169.7	294.3	N.D.
W (ppm)	2	11	9	17	12	8	13
Y (ppm)	0.2	25.3	61.3	66.7	14.4	20.9	64.7
Zn (ppm)	2	66	155	995	34	82	99
laboratory: method		OGL: ICP-MS	OGL: ICP-MS	OGL: ICP-MS	OGL: ICP-MS	OGL: ICP-MS	OGL: ICP-MS
Ce (ppm)	0.07	16.94	114.95	125.98	17.47	14.44	106.19
Cs (ppm)	0.007	0.899	0.387	1.249	0.048	0.113	13.529
Dy (ppm)	0.008	5.026	13.692	14.592	3.054	4.403	12.573
Er (ppm)	0.008	3.376	8.792	9.417	2.031	2.822	8.193
Eu (ppm)	0.005	1.281	1.49	1.51	0.676	1.019	1.389
Gd (ppm)	0.009	4.375	13.515	14.475	2.815	3.945	12.033
Hf (ppm)	0.1	2.6	9.8	8.4	2.1	2.5	9.5
Ho (ppm)	0.003	1.129	2.886	3.132	0.669	0.959	2.721
La (ppm)	0.02	6.29	49.71	54.51	7.39	5.72	46.38
Lu (ppm)	0.003	0.533	1.422	1.428	0.311	0.424	1.236
Nb (ppm)	0.2	3.9	26.7	28.3	3.8	3.7	22.4
Nd (ppm)	0.03	12.16	59.27	64.44	10.11	9.76	53.38
Pr (ppm)	0.006	2.467	14.709	15.899	2.327	2.095	13.499
Rb (ppm)	0.05	21.61	55.92	37.43	0.78	10.65	73.51
Sm (ppm)	0.01	3.53	13.17	14.44	2.42	2.99	11.99
Sr (ppm)	0.5	66.9	37.3	44.1	82	60	201.4
Ta (ppm)	0.17	0.25	1.7	1.76	0.24	0.24	1.48
Tb (ppm)	0.003	0.767	2.23	2.373	0.484	0.699	2.043
Th (ppm)	0.06	0.62	6.42	6.47	0.75	0.59	5.61
Tm (ppm)	0.003	0.508	1.359	1.428	0.3	0.42	1.242
U (ppm)	0.007	0.327	1.611	1.661	0.194	0.152	1.378
Y (ppm)	0.02	29.88	77.35	85.88	17.82	24.9	78.29
Yb (ppm)	0.01	3.39	9.12	9.43	2.04	2.76	8.12
Zr (ppm)	4	93.2	325.5	255.5	84	91	315.3

Sample number		04-BHA-0298	04-BHA-0298B	04-BHA-0310	04-BHA-0311	04-BHA-0312	04-BHA-0314
Township		Loveland	Loveland	Loveland	Loveland	Loveland	Loveland
UTM East NAD83		450758	450758	454533	454852	454949	454469
UTM North NAD83		5388383	5388383	5394965	5394799	5394793	5395216
Rock type		rhyolite	mafic intrusive	massive mafic	pillow lava	pillow lava	leucogabbro
Note							
laboratory: method		ActLabs: XRF	ActLabs: XRF	ActLabs: XRF	ActLabs: XRF	ActLabs: XRF	ActLabs: XRF
	2004 d.l.						
SiO2 (wt%)	0.01	76.21	49.24	45.86	57.17	58.75	48.47
TiO2 (wt%)	0.01	0.12	1.19	0.69	1.76	1.82	1.32
Al2O3 (wt%)	0.01	12.89	15.02	16.83	14.67	14.3	13.58
Fe2O3 (wt%)	0.01	1.76	12.59	10.45	9.26	9.42	14.67
MgO (wt%)	0.01	0.19	6.59	9.15	3.38	3.27	6.6
CaO (wt%)	0.01	0.55	10.47	12.57	6.1	5.95	11.19
Na2O (wt%)	0.01	5.64	2.14	1.23	4.79	4.54	1.7
K2O (wt%)	0.01	2.02	0.91	0.2	0.12	0.21	0.07
MnO (wt%)	0.001	0.049	0.21	0.171	0.124	0.138	0.205
P2O5 (wt%)	0.01	0.02	0.18	0.05	0.24	0.25	0.11
Cr2O3 (wt%)	0.01	-0.01	0.03	0.04	-0.01	0.01	0.02
LOI (wt%)	0.01	0.67	1.64	2.64	1.45	1.28	2.1
TOTAL		100.11	100.21	99.88	99.06	99.93	100.03
laboratory: method		ActLabs: XRF	ActLabs: XRF	ActLabs: XRF	ActLabs: XRF	ActLabs: XRF	ActLabs: XRF
Cr (ppm)	5	-8	160	237	25	26	99
Ni (ppm)	5	-4	81	219	28	32	31
Nb (ppm)	2	28	5	-1	7	9	1
Y (ppm)	2	84	23	14	36	33	27
Zr (ppm)	5	246	89	31	182	181	76
V (ppm)	5	-5	232	193	249	243	369
laboratory: method		OGL: ICP-AES	OGL: ICP-AES	OGL: ICP-AES	OGL: ICP-AES	OGL: ICP-AES	OGL: ICP-AES
Al (ppm)	100	59994	69448	76916	69300	65357	62113
Ba (ppm)	1	340	198	39	32	72	14
Be (ppm)	0.1	1.19	0.33	N.D.	0.5	0.49	0.13
Ca (ppm)	50	3407	69004	81612	40872	40408	73119
Cd (ppm)	2	N.D.	N.D.	N.D.	N.D.	N.D.	N.D.
Co (ppm)	1	2	45	57	34	39	50
Cr (ppm)	1	16.64	155.57	196.44	32.91	58.67	89.72
Cu (ppm)	3	4	10	79	N.D.	N.D.	83
Fe (ppm)	100	12029	79961	65856	60788	61166	92059
K (ppm)	60	12434	6391	1387	554	1257	273
Li (ppm)	1	9	17	18	7	7	4
Mg (ppm)	70	1036	36490	49639	18623	17693	35525
Mn (ppm)	1	311	1332	1037	823	874	1322
Mo (ppm)	8	N.D.	N.D.	N.D.	N.D.	N.D.	N.D.
Na (ppm)	150	42317	15015	8879	33116	32677	12027
Ni (ppm)	3	N.D.	97	221	42	49	56
P (ppm)	10	N.D.	662	74	995	1006	346
S (ppm)	43	51	69	>400	N.D.	N.D.	>400
Sc (ppm)	0.3	2.8	32.3	28.5	24.2	24.8	43.2
Sr (ppm)	0.7	81.4	153.3	103.8	126.4	135.7	98.1
Ti (ppm)	10	608	6080	3229	10183	10371	6876
V (ppm)	1	0.7	205.3	187.2	218.7	215.9	>320.0
W (ppm)	2	8	10	3	6	8	N.D.
Y (ppm)	0.2	75.8	18.8	11.4	31.8	29.5	23
Zn (ppm)	2	72	170	53	19	36	77
laboratory: method		OGL: ICP-MS	OGL: ICP-MS	OGL: ICP-MS	OGL: ICP-MS	OGL: ICP-MS	OGL: ICP-MS
Ce (ppm)	0.07	128.54	15.5	4.38	43.91	44.38	12.57
Cs (ppm)	0.007	0.641	1.588	0.206	0.12	0.134	0.096
Dy (ppm)	0.008	15.831	4.043	2.222	6.846	6.169	4.739
Er (ppm)	0.008	10.169	2.527	1.454	4.255	3.878	3.121
Eu (ppm)	0.005	1.71	1.147	0.566	1.786	1.533	1.115
Gd (ppm)	0.009	15.136	3.926	1.884	6.798	6.3	4.143
Hf (ppm)	0.1	8.9	2.4	0.9	4.8	4.8	2.2
Ho (ppm)	0.003	3.35	0.863	0.495	1.441	1.305	1.037
La (ppm)	0.02	58.2	6.11	1.56	17.61	17.75	4.73
Lu (ppm)	0.003	1.457	0.378	0.222	0.617	0.604	0.469
Nb (ppm)	0.2	28.4	4.6	1.3	10.4	10.3	3.4
Nd (ppm)	0.03	65.95	11.01	3.91	26.52	26.49	9.72
Pr (ppm)	0.006	16.272	2.218	0.746	6.09	6.078	1.932
Rb (ppm)	0.05	53.47	33.3	5.74	1.22	3.61	0.39
Sm (ppm)	0.01	14.67	3.15	1.38	6.29	5.98	3.13
Sr (ppm)	0.5	89.3	169.6	116.4	140.7	149.8	111.6
Ta (ppm)	0.17	1.74	0.27	N.D.	0.58	0.58	0.21
Tb (ppm)	0.003	2.578	0.649	0.34	1.106	1.002	0.724
Th (ppm)	0.06	6.27	0.47	0.11	1.34	1.3	0.39
Tm (ppm)	0.003	1.479	0.367	0.217	0.616	0.572	0.461
U (ppm)	0.007	1.359	0.371	0.044	0.363	0.357	0.113
Y (ppm)	0.02	95.4	22.72	12.94	38.44	34.7	27.29
Yb (ppm)	0.01	9.62	2.41	1.44	4.04	3.78	3.05
Zr (ppm)	4	278.6	95.9	32	193.9	193.2	78.9

Sample number		04-BHA-0315A	04-BHA-0315B	04-BHA-0317	04-BHA-0318	04-BHA-0320	04-BHA-0323A
Township		Macdiarmid	Macdiarmid	Macdiarmid	Macdiarmid	Macdiarmid	Macdiarmid
UTM East NAD83		460196	459941	458275	458058	458445	458166
UTM North NAD83		5388440	5388579	5389174	5389287	5389886	5391159
Rock type		pillow lava	mafic intrusive	silicified mafic volcanic?	pillow lava	massive mafic volcanic	gabbro
Note							
laboratory: method		ActLabs: XRF	ActLabs: XRF	ActLabs: XRF	ActLabs: XRF	ActLabs: XRF	ActLabs: XRF
	2004 d.l.						
SiO2 (wt%)	0.01	52.81	48.99	61.62	56.04	49.21	52.65
TiO2 (wt%)	0.01	1.47	1.71	0.79	0.84	1.62	0.88
Al2O3 (wt%)	0.01	16.02	13.74	15.56	15.96	16.41	13.72
Fe2O3 (wt%)	0.01	11.38	16.65	5.67	8.63	12.41	13.24
MgO (wt%)	0.01	2.11	4.73	3.71	4.97	6.92	5.6
CaO (wt%)	0.01	9.83	9.82	5.05	6.6	5.91	9.21
Na2O (wt%)	0.01	4.23	1.2	5.49	4.12	3.79	2.53
K2O (wt%)	0.01	0.33	0.06	0.17	0.45	0.28	0.29
MnO (wt%)	0.001	0.203	0.276	0.074	0.121	0.15	0.207
P2O5 (wt%)	0.01	0.23	0.28	0.16	0.16	0.19	0.08
Cr2O3 (wt%)	0.01	0.02	-0.01	0.01	0.01	0.02	-0.01
LOI (wt%)	0.01	1.15	2.65	1.59	2.23	3.14	1.83
TOTAL		99.78	100.1	99.89	100.14	100.05	100.22
laboratory: method		ActLabs: XRF	ActLabs: XRF	ActLabs: XRF	ActLabs: XRF	ActLabs: XRF	ActLabs: XRF
Cr (ppm)	5	17	11	66	60	146	8
Ni (ppm)	5	22	29	59	64	68	14
Nb (ppm)	2	3	7	4	4	5	-1
Y (ppm)	2	24	28	21	21	24	22
Zr (ppm)	5	97	109	144	138	122	68
V (ppm)	5	298	304	127	145	256	269
laboratory: method		OGL: ICP-AES	OGL: ICP-AES	OGL: ICP-AES	OGL: ICP-AES	OGL: ICP-AES	OGL: ICP-AES
Al (ppm)	100	73802	63031	72770	74494	76365	62858
Ba (ppm)	1	95	17	62	111	94	62
Be (ppm)	0.1	0.37	0.3	0.38	0.35	0.25	0.16
Ca (ppm)	50	66517	65167	34029	43453	38716	60490
Cd (ppm)	2	N.D.	N.D.	N.D.	N.D.	N.D.	N.D.
Co (ppm)	1	38	50	25	33	39	54
Cr (ppm)	1	39.55	12.78	71.63	64.87	127.64	11.49
Cu (ppm)	3	9	72	29	49	N.D.	40
Fe (ppm)	100	72344	>100000	37039	54727	80851	85242
K (ppm)	60	640	296	1151	3171	1892	1875
Li (ppm)	1	2	10	5	9	23	5
Mg (ppm)	70	11294	25664	20592	27430	38969	30943
Mn (ppm)	1	1282	1752	480	738	961	1334
Mo (ppm)	8	N.D.	N.D.	N.D.	N.D.	N.D.	N.D.
Na (ppm)	150	30483	8203	38504	27746	26123	17273
Ni (ppm)	3	91	48	68	80	84	34
P (ppm)	10	882	1078	616	554	744	253
S (ppm)	43	49	87	56	>400	N.D.	>400
Sc (ppm)	0.3	23.3	27.3	16.7	18.1	27.3	34.5
Sr (ppm)	0.7	129.8	232.5	153.5	138.1	145	68.3
Ti (ppm)	10	7895	9244	4073	4234	8881	4408
V (ppm)	1	281	284.9	121.8	134.2	215.4	255.6
W (ppm)	2	5	5	5	6	6	13
Y (ppm)	0.2	20.8	23.8	17	17	20.2	18.5
Zn (ppm)	2	69	98	44	62	64	57
laboratory: method		OGL: ICP-MS	OGL: ICP-MS	OGL: ICP-MS	OGL: ICP-MS	OGL: ICP-MS	OGL: ICP-MS
Ce (ppm)	0.07	38.77	45.08	31.16	29.37	28.15	12.79
Cs (ppm)	0.007	0.138	0.211	0.178	0.437	0.217	0.084
Dy (ppm)	0.008	4.424	5.082	3.672	3.637	4.371	3.74
Er (ppm)	0.008	2.718	3.162	2.165	2.251	2.56	2.457
Eu (ppm)	0.005	1.652	1.76	1.086	0.959	1.535	0.767
Gd (ppm)	0.009	4.762	5.389	3.96	3.705	4.633	3.14
Hf (ppm)	0.1	2.6	3	3.7	3.6	3.3	2
Ho (ppm)	0.003	0.921	1.084	0.752	0.772	0.895	0.812
La (ppm)	0.02	15.99	17.71	13.86	12.9	11.19	4.88
Lu (ppm)	0.003	0.395	0.447	0.292	0.33	0.352	0.361
Nb (ppm)	0.2	4.2	4.9	6.3	6.1	6.2	2.9
Nd (ppm)	0.03	22.96	26.48	16.59	15.75	17.95	7.98
Pr (ppm)	0.006	5.275	6.12	3.977	3.808	3.917	1.764
Rb (ppm)	0.05	0.77	0.48	3.42	14.88	6.15	4.43
Sm (ppm)	0.01	4.7	5.48	3.74	3.57	4.44	2.37
Sr (ppm)	0.5	145.3	263.2	167.1	149.5	161	75.9
Ta (ppm)	0.17	0.23	0.26	0.44	0.42	0.37	0.19
Tb (ppm)	0.003	0.734	0.859	0.616	0.605	0.733	0.573
Th (ppm)	0.06	0.9	1.07	1.76	1.56	0.82	0.65
Tm (ppm)	0.003	0.392	0.464	0.308	0.33	0.367	0.361
U (ppm)	0.007	0.216	0.231	0.453	0.385	0.184	0.17
Y (ppm)	0.02	25.04	28.25	19.66	20.21	23.76	21.32
Yb (ppm)	0.01	2.56	2.97	1.96	2.16	2.38	2.32
Zr (ppm)	4	101.3	116.8	149.8	143.7	135.2	71.8

Sample number		04-BHA-0323B	04-BHA-0324	04-BHA-0325B	04-BHA-0327D	04-BHA-0328	04-BHA-0330
Township		Macdiarmid	Macdiarmid	Loveland	Macdiarmid	Loveland	Macdiarmid
UTM East NAD83		458036	458624	452160	456182	453840	457169
UTM North NAD83		5391104	5391136	5390385	5395354	5389450	5394039
Rock type		gabbro	pillow lava	rhyolite	massive mafic volcanic	pillow lava	pillow lava
Note							
laboratory: method		ActLabs: XRF	ActLabs: XRF	ActLabs: XRF	ActLabs: XRF	ActLabs: XRF	ActLabs: XRF
	2004 d.l.						
SiO2 (wt%)	0.01	52.85	56.84	76.69	54.84	60.19	50.84
TiO2 (wt%)	0.01	0.81	0.9	0.14	1.07	0.7	0.81
Al2O3 (wt%)	0.01	13.97	15.71	11.47	17.16	16.32	16.36
Fe2O3 (wt%)	0.01	13.15	7.93	2.25	8.27	7.08	6.99
MgO (wt%)	0.01	5.29	5.02	0.31	3.96	3.88	3.33
CaO (wt%)	0.01	8.79	6.33	2.05	7.77	3.87	11.12
Na2O (wt%)	0.01	2.84	4.86	2.52	3.72	5.29	3.6
K2O (wt%)	0.01	0.47	0.52	2.49	1.32	0.65	0.13
MnO (wt%)	0.001	0.209	0.128	0.032	0.122	0.107	0.17
P2O5 (wt%)	0.01	0.09	0.14	0.02	0.21	0.15	0.04
Cr2O3 (wt%)	0.01	-0.01	0.02	-0.01	-0.01	-0.01	0.03
LOI (wt%)	0.01	1.5	1.67	0.93	1.59	1.84	6.76
TOTAL		99.96	100.07	98.89	100.02	100.07	100.18
laboratory: method		ActLabs: XRF	ActLabs: XRF	ActLabs: XRF	ActLabs: XRF	ActLabs: XRF	ActLabs: XRF
Cr (ppm)	5	-8	111	-8	19	34	151
Ni (ppm)	5	9	86	-4	49	61	172
Nb (ppm)	2	1	2	24	9	2	-1
Y (ppm)	2	21	19	66	22	21	14
Zr (ppm)	5	68	109	299	116	139	37
V (ppm)	5	249	184	-5	183	129	205
laboratory: method		OGL: ICP-AES	OGL: ICP-AES	OGL: ICP-AES	OGL: ICP-AES	OGL: ICP-AES	OGL: ICP-AES
Al (ppm)	100	64960	73211	52401	78066	75205	74757
Ba (ppm)	1	117	200	927	420	169	49
Be (ppm)	0.1	0.14	0.27	1.23	0.34	0.4	N.D.
Ca (ppm)	50	58434	42485	14132	52065	25542	70170
Cd (ppm)	2	N.D.	N.D.	N.D.	N.D.	N.D.	N.D.
Co (ppm)	1	54	35	1	30	28	49
Cr (ppm)	1	8.92	118.01	15.17	28.82	40.45	140.12
Cu (ppm)	3	46	46	14	N.D.	47	44
Fe (ppm)	100	85579	51060	14751	53170	46355	44513
K (ppm)	60	3140	3684	17604	9521	4586	750
Li (ppm)	1	4	6	8	18	14	9
Mg (ppm)	70	29332	27531	1605	21342	21561	17608
Mn (ppm)	1	1345	809	203	753	674	1031
Mo (ppm)	8	N.D.	N.D.	N.D.	N.D.	N.D.	N.D.
Na (ppm)	150	19844	34383	17696	25668	36686	24136
Ni (ppm)	3	30	96	N.D.	63	73	163
P (ppm)	10	273	501	N.D.	779	516	42
S (ppm)	43	>400	264	N.D.	N.D.	62	100
Sc (ppm)	0.3	33.2	21.1	3.3	20.7	16.1	25.8
Sr (ppm)	0.7	102.6	118.9	134.8	260	119.8	67
Ti (ppm)	10	4075	4668	650	5502	3536	4043
V (ppm)	1	239	165.7	N.D.	162.5	114.6	200.6
W (ppm)	2	4	9	8	9	10	8
Y (ppm)	0.2	18.4	14.8	57.8	18.4	16.9	11.5
Zn (ppm)	2	70	60	27	82	65	37
laboratory: method		OGL: ICP-MS	OGL: ICP-MS	OGL: ICP-MS	OGL: ICP-MS	OGL: ICP-MS	OGL: ICP-MS
Ce (ppm)	0.07	12.09	22.11	102.09	35.03	32.27	5.22
Cs (ppm)	0.007	0.169	0.142	4.243	3.443	0.429	0.158
Dy (ppm)	0.008	3.671	3.036	12.735	3.955	3.479	2.248
Er (ppm)	0.008	2.4	1.88	8.238	2.339	2.185	1.436
Eu (ppm)	0.005	0.763	0.92	1.874	1.364	0.9	0.59
Gd (ppm)	0.009	3.104	3.091	12.258	4.192	3.592	1.979
Hf (ppm)	0.1	2	2.7	9.9	3.1	3.6	1
Ho (ppm)	0.003	0.799	0.639	2.72	0.816	0.734	0.486
La (ppm)	0.02	5.02	9.61	43.27	14.78	14.98	1.88
Lu (ppm)	0.003	0.352	0.275	1.29	0.341	0.324	0.204
Nb (ppm)	0.2	2.8	4.7	24.4	5.2	6.2	1.6
Nd (ppm)	0.03	7.61	12.16	54.63	19.34	16	4.34
Pr (ppm)	0.006	1.666	2.867	13.29	4.635	4.003	0.815
Rb (ppm)	0.05	11.42	9.53	98.43	44.63	19.75	2.35
Sm (ppm)	0.01	2.31	2.86	12.05	4.27	3.62	1.43
Sr (ppm)	0.5	114.5	129.9	148.2	290.2	131.5	75.8
Ta (ppm)	0.17	0.2	0.3	1.6	0.34	0.44	N.D.
Tb (ppm)	0.003	0.56	0.509	2.035	0.656	0.574	0.354
Th (ppm)	0.06	0.66	0.9	6.09	1.4	1.84	0.15
Tm (ppm)	0.003	0.351	0.276	1.285	0.342	0.323	0.212
U (ppm)	0.007	0.173	0.254	1.501	0.339	0.456	0.046
Y (ppm)	0.02	21.54	17.28	74.2	21.68	19.77	12.93
Yb (ppm)	0.01	2.36	1.79	8.44	2.23	2.08	1.36
Zr (ppm)	4	73.7	111.1	329.2	123.8	146.6	36.5

Sample number		04-BHA-0333A	04-BHA-0333B	04-BHA-0333C	04-BHA-0335	04-BHA-0336	04-BHA-0340
Township		Thorburn	Thorburn	Thorburn	Loveland	Loveland	Loveland
UTM East NAD83		453889	453689	453569	454022	455087	455396
UTM North NAD83		5395611	5395637	5395774	5392075	5391784	5394515
Rock type		felsic clast	felsic clast	gabbro	massive basalt	massive basalt	pillow lava
Note							
laboratory: method		ActLabs: XRF	ActLabs: XRF	ActLabs: XRF	ActLabs: XRF	ActLabs: XRF	ActLabs: XRF
	2004 d.l.						
SiO2 (wt%)	0.01	68.08	59.63	45.69	60.26	59.86	56.55
TiO2 (wt%)	0.01	0.74	0.62	0.77	0.94	0.78	1.92
Al2O3 (wt%)	0.01	14.7	14.64	16.28	14.55	15.08	14.45
Fe2O3 (wt%)	0.01	3.12	4.5	12.06	8.94	7.83	10.02
MgO (wt%)	0.01	1.82	2.41	9.69	2.89	3.76	3.23
CaO (wt%)	0.01	2.99	6.95	9.23	5.53	6.09	6.37
Na2O (wt%)	0.01	5.14	4.92	1.3	4.92	3.94	4.72
K2O (wt%)	0.01	1.01	0.53	1.28	0.57	0.4	0.26
MnO (wt%)	0.001	0.046	0.097	0.194	0.152	0.116	0.176
P2O5 (wt%)	0.01	0.21	0.12	0.05	0.16	0.16	0.28
Cr2O3 (wt%)	0.01	-0.01	0.01	0.03	-0.01	0.01	-0.01
LOI (wt%)	0.01	2	5.66	3.37	0.96	1.74	2.31
TOTAL		99.85	100.09	99.95	99.86	99.77	100.28
laboratory: method		ActLabs: XRF	ActLabs: XRF	ActLabs: XRF	ActLabs: XRF	ActLabs: XRF	ActLabs: XRF
Cr (ppm)	5	-8	87	197	14	80	22
Ni (ppm)	5	10	44	157	33	53	34
Nb (ppm)	2	5	3	-1	6	4	8
Y (ppm)	2	27	15	15	30	20	36
Zr (ppm)	5	196	114	35	178	134	184
V (ppm)	5	50	108	227	168	142	278
laboratory: method		OGL: ICP-AES	OGL: ICP-AES	OGL: ICP-AES	OGL: ICP-AES	OGL: ICP-AES	OGL: ICP-AES
Al (ppm)	100	67397	67056	75266	64074	67461	65532
Ba (ppm)	1	335	151	622	168	138	95
Be (ppm)	0.1	0.34	0.38	0.16	0.44	0.32	0.41
Ca (ppm)	50	19788	45793	58839	35657	40115	40861
Cd (ppm)	2	N.D.	N.D.	N.D.	N.D.	N.D.	N.D.
Co (ppm)	1	10	19	56	27	31	37
Cr (ppm)	1	12.47	81.45	193.98	19.63	90.66	29.34
Cu (ppm)	3	5	42	77	54	60	N.D.
Fe (ppm)	100	20379	29034	77328	56338	50420	65165
K (ppm)	60	7000	3435	8926	3551	2530	1526
Li (ppm)	1	6	8	17	7	6	8
Mg (ppm)	70	9994	13034	53947	14936	20283	17367
Mn (ppm)	1	309	627	1238	932	711	1129
Mo (ppm)	8	N.D.	N.D.	N.D.	N.D.	N.D.	N.D.
Na (ppm)	150	35225	32744	9214	33576	26280	30899
Ni (ppm)	3	20	57	199	47	69	49
P (ppm)	10	814	443	119	588	577	1073
S (ppm)	43	>400	>400	>400	121	>400	N.D.
Sc (ppm)	0.3	11.3	13.2	31.7	18.1	17.3	26.3
Sr (ppm)	0.7	141.9	143.3	130.6	161.6	153.2	121.7
Ti (ppm)	10	3804	3125	3874	4660	3862	10674
V (ppm)	1	46.3	91.7	213.7	142.4	129	234.2
W (ppm)	2	9	11	7	10	17	10
Y (ppm)	0.2	23.1	11.7	12.4	24.9	16	31.7
Zn (ppm)	2	7	44	75	62	47	59
laboratory: method		OGL: ICP-MS	OGL: ICP-MS	OGL: ICP-MS	OGL: ICP-MS	OGL: ICP-MS	OGL: ICP-MS
Ce (ppm)	0.07	38.3	23.64	4.64	38.95	27.56	45.16
Cs (ppm)	0.007	0.321	0.239	0.922	0.489	0.248	0.172
Dy (ppm)	0.008	4.835	2.275	2.478	5.116	3.276	6.673
Er (ppm)	0.008	3.145	1.431	1.598	3.241	2.034	4.117
Eu (ppm)	0.005	0.884	0.916	0.618	1.291	1.041	1.662
Gd (ppm)	0.009	4.704	2.466	2.104	5.091	3.392	6.732
Hf (ppm)	0.1	5.1	2.9	1	4.6	3.2	4.8
Ho (ppm)	0.003	1.035	0.48	0.541	1.084	0.685	1.387
La (ppm)	0.02	17.61	11.16	1.67	17.26	12.46	18.53
Lu (ppm)	0.003	0.491	0.22	0.237	0.491	0.301	0.605
Nb (ppm)	0.2	8.4	4.9	1.4	7.4	5.9	10.5
Nd (ppm)	0.03	20.11	11.44	4.19	20.75	14.42	27.59
Pr (ppm)	0.006	4.806	2.935	0.767	4.96	3.493	6.299
Rb (ppm)	0.05	21.25	9.9	24.4	15.02	7.88	4.23
Sm (ppm)	0.01	4.58	2.48	1.47	4.81	3.19	6.35
Sr (ppm)	0.5	152	157.8	148.1	181.6	172.6	138
Ta (ppm)	0.17	0.59	0.34	N.D.	0.5	0.37	0.57
Tb (ppm)	0.003	0.776	0.385	0.373	0.838	0.541	1.096
Th (ppm)	0.06	2.36	1.34	0.12	1.99	1.01	1.19
Tm (ppm)	0.003	0.473	0.217	0.238	0.484	0.301	0.6
U (ppm)	0.007	0.602	0.331	0.051	0.535	0.282	0.295
Y (ppm)	0.02	28.06	13.2	13.95	29.38	18.77	38.1
Yb (ppm)	0.01	3.1	1.42	1.58	3.18	1.99	3.94
Zr (ppm)	4	206.1	121.2	34.1	185.7	135.5	198

Sample number		04-BHA-0346	04-BHA-0350	04-BHA-0357	04-BHA-0362	04-BHA-0372	04-BHA-0378
Township		Macdiarmid	Macdiarmid	Loveland	Loveland	Macdiarmid	Loveland
UTM East NAD83		456382	456420	448723	449553	456865	452720
UTM North NAD83		5390706	5391302	5389582	5387741	5388365	5389347
Rock type		pillow lava	pillow lava	rhyolite	rhyolite	gabbro	pillow lava
Note							
laboratory: method	2004 d.l.	ActLabs: XRF	ActLabs: XRF	ActLabs: XRF	ActLabs: XRF	ActLabs: XRF	ActLabs: XRF
SiO2 (wt%)	0.01	57.48	58.95	77.67	54.2	53.85	74.23
TiO2 (wt%)	0.01	0.82	0.78	0.13	0.84	0.32	0.15
Al2O3 (wt%)	0.01	15.98	15.67	10.91	17.58	15.33	12.35
Fe2O3 (wt%)	0.01	8.27	7.78	2.74	9.25	8.87	2.67
MgO (wt%)	0.01	4.53	3.51	0.47	4.81	9.14	0.33
CaO (wt%)	0.01	5.21	8.1	5.05	7.64	8.14	1.46
Na2O (wt%)	0.01	4.57	3.52	0.64	3.92	2.11	3.5
K2O (wt%)	0.01	0.66	0.19	1.45	0.73	0.31	2.79
MnO (wt%)	0.001	0.161	0.115	0.048	0.143	0.158	0.045
P2O5 (wt%)	0.01	0.15	0.14	0.01	0.16	0.05	0.02
Cr2O3 (wt%)	0.01	0.01	0.01	-0.01	0.01	0.06	-0.01
LOI (wt%)	0.01	2.26	1.66	1.07	0.71	2.03	1.17
TOTAL		100.1	100.42	100.18	99.99	100.37	98.7
laboratory: method		ActLabs: XRF	ActLabs: XRF	ActLabs: XRF	ActLabs: XRF	ActLabs: XRF	ActLabs: XRF
Cr (ppm)	5	61	72	-8	-8	446	73
Ni (ppm)	5	70	67	-4	-4	203	89
Nb (ppm)	2	3	3	25	35	1	5
Y (ppm)	2	23	20	71	92	11	23
Zr (ppm)	5	135	122	239	280	53	137
V (ppm)	5	158	140	-5	-5	90	159
laboratory: method		OGL: ICP-AES	OGL: ICP-AES	OGL: ICP-AES	OGL: ICP-AES	OGL: ICP-AES	OGL: ICP-AES
Al (ppm)	100	71645	69459	48036	56110	68805	79152
Ba (ppm)	1	336	66	182	414	49	140
Be (ppm)	0.1	0.3	0.36	1.23	1.83	0.17	0.32
Ca (ppm)	50	33903	51896	34052	9366	52432	48297
Cd (ppm)	2	N.D.	N.D.	N.D.	N.D.	N.D.	N.D.
Co (ppm)	1	32	28	3	2	49	35
Cr (ppm)	1	62.82	76.72	15.84	26.92	388.86	83.33
Cu (ppm)	3	31	11	22	3	63	45
Fe (ppm)	100	53362	48826	17628	17943	56498	58672
K (ppm)	60	4576	1182	9504	19350	1919	4986
Li (ppm)	1	8	4	16	13	14	7
Mg (ppm)	70	24460	18592	2161	1433	50306	25943
Mn (ppm)	1	1019	721	313	301	1003	906
Mo (ppm)	8	N.D.	N.D.	N.D.	N.D.	N.D.	N.D.
Na (ppm)	150	30569	22250	4539	24677	14017	26144
Ni (ppm)	3	85	77	4	4	205	99
P (ppm)	10	503	497	N.D.	N.D.	130	553
S (ppm)	43	>400	N.D.	282	43	45	62
Sc (ppm)	0.3	18.5	17.3	3.6	4.3	17.1	20.3
Sr (ppm)	0.7	115.3	150	62.7	81.7	162.1	146.2
Ti (ppm)	10	4108	3834	585	678	1429	4089
V (ppm)	1	142.9	137.1	N.D.	N.D.	74.9	143.5
W (ppm)	2	13	11	15	11	9	10
Y (ppm)	0.2	18.2	16.2	62.8	80.6	7.4	17.9
Zn (ppm)	2	92	16	34	90	58	74
laboratory: method		OGL: ICP-MS	OGL: ICP-MS	OGL: ICP-MS	OGL: ICP-MS	OGL: ICP-MS	OGL: ICP-MS
Ce (ppm)	0.07	29.14	24.69	105.69	117.64	12.63	32.12
Cs (ppm)	0.007	0.173	0.12	1.717	1.399	0.422	0.493
Dy (ppm)	0.008	3.873	3.401	12.743	15.252	1.369	3.786
Er (ppm)	0.008	2.37	2.15	8.372	10.915	0.886	2.358
Eu (ppm)	0.005	1.078	0.961	1.439	1.365	0.551	1.084
Gd (ppm)	0.009	3.786	3.369	12.075	13.692	1.298	3.814
Hf (ppm)	0.1	3.5	3.1	8.8	10.6	1.4	3.5
Ho (ppm)	0.003	0.815	0.707	2.736	3.423	0.285	0.788
La (ppm)	0.02	13.45	11.2	48.17	51.72	6.14	14.65
Lu (ppm)	0.003	0.353	0.308	1.286	1.708	0.147	0.348
Nb (ppm)	0.2	5.7	5.3	26.3	35.4	2.2	6.3
Nd (ppm)	0.03	15.57	13.27	54.12	60.21	5.94	16.47
Pr (ppm)	0.006	3.731	3.13	13.428	14.721	1.511	4.034
Rb (ppm)	0.05	11.07	3.75	80.09	121.56	8.98	25.34
Sm (ppm)	0.01	3.52	3.15	11.73	13.14	1.25	3.69
Sr (ppm)	0.5	129.4	168.6	68.4	89.3	186.2	167.6
Ta (ppm)	0.17	0.39	0.35	1.71	2.26	N.D.	0.42
Tb (ppm)	0.003	0.615	0.554	2.001	2.33	0.217	0.607
Th (ppm)	0.06	1.5	1.29	5.74	7.76	0.64	1.56
Tm (ppm)	0.003	0.354	0.312	1.268	1.706	0.139	0.342
U (ppm)	0.007	0.378	0.335	1.421	1.91	0.16	0.393
Y (ppm)	0.02	21.35	19.1	75.65	98.95	8	21.93
Yb (ppm)	0.01	2.3	2.02	8.41	11.06	0.91	2.27
Zr (ppm)	4	142.7	126.2	273.7	316.5	59.6	144.6

Sample number		04-BHA-0379	04-BHA-0410	04-BHA-0450	04-BHA-0451	04-BHA-0452	04-BHA-0453
Township		Jamieson	Godfrey Township	Robb Township	Jamieson	Jamieson	Jamieson
UTM East NAD83		459427	458132	452605	456181	456784	458128
UTM North NAD83		5379027	5373042	5382916	5381978	5381353	5383148
Rock type		rhyolite	gabbro	rhyolite	rhyolite	rhyolite	rhyolite
Note				Exp. Alliance DDH HM98-31 110.5m	Falconbridge DDH J41-03 444.0m	Falconbridge DDH J41-06 217.0m	Falconbridge DDH J52-03 95.2m
laboratory method	2004 d.l.	ActLabs XRF	ActLabs XRF	ActLabs XRF	ActLabs XRF	ActLabs XRF	ActLabs XRF
SiO2 (wt%)	0.01	73.88	48.23	78.68	72.43	71.36	79.85
TiO2 (wt%)	0.01	0.33	1.16	0.17	0.29	0.31	0.14
Al2O3 (wt%)	0.01	11.83	14.46	11.93	11.4	11.65	10.01
Fe2O3 (wt%)	0.01	3.11	13.97	0.41	4.48	5.64	2.3
MgO (wt%)	0.01	0.26	6.36	0.49	0.65	0.33	0.28
CaO (wt%)	0.01	0.72	10.22	1.05	1.2	1.55	1.13
Na2O (wt%)	0.01	0.85	1.68	4.86	1.63	2.43	2.87
K2O (wt%)	0.01	7.92	0.16	1.1	5.44	4.26	1.99
MnO (wt%)	0.001	0.057	0.214	0.009	0.089	0.133	0.037
P2O5 (wt%)	0.01	0.04	0.13	0.02	0.03	0.04	0.02
Cr2O3 (wt%)	0.01	-0.01	0.01	-0.01	-0.01	-0.01	-0.01
LOI (wt%)	0.01	0.86	3.69	1.17	2.26	2.1	1.63
TOTAL		99.84	100.29	99.88	99.89	99.8	100.25
laboratory method		ActLabs XRF	ActLabs XRF	ActLabs XRF	ActLabs XRF	ActLabs XRF	ActLabs XRF
Cr (ppm)	5	-8	119	-8	-8	-8	-8
Ni (ppm)	5	-4	73	-4	-4	-4	-4
Nb (ppm)	2	33	2	17	16	17	14
Y (ppm)	2	134	27	53	91	90	42
Zr (ppm)	5	602	94	280	481	472	285
V (ppm)	5	-5	264	-5	7	-5	-5
laboratory method		OGL ICP-AES	OGL ICP-AES	OGL ICP-AES	OGL ICP-AES	OGL ICP-AES	OGL ICP-AES
Al (ppm)	100	52318	60983	50849	50171	53532	45080
Ba (ppm)	1	1124	48	153	555	853	340
Be (ppm)	0.1	1.02	0.19	1.06	1.18	0.85	0.86
Ca (ppm)	50	4851	63128	6740	7983	10771	7894
Cd (ppm)	2	N.D.	N.D.	N.D.	N.D.	N.D.	N.D.
Co (ppm)	1	3	50	2	3	3	2
Cr (ppm)	1	16.52	80.15	14.19	11.44	9.11	12.35
Cu (ppm)	3	3	66	N.D.	N.D.	5	N.D.
Fe (ppm)	100	20345	83856	2594	29262	37551	15089
K (ppm)	60	>50000	1011	6530	35411	29128	12440
Li (ppm)	1	5	10	2	7	12	7
Mg (ppm)	70	1278	32445	2578	3446	1727	1529
Mn (ppm)	1	367	1267	40	572	885	228
Mo (ppm)	8	N.D.	N.D.	N.D.	N.D.	N.D.	N.D.
Na (ppm)	150	5371	10818	30925	10775	16678	20144
Ni (ppm)	3	6	81	5	6	6	3
P (ppm)	10	95	433	17	67	97	N.D.
S (ppm)	43	44	177	N.D.	65	>400	46
Sc (ppm)	0.3	4.6	31.6	2.8	4.9	7	2.9
Sr (ppm)	0.7	24.3	102.8	50.9	31.4	75.7	47.1
Ti (ppm)	10	1586	5616	812	1406	1562	653
V (ppm)	1	1	245.1	1.5	4.7	N.D.	N.D.
W (ppm)	2	12	8	8	16	10	16
Y (ppm)	0.2	>120.0	21.8	41.7	80.7	82.8	36.2
Zn (ppm)	2	60	36	N.D.	45	59	19
laboratory method		OGL ICP-MS	OGL ICP-MS	OGL ICP-MS	OGL ICP-MS	OGL ICP-MS	OGL ICP-MS
Ce (ppm)	0.07	147.33	16.45	73.97	99.4	96.58	90.6
Cs (ppm)	0.007	0.846	0.07	0.234	0.695	0.942	1.125
Dy (ppm)	0.008	28.308*	4.773	9.034	16.705	17.142	9.002
Er (ppm)	0.008	18.545	3.113	6.272	11.343	11.305	5.229
Eu (ppm)	0.005	3.544	1.057	1.012	2.341	2.143	1.348
Gd (ppm)	0.009	24.323*	4.211	8.718	14.926	15.14	10.494
Hf (ppm)	0.1	19.2	2.6	9.7	13.6	14	8.9
Ho (ppm)	0.003	6.052	1.038	1.975	3.697	3.694	1.753
La (ppm)	0.02	62.25	6.58	31.58	42.86	42.3	41.06
Lu (ppm)	0.003	2.733	0.457	1.011	1.695	1.676	0.818
Nb (ppm)	0.2	35.6	3.9	21.9	20.5	20.2	21.3
Nd (ppm)	0.03	85.31	11.53	39.49	55.67	53.62	48.15
Pr (ppm)	0.006	19.528	2.371	9.522	13.1	12.764	11.701
Rb (ppm)	0.05	125.8	2.14	17.36	91.66	109.95	51.01
Sm (ppm)	0.01	21.07	3.33	8.94	13.48	13.2	10.54
Sr (ppm)	0.5	26	121.7	57.5	34.2	80.7	51.3
Ta (ppm)	0.17	2.37	0.24	1.66	1.37	1.39	1.36
Tb (ppm)	0.003	4.324	0.736	1.439	2.577	2.637	1.601
Th (ppm)	0.06	10.13	0.6	7.68	6.47	7.32	5.27
Tm (ppm)	0.003	2.787	0.455	0.983	1.71	1.707	0.785
U (ppm)	0.007	2.748	0.155	1.798	1.751	1.815	1.224
Y (ppm)	0.02	>120.00	27.7	53.27	97.45	99.72	45.36
Yb (ppm)	0.01	18.24	3.01	6.57	11.16	11.17	5.33
Zr (ppm)	4	665.3	97.4	295.9	513.8	510	310.2

Sample number		04-BHA-0454	04-BHA-0455	04-BHA-0462
Township		Robb Township	Robb Township	Robb Township
UTM East NAD83		455511	453956	451049
UTM North NAD83		5381580	5383232	5381502
Rock type		pillow lava	pillow lava	granophyre
Note		Falconbridge DDH R46-09 270.7m	Falconbridge DDH R55-04 638.0m	
laboratory method		ActLabs XRF	ActLabs XRF	ActLabs XRF
	2004 d.l.			
SiO2 (wt%)	0.01	52.28	50.47	74.56
TiO2 (wt%)	0.01	1.26	1.58	0.34
Al2O3 (wt%)	0.01	14.17	14.37	12.66
Fe2O3 (wt%)	0.01	12.2	13.18	2.55
MgO (wt%)	0.01	6.81	3.82	0.63
CaO (wt%)	0.01	7.06	11.23	3.17
Na2O (wt%)	0.01	2.86	0.28	4.58
K2O (wt%)	0.01	0.58	0.14	0.39
MnO (wt%)	0.001	0.184	0.312	0.023
P2O5 (wt%)	0.01	0.14	0.15	0.06
Cr2O3 (wt%)	0.01	0.01	0.01	-0.01
LOI (wt%)	0.01	2.68	4.78	0.89
TOTAL		100.24	100.32	99.84
laboratory method		ActLabs XRF	ActLabs XRF	ActLabs XRF
Cr (ppm)	5	13	70	-8
Ni (ppm)	5	19	49	-4
Nb (ppm)	2	3	7	26
Y (ppm)	2	30	37	112
Zr (ppm)	5	101	104	382
V (ppm)	5	326	397	5
laboratory method		OGL ICP-AES	OGL ICP-AES	OGL ICP-AES
Al (ppm)	100	63601	66910	72992
Ba (ppm)	1	145	24	115
Be (ppm)	0.1	0.24	0.56	1.51
Ca (ppm)	50	45580	75293	25073
Cd (ppm)	2	N.D.	N.D.	N.D.
Co (ppm)	1	56	53	7
Cr (ppm)	1	17.75	56.67	15.4
Cu (ppm)	3	85	66	N.D.
Fe (ppm)	100	76767	85930	20698
K (ppm)	60	3902	788	3280
Li (ppm)	1	11	8	3
Mg (ppm)	70	36732	21053	3525
Mn (ppm)	1	1162	2031	165
Mo (ppm)	8	N.D.	N.D.	N.D.
Na (ppm)	150	18802	1838	38755
Ni (ppm)	3	45	62	6
P (ppm)	10	503	529	170
S (ppm)	43	>400	>400	59
Sc (ppm)	0.3	38.3	40.3	4.4
Si (ppm)	0.7	128.9	186.3	139.4
Ti (ppm)	10	6470	7879	1765
V (ppm)	1	293.2	>320.0	7.2
W (ppm)	2	15	5	N.D.
Y (ppm)	0.2	26.2	30	107.6
Zn (ppm)	2	142	115	50
laboratory method		OGL ICP-MS	OGL ICP-MS	OGL ICP-MS
Ce (ppm)	0.07	19.74	18.74	32.22
Cs (ppm)	0.007	0.196	0.069	0.17
Dy (ppm)	0.008	5.174	6.58	19.294
Er (ppm)	0.008	3.375	4.241	13.013
Eu (ppm)	0.005	1.252	1.37	2.758
Gd (ppm)	0.009	4.646	5.548	15.188
Hf (ppm)	0.1	2.8	3	14.1
Ho (ppm)	0.003	1.137	1.404	4.251
La (ppm)	0.02	8.09	7.67	10.81
Lu (ppm)	0.003	0.497	0.624	1.919
Nb (ppm)	0.2	4.5	4.5	23.1
Nd (ppm)	0.03	13.32	13.41	30.83
Pr (ppm)	0.006	2.85	2.73	5.42
Rb (ppm)	0.05	14.17	2.3	7.01
Sm (ppm)	0.01	3.74	4.12	11.7
Sr (ppm)	0.5	145.8	209.3	125
Ta (ppm)	0.17	0.28	0.28	1.55
Tb (ppm)	0.003	0.808	0.995	2.856
Th (ppm)	0.06	0.81	0.78	5.04
Tm (ppm)	0.003	0.505	0.627	1.948
U (ppm)	0.007	0.239	0.221	0.721
Y (ppm)	0.02	30.69	37.54	109.92
Yb (ppm)	0.01	3.26	4.06	12.69
Zr (ppm)	4	103.4	104.6	475.1

Metric Conversion Table

Conversion from SI to Imperial			Conversion from Imperial to SI		
SI Unit	*Multiplied by*	*Gives*	*Imperial Unit*	*Multiplied by*	*Gives*
			LENGTH		
1 mm	0.039 37	inches	1 inch	**25.4**	mm
1 cm	0.393 70	inches	1 inch	**2.54**	cm
1 m	3.280 84	feet	1 foot	**0.304 8**	m
1 m	0.049 709	chains	1 chain	20.116 8	m
1 km	0.621 371	miles (statute)	1 mile (statute)	**1.609 344**	km
			AREA		
1 cm^2	0.155 0	square inches	1 square inch	**6.451 6**	cm^2
1 m^2	10.763 9	square feet	1 square foot	**0.092 903 04**	m^2
1 km^2	0.386 10	square miles	1 square mile	2.589 988	km^2
1 ha	2.471 054	acres	1 acre	0.404 685 6	ha
			VOLUME		
1 cm^3	0.061 023	cubic inches	1 cubic inch	**16.387 064**	cm^3
1 m^3	35.314 7	cubic feet	1 cubic foot	0.028 316 85	m^3
1 m^3	1.307 951	cubic yards	1 cubic yard	0.764 554 86	m^3
			CAPACITY		
1 L	1.759 755	pints	1 pint	0.568 261	L
1 L	0.879 877	quarts	1 quart	1.136 522	L
1 L	0.219 969	gallons	1 gallon	**4.546 090**	L
			MASS		
1 g	0.035 273 962	ounces (avdp)	1 ounce (avdp)	28.349 523	g
1 g	0.032 150 747	ounces (troy)	1 ounce (troy)	**31.103 476 8**	g
1 kg	2.204 622 6	pounds (avdp)	1 pound (avdp)	**0.453 592 37**	kg
1 kg	0.001 102 3	tons (short)	1 ton (short)	**907.184 74**	kg
1 t	1.102 311 3	tons (short)	1 ton (short)	**0.907 184 74**	t
1 kg	0.000 984 21	tons (long)	1 ton (long)	**1016.046 908 8**	kg
1 t	0.984 206 5	tons (long)	1 ton (long)	**1.016 046 90**	t
			CONCENTRATION		
1 g/t	0.029 166 6	ounce (troy)/ ton (short)	1 ounce (troy)/ ton (short)	34.285 714 2	g/t
1 g/t	0.583 333 33	pennyweights/ ton (short)	1 pennyweight/ ton (short)	1.714 285 7	g/t

OTHER USEFUL CONVERSION FACTORS

	Multiplied by	
1 ounce (troy) per ton (short)	31.103 477	grams per ton (short)
1 gram per ton (short)	0.032 151	ounces (troy) per ton (short)
1 ounce (troy) per ton (short)	20.0	pennyweights per ton (short)
1 pennyweight per ton (short)	0.05	ounces (troy) per ton (short)

Note: Conversion factors which are in bold type are exact. The conversion factors have been taken from or have been derived from factors given in the Metric Practice Guide for the Canadian Mining and Metallurgical Industries, published by the Mining Association of Canada in co-operation with the Coal Association of Canada.

ISSN 0826-9580
ISBN 0-7794-7991-2